STUDIES ON DYNAMICS AND CONTROL OF DISTILLATION COLUMNS

by

Elling Wælgaard Jacobsen

A Thesis Submitted for the Degree of

Dr.Ing.

University of Trondheim

The Norwegian Institute of Technology

Trondheim, December 1991

ACKNOWLEDGEMENTS

I am indebted to my supervisor Sigurd Skogestad who has been a most inspiring and encouraging supervisor. In addition to his fruitful contributions in numerous discussions, he has also been a very nice supervisor on a more personal level. I was extremely happy when Sigurd accepted me as a Dr.Ing. student. Now, almost four years later, I know that I had good reasons for being happy. It has been four great, although demanding, years.

I am also indebted to Manfred Morari who was my supervisor while I spent the first six months of 1990 at Caltech. I really enjoyed my stay at Caltech, and feel that it I learned a lot from it.

Thanks also to past and present members of the process control groups at NTH and Caltech for a good time. In particular, I would like to thank Petter Lundström whom I worked close with the first part of this study. Petter and I have shared many fruitful discussions as well as Telemark skiing in Sweden (!), beaching in California etc.

Many friends have been important to me over these years. In particular, I have shared lots of good time with Tor Grande. Tor and I have had several interesting discussions on our research projects as well as many discussions on less serious matters. We have also shared many late night wake-up coffees and even later night refreshing beers. Thanks also to the members of "Jaktlaget" for all the nice hunting trips and subsequent dinners.

Despite the fact that I have spent most of the last four years in my office, I was lucky enough to meet the girl I love. In addition to simply making me very happy, Gry has given me all the support I needed through the rather demanding last months of this work.

My family has always been very important to me, and I dedicate this thesis to my mother and father who have given me such a good life.

Financial support from the Royal Norwegian Council for Scientific and Industrial Research (NTNF) is greatfully acknowledged.

ABSTRACT

Distillation is an important industrial unit operation in which a given feed is separated into two or more products of different compositions. The separation requires input of relatively large amounts of energy. Improved composition control of distillation columns may reduce the energy requirements significantly, and will in addition yield improved product recovery. A prerequisite for obtaining tighter composition control is a basic understanding of the column behavior. This thesis addresses different aspects of the dynamic behavior as well as control of distillation columns.

It is shown that simple distillation columns, even with ideal vapor-liquid equilibrium, may have multiple steady-state solutions and unstable operating points. Two fundamentally different sources for the multiplicity and instability are presented. The dynamics and control of columns with unstable operating points are also addressed.

Low-order dynamic models are frequently used in control studies of distillation columns. Such models are studied in this thesis, and it shown that they in many cases have fundamental shortcomings which make them poor for feedback control studies. It is also shown that it is the high-frequency behavior (initial time response) which is most important to capture in a dynamic model for feedback control studies. One important conclusion is that the flow dynamics should be included in the dynamic model of a distillation column.

Most researchers aiming at improving the composition control of distillation columns, focus on improving the control algorithms. However, distillation columns have inherent control limitations which limits the performance, even of the "best" controller. In this thesis it is shown that the control limitations may be significantly reduced by modifying the *column design.*

In homogeneous azeotropic distillation an entrainer is added to make the separation feasible. The entrainer feed may be used to optimize the column in terms of utility consumption. In this thesis the effect of operating conditions on the controllability of homogeneous azeotropic columns is discussed. It is shown that tight composition control may be achieved in the optimal region of operation, and that overloading the column with entrainer does not improve the controllability.

Contents

Chapter 1

Introduction

Distillation is the most important unit operation in chemical engineering. The principal aim of a distillation column is to separate a given feed into two or more products of different compositions. The separation requires input of relatively large amounts of energy. In the chemical process industry, distillation often involves 30-40 % of the total investment and energy costs. Distillation is also a major energy consumer in a broader perspective; in the USA about 3% of the total energy consumption is spent in distillation (Mix and Dweck, 1982). Similar numbers are probably found for the rest of the western hemisphere. The energy requirements may be reduced significantly through improved operation. This is achieved not only through more optimal column design, but requires in addition a control system which is able to maintain the optimal conditions. Tight control of distillation columns is consequently important for energy savings, and will also yield increased profit through improved product recovery. In addition, distillation columns provide a very challenging example for applying general methods within the field of process dynamics, controller design and analysis in general. The importance of distillation operation is reflected in the very large number of articles and books published on this subject over the years.

1.1 Distillation modelling

A prerequisite for tight composition control of distillation columns is a basic understanding of the column behavior. Some insight may be achieved through experiments on operating columns. However, in order to gain more general insight, mathematical models of the process are needed. One of the main advantages of a model is that it may be simplified, thereby allowing for a better understanding of the different effects contributing to the overall behavior.

Formulating a steady-state or dynamic model of a distillation column is usually rela-

tively simple. However, the resulting model will in most cases contain a very large number of equations which are nonlinear by nature. Solving the model therefore represented the main challenge in the early days of distillation modelling. The first models of distillation columns, developed in the 1920's to 30's, were strongly simplified and treated only the steady-state behavior. These included graphical methods (McCabe and Thiele, 1925) and simple short-cut models (Gilliland and Reed, 1942). The models were based on rather restrictive assumptions, but yielded important insight into the steady-state behavior of distillation columns. One of the first *dynamic* models was solved by Marshall and Pigford (1947) who used simple linear equations and solved them by Laplace transformations. The introduction of the digital computer in the 1950's allowed for more complex models to be solved. Rosenbrock (1957) solved a nonlinear, although relatively simple, dynamic model of a binary column on a digital computer. However, the computer power was rather limited, which is reflected in the comment by Rosenbrock: *"No arrangements are made at present for carrying out the heat-balance automatically. If necessary the machine can be stopped after a few time-steps and the flows corrected by hand calculation. Further time-steps can then be calculated by the machine, and so on"*. In the years following, computer power became readily available, allowing for large and complex systems of nonlinear differential and algebraic equations to be solved, and many papers have been published on the steady-state and dynamic behavior of distillation columns over the last 30 years.

Most papers on distillation dynamics present mainly numerical or experimental results. The results are in most cases application specific and therefore difficult to generalize. Relatively few papers have attempted to establish more general results. However, some important qualitative properties of distillation dynamics have been proposed. Two of the more important ones, both discussed in this thesis, are:

1) *The operating points of binary distillation columns are unique and asymptotically stable.* This conjecture is based on results by several authors (e.g., Rosenbrock, 1960, 1962; Doherty and Perkins 1982; Sridhar and Lucia, 1989). Doherty and Perkins (1982) provide a review of studies on the uniqueness and stability of operating points in homogeneous distillation. The result is somewhat surprising in view of the strong nonlinearity of the dynamic model of a distillation column. However, it is important to note that most of the studies include the restrictive assumptions of constant molar flows (neglected energy balance) as well as all flows measured in molar units. In this thesis it is shown that without these assumptions, even ideal binary distillation columns may have multiple steady-state solutions as well as unstable operating points.

2) *The overall composition dynamics of most distillation columns are well approximated by a linear first-order response.* This has been shown in several theoretical papers (e.g., Davidson, 1956; Moczek et.al., 1965) and has been confirmed by experimental results (McNeill and Sachs, 1969). This result is also somewhat surprising as the set of equations governing distillation dynamics is of high order and strongly nonlinear. The main explanation given is the large interactions between the trays which cause all trays in the column to have similar composition responses (Moczek et.al., 1965). It is important to note that the time constant of the overall response in general will depend on the size of the perturbation made. However, this non-linearity may be effectively counteracted by using logarithmic compositions (Shinskey, 1984; Skogestad, 1987). The fact that the composition dynamics of distillation columns have a relatively simple nature is important as it allows for simple low-order models to be used for certain dynamic studies where insight is important. In distillation control, linear low-order models are commonly used as a consequence of the theoretical results. However, in this thesis it is shown that such models in many cases will have fundamental shortcomings which make them poor for control studies.

The overall composition dynamics of distillation columns are known to be sluggish. However, for feedback control studies it is important to concentrate not only on the overall dynamic behavior, but to incorporate also "fast" dynamic effects. Such effects include possible RHP-zeros and lags caused by the flow dynamics. In particular, it has been demonstrated that the lag caused by the liquid flow dynamics is important for feedback control properties of distillation columns (Skogestad et.al., 1990).

The major part of studies on the behavior of distillation columns have been restricted to systems with relatively ideal thermodynamics. More recently, however, there has been a growing interest in the distillation of more complex mixtures. In particular, there is active research in the field of azeotropic distillation. Most papers in this field treat the steady-state behavior, although some recent papers consider the dynamic behavior of such columns (e.g., Doherty and Perkins, 1978; Andersen et.al., 1991). The dynamic behavior of homogeneous azeotropic distillation columns are discussed briefly in this thesis.

1.2 Distillation Control

Control theory is, similar to distillation modelling, a new science, developing from the 1930's. The first studies on distillation control were published in the 1940's (e.g., Boyd, 1946). Since then there has been published a vast number of articles as well as books on composition control of distillation columns. Most of the research have aimed at testing particular control strategies, and there has been a lot of simulation studies, from which it is difficult to deduce general results. However, general results have been established

governing the inherent control limitations in distillation. The main control limitation is the strong interactions between the top and bottom of the column (Rijnsdorp, 1965), or equivalently, the ill-conditioning (Skogestad, 1987). This applies in particular to columns with high purity products.

A two-product distillation column may usually be described as a 5×5 system in control terms. That is, there are 5 manipulated variables and 5 primary outputs. The optimal controller should use all available information (measurements, process model, expected disturbances) and manipulate all five inputs to keep all the outputs as close as possible to their desired values. However, in practice few columns, if any, are controlled using a full 5×5 controller. Instead, a decentralized system with single-loop controllers is used in most cases. The main reasons are that such a controller is easier to understand and tune and also more failure tolerant. When using a decentralized control structure the control design may be divided into three steps: 1) Choose inputs to use for level and pressure control. 2) Design level and pressure controllers 3) Design composition controllers. In many cases steps 1 and 2 are made without considering the implications for the last step. However, as shown by several authors (e.g., Shinskey, 1967, 1984; Waller, 1986; Skogestad et.al., 1990) the selection of which inputs to use for level control is of vital importance for the remaining composition control problem. Different configurations will have different control properties. The selection of which inputs to use for composition control has received a major part of the attention in the distillation control literature over the last decade.

Having decided which inputs to use for level control, the remaining control problem is not too difficult. The design of level and pressure controllers is relatively simple, and guidelines are available in the literature (Shinskey, 1984). The final decision to be made is whether a "full" 2×2 controller should be used for composition control. In academia the use of decouplers has been discussed for a long time (e.g., Weischedel and McAvoy, 1980). The main reason for employing decouplers is to counteract the strong interactions between the top and bottom of the column, or equivalently, compensate for the strong directionalities (ill-conditioning). Skogestad (1987) introduced the concept of robust control in distillation, that is, controller design taking uncertainties in the model and the plant into account. In cases where the interactions are large decouplers will perform poorly in the presence of certain types of uncertainty. This motivates the use of single-loop controllers also for composition control.

Most studies aimed at improving the control of distillation columns are limited to selecting inputs for composition control and consideration of different control algorithms. In this thesis it is considered whether changing the *column design* may reduce some of

the inherent control limitations, thereby improving the control performance.

Most studies in the distillation control literature treats the case of ideal binary distillation. Few papers have treated the control of more complex distillations. In this thesis the control of homogeneous azeotropic columns is studied.

1.3 Thesis Overview

This thesis addresses different aspects of modelling and control of distillation columns. Each chapter is written as an article, and may thus be read independently. Literature references are also given in each chapter. The thesis is naturally divided into three parts:

Part I: Multiplicity and instability in distillation columns.

The studies on multiplicity in distillation were initiated during an attempt to reproduce some experimental results on distillation of an ethanol-water mixture presented in Waller et.al. (1988). By simulations it was found that the specifications given in the paper, which were flows on a mass rate basis, yielded two possible solutions in terms of compositions. One of the solutions corresponded closely to the profile given by Waller et.al., while the second solution had widely different compositions. In order to understand the source of the multiplicity, significant amounts of work were put into analyzing the rather complex model. Several authors had claimed that multiplicity was impossible for binary distillation, and it was assumed that the multiplicity were due to the thermodynamic complexity of the mixture. Attempts of applying different matrix techniques as well as Lyapunov functions failed due to the large complexity of the system studied. However, by simplifying the model, it became clear that the reason for the multiplicity was rather simple and independent of the thermodynamic complexity of the mixture.

Chapter 2 presents results showing that homogeneous distillation columns may display multiple steady-state solutions, even in the case of ideal binary distillation. Two fundamentally different sources are presented for the multiplicity. In both cases pitchfork bifurcation points are found, resulting in several possible steady-state solutions in terms of outputs (i.e., compositions) for a given set of inputs (i.e., flows). It is shown that for certain specifications there may exist up to five possible solutions. Some of the solutions are found to be unstable.

The dynamic behavior and control of ideal binary distillation columns with multiple solutions are discussed in Chapter 3. Evidence are provided for the instability of certain operating points. It is shown that an open-loop unstable operating point may be stabilized with feedback control of a composition or a temperature. If the control is not sufficiently

tight, the column may go into a stable limit cycle. Finally, possible implications of the instability for dual composition control are discussed.

Part II: Low-order dynamic models for distillation columns.

Low-order dynamic models are commonly used in the distillation control literature. Chapter 4 presents results showing that such models in many cases are inconsistent in that they contain an excessive number of slow poles compared to the process. This has important implications for feedback control. The results are relevant also for other ill-conditioned processes.

Chapter 5 discusses how to obtain low-order models for robust control of distillation columns. Low-order models obtained from physical insight as well as mathematically reduced models are considered. In addition, the problem of obtaining low-order models from experimental data is discussed. It should be noted that this paper was written before the results in Chapter 4 were found, and that the paper includes models that are inconsistent according to Chapter 4. However, the models suggested are shown to be reasonable for two-point (dual composition) control of distillation columns.

Part III: Trade-offs between design and control of distillation columns.

Chapter 6 discusses a few design modifications of distillation columns which may improve the controllability. The main objectives are to reduce the interactions between the top and bottom of the column as well as the disturbance sensitivity. It is shown that some of the modifications may yield a significant improvement in the controllability of high-purity columns.

Homogeneous azeotropic distillation columns have an extra degree of freedom in the amount of entrainer added to enable the separation. This degree of freedom may be used to optimize the column for a given separation. Chapter 7 discusses how the selection of operating points affects the controllability of such columns. This work was carried out at California Institute of Technology under the guidance of Manfred Morari during a visit there in 1990.

A final summary and suggestions for future research are given in Chapter 8.

Preliminary versions of the papers presented in this thesis have appeared at several conferences:

Chapter 2: 1990 AIChE Annual Meeting (paper 133a).

Chapter 3: 40th Canadian Chemical Engineering Conference (paper 1241) and
1991 American Control Conference. (Proceedings, p.773-778).

Chapter 5: 1990 IFAC World Congress. (Preprints, p.213-219).

Chapter 6: EFChE Symposium COPE-91. (Proceedings, p.123-128).

Chapter 7: 1990 AIChE Annual Meeting (paper 211d).

In addition to the work presented in this thesis, the author have participated in other research projects governing distillation dynamics and control during the course of study. The results of these projects are presented in the following articles:

Skogestad, S., P. Lundström and E.W. Jacobsen, 1990, "Selecting the Best Distillation Control Configuration", *AIChE J.*, **36**, 5, 753-764.

Skogestad, S., E.W. Jacobsen and M. Morari, 1990, "Inadequacy of Steady-State Analysis for Feedback Control: Distillate-Bottom Control of Distillation Columns", *Ind.Eng.Chem.Res.*, **29**, 12, 2339-2346.

REFERENCES

Andersen, H.W., L. Laroche and M. Morari, 1991, "Dynamics of Homogeneous Azeotropic Distillation Colunms", *Ind.Eng.Chem.Res.*, **30**, 1846-1855.

Boyd, D.M., 1946, "Control of Fractionating Columns", *Petroleum Refiner*, **25**, 4, 147-151.

Davidson, J.F., 1956, "The Transient Behavior of Plate Distillation Columns", *Trans.Inst.Chem.Eng.*, **34**, 44-52.

Doherty, M.F. and J.D. Perkins, 1978, "On the Dynamics of Distillation Processes - I. The Simple Distillation of Multicomponent Non-Reacting Homogeneous Liquid Mixtures", *Chem.Eng.Sci.*, **33**, 569-578.

Doherty, M.F. and J.D. Perkins, 1982, "On the Dynamics of Distillation Processes-IV. Uniqueness and Stability of the Steady-State in Homogeneous Continuous Distillation", *Chem.Eng.Sci*, **37**, 3, 381-392

Gilliland, E.R. and C.E. Reed, 1942, "Degrees of Freedom in Multicomponent Absorption and rectification Columns", *Ind.Eng.Chem.*, **34**, 551-557.

Marshall, W.R. and R.L. Pigford, 1947, "The Application of Differential Equations to Chemical Engineering Problems", *University of Delaware*, Delaware, USA.

McCabe, W.L. and E.W. Thiele, 1925, "Graphical Design of Fractionating Columns", *Ind.Eng.Chem.*, **17**, 605-611.

McNeill, G.A. and J.D. Sachs, 1969, "High Performance Column Control", *Chem.Eng.Prog.*, **65**, 3, 33-39.

Mix, T.W. and J.S. Dweck, 1982, "Conserving Energy in Distillation", *Industrial Energy-Conservation Manual No. 13*, MIT Press, Cambridge, MA.

Moczek, J.S., R.E. Otto and T.J. Williams, 1965, "Approximation Models for the Dynamic Response of Large Distillation Columns", *Chem.Eng.Prog.Symp.Ser*, **61**, 55, 136-146.

Rijnsdorp, J.E., 1965, "Interactions in Two-Variable Control Systems for Distillation Columns, 1-2", *Automatica*, **1**, 15-52.

Rosenbrock, H.H., 1957, "An Investigation of the Transient Response of a Distillation Column. Part I.", *Trans.Instn.Chem.Engrs.*, **35**, 347-351.

Rosenbrock, H.H., 1960, "A Theorem of "Dynamic Conservation" for Distillation", *Trans.Instn. Chem.Engrs.*, **38**, 20, 279-287.

Rosenbrock, H.H., 1962, "A Lyapunov Function with Applications to Some Nonlinear Physical Problems", *Automatica*, **1**, 31-53.

Shinskey, F.G., 1967, *Process Control Systems*, McGraw-Hill, New York.

Shinskey, F.G. 1984, *Distillation Control. 2nd ed.*, McGraw-Hill, New York.

Skogestad, S., 1987, "Studies on Robust Control of Distillation Columns", Ph.D. Thesis, California Institute of Technology, USA.

Skogestad, S., P. Lundström and E.W. Jacobsen, 1990, "Selecting the Best Distillation Control Configuration", *AIChE J.*, **36**, 5, 753-764.

Sridhar, L.N. and A. Lucia, 1989, "Analysis and Algorithms for Multistage Separation Processes", *Ind.Eng.Chem.Res.*, **28**, 793-803.

Waller, K.V., 1986, "Distillation Control System Structures", *Prepr. IFAC Symposium DYCORD 86*, Bournemouth, UK.

Waller, K.V., K.E. Häggblom, P.M. Sandelin and D.H. Finnerman, 1988, "Disturbance Sensitivity of Distillation Control Structures", *AIChE J.*, **34**, 5, 853-858.

Weischedel, K. and T.J. McAvoy, 1980, "Feasibility of Decoupling in Conventionally Controlled Distillation Columns", *Ind.Eng.Chem.Fundamen.*, **19**, 379-384.

Chapter 2

Multiple Steady-States in Ideal Two-Product Distillation

Elling W. Jacobsen and Sigurd Skogestad

Chemical Engineering
University of Trondheim - NTH
N-7034 Trondheim
Norway

Published in *AIChE J.*, **37**, 4, 499-511, 1991

Abstract

Simple distillation columns with ideal VLE (vapor-liquid equilibrium) may display multiple steady-state solutions. Two fundamentally different sources for the multiplicity are presented. In both cases one may get the unexpected result that increasing reflux makes separation worse in the top part of the column. This will correspond to an unstable operating point.

The first type of multiplicity is found for columns with mass or volume inputs (e.g., mass reflux and molar boilup). Even for the case of constant molar flows the transformation from the actual input units to molar units may become singular, resulting in multiple steady-state solutions. The results are highly relevant in practice as industrial columns usually will have inputs on a mass or volume basis. The second type of multiplicity is found for specifications on a molar basis (e.g., molar reflux and molar boilup) and depends on the presence of an energy balance in the model. The multiplicity is caused by interactions between flows and compositions in the column.

2.1 Introduction

The issue of multiple steady-states (multiplicity) in distillation columns has been studied extensively over the last 30 years. A literature review on homogeneous (one liquid phase) distillation is given by Doherty and Perkins (1982). Rosenbrock (1960,1962) was the first to prove, using a Krasovski form of the Lyapunov function, that multiplicity is impossible for the binary case with constant molar flows (neglecting the energy balance). Doherty and Perkins (1982) conclude that multiple steady-states is impossible for single-staged "columns" and for any multistage column separating a binary mixture. Sridhar and Lucia (1989) include the energy balance in the model and conclude under certain assumptions that also in this case binary distillation columns will exhibit unique solutions. They do, however, study only two different sets of specifications (i.e., $Q_D Q_B$ and LB).

In a simulation study Magnussen et.al. (1979) report multiple solutions for a non-ideal mixture of water-ethanol-benzene. The authors do not give any explanation for their results, and the multiplicity was only predicted by the NRTL and UNIQUAC activity coefficient models. Their results have been studied and reproduced in several other simulations (Prokopakis and Seider, 1983; Kovach and Seider, 1987; Venkataraman and Lucia, 1988). The main reason for the multiplicity in this case is the non-ideality in terms of potential liquid-liquid phase split in the mixture (Lucia et al., 1989). Widagdo et.al (1989) report multiplicity for another heterogeneous system.

Chavez et.al. (1986) and Lin et.al. (1987) find multiple steady-state solutions in interlinked distillation columns. The multiplicity they find, however, is due to the interlinking and is not found in single columns.

For the first time, we present examples of multiplicity in distillation columns with ideal thermodynamics. Two fundamentally different types of multiplicity are presented: I) multiplicity in input transformations and II) multiplicity for molar flows.

I. Multiplicity in input transformations. Common for all the studies mentioned above is that the authors have assumed the independent flows (e.g., reflux L and boilup V) to be given on a *molar* basis. In fact, this is not even mentioned as an assumption, but simply taken for granted. The main reason for using molar flows is that they enter directly into the tray material balances and thus determine the separation in the column. In addition, there must have been a belief that using other units for the flows would not alter the fundamental results. However, we believe that in real columns most streams, in particular liquid streams, are *not* given on a molar basis but rather on a mass or volume basis. The transformation from mass or volume flows to molar flow rates depends on the compositions in the column and is nonlinear. As shown in this work, this transformation is singular in some cases, leading to multiplicity and instability even in ideal two-product distillation.

II. Multiplicity for molar inputs. We present results showing that also for specification of molar inputs we may get multiplicity in ideal distillation. The multiplicity is found for specification of molar reflux and boilup and depends on the presence of an energy balance in the model. The interaction between flows and compositions in the column may lead to multiple solutions, one of which is unstable. Also the multiplicity found here may be experienced in real columns as it is the size of the molar flows that determine separation in distillation. This type of multiplicity will in addition be important for simulations since

specifications usually are on a molar basis.

The term "multiplicity" used above refers to the case of *output multiplicity*, that is, when there for a given value of the independent variables (inputs such as reflux and boilup) exists several possible sets of dependent variables (outputs such as product compositions). This is similar to the classical example of multiplicity in exothermic chemical reactors in which two stable and one unstable steady-states exist.

Another kind of multiplicity which is only briefly discussed in this paper is *input multiplicity*. This is when there for a given value of the output exists several possible sets of inputs. It is quite common in chemical engineering, and may occur whenever there is an extremum in the relationship between the input and the output. For example, for multicomponent distillation columns the relationship between product flow and concentration of intermediate component generally has a maximum as will be discussed later. In terms of control, output multiplicity is generally related to poles crossing the imaginary axis (unstable operating points), while input multiplicity is related to zeros crossing through the origin (changes in sign of gain and inverse response). A pole at the imaginary axis corresponds to a singularity in the transfer-function from input to output, while a zero at the imaginary axis corresponds to a singularity in the transfer-function from output to input.

In this paper we shall consider output multiplicity in distillation columns from a steady-state point of view only. The implications for dynamics and control are discussed in another paper (Jacobsen and Skogestad, 1990). We start the paper by considering multiplicity for the case of input units other than molar (Part I). Here, we assume constant molar flows, i.e., we neglect the energy balance. In considering multiplicity for molar inputs (Part II), we include the energy balance in the model. This is a requirement for getting multiple steady-states for molar inputs. Finally we present results for the case when both types of output multiplicity may appear.

Part I. Multiple Steady-States for Mass or Volume Inputs

We consider the simplest case with binary mixtures, constant relative volatility (ideal VLE) and constant molar flows. Similar results are obtained also in columns with more non-ideal behavior.

Rosenbrock (1960, 1962) have shown that multiplicity is impossible in the binary, constant molar flow case, i.e., for a given L and V (molar basis) there exist only one possible steady-state. For example, the top composition $y_D = g(L, V)$ is a unique function of L and V in the constant molar flow case. This also applies if we select as independent variables any other two independent combinations of *molar* flows, for example D and L. However, as discussed below, in real operating columns both flows are almost never specified on a molar basis. In the following we mainly consider the $L_w V$-configuration, with reflux specified on mass basis and with boilup on molar basis. Also discussed is the effect of choosing other flows as independent inputs, for example, the $D_w V$- and LQ_B-

Example	z_F	F	α	N	N_F	M_1	M_2
1. Methanol-Propanol	0.50	1	3.55	8	4	32.04	60.10
2. One-stage column	0.50	1	4.0	1	1	20	40
3. Propanol-Acetic acid	0.50	1	*)	1	1		

- Feed is saturated liquid.
- Total condenser with saturated reflux.

*) α varies in the range 1.85 to 2.25.

Table 2.1: Data for example columns.

configuration. In the latter case the heat input Q_B, which indirectly sets V, is used as an independent variable.

2.2 Introductory Example

Example 1. Data for a methanol-propanol column are given in Table 2.1. The assumption of constant molar flows implies constant vapor and liquid molar flows through the column (except at the feed location). Boilup V is fixed at 2.0 kmol/min and we consider the steady-state solutions with reflux L_w in the range 47 to 55 kg/min. The results are summarized in Table 2.2 and in Figure 2.1. For L_w between 48.8 and 52.2 kg/min there exists three steady-state solutions. For example, with $V = 2.0$ kmol/min and $L_w = 50$ kg/min we get the three steady-states II, III and IV in Table 2.2. With fixed values of L_w and V the solutions on the upper and lower branches on Figure 2.1 are stable, whereas the solutions on the intermediate branch (e.g., steady-state III) are unstable. The reason for this multiplicity is the transformation $L = L_w/M$ between mass and molar reflux. As seen from Figure 2.1 this transformation is not unique for L_w in the region 48.8 and 52.2 kg/min.

	L [kmol/min]	D [kmol/min]	L_w [kg/min]	y_D	x_B
I	1.064	0.936	48.00	0.534	3.10e-3
II	1.143	0.857	50.00	0.584	3.50e-3
III	1.463	0.537	50.00	0.9237	7.60e-3
IV	1.555	0.445	50.00	0.9969	0.104
V	1.650	0.350	53.00	0.9984	0.233

- Constant molar flows.

Table 2.2: Steady-state solutions for methanol-propanol column with V=2.0 kmol/min and L_w in the range 48 to 53 kg/min.

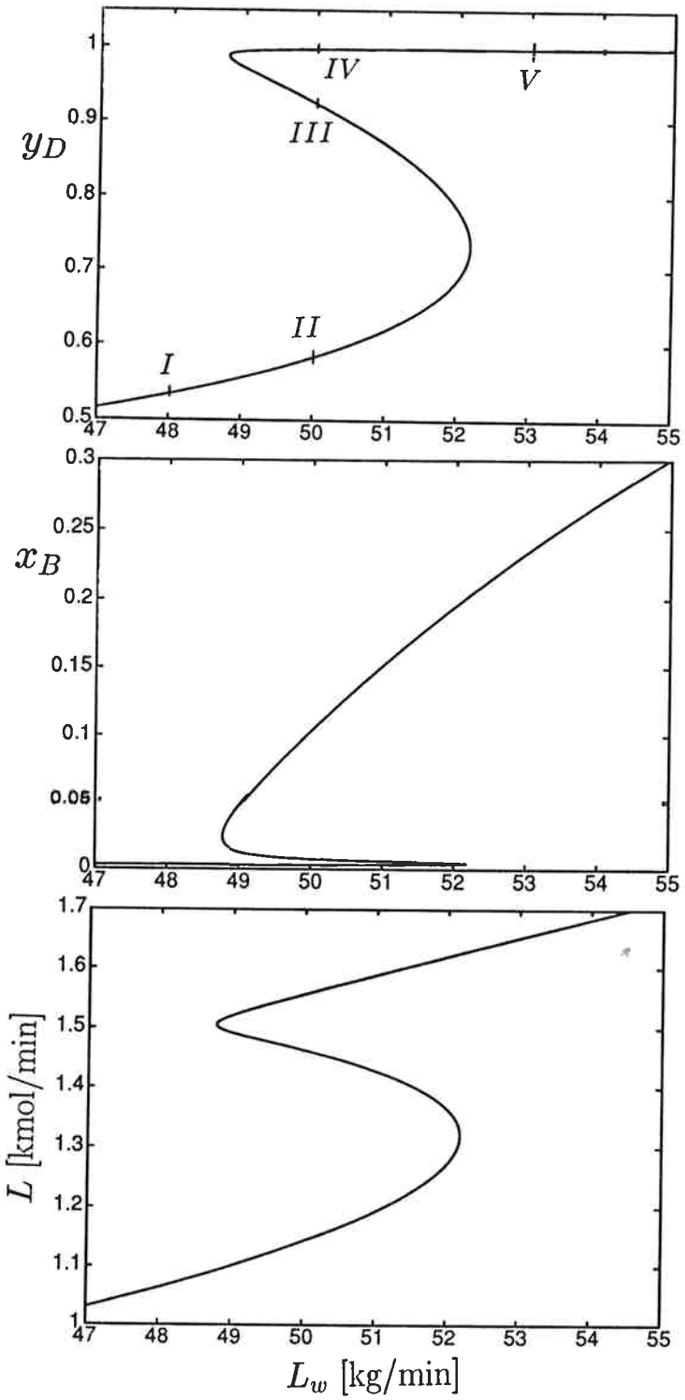

Figure 2.1: Multiple steady-states for mass reflux L_w for the methanol-propanol column assuming constant molar flows. Boilup V=2.0 kmol/min.

2.3 Specification of Flows in Distillation Columns.

We discuss here which units are most often encountered for the flows in distillation columns during operation.

Configurations. Consider the two-product distillation column in Figure 2.2. If the feed to the column is given there are at least four flows that might be specified: reflux L, boilup V, distillate (top product) flow D, and bottoms flow B. However, for a given column there are only two degrees of freedom at steady-state, that is, only two of these flows may be specified independently. A specific choice of two independent flows is denoted as a "configuration". The term comes from process control and is the independent variables from a control point of view. Let n (or no subscript) denote molar flow in kmol/min, w (or as subscript) mass flow in kg/min, q (or as subscript) denote volumetric flow in m^3/min. For example, L is reflux in kmol/min, L_w in kg/min and L_q in m^3/min. Furthermore, v (m/min) is the linear velocity, M (kg/kmol) is the mole weight, ρ (kg/m^3) is the density, and A (m^2) is the cross-sectional area. We have

$$w = Mn = \rho q \tag{2.1}$$

$$q = Mn/\rho = Av \tag{2.2}$$

For example, $L_w = \rho L_q = ML$. The mole weight M is often a strong function of composition (operating point). For liquids, the density ρ is usually a relatively weak function of composition, but the molar volume M/ρ is often a strong function of composition. For gases, the molar volume M/ρ is weakly dependent on composition.

Liquid flows without measurements. In this case, the liquid flow is usually changed either by adjusting a valve position or the power to a pump. In the first case, assume that the pressure drop Δp_V across the valve is constant. Then for turbulent flow $\Delta p_V = \hat{k}(z)\rho v^2 = k(z)qw$ where k is a function of the valve position z. That is, fixing the valve position is the same as fixing the geometric average of mass and volumetric flow rate, $\sqrt{qw}$. In the second case, assume that the pressure drop across the pump Δp_p is fixed. The power is given by $P = \Delta p_p q$ and fixing the power is the same as fixing the volumetric flow rate q. In both cases it is most natural to specify the flow on a volumetric or mass basis (as noted above these are usually not too different). In the special case, if a partial condenser is used, then the reflux may be given indirectly by the cooling duty and it may be reasonable to assume reflux to be given on a molar basis.

Liquid flows with measurements. In many cases, the valve position or pump power is adjusted to keep the *measured* value of the flow constant. Most liquid flow measurements are on a mass or volumetric basis (or mixed). For example, the flow is often inferred by measuring the pressure drop over a fixed restriction in a pipe, such as an orifice or venturi. As noted above, the pressure drop is proportional to the product qw, and hence one gets a measure of the geometric average of the mass and volumetric flow rate. Other measuring devices give a direct measure of volumetric flow rate q, such as displacement meters, turbine meters and magnetic meters. Direct measurements of mass flow rates also exist. However, for liquids no direct measurement of molar flow rate is in common use.

Boilup V. This is a vapor flow. However, usually the amount of boilup is given indirectly by the heat input Q_B to the reboiler. An energy balance around the reboiler

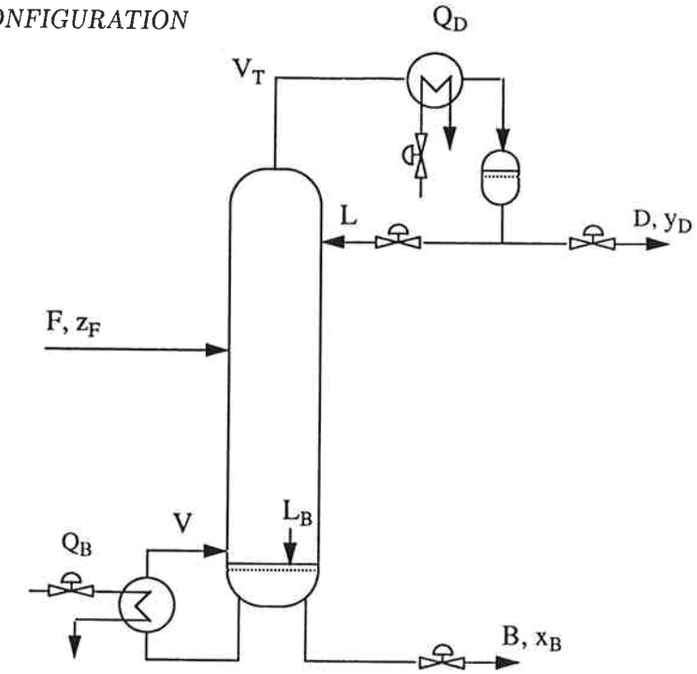

Figure 2.2: Two product distillation column.

gives

$$Q_B = V(H_1^V - H_2^L) + B(H_1^L - H_2^L) \tag{2.3}$$

where H_i^V and H_i^L are the molar enthalpies on tray i of the vapor and liquid phases, respectively. Neglecting changes in the liquid enthalpy yields

$$Q_B \approx V(H_1^V - H^L) = V\Delta H_1^{vap} \tag{2.4}$$

where ΔH_1^{vap} is the heat of vaporization in the reboiler. In many cases ΔH_1^{vap} is only weakly dependent on composition and specifying Q_B is almost the same as fixing the molar boilup V. However, for widely different components or strongly nonideal systems, this may not be the case.

Therefore, it can be summarized that:

- For liquids, it is most natural to specify the flow rate on a volumetric or mass basis. In a distillation column, L, D and B are usually liquids.
- It seems reasonable in many cases to assume the boilup V to be given on a molar basis.

2.4 L_wV-Configuration

This choice of independent variables is very common industrially, and the introductory example showed that it may display multiple steady-states. Consider the simplest case

with a binary separation, and let subscript 1 denote the most volatile ("light") component and 2 the least volatile component. The transformation between mass and molar reflux is given by:

$$L = L_w/M; \quad M = y_D M_1 + (1 - y_D)M_2 \tag{2.5}$$

where M_i is the molecular weight of the individual components. We might expect L to increase uniformly with L_w, that is, $dL/dL_w > 0$ such that an increase in the mass reflux L_w will always increase the molar flow L. However, because M is a function of composition (y_D) and thereby of L_w this may not be the case. Assume that the molar boilup V is fixed, and differentiate both sides of $L_w = LM$ with respect to L

$$\left(\frac{\partial L_w}{\partial L}\right)_V = M + L(M_1 - M_2)\left(\frac{\partial y_D}{\partial L}\right)_V \tag{2.6}$$

A possible negative slope, $(\partial L_w/\partial L)_V < 0$, will correspond to an unstable operating point and is explained by two opposing effects. Since these effects have different time constants, it is most instructive to consider the dynamic response (although we are here interested in the steady-state effect). Consider an increase in L. Initially, $L_w = LM$ always increases because M is unchanged. However, as a result of the increase in L, the fraction of light component will start increasing (see Appendix 2) and hence M will change. If $M_2 > M_1$ (which is usually the case), M will decrease and the resulting decrease in L_w may eventually offset the initial increase. Note that multiple steady-states and instability will not occur for the L_wV-configuration when $M_2 < M_1$.

The instability may be explained physically as follows: Assume $M_2 > M_1$ and that L_w and V are constant. The column is perturbed slightly such that y_D increases by Δy_{D1}. This reduces M and thus increases L by $\Delta L_1 = (\partial L/\partial y_D)_{L_w}\Delta y_{D1}$. The increased L will subsequently increase y_D even more. If this second increase $\Delta y_{D2} = (\partial y_D/\partial L)_V \Delta L_1$ is larger than the initial perturbation Δy_{D1}, then the column will start drifting away and we have instability. The condition for instability then becomes $\Delta y_{D2} > \Delta y_{D1}$ or

$$\left(\frac{\partial y_D}{\partial L}\right)_V \left(\frac{\partial L}{\partial y_D}\right)_{L_w} > 1 \tag{2.7}$$

which may shown to be equivalent to having a negative slope in (2.6). Note that this derivation is not rigorous as it is based on steady-state arguments only. A more detailed analysis using dynamics is given in Jacobsen and Skogestad (1990).

The fact that an operating point is unstable does not necessarily imply that there exists another stable operating point for the same values of L_w and V (see Figure 2.4). For example, if L starts increasing as discussed above, it may reach a point where the specified value of L_w corresponds to a $L > V_T$. This is impossible as it would drain the condenser or require a negative distillate flow D. In practice, the operator would then have to increase V or reduce L_w. However, as shown in the introductory example, there does exist cases where multiple steady-states exist for a given L_w and V. This happens when there for the given V exist points (values of L_w) where the transformation from L_w to L is singular (i.e., $\partial L/\partial L_w = \infty$ or $\partial L_w/\partial L = 0$ in (2.6)).

2.4.1 Analytical treatment

To understand the characteristics of columns in which multiplicity and instability are most likely to occur, the ideal case with constant molar flows and constant relative volatility is considered. From (2.6) we know that for binary separations instability occurs at operating points where

$$y_D + L\left(\frac{\partial y_D}{\partial L}\right)_V > \frac{M_2}{M_2 - M_1} \tag{2.8}$$

Here we have assumed $M_2 > M_1$ which is a necessary condition for instability for this configuration. To understand the implications of condition (2.8), we need an analytical expression for the gain $(\partial y_D/\partial L)_V$. We shall consider a one-stage column where exact expressions are easily derived, and subsequently a multistage column where good approximations exist.

One-stage column

Example 2. Consider the simple column in Figure 2.3 with one theoretical stage (the reboiler) and a total condenser. This is the simplest column for which the instability and multiplicity may be observed. Of course, such a column will never be operated in practice because the reflux is simply wasting energy and has no effect on separation. The following equations apply

$$Fz_F = Dy_D + Bx_B \tag{2.9}$$

$$D = V - L; \quad B = L + F - V \tag{2.10}$$

$$\alpha = \frac{y_D(1 - x_B)}{(1 - y_D)x_B} \tag{2.11}$$

$$L_w = LM; \quad M = y_D M_1 + (1 - y_D)M_2 \tag{2.12}$$

Let $\alpha = 4.0, z_F = 0.5, M_1 = 20$ kg/kmol and $M_2 = 40$ kg/kmol. Consider a nominal operating point with $V = 4.7$ kmol/min and $L = 4.2$ kmol/min. From (2.9)-(2.12) we get $D = B = 0.5$ kmol/min, $x_B = 0.33, y_D = 0.67$ and $L_w = 112$ kg/min. However, this is not the only possible steady-state with $V = 4.7$ kmol/min and $L_w = 112$ kg/min. Table 2.3 shows that there exist two other solutions with $y_D = 0.56$ and $y_D = 0.76$, respectively. The results are shown graphically in Figure 2.4 b). Note that the nominal steady-state with y_D=0.67 is in the region where the relationship between L_w and L has a negative slope and thus is unstable with V and L_w as independent variables.

The effect of increasing the internal flows is illustrated by Figure 2.4 c) where V has been increased from 4.7 to 7.0 kmol/min. Here the relationship between L and L_w has a negative slope over the entire region. The two stable branches have disappeared and we have only one *unstable* solution for any given L_w. On the other hand, for low values of the internal flows there exists only one *stable* solution. This is illustrated by Figure 2.4 a) where $V = 4.0$ kmol/min.

Differentiating (2.9)-(2.11) yields the following exact expression for the gain

$$\left(\frac{\partial y_D}{\partial L}\right)_V = \frac{(1 - y_D)y_D(y_D - x_B)}{Bx_B(1 - x_B) + Dy_D(1 - y_D)} \tag{2.13}$$

L [kmol/min]	D [kmol/min]	L_w [kg/min]	y_D
3.7	1.0	111.00	0.500
3.9	0.8	112.01	0.564
4.2	0.5	112.00	0.667
4.5	0.2	111.99	0.756
4.7	0.0	112.80	0.800

Table 2.3: Steady-state solutions for one-stage column with $V = 4.7$ kmol/min and L in the range 3.7 to 4.7 kmol/min.

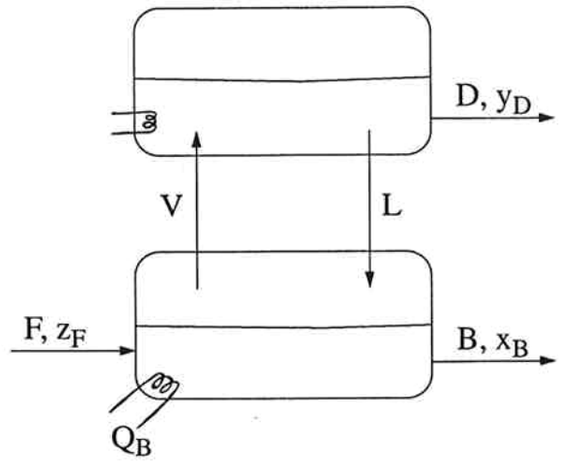

Figure 2.3: One-stage column with total condenser.

Condition (2.8) for instability then becomes

$$y_D + L\frac{(1-y_D)y_D(y_D-x_B)}{Bx_B(1-x_B)+Dy_D(1-y_D)} > \frac{M_2}{M_2-M_1} \tag{2.14}$$

The gain (2.13) varies only moderately with operating conditions for a single-stage column. Thus, we conclude from (2.14) that any operating point may be unstable with the L_wV-configuration, provided the internal flows (L) are sufficiently large.

To test stability of the nominal operating point in Example 2, let $D = B = 0.5, x_B = 0.33, y_D = 0.67, M_2/(M_2 - M_1) = 2$ and derive from (2.14) the instability condition $L > 4.0$. Since we have L=4.2 the operating point is unstable.

Multistage column

Somewhat surprisingly, the analytical results for the one-stage column carry over almost directly to the multistage case. For example, expression (2.13) for the gain $(\partial y_D/\partial \mathrm{L})_V$ is a

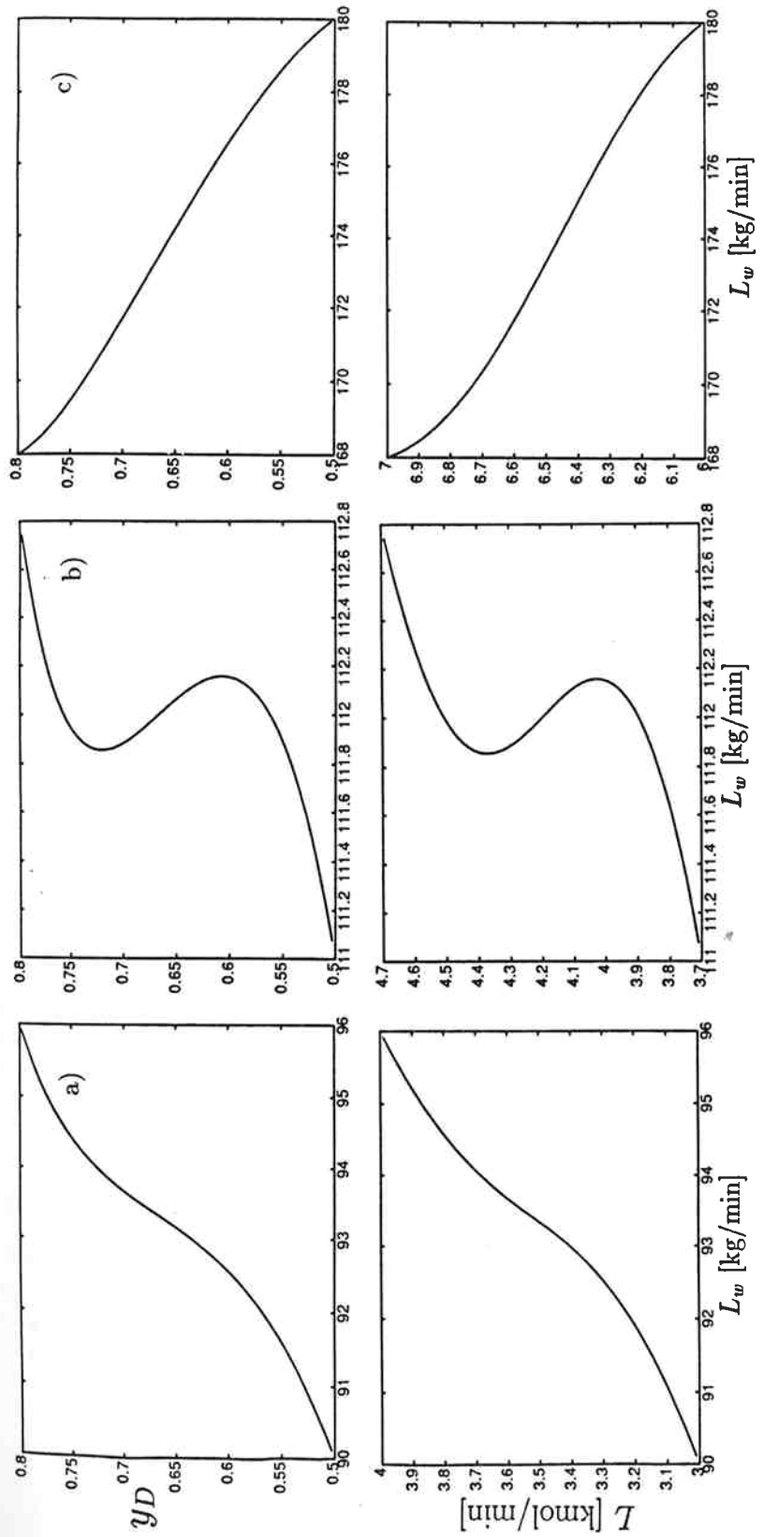

Figure 2.4: Steady-state solutions as a function of mass reflux L_w for one-stage column with $\alpha = 4$.a) $V = 4.0$ kmol/min - Unique stable solution. b) $V = 4.7$ kmol/min - Multiple solutions. c) $V = 7.0$ kmol/min - Unique unstable solution.

good approximation for multistage columns with constant relative volatility and constant molar flows (e.g., Skogestad and Morari, 1987b). The reason is that the overall separation factor

$$S = \frac{y_D(1-x_B)}{(1-y_D)x_B} \tag{2.15}$$

usually does not change very much with operating conditions and may be assumed constant when estimating the gain (for a one-stage column the separation factor is equal to the relative volatility α). Equation (2.15) then takes the place of (2.11), and assuming S constant yields the same expression for the gain as for the one-stage column. [The exact expression when S is not constant is

$$\left(\frac{\partial y_D}{\partial L}\right)_V = \frac{(1-y_D)y_D(y_D-x_B)}{Bx_B(1-x_B)+Dy_D(1-y_D)}\left(1+\frac{Bx_B(1-x_B)}{y_D-x_B}\left(\frac{\partial \ln S}{\partial L}\right)_V\right) \tag{2.16}$$

The only assumption made here is the one of constant molar flows such that (2.10) applies. Equation (2.16) shows that the effect of changes in S on the gain is always negligible when the bottom product is pure, i.e., $x_B \approx 0$.]

The main difference from the single-stage case is that in a multistage column the compositions and the gain (2.13) may change drastically with operating conditions. To study this effect consider the following three cases:

I) Top impure, bottom pure ($x_B \ll (1-y_D)$). Equation (2.13) is simplified to:

$$\left(\frac{\partial y_D}{\partial L}\right)_V \approx \frac{y_D - x_B}{D} \approx \frac{y_D}{D} \tag{2.17}$$

II) Equal purity in top and bottom ($x_B \approx (1-y_D)$). Equation (2.13) is simplified to:

$$\left(\frac{\partial y_D}{\partial L}\right)_V \approx \frac{y_D - x_B}{F} \approx \frac{1}{F} \tag{2.18}$$

III) Top pure, bottom impure ($x_B >> (1-y_D)$). Equation (2.13) is simplified to:

$$\left(\frac{\partial y_D}{\partial L}\right)_V \approx \frac{1-y_D}{Bx_B} \approx 0 \tag{2.19}$$

Recall the instability condition (2.8). We conclude that instability is unlikely in case *III*, when the top product is pure relative to the bottom product. The approximate condition for instability in case *I* when the bottom product is pure ($x_B \approx 0$) becomes

$$y_D(1+L/D) > \frac{M_2}{M_2 - M_1} \tag{2.20}$$

From this derivation we conclude that instability with the L_wV-configuration is most likely to be observed in the following cases: 1) Bottom product relatively pure ($x_B \ll (1-y_D)$), 2) molecular weight of light component much smaller than of heavy component, and 3) L/D large. We note that any column with $M_1 < M_2$ may become unstable with sufficiently large L/D.

In practice, conditions 2) and 3) often are not satisfied at the same time. First, large values of L/D should be used only for difficult separations (α close to one) which usually involve components with similar molecular weights. Second, columns with large values of L/D (greater than five according to Luyben, 1979) usually are not operated with the L_wV-configuration at all. The reason usually given for this is that controlling the condenser level with a small stream is difficult, and reflux L should be used for level control whenever L/D is large. While this argument certainly is true, it is also possible that open-loop instability of the L_wV-configuration may have caused the poor observed behavior.

2.5 Other Configurations

2.5.1 D_wV-configuration

We have

$$D = D_w/M \tag{2.21}$$

where M is defined by (2.5). Differentiation yields the following condition for instability

$$\left(\frac{\partial D_w}{\partial D}\right)_V = M + D(M_1 - M_2)\left(\frac{\partial y_D}{\partial D}\right)_V < 0 \tag{2.22}$$

Note that the condition for instability is almost independent of the size of the internal flows. Since $(\partial y_D/\partial D)_V$ is essentially always negative (Appendix 1), we see from (2.22) that a necessary condition for instability or singularity is that $M_1 > M_2$, i.e. the most volatile component must have the largest molecular weight. This implies that we have the opposite case as compared to the L_wV-configuration. Thus, non-uniqueness and instability in a given operating point with the L_wV-configuration is avoided by using the D_wV-configuration instead. During operation, this is accomplished by changing condenser level control from using distillate to using reflux.

In fact, it seems very unlikely that multiple steady-states or instability may ever occur for this configuration: Consider the case $M_1 > M_2$. As we have no multiplicity for the *molar* DV-configuration (Doherty and Perkins, 1982) the gains $(\partial y_D/\partial D)_V$ and $(\partial x_B/\partial D)_V$ are negative (see Appendix 1). An analysis of the differentiated component material balance (2.9) then gives $(\partial y_D/\partial D)_V > -y_D/D$. For the worst case with $(\partial y_D/\partial D)_V = -y_D/D$ the condition for instability (2.22) becomes $M_2 < 0$ which of course is impossible.

2.5.2 LQ_B-configuration

We have assumed the boilup to be measured on a molar basis. However, as discussed previously, the boilup will often be set indirectly by the amount of heat input, Q_B, to the reboiler. The energy balance for the reboiler when liquid enthalpy changes are neglected yields (2.4)

$$V \approx Q_B/\Delta H^{vap}(x_B) \tag{2.23}$$

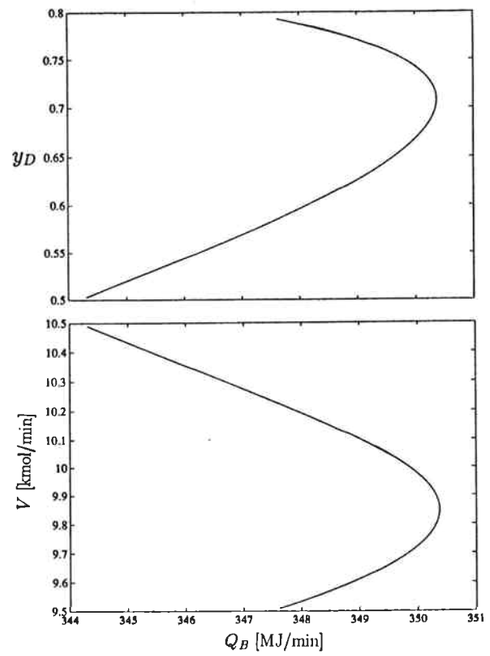

Figure 2.5: Multiple steady-states for heat input Q_B for one-stage propanol-acetic acid column. Reflux $L = 9.5$ kmol/min

Here we have indicated that the heat of vaporization, ΔH^{vap}, in general depends on the composition in the reboiler, x_B. Note the similarity between this transformation and the transformation $L = L_w/M(y_D)$ studied above. For simplicity assume reflux to be kept constant on a molar basis, and consider a binary mixture where x_B is the mole fraction of light component. The differential of Q_B with respect to V becomes

$$\left(\frac{\partial Q_B}{\partial V}\right)_L = \Delta H^{vap} + V\frac{d\Delta H^{vap}}{dx_B}\left(\frac{\partial x_B}{\partial V}\right)_L \tag{2.24}$$

and we have instability if this slope is negative. For constant molar flows $(\partial x_B/\partial V)_L$ is always negative (Appendix 2), and we see from (2.24) that a necessary condition for instability or singularity is that $d\Delta H^{vap}/dx_B > 0$ for the actual value of x_B. This is not too common in practice. It will be the case when the lightest component has the largest heat of vaporization, but may also happen for non-ideal systems where this is not the case.

A similar analysis as for the L_wV-configuration shows that instability is most likely for the LQ_B-configuration when the internal flows are large and when the bottom product is relatively unpure.

Example 3. One-Stage propanol-acetic acid column. Propanol is the more volatile component and the relative volatility, α, is in the range 1.85 to 2.25. The heat of vaporizations are 41.2 kJ/mol for propanol and 23.7 kJ/mol for acetic acid, implying that multiplicity is possible. In this example we use the exact energy balance (2.3), and the Van Laar activity coefficient model the vapor-liquid equilibrium. Consider a nominal operating point with reflux $L = 9.5$ kmol/min and boilup $Q_B = 349$ MJ/min. We obtain two steady-state solutions for these specifications: 1) $y_D = 0.596$ and 2) $y_D = 0.787$. If we could allow for negative product flows, we would get three solutions. Solution 1 is unstable while solution 2 is stable. The multiplicity is illustrated graphically in Figure 2.5.

2.5.3 Other cases

As seen from the above, possible singularities in the transformation of streams depends on the choice of configuration, or in terms of steady-state simulation, the specification of flows. Singularity occurs when $\partial w/\partial n$ is zero. For liquid flows we conclude that singularity may occur for reflux L_w and bottoms product B_w when $M_2 > M_1$, while distillate D_w and boilup V_w require the opposite, i.e., $M_1 > M_2$. This is easily seen from the sign of the respective gains (Appendix 1 and 2). However, as noted above, singularity seems unlikely to occur for D_w or B_w. For ratio inputs, singularities are also unlikely in most cases. For example, (L/D) is independent of composition provided the column has a total condenser and L and D are measured in the same units.

Part II. Multiple Steady-States for Molar Inputs

We have discussed the multiplicity resulting from the use of input units other than molar. In Part II, we consider the multiplicity that may occur when molar reflux and boilup are used as specifications (i.e., LV-configuration). This type of multiplicity does not occur for the case of constant molar flows, and thus depends on the energy balance.

2.6 LV-Configuration

Example 1, continued. We will continue to study the methanol-propanol column in Table 2.1. We now include an energy balance on each tray where we previously assumed constant molar flows (see Table 2.4):

$$Q_i + V_{i-1}H^V_{i-1} + L_{i+1}H^L_{i+1} - V_iH^V_i - L_iH^L_i + F_iH^F_i = 0 \tag{2.25}$$

Here subscript i denotes tray number (trays are numbered from the bottom). We assume constant relative volatility as before, while enthalpies are computed from the equations given in Table 2.4.

$H_i^L = 16.67e^{-1.087x_i}$
$H_i^V = 13.49e^{-3.98x_i} + 43.97e^{-0.088x_i}$

- Reference state: Pure components as liquid at $0°C$.
- x_i denotes mole fraction methanol in liquid phase.

Table 2.4: Saturated molar enthalpies (kJ/mol) for methanol-propanol system at a pressure of 1 atm.

	L [kmol/min]	D [kmol/min]	y_D	x_B
I	4.60	0.535	0.9324	2.474e-3
II	4.70	0.505	0.9845	6.344e-3
III	4.70	0.406	0.9993	0.1587
IV	4.70	0.0866	0.9997	0.4526

- The energy balance is included in the model.

Table 2.5: Steady-state solutions for methanol-propanol column with boilup V=4.5 kmol/min.

Molar boilup V is kept constant constant at 4.5 kmol/min and we consider solutions for *molar* reflux between 4.6 and 4.75 kmol/min. Some solutions are given in Table 2.5. From the table we see that for L = 4.70 kmol/min we get the three solutions II, III and IV. Solution III is found to be unstable. The multiplicity is graphically illustrated in Figure 2.6.

Similar results were obtained with commercial simulators using consistent thermodynamic data for VLE and enthalpy (e.g., SRK equation of state) which satisfy the Gibbs-Duhem equation.

Analytical Treatment. The example above shows that we may have multiplicity for the LV-configuration, even in ideal binary distillation. To understand the source of the multiplicity, the transformation between the DV-configuration, which yields unique solutions in terms of compositions in all examples studied, and the LV-configuration is examined.

Consider the gain $(\partial y_D/\partial L)_V$. This gain is usually positive, but as seen above (Figure 2.6) it may be negative in some cases, and the operating point will then be unstable. We have

$$\left(\frac{\partial y_D}{\partial L}\right)_V = \left(\frac{\partial y_D}{\partial D}\right)_V \left(\frac{\partial D}{\partial L}\right)_V \tag{2.26}$$

where the gain $(\partial y_D/\partial D)_V$ is essentially always negative (Appendix 1). For constant molar flows $(\partial D/\partial L)_V = -1$ and $(\partial y_D/\partial L)_V$ is positive. However, due to the energy

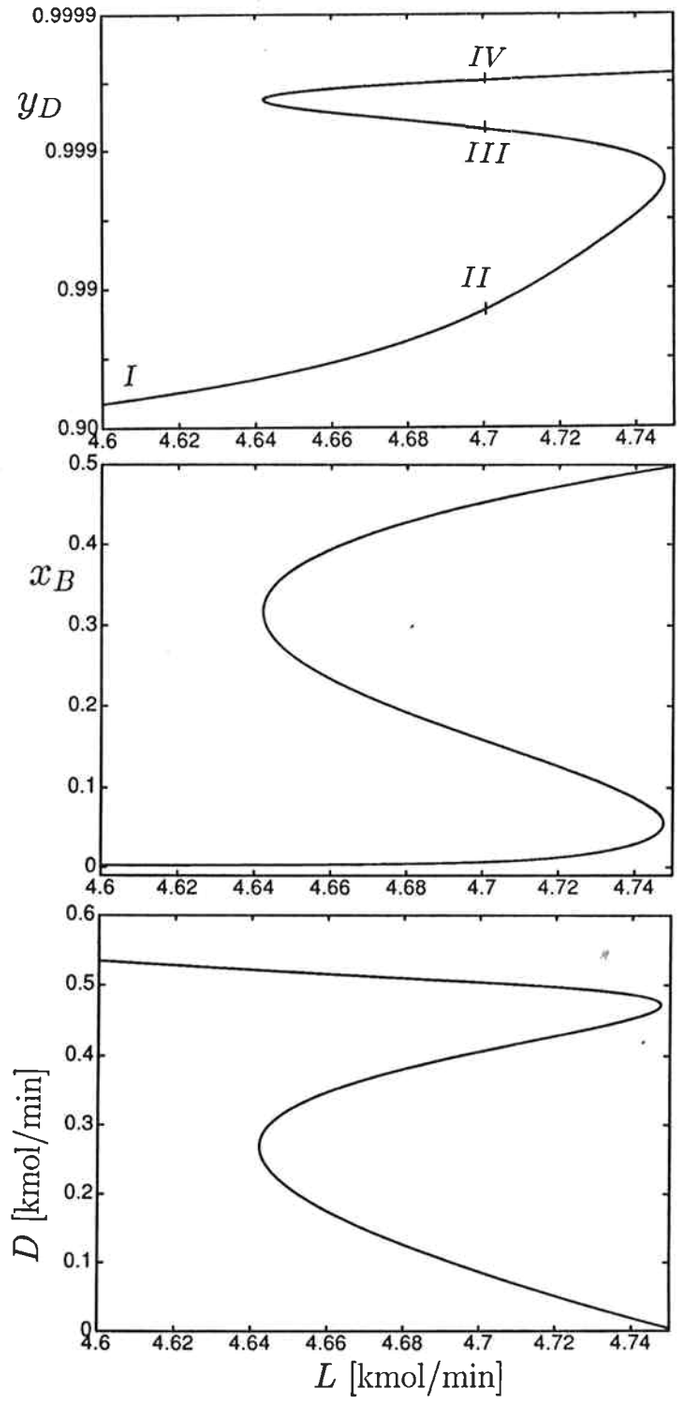

Figure 2.6: Multiple steady-states for molar reflux L for methanol-propanol column. Boilup V=4.5 kmol/min. Energy balance included.

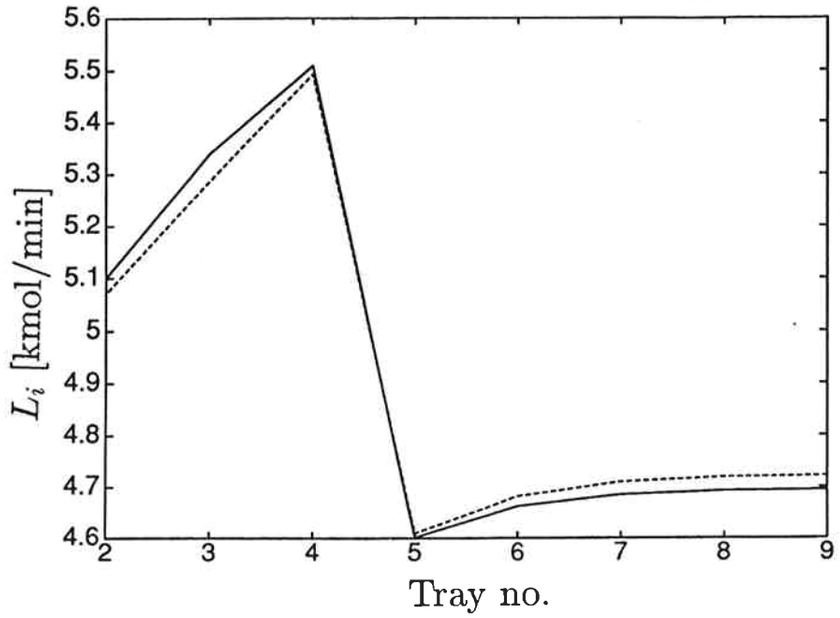

Figure 2.7: Liquid flow profiles for two molar refluxes in the unstable region of the methanol-propanol column. Boilup V=4.5 kmol/min. (—— original, - - - - after increase in L). Energy balance included.

balance, the flows inside the column depend on the compositions and instability occurs if

$$\left(\frac{\partial D}{\partial L}\right)_V > 0 \tag{2.27}$$

Using the material balances around the condenser ($V_T = L + D$) and around the column interior ($L + V = L_B + V_T$) yields

$$\left(\frac{\partial D}{\partial L}\right)_V = -1 + \left(\frac{\partial V_T}{\partial L}\right)_V = -\left(\frac{\partial L_B}{\partial L}\right)_V \tag{2.28}$$

and (2.27) is equivalent to

$$\left(\frac{\partial L_B}{\partial L}\right)_V < 0 \tag{2.29}$$

Here V_T denotes vapor flow from top tray to the condenser, and L_B is liquid flow from bottom tray to the reboiler. This means that in the unstable region an increase in reflux will result in a decrease in liquid flows in the lower part of the column. This is illustrated in Figure 2.7 where we have plotted two liquid flow profiles in the unstable region for the methanol-propanol column.

Neglecting changes in liquid enthalpy with composition yields the following relationship between boilup V and vapor flow from top tray V_T (saturated liquid feed)

$$V_T = \frac{\Delta H_1^{vap}}{\Delta H_T^{vap}} V \tag{2.30}$$

The instability condition (2.27) is equivalent to

$$\left(\frac{\partial L}{\partial D}\right)_V = -1 + \left(\frac{\partial V_T}{\partial D}\right)_V > 0 \tag{2.31}$$

and we get

$$\left(\frac{\partial L}{\partial D}\right)_V = -1 + \frac{\left(\frac{d\Delta H^{vap}}{dx}\right)_{x=x_B}\left(\frac{\partial x_B}{\partial D}\right)_V \Delta H_T^{vap} - \left(\frac{d\Delta H^{vap}}{dx}\right)_{x=x_T}\left(\frac{\partial x_T}{\partial D}\right)_V \Delta H_1^{vap}}{(\Delta H_T^{vap})^2} V \tag{2.32}$$

Assuming no multiplicity for the DV-configuration implies that $\left(\frac{\partial x_i}{\partial D}\right)_V$ always will be negative (Appendix 1). Furthermore, in most systems $\left(\frac{d\Delta H^{vap}}{dx}\right)$ will be negative, that is, the heat of vaporization decreases with fraction of most volatile component. From (2.32) we see that in this case instability will be most likely when the magnitude of $\left(\frac{\partial x_B}{\partial D}\right)_V$ is large and the magnitude of $\left(\frac{\partial x_T}{\partial D}\right)_V$ is small. This will happen when we have high purity in the top and a relatively unpure bottom product. This agrees with the results found for the methanol-propanol column (Table 2.5 and Figure 2.6), where instability was found for top composition between 0.9984 and 0.9996, and bottom composition between 0.3152 and 0.0580. In the case where $\left(\frac{d\Delta H^{vap}}{dx}\right)$ is positive, instability will be most likely when the bottom product is pure while the top product is relatively unpure. We also see from (2.32) that instability is favored by high internal flows (i.e., large V).

Similar relations are obtained when considering changes in molar boilup. In this case, the transformation between the LB- and LV-configuration is considered. Instability is equivalent to

$$\left(\frac{\partial V_T}{\partial V}\right)_L < 0 \tag{2.33}$$

We conclude that the multiplicity found for the LV- configuration is due to the interactions between flows and compositions in the column. The flows affect compositions through the material balance, while compositions will affect the flows through the energy balance. In some regions this interaction leads to an inversed gain in compositions compared to what we find for constant molar flows (e.g., $\left(\frac{\partial y_D}{\partial L}\right)_V < 0$) and we get multiple steady-state solutions, one of which is unstable. Rademaker et.al. (1975) claim that the influence of compositions on flow rates usually will be negligible. The results we present here show that the influence in many cases will be crucial, leading even to inversed gains and instability in some cases.

2.7 Combination of Mass Inputs and Energy Balance

The two types of multiplicity discussed may occur in the same region of operation for a column. Consider the L_wV-configuration. We have

$$\left(\frac{\partial y_D}{\partial L_w}\right)_V = \left(\frac{\partial y_D}{\partial L}\right)_V \left(\frac{\partial L}{\partial L_w}\right)_V \tag{2.34}$$

Instability (negative slope between L_w and y_D) occurs whenever one of the elements on the right hand side of (2.34) is negative: I) there is a negative slope between molar reflux and mass reflux, or II) there is a negative slope between molar reflux and top composition. Equation (2.34) indicates that there may be a positive slope between mass reflux L_w and top composition y_D if both I and II occur at the same time. However, equation (2.6) for the case $M_2 > M_1$ shows that when $\left(\frac{\partial y_D}{\partial L}\right)_V$ is negative, neither singularity nor negative slope exists between mass and molar reflux. This implies that the instability for the molar reflux usually is preserved when using mass reflux.

Example 1, continued. Figure 2.8 a) shows solutions for the methanol-propanol column using the L_wV-configuration with the energy balance included. Mass reflux is in the range 57 to 60 kg/min while keeping molar boilup at 2.0 kmol/min. Compared to Figure 2.1 which shows the corresponding results for the case of constant molar flows, we see that the range of multiplicity in terms of mass reflux becomes narrower. The reason is that with the energy balance included we get a larger value of $(\partial y_D/\partial L)_V$ in the region of interest. Note that for this value of boilup there is no multiplicity between *molar* reflux L and top composition y_D, i.e., $(\partial y_D/\partial L)_V > 0$.

Figure 2.8 b) shows solutions with mass-reflux in the range 95 kg/min to 103 kg/min while keeping boilup at 3.0 kmol/min. We now have two regions of multiplicity, and due to a partial overlap we get four solutions for mass reflux in the range 95.75 to 96.2 kg/min. If we allowed for negative product flows, we would get five solutions as the lower branch would also overlap. The two lower singular points are caused by a multiplicity between mass reflux L_w and molar reflux L, while the two upper singular points (high purity in top) are caused by a multiplicity between molar reflux L and top composition y_D. This may be seen from the plot of mass reflux versus molar reflux in Figure 2.8 b). The analysis presented earlier in the paper showed that mass-flow instability (type I) is most likely with relatively low purity in the top, while molar flow instability (type II) is most likely with relatively high purity in the top. The results in this example support this analysis.

2.8 Discussion

Global stability. We have derived conditions such as (2.8) to check the local stability of a certain operating point. However, it is not easy to tell if it is globally stable, that is, if it is at a point where we have uniqueness. For Example 1 (Table 2.2), it is easily shown with the use of (2.8) that operating point III is unstable and operating points I, II, IV and V are (locally) stable. It is clear from Figure 2.1 that operating points I and V are globally stable (with the given L_w and V), whereas II and IV are not. However, there exists no simple method to check this directly. To do this analytically one would have to apply some kind of Lyapunov function to the dynamic model, which is not at all straightforward due to the high order and complexity of a dynamic model of a distillation column. In fact, the easiest way to check for global stability is to obtain solutions in the whole range of operation specifying one input and one composition (e.g., boilup V and top composition y_D) in a steady-state simulator and then generate a figure similar to Figure 2.1.

Subcooling. We have not discussed all issues that may be important for multiplicity

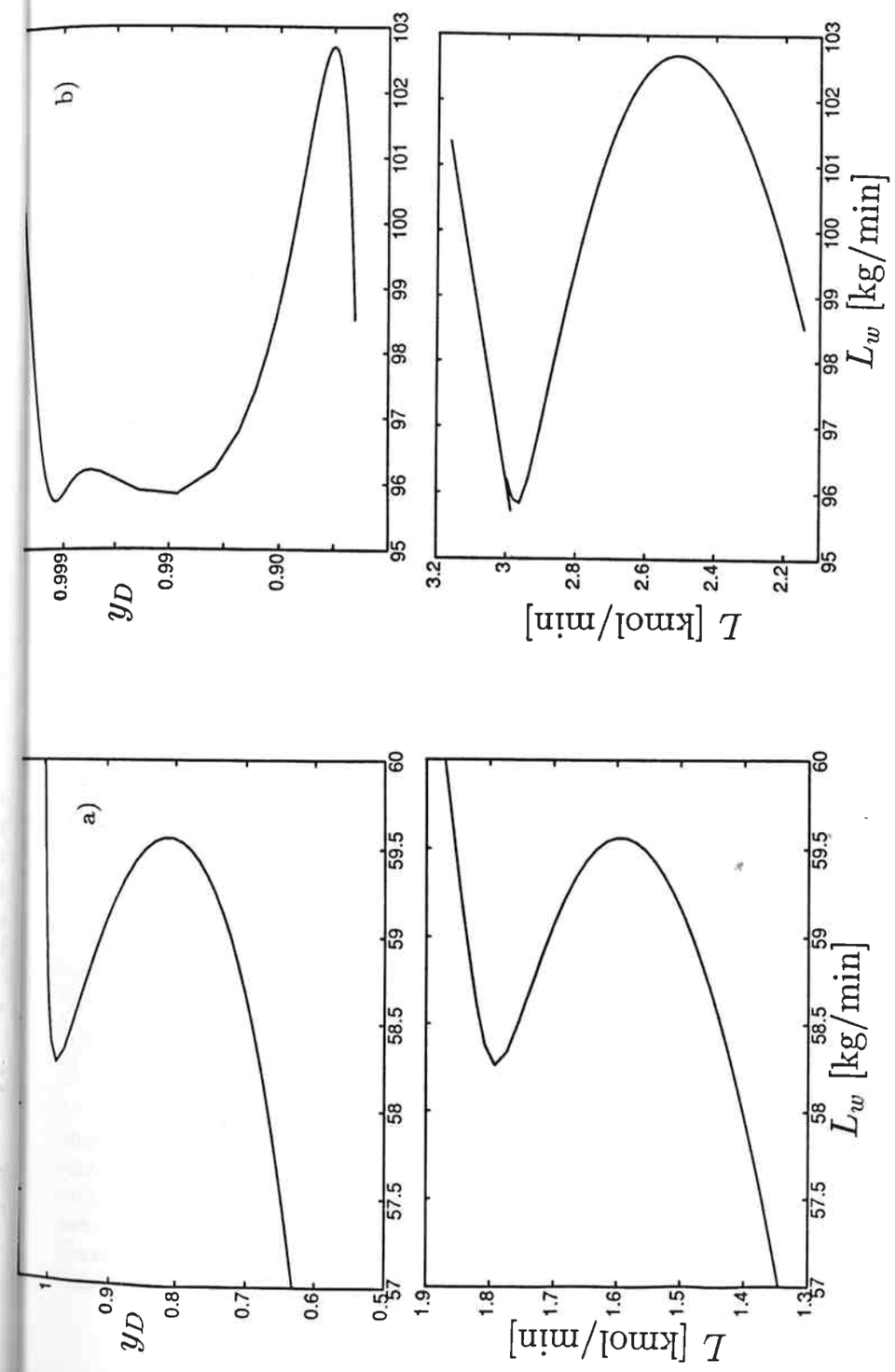

Figure 2.8: Multiple steady-states for mass-reflux L_w for methanol-propanol column with energy balance included in model. a) Boilup V=2.0 kmol/min. b) Boilup V=3.0 kmol/min.

and instability in distillation. For instance, subcooling of the reflux may be important as the degree of subcooling may depend on the temperature and thereby on composition. The separation in the column is determined by the effective reflux $L_{eff} > L$ which takes into account the additional internal reflux caused by subcooling. The degree of subcooling will usually decrease as y_D increases because the top part of the column cools down. With subcooling the second term in (2.7) is therefore reduced in magnitude, and we conclude that subcooling makes instability somewhat less likely for the L_wV-configuration.

Multicomponent mixtures. Introducing additional non-key components will generally make multiplicity and instability less probable. The reason is that the "dead weight" of the non-key components generally will reduce the effect of changes in the compositions of the key components on mole weight, M, and heat of vaporization, ΔH^{vap}.

Volume basis. We have not discussed volume inputs in particular, but the results obtained for mass inputs will in general apply to the volume case. For the case with ideal mixing we need only substitute the molecular weights with the molar volumes in the equations presented. For example, consider the L_qV-configuration. Similar to the mass case, $V_2 > V_1$ is necessary for instability, and in this case the instability condition becomes

$$y_D + L\left(\frac{\partial y_D}{\partial L}\right)_V > \frac{V_2}{V_2 - V_1} \tag{2.35}$$

For most mixtures, the difference in densities between the components are small, and very similar results will be obtained for volume inputs as those found for mass-inputs. For the methanol-propanol example, we have a density of methanol of 795 kg/m^3 and a density of propanol of 806 kg/m^3 at normal conditions, and the results for volume inputs would be almost identical to what is found for mass inputs. For non-ideal mixtures, the volume of mixing must also be accounted for.

Instability during industrial operation. As we have discussed above, instability for the L_wV-configuration is likely to occur during operation if the reflux is large. Since the L_wV-configuration is commonly used in the industry, it is surprising that there has been no previous experimental reports of instability. One possible reason is that multiplicity and instability always have been believed to be impossible in distillation, and consequently observations of instability during operation have been explained in other ways.

During operation the presence of instability and multiple steady-states with the L_wV-configuration may be observed as follows:

- A column may easily be operated at an unstable operating point by use of feedback, for example, by adjusting L_w such that a tray temperature is kept constant. The operating point is (open-loop) unstable if one observes that the steady-state effect of an increase in purity in the top is to decrease L_w. If this column is switched to a manual mode, instability will occur.

- Multiple steady-states may be observed when a column is operated with constant L_w and V (manual control) close to a singular point. A small upset to the column may bring the column past the singular point, and one will observe catastrophic behavior as the entire column profile is changed when the column moves to its new steady-state on another branch (Figure 2.9). Hysteresis may also be experienced during operation, that is, if one takes an input (e.g., L_w) through a singular point the

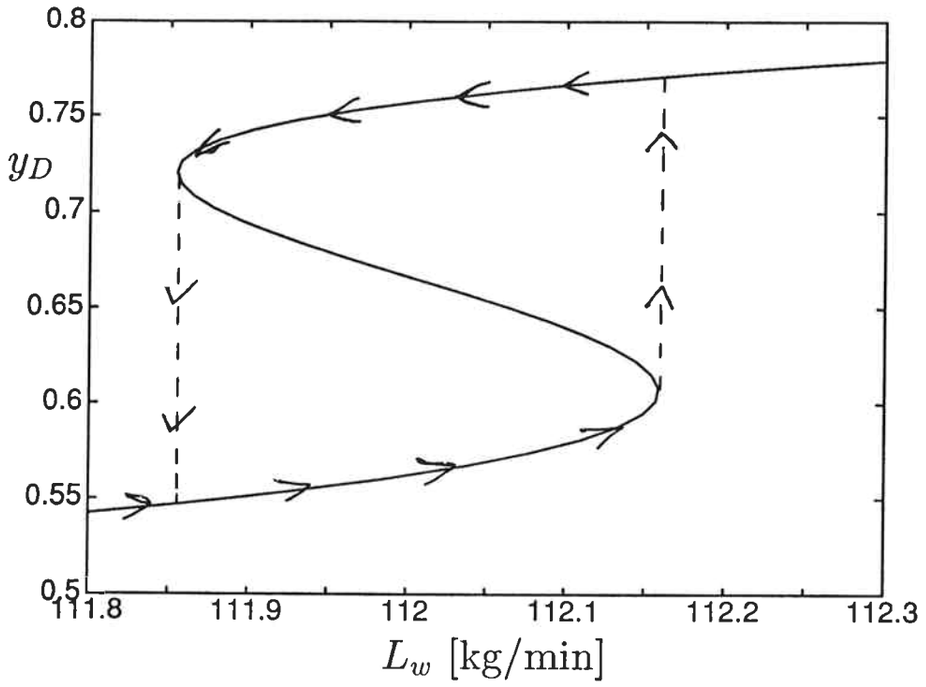

Figure 2.9: Illustration of hysteresis with jump phenomena in distillation.

outputs of the column will jump to totally different values. However, resetting the input to its original value will not force the outputs back to their original values. This closed-loop hysteresis phenomena with jumps at the singular points is well known from catastrophe theory (see e.g. Poston and Stewart (1978)), and is illustrated in Figure 2.9.

Input multiplicity. All results above are for the case of output multiplicity. As mentioned in the introduction, we may also have input multiplicity in distillation columns, at least for multicomponent separations. As an example, consider a separation of components L (light), M (intermediate) and H (heavy). Let z and y represent mole fractions in the feed and top product, respectively. Let V/F be fixed and consider the effect on y_M of varying the top product rate, D. For large values of D ($D \approx F$) there is no separation in the top and we have $y_M \approx z_M$. As D is reduced, y_M *increases* because component H is taken out in the bottom rather than in the top. For $D \approx F(1 - z_H)$ we have the best separation between components M and H, and we have $y_M \approx y_M^* = z_M/(1 - z_H) > z_M$. However, as D is reduced beyond this value, the column starts separating between components L and M, and y_M *decreases*, and for small values of D we have $y_M \approx 0$. Consequently, as illustrated in Figure 2.10, the relationship between D and y_M has a maximum. If y_M is specified between z_M and y_M^* there exists two possible values for D, that is, we have

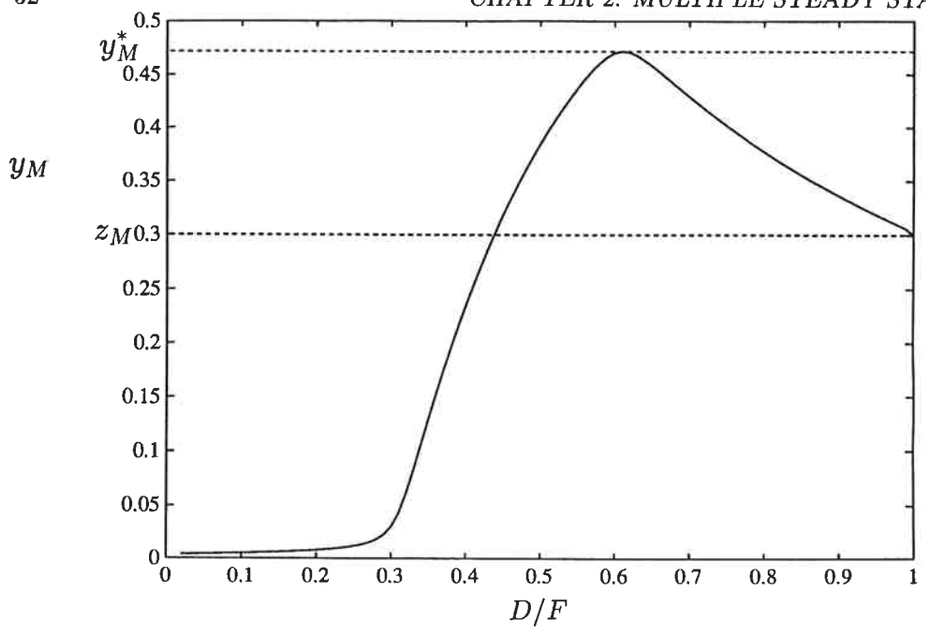

Figure 2.10: Input multiplicity in distillation. Mole fraction of intermediate component in distillate, y_M, as a function of distillate flow rate, D. Column Data: $N = 11$, $N_F = 6$, $z_L = 0.3$,$z_M = 0.3$,$z_H = 0.4$, $\alpha_{LM} = \alpha_{MH} = 2.0$, $V = 2.5$ kmol/min.

input multiplicity. To avoid this problem in a practical situation one should redefine the outputs, for example, by specifying compositions in terms of ratios of key components.

2.9 Conclusions

1. Two-product distillation columns may have multiple steady-state solutions as well as unstable operating points. These results are independent of complex thermodynamics, and are found even for single staged, ideal binary distillation columns.

2. The behavior may be caused by two different effects:

   - Possible singularities in the transformation from the actual independent flows to the molar flows L and V which determine separation in the column. The relationship between mass and molar reflux is $L_w = LM$. An increase in L will in most systems reduce the mole weight M of the top product. If this reduction is sufficiently large, the overall effect may be a decrease in L_w, and the operating point is unstable. This is most likely to happen when; The molecular weight of the light component is much smaller than that of the heavy component, but relative volatility still reasonably close to 1; the bottom product is relatively pure $[x_B \ll (1 - y_D)]$; and the ratio L/D is large.

   - Possible singularities between molar reflux L and top composition y_D due to interactions between flows and compositions in the column. The flows will affect compositions through the material balance while compositions will affect flows through the energy balance. The total effect may result in a negative slope between molar reflux L and top composition y_D, which corresponds to an unstable operating point.

3. For both types of multiplicities the following three operating regimes exist :

   -Internal flows low: no multiplicity, no instability.

   -Internal flows intermediate: multiple steady-states, one of which is unstable. (In some cases there may be two unstable solutions for the L_wV-configuration due to both molar- and mass-input multiplicity in the same region of operation)

   -Internal flows high: no multiple steady-states, all operating points unstable.

APPENDIX 1. Sign of gains $(\partial y_D/\partial D)_V$ and $(\partial x_B/\partial B)_L$.

1. Assume no multiplicity for the DV-configuration, i.e., neither output nor input multiplicity. No output multiplicity (i.e., specifying D and V uniquely determines x_i) seems to apply generally. No input multiplicity (e.g., specifying V and x_i uniquely determines D) seems to always apply to binary mixtures and multicomponent mixtures if we consider the components which distribute to one product, i.e., not for intermediate components. (see Figure 2.10).

2. Let y_D denote the mole fraction in the distillate of the most volatile component. Then

$$\lim_{D\to 0} y_D > z_F; \quad \lim_{D\to F} y_D = z_F \tag{2.36}$$

As y_D decreases when D goes from 0 to F, the gain $(\partial y_D/\partial D)_V$ must be negative for some D. Assumption 1 then implies that the gain is negative for all D, i.e.

$$\left(\frac{\partial y_D}{\partial D}\right)_V < 0. \tag{2.37}$$

Similar reasoning for compositions on other trays gives

$$\left(\frac{\partial x_i}{\partial D}\right)_V < 0 \tag{2.38}$$

for all i.

3. Assuming $(\partial V_T/\partial V)_D$ and $(\partial L_B/\partial L)_D$ non-zero implies that the transformations between the DV- and the LB-configuration are non- singular. Uniqueness for the DV-configuration is then conserved with the LB-configuration.

4. A similar analysis as in 2 above yields

$$\left(\frac{\partial x_i}{\partial B}\right)_L > 0 \tag{2.39}$$

for all i. This also applies to the reboiler where $x_i = x_B$.

APPENDIX 2. Sign of gains $(\partial y_D/\partial L)_V$ and $(\partial x_B/\partial V)_L$ for the case of constant molar flows.

The gain $(\partial y_D/\partial L)_V$ may be written as

$$\left(\frac{\partial y_D}{\partial L}\right)_V = \left(\frac{\partial y_D}{\partial D}\right)_V \left(\frac{\partial D}{\partial L}\right)_V \tag{2.40}$$

For the case of constant molar flows $(\partial D/\partial L)_V = -1$, and (2.40) becomes $(\partial y_D/\partial L)_V = -(\partial y_D/\partial D)_V$. From Appendix 1 it then follows that

$$\left(\frac{\partial y_D}{\partial L}\right)_V > 0 \tag{2.41}$$

Similarly, we find

$$\left(\frac{\partial x_B}{\partial V}\right)_L < 0 \tag{2.42}$$

When the energy balance is included the sign of the gains $(\partial y_D/\partial L)_V$ and $(\partial x_B/\partial V)_L$ may take either sign as shown in Part II of this paper.

NOMENCLATURE (see also Figure 2.2)

B - bottoms flow (kmol/min)
D - distillate flow (kmol/min)
F - feed rate (kmol/min)
H^L - liquid phase enthalpy (kJ/kmol)
H^V - vapor phase enthalpy (kJ/kmol)
ΔH^{vap} - heat of vaporization (kJ/kmol)
L - reflux flow rate (kmol/min)
L_B - liquid flow from bottom tray (kmol/min)
M - mole weight, usually of top product (kg/kmol)

M_1 - pure component mole weight of most volatile component (kg/kmol)
M_2 - pure component mole weight of least volatile component (kg/kmol)
N - no. of theoretical stages in column
N_F - feed stage location (1-reboiler)
Δp - pressure drop (atm)
Q_B - heat input to reboiler (kJ/min)
Q_D - heat removal in condenser (kJ/min)
$S = \frac{y_D(1-x_B)}{(1-y_D)x_B}$ - separation factor (binary mixture)
V - boilup from reboiler (kmol/min) (determined indirectly by heating Q_B)
V_T - vapor flow rate from top tray (kmol/min) (determined indirectly by cooling Q_D)
V_1 - pure component molar volume of most volatile component (m^3/kmol)
V_2 - pure component molar volume of least volatile component (m^3/kmol)
x_B - mole fraction of most volatile component in bottom product
x_i - mole fraction of most volatile component on tray i
y_D - mole fraction of most volatile component in distillate (top product)
z_F - mole fraction of most volatile component in feed

Greek symbols

$\alpha = \frac{y_i/x_i}{(1-y_i)/(1-x_i)}$ - relative volatility (binary mixture)
ρ - density (kg/m^3)

Subscripts
q - flow rate in m^3/min
w - flow rate in kg/min

REFERENCES

Chavez, C. , J.D. Seader and T.L. Wayburn, 1986, "Multiple Steady-State Solutions for Interlinked Separation Systems", *Ind.Eng.Chem.Fund.*, **25**, 566-576

Doherty, M.F. and Perkins, J.D., 1982, "On the Dynamics of Distillation Processes-IV. Uniqueness and Stability of the Steady-State in Homogeneous Continuous Distillation", *Chem.Eng.Sci*, **37**, 3, 381-392

Jacobsen, E.W. and S. Skogestad, 1990, "Dynamics and Control of Unstable Distillation Columns", Presented at Canadian Chem.Eng.Conf., Halifax, Canada, July, 1990.

Kovach, J.W. and W.D. Seider, 1987, "Heterogeneous Azeotropic Distillation - Homotopy Continuation Methods", *Comput.Chem.Engng.*, **11**, 6, 593-606

Lin, W.J., J.D. Seader and T.L. Wayburn, 1987,"Computing Multiple Solutions to Systems of Interlinked Separation Columns", *AIChE J.*, **33**,886

Lucia, A, L.N. Sridhar and X. Guo, 1989, "Analysis of Multicomponent, Multistage Separation Process", AIChE Annual Meeting, San Francisco.

Luyben, W.L., 1979, "Introduction and Overview of Distillation Column Control", Presented at AIChE Workshop, Tampa, Florida.

Magnussen T., M.L. Michelsen and Aa. Fredenslund, 1979, "Azeotropic Distillation using UNIFAC", *Inst.Chem.Eng.Symp.Ser.*, **56**, pp. 4.2/1-4.2/19.

Poston, T. and I. Stewart, 1978, *Catastrophe Theory and its Applications*, Pitman, London

Prokopakis, G.J. and W.D. Seider, 1983, "Feasible Specifications in Azeotropic Distillation", *AIChE J.*, **29**, 1, 49-60.

Rademaker, O., J.E. Rijnsdorp and A. Maarleveld, 1975, *Dynamics and Control of Continuous Distillation Units*, Elsevier, Amsterdam.

Rosenbrock, H.H., 1960, "A Theorem of "Dynamic Conservation" for Distillation", *Trans.Ins. Chem.Engrs.*, **38**, 20, 279-287.

Rosenbrock, H.H., 1962, "A Lyapunov Function with Applications to Some Nonlinear Physical Problems", *Automatica*, **1**, 31-53.

Ryskamp, C. J., 1980, "New Strategy Improves Dual Composition Column Control", *Hydrocarb.Proc.*, **59**, 6, 51.

Sridhar, L.N. and A. Lucia, 1989, "Analysis and Algorithms for Multistage Separation Processes", *Ind.Eng.Chem.Res.*, **28**, 793-803.

Skogestad, S. and M. Morari, 1987, "Understanding the Dynamic Behavior of Distillation Columns", *Ind.Eng.Chem.Res.*, **27**, 10, 1848-1862.

Skogestad, S. and M. Morari, 1987b, "A Systematic Approach to Distillation Column Control", *I.Chem.E. Symposium Series*, **104**, A71-86.

Venkataraman, S. and A. Lucia, 1988, "Solving Distillation Problems by Newton-like Methods", *Comput.Chem.Engng.*, **12**, 1, 55-69

Widagdo, S., W.D. Seider and D.H. Sebastian, 1989, "Bifurcation Analysis in Heterogeneous Azeotropic Distillation", *AIChE J.*, **35**, 9, 1457-1464

Chapter 3

Dynamics and Control of Unstable Distillation Columns

Elling W. Jacobsen and Sigurd Skogestad

Chemical Engineering
University of Trondheim - NTH
N-7034 Trondheim
Norway

Submitted to *Chem.Eng.Sci.*

Abstract

The paper addresses dynamics and control of distillation columns operated at open-loop unstable operating points. The fact that ideal two-product distillation columns may have multiple steady-states and right half plane poles has only recently been recognized. This paper discusses in detail the dynamics and control implications. It is shown that with reflux and boilup as independent variables the operating points become unstable if the internal flows are sufficiently large. An open-loop unstable operating point may be stabilized by use of one-point control, i.e., feedback control of a column composition or temperature. If the control is not sufficiently tight, the column may go into a stable limit cycle. It is shown that the open-loop right half plane pole may worsen the control performance when both product compositions are under feedback control. Finally, it is shown that with distillate flow and boilup as independent variables the operating points may become unstable if the level control is not sufficiently tight. The column may also in this case go into a stable limit cycle.

3.1 Introduction

Distillation is undoubtly the most studied unit operation in the process control literature. However, in all previous studies the column dynamics have been assumed to be asymptotically stable (with level and pressure loops closed). The main reason is that most authors have considered dynamic models with constant molar flows (neglected energy balance) and in addition assumed the inputs (e.g., reflux and boilup) to be given on a molar basis.

For the case of molar inputs there exists several papers on uniqueness and asymptotic stability of the operating points in homogeneous distillation. Most papers treats the constant molar flow case (neglected energy balance), e.g., Lapidus and Amundson, 1950; Acrivos and Amundson, 1955; Rosenbrock 1960, 1962. Doherty and Perkins (1982) provide a review of results published in this area, and conclude that, for constant molar flows, multiplicity and instability is impossible for single-staged "columns" and any multistage column separating a binary mixture. Sridhar and Lucia (1989) include the energy balance in the model and conclude under certain assumptions that also in this general case binary distillation columns will exhibit unique and stable solutions. They do, however, only study a limited set of specifications, namely $Q_D Q_B$ and LB.

However, in a recent paper Jacobsen and Skogestad (1991) report two kinds of multiplicity which may occur in distillation. 1) Jacobsen and Skogestad (1991) argue that columns under operation only in rare cases have all the manipulated inputs on a molar basis. For instance, fixing the valve position will normally correspond closely to fixing the geometric average of mass and volumetric flow-rate. As they show, the transformation from mass- or volume flows to molar flows is nonlinear due to the composition dependence and may in some cases become singular, even for the binary case with constant molar flows. A singularity in the input transformation will imply that there exist multiple solutions in terms of outputs (compositions) for a given set of inputs (flows). One of the solutions will be unstable. 2) In addition, Jacobsen and Skogestad show that when the energy balance is included in the model, even molar inputs may yield multiple solutions. Both types of multiplicity and instability may be experienced in industrial columns operated with inputs on a mass- or volume basis.

Jacobsen and Skogestad (1991) treat the multiplicity only from a steady-state point of view. In this paper we study the dynamics of columns with multiple solutions, and consider the implications of open-loop instability for feedback control. The last point is important as previous studies on distillation control have assumed open-loop stability, and we investigate whether the achieveable closed-loop performance is influenced by the open-loop instability.

We start the paper with a brief summary of the previous results on steady-state multiplicity caused by singularity in the input transformation. We prove the instability for this case and consider the overall dynamics of columns with right half plane (RHP) poles. Finally, we consider whether any fundamental new control problems are introduced by the multiplicity and instability.

We limit ourselves to discuss mainly one control configuration (set of specifications), namely the case where mass reflux L_w and molar boilup V (V is closely related to the heat input Q_B) are used as independent variables. This is the most widespread configuration in industry, and is the configuration for which multiplicity and instability is most likely

to occur (Jacobsen and Skogestad, 1991). With this configuration the product flows (D_w and B_w) are used to control the condenser and reboiler levels (M_D and M_B). We here assume perfect level control, but this assumption is not important since the composition response is only weakly dependent on the level control when reflux and boilup are used as independent variables. At the end of the paper we consider the case with distillate flow D_w and boilup V as independent inputs, and show that with this configuration the responses are strongly dependent on the level control; the operating points may even become unstable if the level control is not sufficiently tight.

In most of the paper we consider the simplest case with constant molar flows, i.e., we neglect the energy balance. Towards the end of the paper we consider the instability that may be caused by including the energy balance.

3.2 Results on Steady-State Multiplicity in Ideal Distillation

We give here a brief review of the results on multiplicity caused by singularity in the input transformation presented in Jacobsen and Skogestad (1991).

Consider the two-product distillation column in Figure 3.1. If the feed to the column is given there are at least four flows that may be specified: reflux L, boilup V, distillate D and bottoms flow B. However, for a given column there are only two degrees of freedom at steady-state, that is, only two of these flows may be specified independently. A specific choice of two independent variables is denoted a "configuration".

Jacobsen and Skogestad (1991) provide an example of steady-state multiplicity in a column separating a mixture of methanol and n-propanol. The column has mass reflux and molar boilup as independent variables, i.e., $L_w V$-configuration. Data for the column are given in Table 3.1. Note that the energy balance is excluded, i.e., constant molar flows are assumed. Some steady-state solutions are given in Table 3.2, and we see that for a specification of mass reflux $L_w = 50.0$ kg/min and molar boilup $V = 2.0$ kmol/min we have three possible solutions II, III and IV in terms of compositions. The multiplicity is graphically illustrated in Figure 3.2.

The observed multiplicity is caused by the transformation between the actual flow-rates (mass) and the molar flow-rates which determine separation. For a binary mixture the transformation between mass reflux, L_w, and molar reflux, L, is given by

$$L = L_w/M; \quad M = y_D M_1 + (1 - y_D) M_2 \tag{3.1}$$

Here M_i denotes the molecular weight of the individual components. One might expect the molar reflux to increase monotonically with the mass reflux, that is, $(\partial L/\partial L_w)_V > 0$. However, because M is a function of composition, y_D, and thereby of L_w, this might not be the case. Assuming molar boilup V fixed and differentiating $L_w = LM$ on both sides with respect to L yields

$$\left(\frac{\partial L_w}{\partial L}\right)_V = M + L(M_1 - M_2)\left(\frac{\partial y_D}{\partial L}\right)_V \tag{3.2}$$

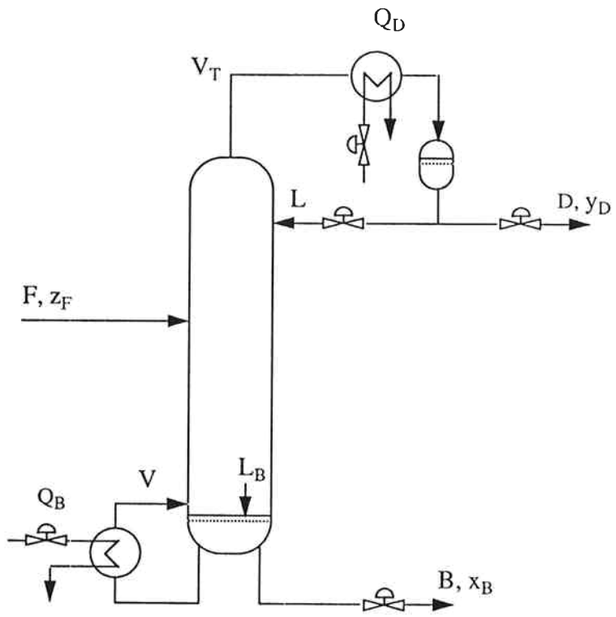

Figure 3.1: Two product distillation column.

z_F	F	α	N	N_F	M_1	M_2
0.50	1	3.55	8	4	32.04	60.10

- Feed is saturated liquid.
- Total condenser with saturated reflux.
- Liquid holdups are $M_{Li}/F = 0.5min$
- L_wV-configuration: $M_D/F = M_B/F = 0.5min$
- D_wV-configuration: $M_D/F = M_B/F = 5.0min$
- Flow dynamics included in dynamic simulations.
- Constant pressure.

Table 3.1: Data for Methanol-Propanol Column.

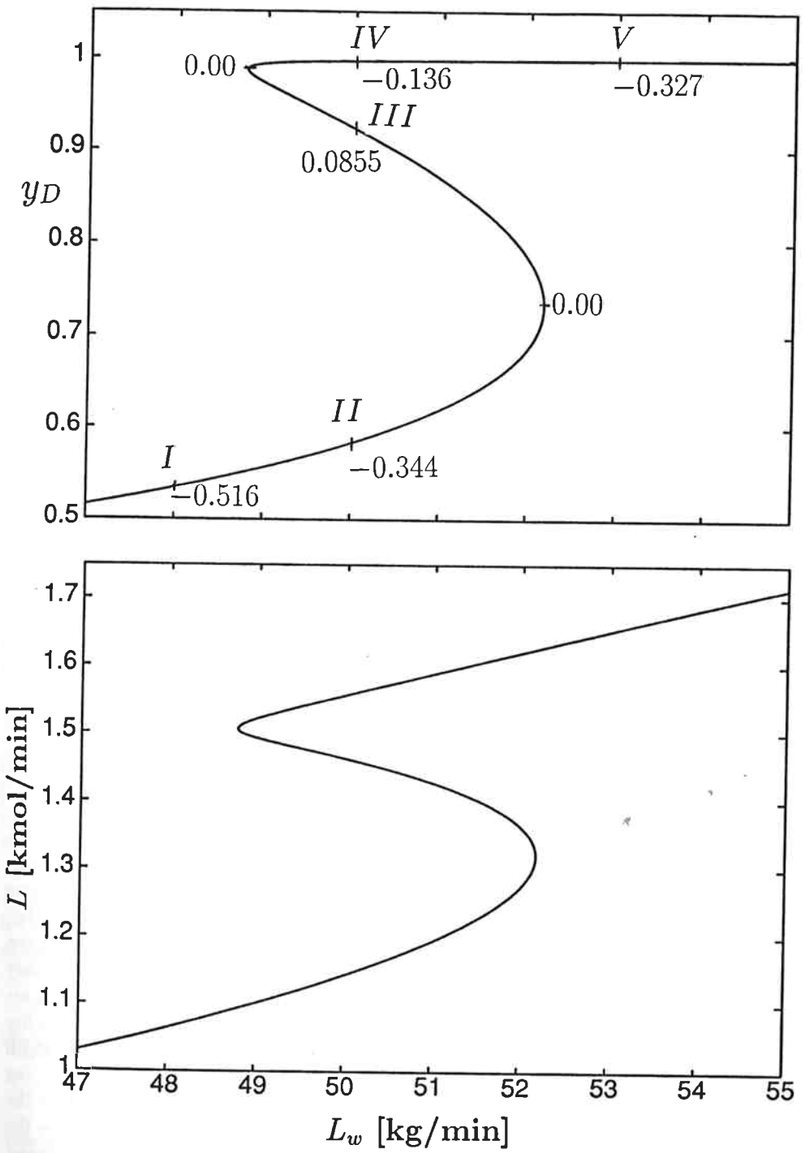

Figure 3.2: Methanol-propanol column with constant molar flows: Multiple steady-states for L_wV-configuration. Mass reflux L_w is varied while molar boilup V is fixed at 2.0 kmol/min. On the upper plot the corresponding maximum eigenvalue is shown at some of the steady-state solutions.

	L [kmol/min]	D [kmol/min]	L_w [kg/min]	y_D	x_B
I	1.064	0.936	48.00	0.534	3.10e-3
II	1.143	0.857	50.00	0.584	3.50e-3
III	1.463	0.537	50.00	0.9237	7.80e-3
IV	1.555	0.445	50.00	0.9969	0.104
V	1.650	0.350	53.00	0.9984	0.233

- Constant molar flows.

Table 3.2: Steady-state solutions for methanol-propanol column with V=2.0 kmol/min and L_w in the range 48 to 53 kg/min.

For $M_1 < M_2$, which is usually the case (the most volatile component has the smallest molecular weight), the second term on the right hand side of (3.2) will be negative and the total differential may take either sign. The transformation from L_w to L will be singular when $(\partial L_w/\partial L)_V = 0$. A singular point will correspond to a bifurcation point, and the number of solutions changes from one to three. Jacobsen and Skogestad (1991) state that solutions with $(\partial L_w/\partial L)_V < 0$ (middle branch in Figure 3.2) correspond to unstable operating points, but they do not prove this rigorously.

3.3 Open-Loop Dynamics and Instability for L_wV-configuration

The maximum eigenvalue in selected operating points of the methanol-propanol column with constant molar flows and the L_wV-configuration are shown in Figure 3.2. From the figure we observe that the eigenvalues at the upper and lower branches are negative, implying stability, while those at the intermediate branch (negative slope) are positive, implying instability of the operating points. Note that the unstable operating points only have a single eigenvalue in the right half plane. The eigenvalues at the singular points are zero as expected since they correspond to bifurcation points. The open-loop instability at the intermediate branch is illustrated by the nonlinear simulations in Figure 3.3 which shows the responses in top composition y_D to small changes in mass-reflux L_w (keeping boilup V fixed) at the unstable operating point III. The simulations indicate that the two stable solutions II and IV have equally large regions of attraction as seen from the unstable solution III. The purpose of the rest of this section is to prove the observed instability at the intermediate branch and to compare the dynamics of columns with mass or volume inputs with those found for models with molar inputs.

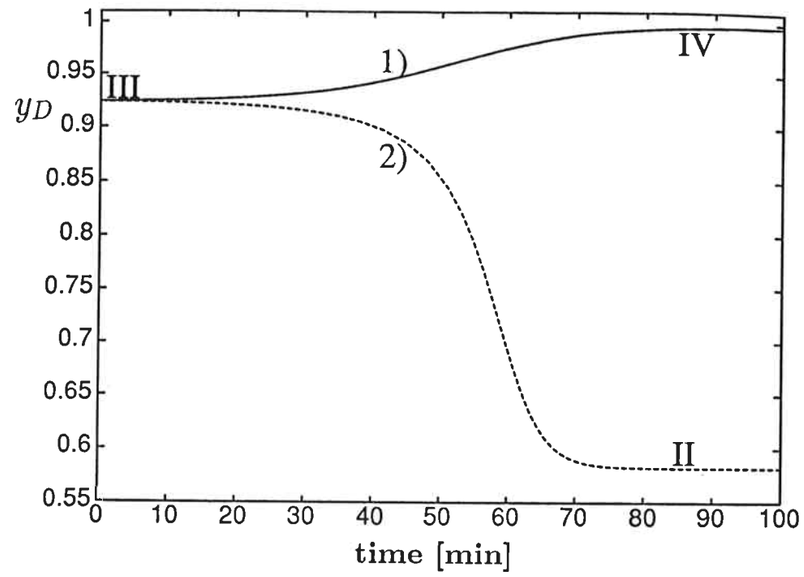

Figure 3.3: Nonlinear open-loop simulation of methanol-propanol column at unstable operating point III in Figure 3.1. 1) Small increase in mass reflux L_w. 2) Small decrease in mass reflux L_w. Boilup $V = 2.0$ kmol/min. Constant molar flows.

3.3.1 Conditions for instability

One-stage column Consider the simple column in Figure 3.4 with one theoretical stage (the reboiler) and a total condenser. Of course, such a column will never be operated in practice because the reflux is simply wasting energy and has no effect on separation. However, we start by analyzing this column due to the simplicity of the dynamic model. As Jacobsen and Skogestad (1991) show, even such a simple column with ideal thermodynamics may have multiple steady-state solutions. Assume binary separation, liquid feed, constant holdup in the reboiler (M_L) and negligible holdup in the condenser. The dynamic model of the column becomes:

$$M_L \frac{dx_B}{dt} = Fz_F - Dy_D - Bx_B \tag{3.3}$$

We have $D = V - L$ and $D + B = F$ and with L and V as independent variables we get

$$M_L \frac{dx_B}{dt} = F(z_F - x_B) + L(y_D - x_B) + V(x_B - y_D) \tag{3.4}$$

Linearization, Laplace transformation and introduction of deviation variables assuming F, z_F and V constant yields

$$sM_L\Delta x_B(s) = -D\Delta y_D(s) - B\Delta x_B(s) + (y_D - x_B)\Delta L(s) \tag{3.5}$$

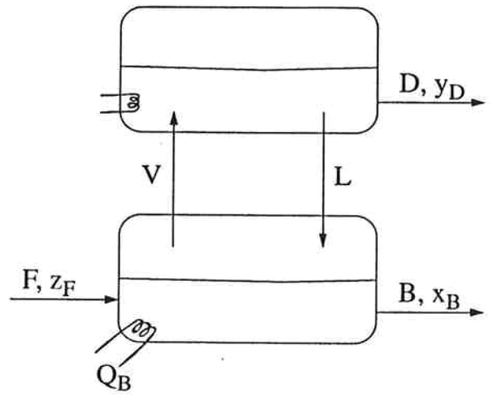

Figure 3.4: One-stage column with total condenser.

Assuming constant relative volatility α yields the following relation between $\Delta y_D(s)$ and $\Delta x_B(s)$

$$\frac{\Delta y_D(s)}{\Delta x_B(s)} = \frac{\alpha}{(1+(\alpha-1)x_B)^2} = K(x_B) \tag{3.6}$$

Equation (3.5) then becomes

$$\Delta x_B(s) = \frac{y_D - x_B}{M_L s + a}\Delta L(s) \tag{3.7}$$

where

$$a = KD + B \tag{3.8}$$

As all terms in (3.8) are positive, the pole $-a/M_L$ is always negative, implying that all operating points are stable when molar reflux L and molar boilup V are independent variables.

Now consider mass reflux L_w as an input instead of molar reflux $L = L_w/M$. By linearization we obtain for binary separations

$$\Delta L = \frac{1}{M}\Delta L_w + L\frac{M_2 - M_1}{M}K\Delta x_B \tag{3.9}$$

Substituting (3.9) into (3.7) we obtain the following transfer-function between liquid composition, $\Delta x_B(s)$, and mass reflux $\Delta L_w(s)$:

$$\Delta x_B(s) = \frac{y_D - x_B}{M_L s + a_w}\frac{\Delta L_w(s)}{M} \tag{3.10}$$

where

$$a_w = KD + B - (y_D - x_B)\frac{M_2 - M_1}{M}KL \tag{3.11}$$

The operating point is unstable for $a_w < 0$. At steady-state (3.6), (3.7) and (3.8) yield

$$\left(\frac{\partial y_D}{\partial L}\right)_V = \frac{y_D - x_B}{D + B/K} \tag{3.12}$$

and from (3.2) we find that instability ($a_w < 0$) is equivalent to a negative slope for $(dL_w/dL)_V$.

Multistage column Although the dynamic model of a multistage distillation column is of high order, it is well known that the overall composition dynamics in distillation columns may be well approximated by a first order response (e.g., Davidson, 1956, Skogestad and Morari, 1987). This implies that we may approximate the transfer-function from molar reflux L to top composition y_D with

$$\left(\frac{\partial y_D}{\partial L}\right)_V(s) \approx \frac{k^{LV}_{y_D L}}{1+\tau_1 s} \tag{3.13}$$

where $k^{LV}_{y_D L}$ ($= (\partial y_D/\partial L)_V$ in (3.2)) is the steady-state gain and τ_1 is the dominant time-constant (we assume stability, $\tau_1 > 0$, which always holds for the case of constant molar flows). We now want to derive the transfer function $(\partial y_D/\partial L_w)_V(s)$. With V constant the total differential of y_D may be written

$$dy_D(s) = \left(\frac{\partial y_D}{\partial L}\right)_V(s)dL(s) \tag{3.14}$$

Here $L = L_w/M$ is a function of both L_w and y_D and we get

$$dL(s) = \left(\frac{\partial L}{\partial L_w}\right)_{y_D}(s)dL_w(s) + \left(\frac{\partial L}{\partial y_D}\right)_{L_w}(s)dy_D(s) \tag{3.15}$$

Combining (3.14) and (3.15) yields:

$$\left(\frac{\partial y_D}{\partial L_w}\right)_V(s) = \frac{\left(\frac{\partial L}{\partial L_w}\right)_{y_D}\left(\frac{\partial y_D}{\partial L}\right)_V(s)}{1 - \left(\frac{\partial L}{\partial y_D}\right)_{L_w}\left(\frac{\partial y_D}{\partial L}\right)_V(s)} \tag{3.16}$$

The Laplace variable s has been deleted for $(\partial L/\partial L_w)_{y_D}$ and $(\partial L/\partial y_D)_{L_w}$ since the relationship $L = L_w/M$ is purely static. For a binary mixture

$$\left(\frac{\partial L}{\partial L_w}\right)_{y_D} = y_D M_1 + (1-y_D)M_2 \tag{3.17}$$

$$\left(\frac{\partial L}{\partial y_D}\right)_{L_w} = \frac{L_w(M_2 - M_1)}{(y_D M_1 + (1-y_D)M_2)^2} \tag{3.18}$$

From (3.16) we now find that the dominant pole is given by

$$\lambda_{max} = -\frac{1}{\tau_1}\left(1 - \frac{k^{LV}_{y_D L}L(M_2 - M_1)}{y_D M_1 + (1-y_D)M_2}\right) \tag{3.19}$$

The pole will be in the right half plane when

$$\frac{k_{y_DL}^{LV} L(M_2 - M_1)}{y_D M_1 + (1 - y_D) M_2} > 1 \tag{3.20}$$

This is exactly the same criterion as Jacobsen and Skogestad (1991) found for a negative slope between mass and molar reflux. Thus, a sufficient condition for instability for the L_wV-configuration is

$$\left(\frac{\partial L}{\partial L_w}\right)_V < 0 \tag{3.21}$$

This means that solution branches with a negative slope between L and L_w represent unstable solutions, provided the column is stable on a molar basis. This result is in accordance with numerical results.

In the general case with more complex dynamics, (3.13) may be replaced by

$$\left(\frac{\partial y_D}{\partial L}\right)_V (s) = \frac{k_{y_DL}^{LV}(1 + b_1 s + b_2 s^2 + ... + b_{n-1} s^{n-1})}{1 + a_1 s + a_2 s^2 + ... + a_n s^n} \tag{3.22}$$

This follows since the composition dynamics generally have a pole excess of one[1] (e.g., Skogestad and Morari, 1988). We assume "molar" stability, i.e., all $a_i's$ in (3.22) are positive. We may now use the Routh-Hurwitz stability criterion (the coefficients in the pole polynomial of (3.16) should have different signs) to conclude that in the general case (3.20) and (3.21) are sufficient conditions for instability.

Equation (3.19) gives an approximate way of calculating the dominating pole for the L_wV-configuration from data computed for molar inputs. Figure 3.5 shows a comparison of this approximation with the maximum eigenvalue computed from the full linear model with mass reflux. We see that the (3.19) yields a correct value of zero λ_{max} at the singular points, and a fairly good approximation in the whole.

3.3.2 Effect of operating conditions on stability

Jacobsen and Skogestad (1991) provide analytical results on when a negative slope between mass and molar reflux, i.e., instability according to (3.21), is most likely. They show that a negative slope is most likely with large internal flows (i.e., large L and V) and with intermediate purities in the top (i.e., intermediate L for given V). This corresponds to having L and $k_{y_DL}^{LV}$ large, and according to (3.20) this is the case for which instability is most likely. Note that the analytical treatment in Jacobsen and Skogestad (1991) was based on ideal separation with constant relative volatility and constant molar flows. The same assumptions apply to the discussion below.

To study the effect of operating conditions on stability for the L_wV-configuration, consider different values of V, and for each value let L vary between $L_{min} = V - F$ ($B = 0$) and $L_{max} = V$ ($D = 0$) (Note that these variations in L and V are purely static). On the basis of the analytical results in Jacobsen and Skogestad (1991) we get three different cases of operation depending on the size of the internal flows:

[1]For the case with a total condenser there will be a pole excess of two in (3.22).

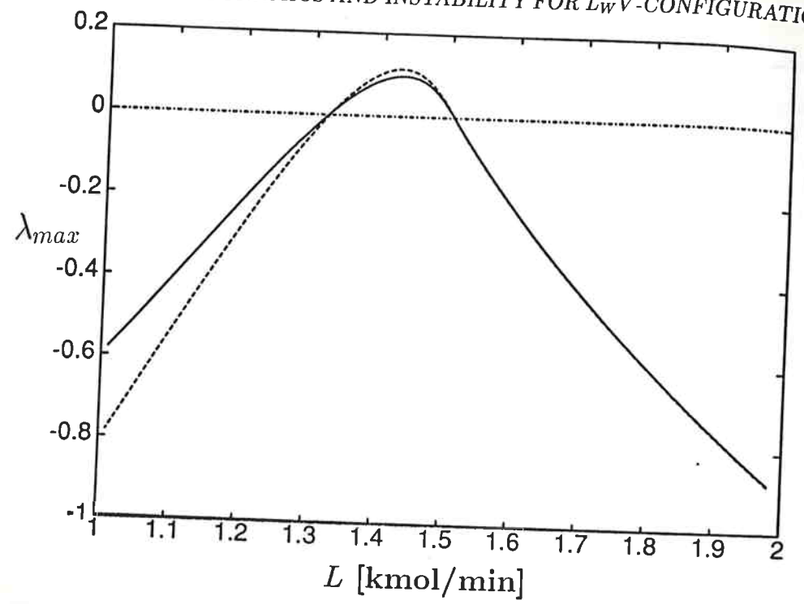

Figure 3.5: Maximum eigenvalue λ_{max} as a function of molar reflux L for methanol-propanol column with L_wV-configuration and $V = 2.0$ kmol/min. Solid line: exact. Dashed line: Computed from (3.19). Constant molar flows.

A. Internal flows low (V small): The largest pole (λ_{max}) starts out in the LHP for $L = L_{min}$ and moves toward the right as L is increased. However, it does not reach the imaginary axis before it begins to move back. This implies that we have uniqueness with all solutions stable.

B. Internal flows intermediate: The pole λ_{max} starts out in the LHP at L_{min} and moves towards the imaginary axis as L is increased. At some value of L the pole crosses the imaginary axis and moves into the RHP. For some intermediate value of L the pole begins to move back and crosses the imaginary axis again (this time from right to left). In this case we have three solutions, one of which is unstable.

C. Internal flows high (V large): The large value of L_{min} implies that λ_{max} starts out in the RHP and moves further towards the right with increasing L. For some intermediate value of L the pole starts to move back but it never crosses the imaginary axis before $L = L_{max}$. In this case we have uniqueness and all solutions unstable.

The three different regimes of operation are illustrated in Figure 3.6 for the one-stage column studied by Jacobsen and Skogestad (1991). Note that there also may be cases where there are two solutions, of which one is unstable. In this case the third solution would actually correspond to one of the product flows, D or B, being negative.

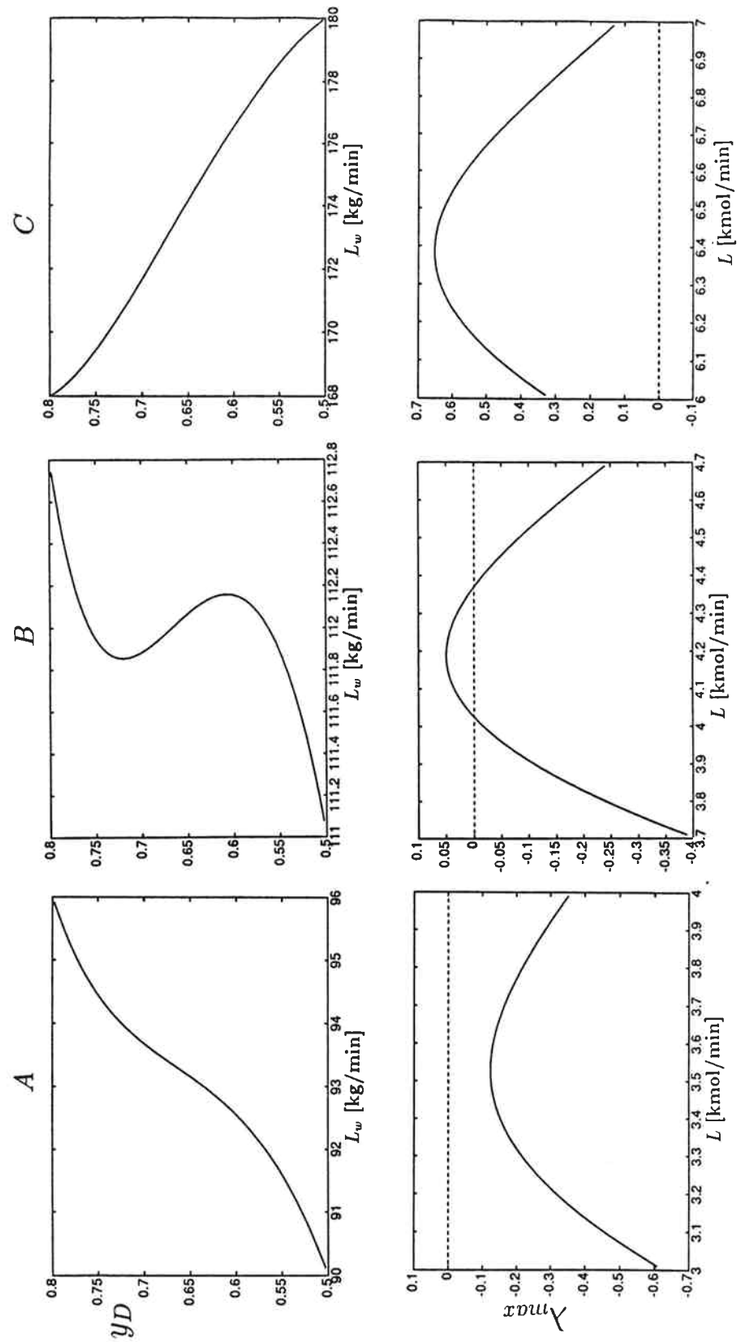

Figure 3.6: Steady-state solutions as a function of mass-reflux L_w for one-stage column with $N = 1$, $F = 1$, $z_F = 0.5$, $M_1 = 20$, $M_2 = 40$ and $\alpha = 4.0$. Lower plot shows corresponding maximum eigenvalue as a function of molar reflux L. A) $V = 4.0$ kmol/min. B) $V = 4.7$ kmol/min. C) $V = 7.0$ kmol/min.

3.3.3 Overall dynamics

The analysis above showed that the dominant (largest) pole, and thereby the stability and low-frequency dynamics, is strongly influenced by the transformation between mass and molar reflux. However, the effect on the high-frequency dynamics is much smaller. Figure 3.7 shows the magnitude and phase of the transfer-functions from L and L_w, respectively, to top composition y_D (keeping boilup V fixed) at operating point III of the methanol-propanol column. From the figure we see that the phase of the two transfer-functions differs with 180 degrees at low frequencies as expected since the transfer function from mass-reflux has a RHP pole and negative low-frequency gain. However, the phases approach each other at intermediate frequencies and become identical at high frequencies. The magnitudes of the two systems are almost identical at all frequencies. Note that the magnitude for the L_wV-configuration has been scaled by M. The fact that the magnitudes are similar also at low frequencies is a coincidence for this operating point. The reason is that the dominant poles are similar in magnitude (-0.098 and 0.086). However, the dynamics of the two systems differ in the region where the phases differ. The most important conclusion to draw from Figure 3.7 is that it is mainly the dominant pole that is influenced by the transformation from mass to molar flows. The initial response (high-frequency behavior) is unaffected. Similar results are obtained for the other three transfer-functions of the 2×2 system.

3.4 Feedback Control

3.4.1 Limitations imposed by RHP poles and zeros

As we have seen, columns operating with mass or volume inputs may be open-loop unstable, and will require feedback control (in addition to level and pressure control) for stabilization. From control theory it is well known that unstable poles by themselves do not represent any bandwidth limitations; on the contrary they put a lower limit on allowable bandwidth of the closed-loop system. Problems will therefore only arise if there are bandwidth limitations like right half plane zeros at frequencies comparable to the right half plane pole ("The system goes unstable before we are able to observe what is happening") or if there are constraints ("we can not counteract the instability").

Freudenberg and Looze (1985, 1988) have extended the Bode Sensitivity Integral Theorem for minimum phase systems to systems containing RHP zeros and RHP poles. Here we consider scalar systems, but similar relations are obtained for multivariable systems if one considers the maximum singular value of the sensitivity function $\bar{\sigma}(S)$ instead of $|S|$.

Consider the sensitivity function $S = (1 + gc)^{-1}$ of the closed-loop system. Ideally we want $S = 0$. However, for all real systems $|S(j\omega)| = 1$ at high frequencies. In addition, for an open-loop system with a pole excess of at least two (satisfied for any real system) and a single real RHP pole p the following limitation applies (Freudenberg and Looze, 1985)

$$\int_0^\infty log|S(j\omega)|d\omega = \pi p \tag{3.23}$$

(With no RHP pole ($p = 0$) (3.23) reduces to the theorem of Bode.) From (3.23) we

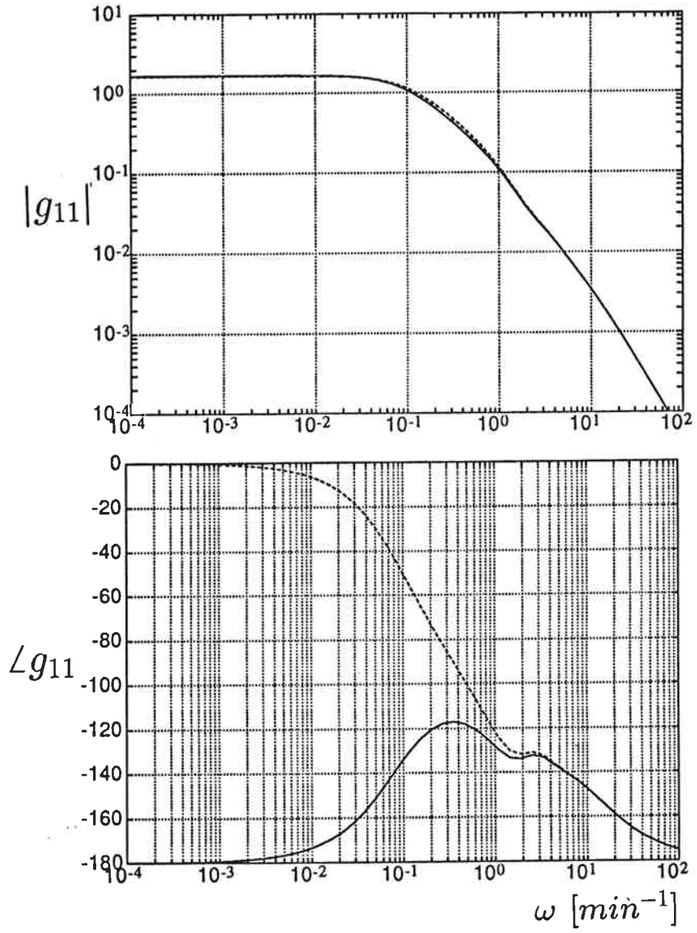

Figure 3.7: Frequency response for transfer-function from reflux to top composition y_D keeping V constant for operating point III of methanol-propanol column. Solid line: mass reflux. Dashed line: molar reflux. The magnitude for mass-reflux L_w is scaled by M. Constant molar flows.

see that we need a frequency range with $|S| > 1$ and that the presence of a RHP-pole increases the area where $|S| > 1$. However, (3.23) does not impose any practical design limitation as the area for $|S| > 1$ may be smoothed out over an arbitrarily large frequency range, and the peak of S may accordingly be made arbitrarily small. Thus, as stated above, the RHP pole will not represent a control limitation if there are no bandwidth constraints present in the system.

However, for an open-loop system with a real RHP pole p and a real RHP zero z, the following restriction applies (Freudenberg and Looze, 1985, 1988)

$$\int_0^\infty log|S(j\omega)|W(z,\omega)d\omega = \pi log|\frac{p+z}{p-z}| \tag{3.24}$$

(With no RHP pole ($p = 0$) the integral equals zero). The weight W is given by

$$W(z,\omega) = \frac{2z}{z^2+\omega^2} \tag{3.25}$$

The form of W (it equals $2/z$ up to $\omega = z$ where is cuts off with a -2 slope.) implies that essentially all the area for $|S| > 1$ has to be at frequencies lower than z, and the sensitivity function must have a peak $|S| > 1$ at $\omega < z$. The peak will have to become increasingly large as the bandwidth frequency (where $|S|$ first reaches 1) approaches z. From (3.24) we also see that as the RHP zero approaches the RHP pole, the peak goes to infinity. This implies that we in general must require

$$p < z \tag{3.26}$$

For the distillation column $p = \lambda_{max}$, and RHP zeros are most likely caused by deadtimes, θ_d, in measurements and actuators. Using a first-order Padé approximation for θ_d results in a RHP zero at $z = 2/\theta_d$. We must then require $\lambda_{max} < 2/\theta_d$, or equivalently $\theta_d < 2/\lambda_{max}$. With a limited structure of the controller, e.g. a PI-controller, we must require a larger distance between the RHP pole and the RHP zero than given by (3.26) in order to stabilize the column.

For a further discussion on the effect of RHP-poles and -zeros on closed-loop performance see Freudenberg and Looze (1985, 1988) and Looze and Freudenberg (1991).

3.4.2 One-point control

Good control of distillation columns usually requires two-point control, i.e., feedback control of both product compositions. However, in order to stabilize an open-loop unstable column one-point control will suffice. This is also the way most industrial columns with composition control are operated. An unstable column operating with the L_wV-configuration may be stabilized by controlling either top or bottom composition, or any other variable related to composition, e.g. a temperature inside the column. The analysis presented above for SISO systems then applies.

For operating point III of the methanol-propanol column the RHP-pole is at $p = 0.086min^{-1}$ and we are unable to stabilize the column with a PI-controller when the deadtime exceeds 11 min. ($z \approx 2/\theta_d = 0.182min^{-1}$). However, composition measurements

in industrial columns (GC-analysis) may typically have deadtimes up to 30 min., and one should then use faster temperature measurements in order to stabilize the column.

Nonlinear Simulations. Figure 3.8 shows nonlinear simulations of the methanol-propanol column using a single-loop PI-controller[2] between top composition y_D and mass-reflux L_w with a 1 minute measurement deadtime included. Molar boilup V is kept constant at 2.0 kmol/min. The figure shows the responses to setpoint changes in y_D from operating point II (open-loop stable) to operating point III (open-loop unstable) and then further on to operating point IV (open-loop stable) (see Figure 3.2 and Table 3.2). A logarithmic measurement $Y_D = ln(1 - y_D)$ was used in the controller as this reduces the nonlinearity of the initial response between different operating points (Skogestad and Morari, 1988). From the figure we see that the controller is able to stabilize the open-loop unstable operating point III with a RHP pole at 0.086 min^{-1}. The simulations also show that the same controller may be used in these three widely differing operating points. The reason is that the initial response (high-frequency dynamics) in terms of logarithmic composition Y_D is similar in all operating points. We would get instability if we used mole fractions, y_D, as is done conventionally. From the plot of mass-reflux L_w against time we see that the steady-state change in the input is zero, showing that the three operating points are multiple solutions.

One should be careful about detuning a controller in an open-loop unstable process as the bandwidth may become lower than the minimum allowable and the operating point becomes closed-loop unstable. This is illustrated in Figure 3.9. where the controller gain has been reduced by a factor of two compared to the simulations in Figure 3.8. Operating point *III* is now closed-loop unstable, and a small setpoint change makes the system start drifting away. However, this does not imply that the column goes globally unstable in the sense that physical constraints are violated. Since there exists steady-state solutions above and below the unstable solution the column goes into a stable limit cycle. If the controller gain is reduced further the limit cycle will continue, but now with a longer period of each cycle and with higher peaks in composition. There will also exist cases where there are no solutions either above or below the unstable solution. In this case the column is likely to go globally unstable as either the condenser (missing upper branch) or reboiler (missing lower branch) would run dry.

3.4.3 Two-point control

As pointed out above, one-point control is sufficient to stabilize an unstable operating point, but high performance control usually requires control of both product compositions. There exist a large amount of literature on two-point control of distillation columns, but everything is based on open-loop stable models. Here we want to investigate whether the potential instability caused by using mass-flows will affect the achieveable closed-loop performance of the column significantly.

In order to compare achieveable performance for the stable model with molar reflux and the unstable process with mass reflux we design controllers with optimized performance for both cases. As a design objective we use the structured singular value, μ (see

[2]Tuned to yield reasonably fast response. Note that Ziegler-Nichols tuning rules resulted in a closed-loop unstable system.

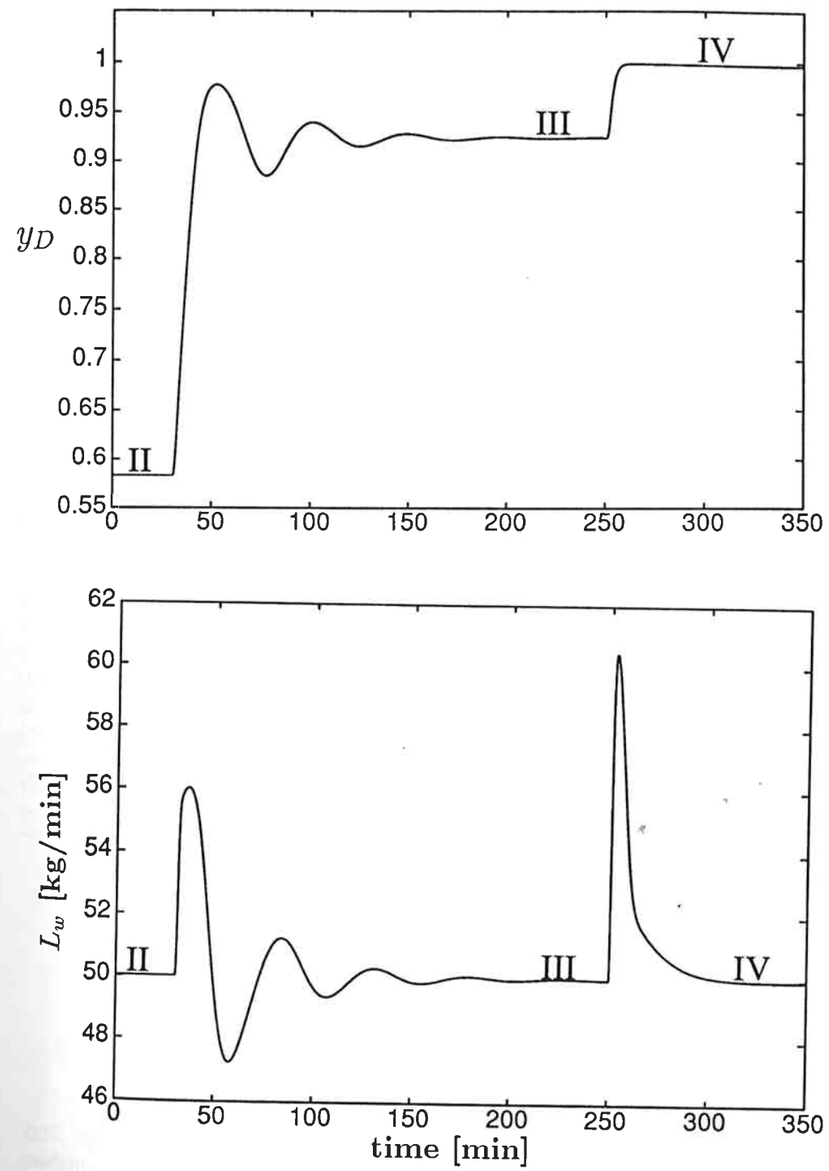

Figure 3.8: Nonlinear simulation of methanol- propanol column with one-point control of top-composition y_D using mass reflux L_w. Setpoint changes from operating point *II* to *III* and from *III* to *IV*. Boilup $V = 2.0$ kmol/min. Controller parameters: $k = 3.0$ and $\tau_I = 11.0$ min. Gain is for logarithmic composition, i.e., $log(1 - y_D)$. Constant molar flows.

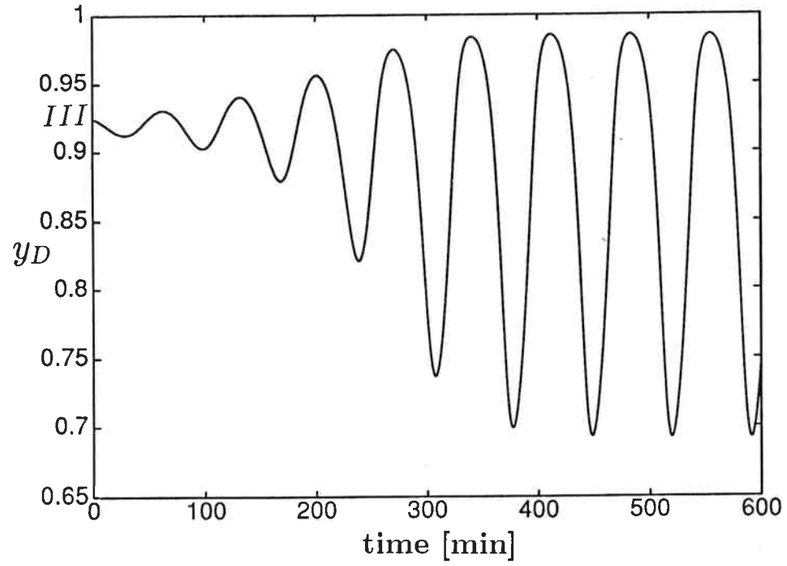

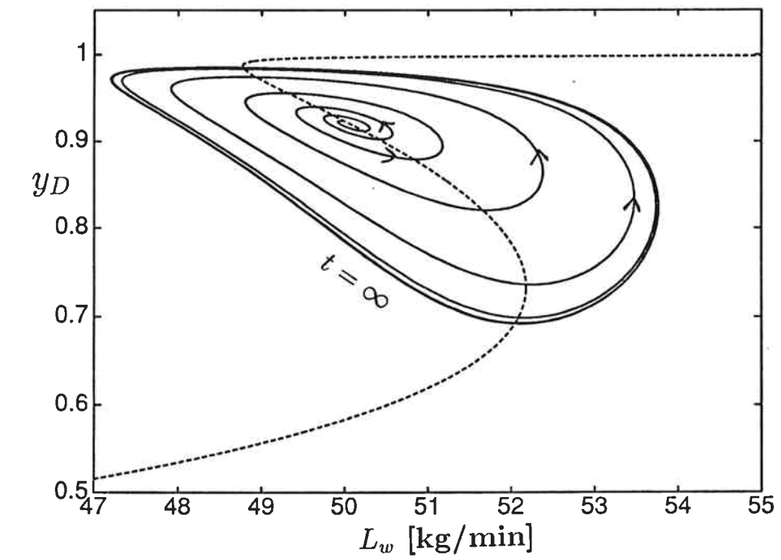

Figure 3.9: Nonlinear simulation of methanol- propanol column with one-point control of top-composition y_D using mass reflux L_w. Controller gain reduced by a factor of 2 compared to Figure 3.8. Upper plot: Time as independent variable. Lower plot: Phase-plane plot. Dashed line shows steady-state solutions. Constant molar flows.

e.g., Skogestad et.al., 1988). This implies that we may include model uncertainty in the design. We use a relative uncertainty weight in each channel given by

$$w_I(s) = 0.20\frac{5\theta_d s + 1}{0.5\theta_d s + 1} \tag{3.27}$$

This means that we allow for a deadtime θ_d in addition to 20 % uncertainty in each input. The performance weight used is given by

$$w_P(s) = \frac{1}{P}\frac{\tau_{CL}s + P}{\tau_{CL}s} \tag{3.28}$$

This implies that the worst case peak of $\bar{\sigma}(S)$ should be less than P, and that the closed-loop time-constant should be less than τ_{CL}. We design single-loop controllers[3] for different values of θ_d, and for each design we adjust the performance weight until a μ-value of 1 is achieved. This is done by first increasing τ_{CL} and then increasing P if necessary. A μ-value of 1 implies that we can guarantee the specified performance for all plants within the model uncertainty.

We will again consider operating point III of the methanol-propanol column with a RHP pole at 0.086 min^{-1}. We use single-loop PID-controllers as this is the preferred control structure in the industry, and also close to optimal (Skogestad and Lundström, 1990). Table 3.3 gives the results for designs with θ_d between 1 and 5 minutes. For a deadtime of 1 min. we see from Table 3.3 that there is only a small difference between the achieved robust performance of the unstable process and the stable model. When the deadtime is increased we must allow for a lower bandwidth as well as a higher peak in the sensitivity function for the open-loop unstable process than for the open-loop stable model. This is as expected from (3.24). For a deadtime of 2 minutes we can only guarantee half the bandwidth for the unstable system compared to the stable model. With a deadtime of 5 minutes (RHP zero $z \approx 0.4min^{-1}$) the response for the LV-configuration is poor (τ_{CL} = 175 min. with a maximum peak P = 3.0), while the response for the L_wV-configuration is unacceptable (τ_{CL} = 455 min. and P = 6.0). This implies that when the operating point is open-loop unstable (with the L_wV-configuration) and the system in addition has significant deadtime one should consider using a different configuration.

[3]Note that decouplers will perform poorly on ill-conditioned plants due to uncertainty sensitivity.

	LV		L_wV	
θ_d [min]	P	τ_{CL} [min]	P	τ_{CL} [min]
1.0	2.5	25	2.5	32
2.0	2.5	59	2.5	140
3.0	2.5	100	3.0	227
4.0	2.5	161	5.0	345
5.0	3.0	175	6.0	455

Table 3.3: Robust performance parameters (see (3.28)) obtained for stable LV-configuration and unstable L_wV-configuration in operating point III of the methanol-propanol column. All parameters for minimized μ_{RP}=1.00 using two single-loop PID controllers.

	k_y	τ_{Iy}	τ_{Dy}	k_x	τ_{Ix}	τ_{Dx}
LV-configuration	0.0687	6.55	2.33	0.0680	5.29	0.180
L_wV-configuration	4.064	32.27	2.91	0.0280	4.79	0.209

Table 3.4: Controller parameters for closed-loop simulations in Figure 3.10. (Correspond to last entry in Table 3.3)

Nonlinear Simulations. Figure 3.10 shows responses to setpoint changes in top composition y_D using two single loop PID-controllers for the LV-configuration and the L_wV-configuration. The simulations include 5 minutes deadtime (using a 1.order Padé approximation) and 20 % input uncertainty. The controller parameters were obtained from the μ-optimal design above, and are given in Table 3.4. The simulations demonstrate the fact that the performance for the case with mass-reflux is clearly worse than for the case with molar reflux. The L_wV-configuration has a much larger overshoot as well as a longer settling period.

3.5 Effect of Including the Energy Balance

To this point we have only considered models with constant molar flows, that is, with the energy balance excluded. However, Jacobsen and Skogestad (1991) show that when the energy balance is included in the model, even molar inputs may yield multiplicity and instability in distillation. The multiplicity is in this case caused by interactions between the flows and compositions inside the column. The flows will affect the compositions through the material balance while the compositions will affect the flows through the energy balance.

Figure 3.11 shows steady-state solutions for the methanol-propanol column with the LV-configuration and the energy balance included in the model. The enthalpy data used are given in Table 3.5. The maximum eigenvalues in selected operating points are also shown in Figure 3.11 and we see that the solution branch with a negative slope between molar reflux L and top composition y_D corresponds to unstable solutions. Note that the eigenvalues were computed with a static energy balance, that is, the energy dynamics were neglected.

To consider the stability properties for the LV-configuration with the energy balance

$$H_i^L = 16.67e^{-1.087x_i}$$
$$H_i^V = 13.49e^{-3.98x_i} + 43.97e^{-0.088x_i}$$

- Reference state: Pure components as liquid at $0°C$.
- x_i denotes mole fraction methanol in liquid phase.

Table 3.5: Saturated molar enthalpies (kJ/mol) for methanol-propanol system at a pressure of 1 atm.

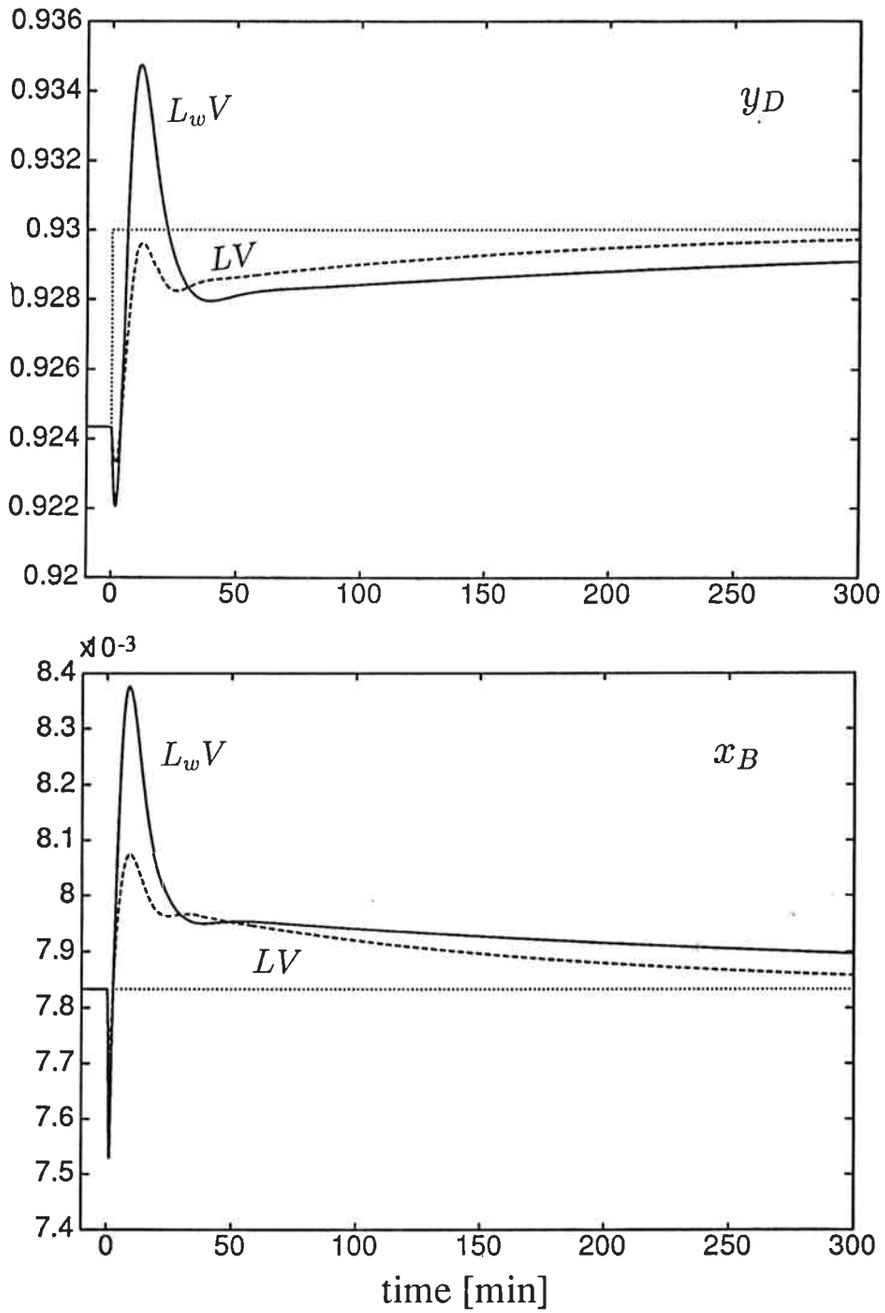

Figure 3.10: Nonlinear simulation of methanol- propanol column at operating point III with two-point control using LV- and L_wV-configuration. Response to a setpoint change in y_D using two single-loop PID controllers. Deadtime θ_d = 5min. PID-settings from Table 3.4. Constant molar flows.

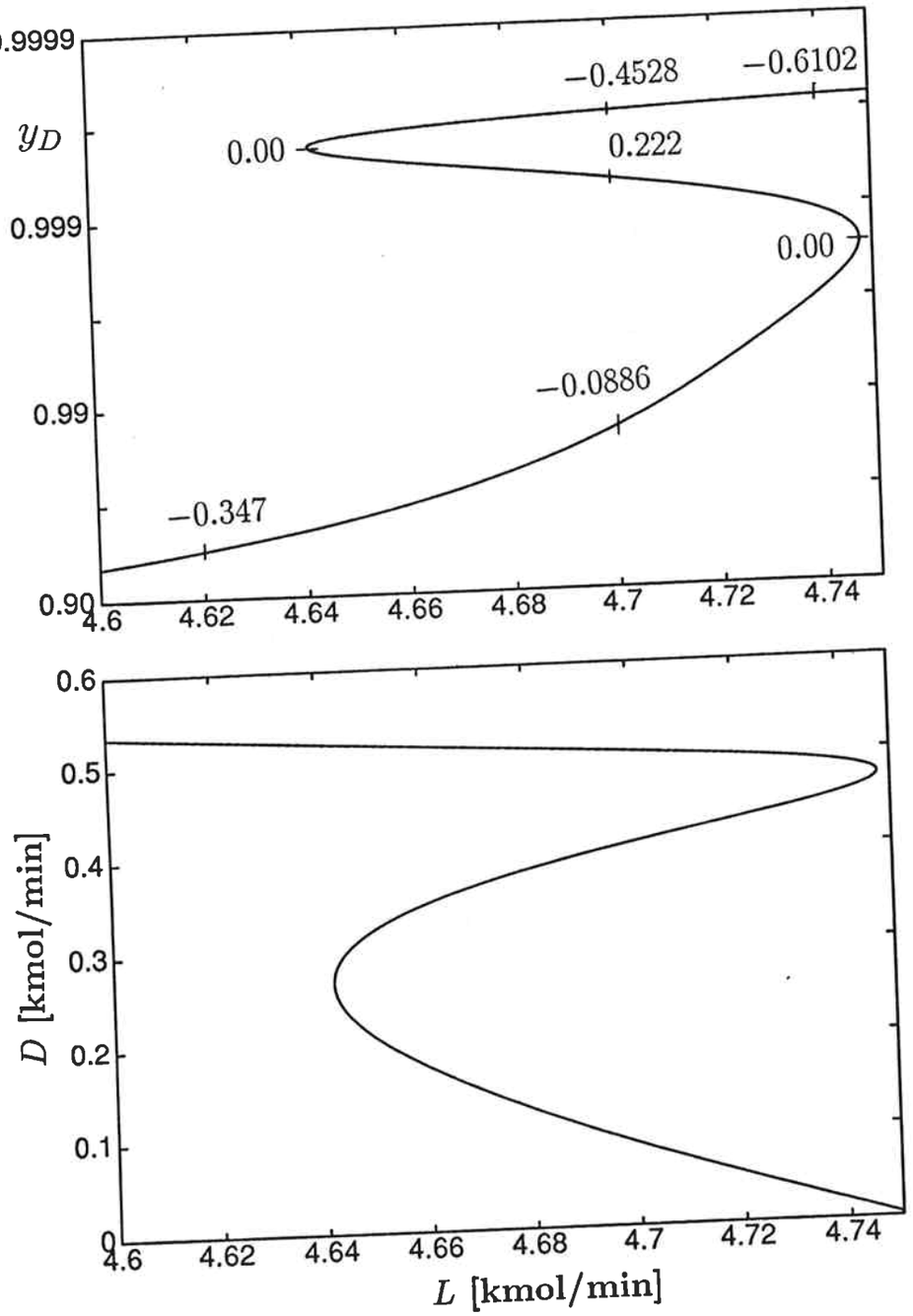

Figure 3.11: Steady-state solutions as a function of molar reflux L for methanol-propanol column with energy balance included. The maximum eigenvalue is shown in selected operating points. Boilup $V = 4.5$ kmol/min.

	L [kmol/min]	D [kmol/min]	y_D	x_B
I	4.60	0.535	0.9324	2.474e-3
II	4.70	0.505	0.9845	6.344e-3
III	4.70	0.406	0.9993	0.1587
IV	4.70	0.0866	0.9997	0.4526

- Energy balance included in model.

Table 3.6: Steady-state solutions for methanol-propanol column with boilup V=4.5 kmol/min.

included we utilize the fact that the DV-configuration in all known cases yields unique solutions (Sridhar and Lucia, 1989, Jacobsen and Skogestad, 1991) which are stable under the assumption of perfect level control (see section 3.7 below). The transfer function from molar reflux L to top composition y_D may be written

$$\left(\frac{\partial y_D}{\partial L}\right)_V(s) = \left(\frac{\partial y_D}{\partial D}\right)_V(s)\left(\frac{\partial L}{\partial D}\right)_V^{-1}(s) \tag{3.29}$$

As before we assume that the composition dynamics for the stable case may be approximated by a first-order response, i.e.,

$$\left(\frac{\partial x_i}{\partial D}\right)_V(s) \approx \frac{k_{x_iD}^{DV}}{1+\tau_1 s} \tag{3.30}$$

A material balance around the condenser yields (assuming perfect level control)

$$L = V_T - D \tag{3.31}$$

where V_T denotes vapor flow to the condenser. For simplicity we neglect changes in the liquid enthalpy with composition, and obtain from an overall static energy balance (saturated liquid feed)

$$V_T = \frac{\Delta H_1^{vap}}{\Delta H_T^{vap}} V \tag{3.32}$$

Here the "heat of vaporization", ΔH_i^{vap}, is the enthalpy of the vapor with each component as pure saturated liquid as reference. (See Appendix for details.) Inserting (3.32) in the material balance (3.31) and differentiating, with ΔH^{vap} a function of composition x only (saturated vapor at constant pressure), yields for a binary mixture

$$\left(\frac{\partial L}{\partial D}\right)_V(s) = -1 + V\frac{\left(\frac{d\Delta H^{vap}}{dx}\right)_{x=x_B}\left(\frac{\partial x_B}{\partial D}\right)_V(s)\Delta H_T^{vap} - \left(\frac{d\Delta H^{vap}}{dx}\right)_{x=x_T}\left(\frac{\partial x_T}{\partial D}\right)_V(s)\Delta H_1^{vap}}{(\Delta H_T^{vap})^2} \tag{3.33}$$

Inserting (3.30) and (3.33) into (3.29) we find that the largest pole of $(\partial y_d/\partial L)_V(s)$ will be

$$\lambda_{max} = -\frac{1}{\tau_1}\left(1 - V\frac{\left(\frac{d\Delta H^{vap}}{dx}\right)_{x=x_B} k^{DV}_{x_BD}\Delta H^{vap}_T - \left(\frac{d\Delta H^{vap}}{dx}\right)_{x=x_T} k^{DV}_{x_TD}\Delta H^{vap}_1}{(\Delta H^{vap}_T)^2}\right) \tag{3.34}$$

Comparing (3.34) and (3.33) we see that the pole will be in the right half plane when $(\partial L/\partial D)_V$ is positive. This is in accordance with the results presented in Jacobsen and Skogestad (1991).

From (3.34) we see that the probability of instability for the LV-configuration will increase with internal flows (i.e., V). This is similar to what was found for the instability caused by the input transformation with the L_wV-configuration. If we assume ideal vapor phase, then $d\Delta H^{vap}/dx = \Delta H^{vap}_L - \Delta H^{vap}_H$ which is the difference in heats of vaporization for the light and heavy component at their normal boiling point. Thus, for the normal case where the most volatile component has the smallest heat of vaporization $(d\Delta H^{vap}/dx_i < 0)$ instability is most likely when we have $|k^{DV}_{x_BD}|$ large relative to $|k^{DV}_{x_TD}|$, which corresponds to having high purity in the top relative to the bottom. Note that this is different from what was found for the L_wV-configuration where instability was found to be most likely with intermediate purities in the top (unpure relative to bottom.)

The singularity caused by interactions between the material and energy balance corresponds to a bifurcation point with a single pole crossing the imaginary axis, similar to what was found for constant molar flows with the L_wV-configuration. The control problems will therefore be similar to what was discussed in section 3.4.

3.5.1 Combining mass flows and energy balance

Jacobsen and Skogestad (1991) show that when both types of multiplicities are present in the same region of operation, a column operating with the L_wV-configuration may have five different solutions, two of which will be unstable. This is illustrated in Figure 3.12 which shows solutions for the methanol-propanol column with L_w in the range 84 to 91 kg/min and $V = 2.7$ kmol/min. In the same figure is also shown the maximum eigenvalue as a function of top composition y_D. The bifurcation (singular) points at low purities in the top are due to singularities between mass reflux and molar reflux, while those at high purities are due to singularities between molar reflux and top composition.

3.6 Other Bifurcation Parameters

So far we have only considered the inputs, e.g. reflux L_w and boilup V, as potential bifurcation parameters. That is, in all studies we have assumed the other parameters, e.g., feed flow F, feed composition z_F, feed liquid fraction q_F, tray efficiency etc., to be fixed. However, it is clear that these parameters will vary during operation and may, similarly to the inputs, cause the column operation to go from open-loop stable to open-loop unstable.

To illustrate this consider Figure 3.13 which shows steady-state solutions for the methanol-propanol column (assuming constant molar flows) with $L_w = 50.0$ kg/min,

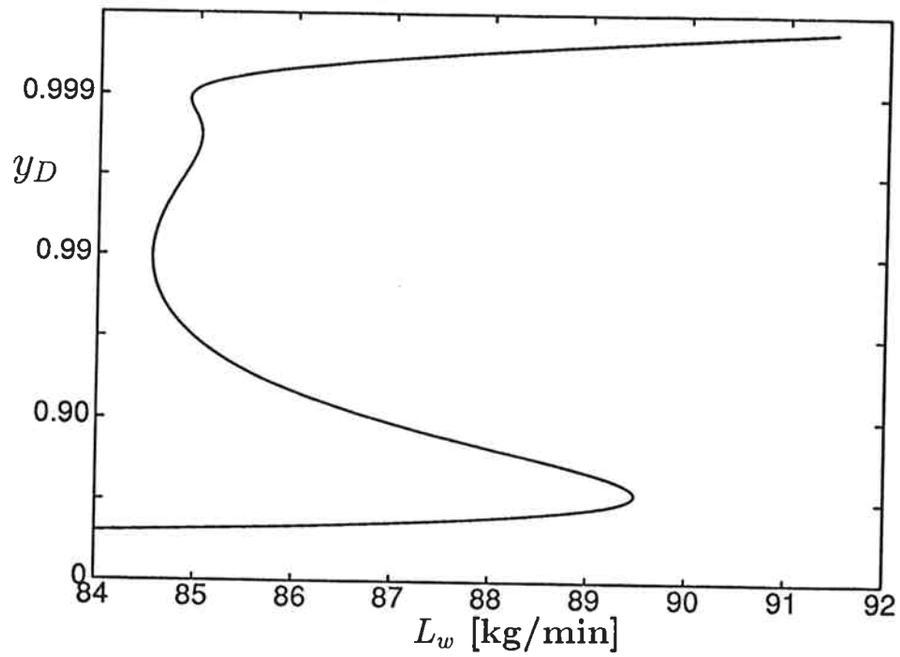

Figure 3.12: Steady-state solutions as a function of mass reflux L_w for methanol-propanol column with energy balance included in model. Lower plot shows the maximum eigenvalue as a function of top composition y_D. Boilup $V = 2.7$ kmol/min.

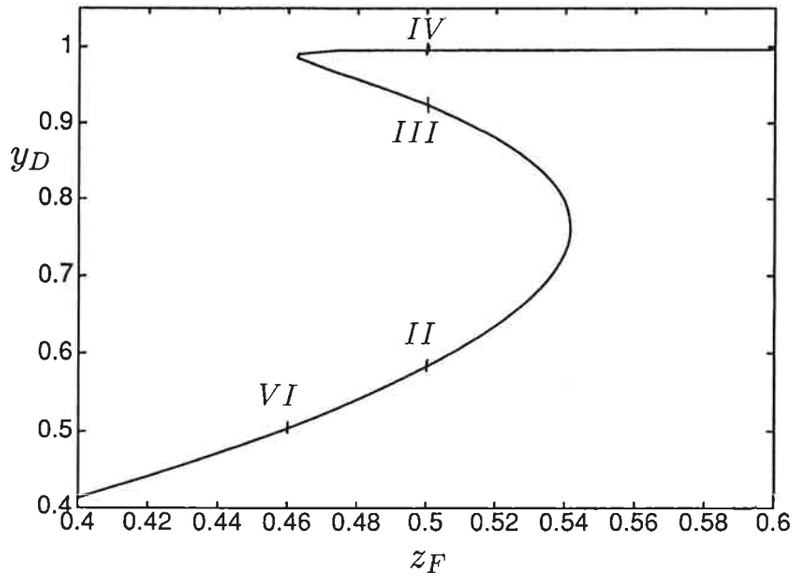

Figure 3.13: Steady-state solutions as a function of feed composition z_F for methanol-propanol column. Reflux $L_w = 50$ kg/min, Boilup $V = 2.0$ kmol/min. Constant molar flows.

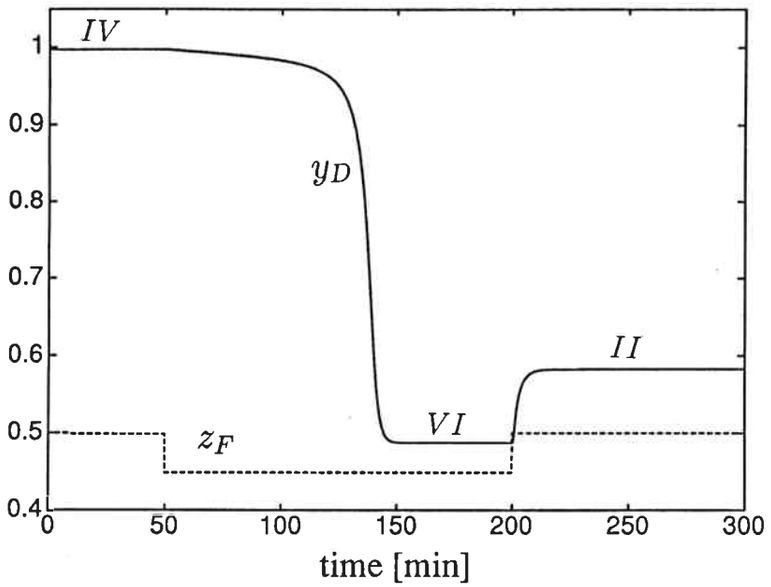

Figure 3.14: Nonlinear open-loop simulation of changes in feed-composition z_F for methanol-propanol column. Reflux $L_w = 50$ kg/min and boilup $V = 2.0$ kmol/min. Roman numbers $II - IV$ refer to Table 3.2 with $z_F = 0.50$. Operating point VI corresponds to $z_F = 0.46$. Constant molar flows.

$V = 2.0$ kmol/min and feed composition z_F in the range 0.40 to 0.60. From the figure we see that there are multiple solutions for z_F in the range 0.46 to 0.54. This implies that disturbances in the feed composition may cause the column to go through a singular point and thereby "jump" to another solution branch. This is illustrated in Figure 3.14 which shows the response in top composition y_D to a change in feed composition z_F from 0.50 (operating point IV in Table 3.2) to 0.46. The figure illustrates how the top composition "jumps" to the lower solution branch and settles in operating point VI. When the feed composition returns to $z_F = 0.50$ the solution remains on the lower branch and settles in operating point II.

3.7 Instability with the $D_w V$-Configuration

We have so far only considered using reflux and boilup as independent variables, e.g., the $L_w V$-configuration. This is also the most widespread configuration in industry. However, there are many different configurations that may be used. For instance, changing condenser level control from using distillate D_w to using reflux L_w results in the $D_w V$-configuration. For all the examples we have have studied this configuration yields a unique steady-state solution in terms of compositions. Furthermore, we have assumed perfect level control, in which the operating point is found to be asymptotically stable. However, here we show that without the assumption of perfect level control the operating point may become unstable also with the $D_w V$-configuration. We start by considering an example and will then explain the results thereof using analytical results.

Example. We will again consider the methanol-propanol column in Table 3.1. The holdups in the reboiler and condenser are increased to $M_D/F = M_B/F = 5.0$ min. We consider the case with constant molar flows, and use distillate flow D_w and boilup V as independent inputs, i.e., $D_w V$-configuration. With this configuration the condenser level is controlled by reflux L_w and the reboiler level is controlled by bottoms flow B_w. The nominal operating point we consider has D_w=18.36 kg/min and V=2.0 kmol/min. For these specifications we obtain y_D=0.9237 and x_B=0.0078, and the steady-state is unique. Note that the operating point corresponds to solution III for the $L_w V$-configuration in

	y_D	x_B	D	λ_{max}
I	0.5207	2.024e-3	0.9601	-0.5323
II	0.9673	6.756e-3	0.5135	7.327e-2
III	0.9978	7.251e-2	0.4620	-1.744e-2
IV	0.99855	0.1236	0.4302	1.7512e-2
V	0.99908	0.2321	0.3493	-5.608e-2

- Energy balance included in model.

Table 3.7: Steady-state solutions for methanol-propanol column with L_w=85 kg/min and $V = 2.7$ mol/min.

Table 3.2 and Figure 3.2, that is, the operating point is unstable with reflux and boilup as independent variables.

We now consider the stability of the of the operating point for different gains K_{M_D} in the condenser level controller. A pure proportional controller is used, i.e., $dL_w(s) = K_{M_D} dM_{Dw}(s)$. We assume perfect level control in the reboiler. Figure 3.15a shows the response in top composition to a small increase in D_w, keeping V constant, with level control gain K_{M_D}=0.10. We see that the response is stable and slightly oscillatory. Figure 3.15a also shows the phase plot of top composition y_D against mass bottoms flow B_w, and we see that the steady-state is a stable spiral attractor. Figure 3.15b shows the corresponding response with K_{M_D}=0.05. The response is now more oscillatory, but the steady-state is still a stable spiral attractor. With K_{M_D} reduced to 0.03 the operating point becomes an unstable spiral as seen from Figure 3.15c. However, the response settles into a stable periodic solution, that is, a stable limit cycle.

The fact that the steady-state changes from a stable spiral to an unstable spiral as the level control gain is reduced implies that a pair of complex conjugate eigenvalues cross the imaginary axis. This may be seen from Figure 3.16a which shows the largest eigenvalues as a function of level control gain K_{M_D}, i.e., the root locus. We see that as the gain is reduced below a value of 0.043, the eigenvalues cross the imaginary axis, and the operating point becomes unstable. The fact that a stable limit cycle appears as the steady-state becomes unstable, implies that the system undergoes a dynamic bifurcation known as the Hopf bifurcation.

3.7.1 Analytical treatment

To understand why the steady-state for the D_wV-configuration becomes unstable, consider the transfer function $(\partial y_D/\partial D_w)_V(s)$ which may be written

$$\left(\frac{\partial y_D}{\partial D_w}\right)_V(s) = \left(\frac{\partial y_D}{\partial L_w}\right)_V(s)\left(\frac{\partial L_w}{\partial D_w}\right)_V(s) \tag{3.35}$$

Here the transfer function $(\partial y_D/\partial L_w)_V(s)$ expresses the effect of reflux on top composition with the L_wV-configuration, and we have seen that it may be unstable with a single RHP pole. For simplicity we consider only the largest pole in the transfer function

$$\left(\frac{\partial y_D}{\partial L_w}\right)_V(s) = \frac{k^{L_wV}}{s-a} \tag{3.36}$$

Here a denotes the maximum eigenvalue for the L_wV-configuration. The transfer function $(\partial L_w/\partial D_w)_V(s)$ may be computed from a material balance around the condenser

$$dL_w(s) = \frac{K_{M_D}}{s}(dV_{Tw}(s) - dL_w(s) - dD_w(s)) \tag{3.37}$$

Differentiation of (3.37) yields

$$\left(\frac{\partial L_w}{\partial D_w}\right)_V(s) = \frac{K_{M_D}}{K_{M_D}+s}(V_T(M_1-M_2)\left(\frac{\partial y_T}{\partial D_w}\right)_V(s) - 1) \tag{3.38}$$

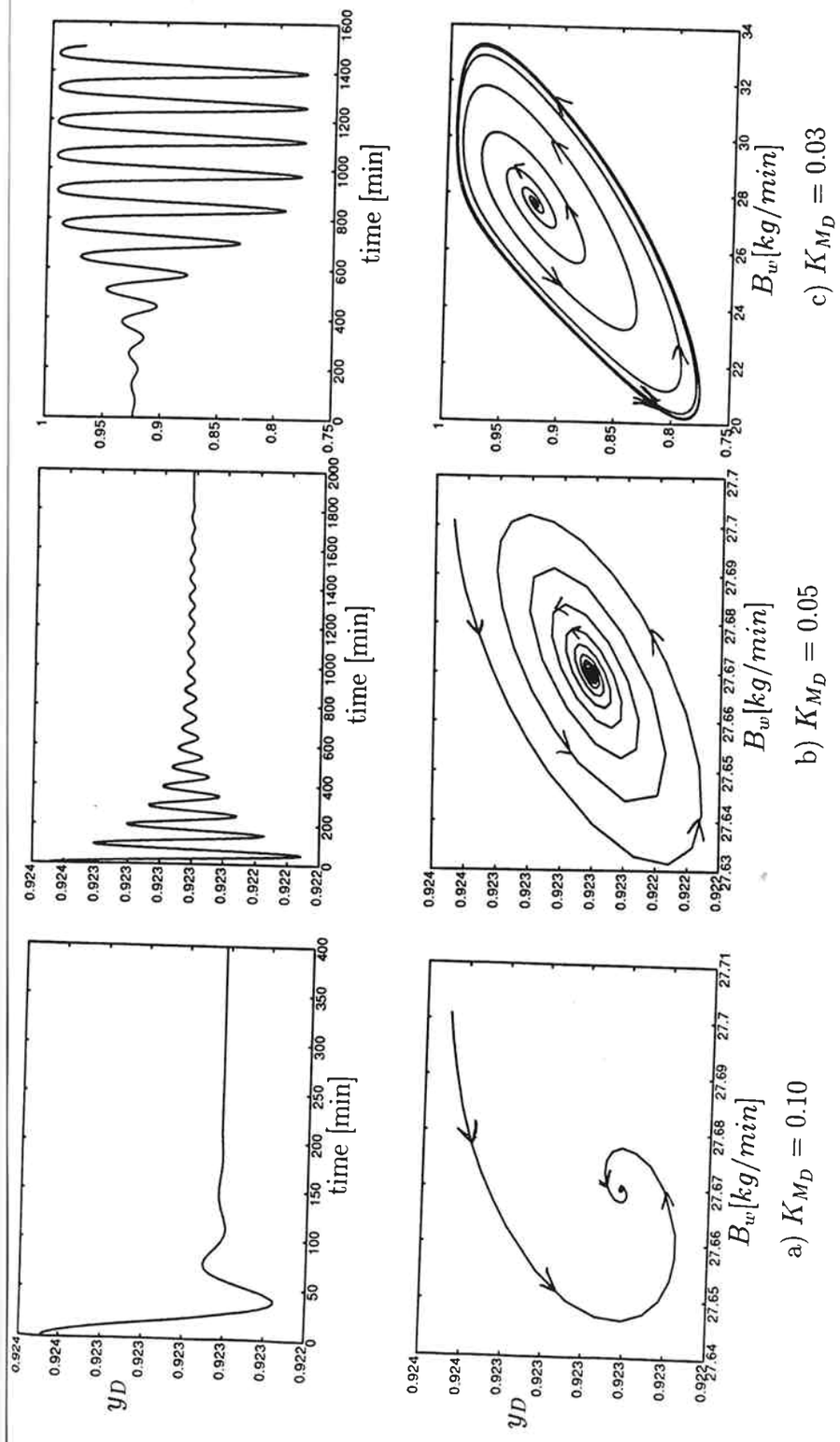

Figure 3.15: Nonlinear open-loop simulation of methanol-propanol column with D_wV-configuration. Responses to small increase in D_w with different gains K_{M_D} in condenser level controller. a) K_{M_D}=0.10. b) K_{M_D}=0.05 c) K_{M_D}=0.03. Upper plot: time as independent variable. Lower plot: Phase-plane plot. Boilup V=2.0 kmol/min. Constant molar flows.

Here y_T denotes the composition of V_T. We assume negligible condenser holdup so that $(\partial y_T/\partial D_w)_V(s) = (\partial y_D/\partial D_w)_V(s)$. Inserting (3.36) and (3.38) into (3.35) yields

$$\left(\frac{\partial y_D}{\partial D_w}\right)_V(s) = \frac{K_{M_D}k^{L_wV}}{s^2 + (K_{M_D} - a)s - K_{M_D}(a + k^{L_wV}V_T(M_1 - M_2))} \tag{3.39}$$

The poles of the transfer function (3.39) become

$$\lambda_{1,2} = -\frac{1}{2}(K_{M_D} - a) \pm \frac{1}{2}\sqrt{(K_{M_D} - a)^2 + 4K_{M_D}(a + k^{L_wV}V_T(M_1 - M_2))} \tag{3.40}$$

Figure 3.16b shows the root locus for the example computed using equation (3.40), and we see that the simple expression (3.40) yields a reasonable prediction of the behavior of the full model in Figure 3.16a.

Let us now use (3.40) to consider the stability of the D_wV-configuration for the two cases when the pole a of the L_wV-configuration is in the LHP and RHP, respectively:
1) Stable L_wV-configuration, $a < 0$: In this case the first term in (3.40) is negative for all values of $K_{M_D} > 0$. Furthermore, the second term under the root in (3.40) is negative and the root will be real with a value less than $(K_{M_D} - a)$ or it will be imaginary. This implies that both eigenvalues in (3.40) are in the LHP, that is, the D_wV-configuration is stable for all values of $K_{M_D} > 0$.
2) Unstable L_wV-configuration, $a > 0$: In this case we have that the first term in (3.40) is positive if $K_{M_D} < a$, that is, at least one of the eigenvalues in (3.40) are in the RHP with $K_{M_D} < a$. The size of K_{M_D} will determine whether the root in (3.40) is imaginary. For $K_{M_D} = a$, i.e., the bifurcation point, we have that the root is imaginary if $k^{L_wV}V_T(M_1 - M_2) < -a$, which is the case in all examples we have studied.

We conclude from the above analysis that a prerequisite for instability with the D_wV-configuration is that the operating point is unstable with the L_wV-configuration. This is not too surprising as the level control for the D_wV-configuration may be viewed as a feedback effect on the L_wV-configuration. If the feedback control is not tight enough, we are not able to stabilize the column, which is similar to what we found for the case of one-point control with the L_wV-configuration. With a gain K_{M_D}=0, i.e., no condenser level control, we see from (3.40) that there will be a RHP pole at a (in addition to a pole at 0), and we effectively have the stability properties of the L_wV-configuration. This may also be seen from the root locus in Figure 3.16a for K_{M_D}=0.

In our example we find that the L_wV-configuration is unstable with a pole $a = 0.047$ (with $M_D/F = M_B/F = 5min.$) and from (3.40) we predict instability for the D_wV-configuration with $K_{M_D} < 0.047$. From the full model we find that instability occurs for $K_{M_D} < 0.043$. The deviation in predicted and computed value is explained by our assumptions of first-order response in (3.36) and negligible condenser holdup in the analytical treatment.

We have shown that the operating points with the D_wV-configuration may become unstable with two complex conjugate eigenvalues crossing the imaginary axis. However, we have seen from the example that a stable limit cycle appears as the steady-state solution goes unstable. The proof of the existence of a stable limit cycle is rather involved for a high-order dynamic model, and is therefore left out here.

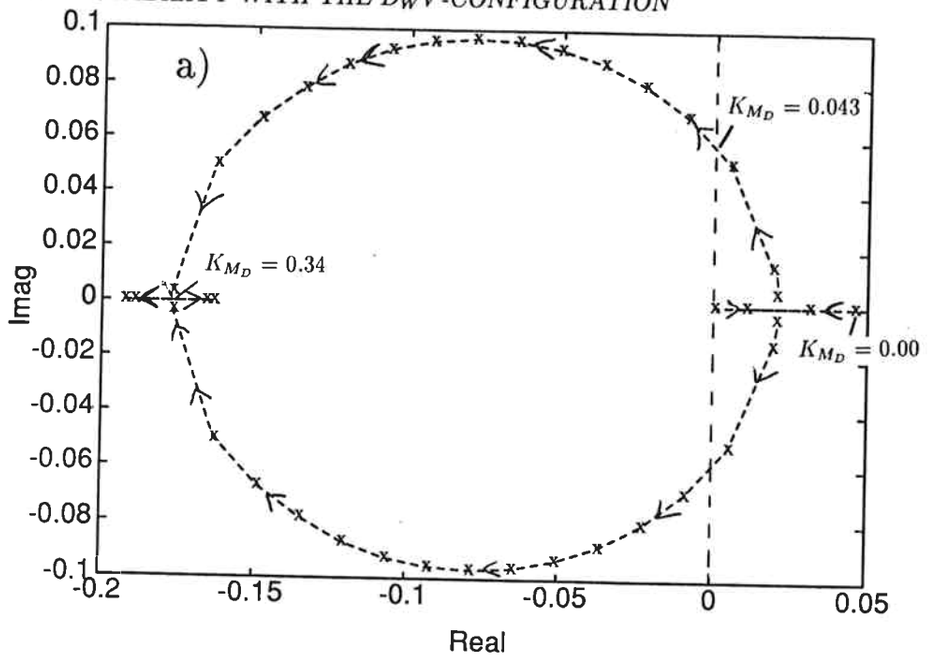

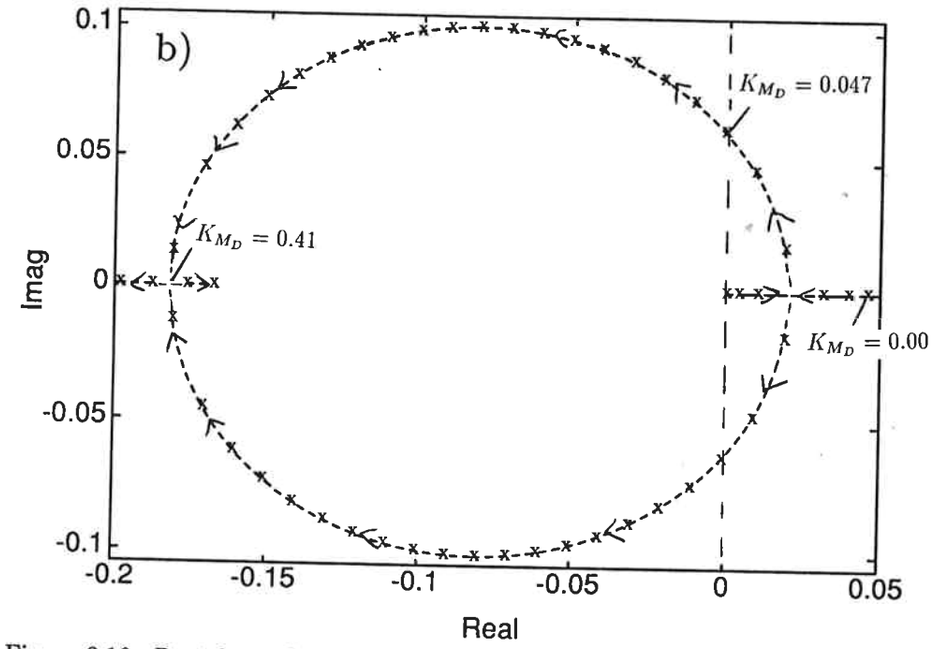

Figure 3.16: Root locus for methanol-propanol column with constant molar flows and D_wV configuration. D_w=18.36 kg/min and V=2.0 kmol/min. Plot shows maximum eigenvalues as function of gain K_{M_D} in condenser level controller (arrows indicate increasing gain). a) Eigenvalues computed from full model. b) Eigenvalues computed from simple expression (3.40).

3.8 Discussion

Other Configurations. We have in this paper only considered two configurations, namely the L_wV- and D_wV-configuration. We have shown that with the L_wV-configuration, the operating points may be open-loop unstable with a single RHP pole. This instability is linked to the existence of multiple steady-state solutions and is independent of the level control tuning. To stabilize an unstable operating point with the L_wV-configuration, feedback control of a temperature or composition is required. For the D_wV-configuration we have shown that instability may result if the level control is not sufficiently tight. Many other configurations are of course also possible, and the type of instability found for the D_wV-configuration is likely to be found with other configurations. For instance, the L_wB_w-configuration may become unstable with too slow reboiler level control. However, Jacobsen and Skogestad (1991) show that output multiplicity and the corresponding type of instability is unlikely with other flows than reflux and boilup as independent variables. Because relatively tight level control usually is easily achieved, one may in most cases avoid instability with the L_wV-configuration by changing to another configuration. However, note that different configurations will also have different control properties like interactions and disturbance sensitivity (e.g., Skogestad et.al., 1990). The choice of a proper configuration should therefore not only be based on open-loop stability properties.

Detecting open-loop instability experimentally. There are several ways to determine whether a column under operation will be open-loop unstable with reflux and boilup as independent variables.

1. L_wV-configuration with one loop closed:

- Increasing the purity in the top of the column corresponds to decreasing reflux, which is opposite to what one would expect. Similar behavior will be seen in the bottom, i.e., increasing purity corresponds to decreasing boilup.
- Detuning the controller makes the column go into a stable limit cycle.
- Turning the controller off causes the column profile to drift away. However, it may be difficult to distinguish this from a "slow" column with a stable pole close to the imaginary axis.

2. Using other configurations:.

- If an increase in distillate flow, i.e., decreasing y_D, results in increased reflux, the operating point will be unstable with the L_wV-configuration. Similarly, if boilup increases when bottoms flow is increased the operating point will be unstable with the L_wV-configuration.

Effect of column design. The methanol-propanol column that we have studied in this paper is not optimally designed for the product compositions of operating point *III* in Table 3.2. In fact it is doubtful that the column would be unstable when optimally designed as the internal flows then would be significantly smaller. This is probably true for many separations, i.e., an optimally designed column will be open-loop stable. However, few industrial columns are operated close to an optimal operating point. One reason is that the desired compositions will change after the column is built. In addition, many operators prefer to use high internal flows (over-purification) in order to assure that specifications are kept when disturbances enter the column. It is therefore likely that many industrial columns may have problems with open-loop instability. The fact that this has not been

reported previously is probably due to the fact that open-loop instability has been believed to be impossible, and problems have therefore been explained by other means.

3.9 Conclusions

1. Two-product distillation columns operating with reflux and boilup as independent inputs may be open-loop unstable with a single right half plane pole. Two different effects may cause the instability:
   - Possible singularities in the transformation between the actual input units and the molar units which determine separation.
   - Possible singularities between molar flows and compositions due to interactions through the material and energy balance.

   In both cases the probability of instability is increased with increased internal flows.
2. An unstable operating point may be stabilized by use of one-point control provided the bandwidth of the controller is sufficiently high, that is, if the measurement delay is sufficiently small. If an operating point becomes closed-loop unstable due to a too low bandwidth, the column may go into a stable limit cycle provided there exists stable solutions above and below the unstable solution.
3. The presence of open-loop instability will worsen the performance of the closed-loop system. This will become more marked as the deadtime in the system is increased.
4. Distillation columns operating with distillate flow and boilup as independent variables may have unstable operating points if the condenser level control is not sufficiently tight. The instability will in this case correspond to a Hopf bifurcation, that is, a pair of complex conjugate eigenvalues cross the imaginary axis and a stable limit cycle appears. A prerequisite for instability with this configuration is that the operating point is unstable with reflux and boilup as independent variables.

Acknowledgements: Financial support from the Royal Norwegian Council for Scientific and Industrial Research (NTNF) is greatfully acknowledged.

APPENDIX. Simplification of the energy balance.

The static energy balance on a single tray may be written (no external heating or cooling)

$$V_{i-1}H^V_{i-1} + L_{i+1}H^L_{i+1} - V_iH^V_i - L_iH^L_i + F_iH^F_i = 0 \tag{3.41}$$

Here subscript i denotes tray-number (reboiler is tray 1), H^V and H^L denotes vapor and liquid enthalpies respectively and H^F feed enthalpy.

As reference state for enthalpies we select pure components as saturated liquids. Then, under the assumptions of no heat of mixing, equal heat capacities for the components and linear boiling point curve we get $H^L_i = 0$ on all trays (this is a common assumption in distillation which yields "constant molar flows" if we in addition assume the same heat of vaporization for all components.) Also assume that the feed is saturated liquid so that $H^F_i = 0$. With these assumptions the energy balance (3.41) becomes

$$V_i\Delta H^{vap}_i = V_{i-1}\Delta H^{vap}_{i-1} \quad ;\Delta H^{vap}_i = H^V_i \tag{3.42}$$

An overall static energy balance then yields

$$V_T\Delta H^{vap}_T = V_1\Delta H^{vap}_1 \tag{3.43}$$

NOMENCLATURE (see also Figure 3.1)

A - State matrix of distillation column
B - bottoms flow (kmol/min)
c - controller
D - distillate flow (kmol/min)
F - feed rate (kmol/min)
g - process transfer function
H^F - enthalpy of feed (kJ/mol)
H^L - saturated liquid enthalpy (kJ/mol)
H^V - saturated vapor enthalpy (kJ/mol)
ΔH^{vap} - $(= H^V - H^L)$ heat of vaporization (for mixture)
K_{M_D} - condenser level control gain
$k^{u_1u_2}_{yu_1}$ - steady-state gain from input u_1 to output y with u_1u_2-configuration.
L - reflux flow rate (kmol/min)
LHP - left half plane
M - molecular weight, usually of top product (kg/kmol)
M_1 - pure component molecular weight of most volatile component (kg/kmol)
M_2 - pure component molecular weight of least volatile component (kg/kmol)
M_L - tray liquid holdup (kmol)
M_D - condenser holdup (kmol)
M_B - reboiler holdup (kmol)
N - no. of theoretical stages in column
N_F - feed stage location (1-reboiler)
P - maximum allowed peak on sensitivity function
p - right half plane pole (min^{-1})

Q_B - heat input to reboiler
Q_D - heat removal in condenser
q_F - liquid fraction in feed
RHP - right half plane
S - sensitivity function
V - boilup from reboiler (kmol/min) (determined indirectly by heating Q)
V_T - vapor flow to condenser (kmol/min)
x_B - mole fraction of most volatile component in bottom product
x_i - mole fraction of most volatile component at tray i
y_D - mole fraction of most volatile component in distillate (top product)
y_T - mole fraction of most volatile component in V_T.
z - right half plane zero (min^{-1})
z_F - mole fraction of most volatile component in feed

Greek symbols

$\alpha = \frac{y_i/x_i}{(1-y_i)/(1-x_i)}$ - relative volatility (binary mixture)
$\lambda_i(A)$ - i'th eigenvalue of A.
$\lambda_{max} = \max_i |\lambda_i(A)|$- maximum eigenvalue = dominant pole
μ - structured singular value
$\bar{\sigma}$ - maximum singular value
τ_{CL} - required closed-loop time constant (min)
θ_d - deadtime (min)
ω - frequency (min^{-1})

Subscripts

w - flow rate in kg/min
H - least volatile component
L - most volatile component

REFERENCES

Acrivos, A. and N.R. Amundson, 1955, "Application of Matrix Mathematics to Chemical Engineering Problems", *Ind.Eng.Chem.*, **47**, 8, 1533-1541

Davidson, J.F., 1956, "The Transient Behavior of Plate Distillation Column", *Trans.Inst.Chem.En.* **34**, 44-52.

Doherty, M.F. and J.D. Perkins, 1982, "On the Dynamics of Distillation Processes-IV. Uniqueness and Stability of the Steady-State in Homogeneous Continuous Distillation", *Chem.Eng.Sci*, **37**, 3, 381-392

Freudenberg, J.S. and D.P. Looze, 1985, "Right Half Plane Poles and Zeros and Design Tradeoffs in Feedback Systems", *IEEE Trans.Autom.Control*, **AC-30**, 555-565.

Freudenberg, J.S. and D.P. Looze, 1988, "Frequency Domain Properties of Scalar and Multivariable Feedback Systems", Springer-Verlag

Jacobsen, E.W. and S. Skogestad, 1991, "Multiple Steady-States in Ideal Two-Product Distillation", *AIChE J.*, **37**, 4, 499-511.

Lapidus, L. and N.R. Amundson, 1950, "Stagewise Absorption and Extraction Equipment - Transient and Unsteady State Operation", Ind.Eng.Chem., **42**, 1071-1078.

Looze, D.P. and J.S. Freudenberg, 1991, "Limitations of Feedback Properties Imposed by Open-Loop Right Half Plane Poles", *IEEE Trans.Autom.Control*, **36**, 6, 736-739.

Luyben, W. L., 1979, "Introduction and Overview of Distillation Column Control", AIChE Workshop, Tampa, FL.

Rosenbrock, H.H., 1960, "A Theorem of "Dynamic Conservation" for Distillation", *Trans.Instn. Chem.Engrs.*, **38**, 20, 279-287.

Rosenbrock, H.H., 1962, "A Lyapunov Function with Applications to Some Nonlinear Physical Problems", *Automatica*, **1**, 31-53.

Shinskey, F.G., 1984, *Distillation Control*, 2nd ed., McGraw-Hill, New York.

Sridhar, L.N. and A. Lucia, 1989, "Analysis and Algorithms for Multistage Separation Processes", *I & EC Res.*, **28**, 793-803.

Skogestad, S. and M. Morari, 1987, "The Dominant Time Constant for Distillation Columns", *Comp.Chem.Eng*, **11**, 6, 607-617.

Skogestad, S., M. Morari and J.C. Doyle, 1988, "Robust Control of Ill-Conditioned Plants: High-Purity Distillation", *IEEE Trans. Autom. Control*, **33**, 12, 1092-1105

Skogestad, S. and M. Morari, 1988, "Understanding the Dynamic Behavior of Distillation Columns", *Ind. & Eng. Chem. Research*, **27**, 10, 1848-1862.

Skogestad, S. and P. Lundström, 1989, "Mu-Optimal LV-Control of Distillation Columns", *Comp.Chem.Eng.*, **14**, 4/5, 401-413.

Skogestad, S., P. Lundström, E.W. Jacobsen, 1990, "Selecting the Best Distillation Control Structure", *AIChE J.*, **36**, 5, 753-764.

Chapter 4

Inconsistencies in Dynamic Models for Ill-Conditioned Plants -
with Application to Low-Order Models of Distillation Columns.

Elling W. Jacobsen and Sigurd Skogestad

Chemical Engineering
University of Trondheim - NTH
N-7034 Trondheim
Norway

Submitted to *Chem.Eng.Sci.*

Abstract

The open-loop responses of ill-conditioned processes often take the form of almost pure first-order dynamics. Physically, a single pole (state), resulting from interactions, is dominating all the individual responses, and it is difficult to identify the other poles of the process. Attempting to define a model using only the dominant time-constant of the process corresponds to assuming singular dynamics, and is inconsistent unless the process actually is singular at all frequencies, including the steady-state. As we show here, the realization of such a model will contain several poles equal to the dominating pole of the process. The number of poles is determined by the rank of the steady-state matrix. It is shown that the model, although seamingly a reasonable approximation for open-loop dynamics, yields a poor prediction of the closed-loop behavior of the process.

The emphasis of the paper is on high-purity distillation. However, the results are relevant also for other ill-conditioned processes and the paper includes a heat-exchanger example.

4.1 Introduction

When obtaining dynamic models for process control one usually seeks simple linear models. The traditional approach has been to obtain low-order transfer-functions by fitting open-loop responses of a plant or full-order nonlinear model. This is also the usual approach for multivariable processes where the transfer-matrix usually is obtained by fitting the elements *independently*. For ill-conditioned processes, like high-purity distillation columns, this will often result in first-order (plus delay) transfer-functions with equal or similar time-constants in all elements.

Fitting the elements of the transfer-matrix from individual open-loop responses is a poor approach due to several circumstances. Skogestad and Morari (1988) argue that this may easily lead to poor models for ill-conditioned processes unless one explicitly takes into account the coupling between the gains of the different elements. In particular one is not able to obtain a good model of the low-gain direction of the plant, and the model will easily have the wrong sign of the determinant at steady-state. (Andersen et.al., 1988, Skogestad and Morari, 1988).

In this paper we show that such an approach, based on matching the steady-state, often leads to models with an excessive number of slow poles (large time-constants). The reason is that one is not able to account for the faster poles of the process which are difficult to observe from the open-loop responses. In ill-conditioned processes the dominating pole is usually a result of interactions, and is thus shared by all the transfer-matrix elements. One may attempt to take this into consideration and formulate a model with only a single time-constant. However, for an $n \times n$ process we need at least n states for the model to be non-singular, and the resulting model will contain n poles equal to the dominating pole of the process.

Most authors, however, fit the transfer-matrix using different time-constants in the different elements without considering whether there are one or several dominating poles in the process (e.g., Shunta and Luyben, 1972, Waller et.al., 1988). For ill-conditioned processes this will usually yield several slightly different time-constants, all in the magnitude of the dominating time-constant of the process. Again, we effectively get a model with excessive slow poles, and the resulting model is inconsistent on physical grounds.

Both types of models discussed above will, due to the inconsistency, usually result in a poor prediction of the closed-loop behavior of the plant. This is the subject of this paper.

We start the paper with an example of an inconsistent low-order model of an ill-conditioned process. The model, although seamingly a good open-loop description of the plant, is shown to yield unexpected behavior when one control loops is closed ("one-point control"). The results in this example are subsequently explained using analytical results. We then briefly discuss what types of processes that are likely to be modelled with an excessive number of slow poles. Most papers on distillation control treat the case when both composition loops are closed ("two-point control"), and the quality of models with excessive slow poles for this case is also treated in the paper. In the last section we discuss the specific problem of obtaining good low-order models for distillation columns.

All the results presented in this paper are for 2×2 processes, i.e., two inputs and two outputs. However, the results are of relevance also for higher dimensional processes.

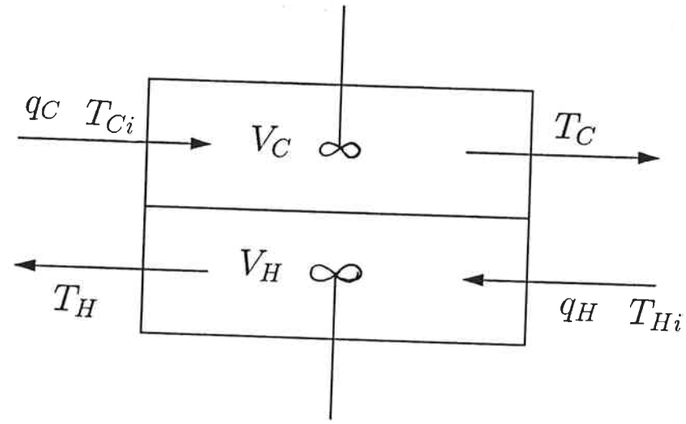

Figure 4.1: Simplified representation of heat-exchanger.

$V_C = V_H$ $[m^3]$	$q_C = q_H$ $[m^3/min]$	T_{Ci} $[°C]$	T_{Hi} $[°C]$	T_C $[°C]$	T_H $[°C]$	UA $[kJ/°Cmin]$	ρ $[kg/m^3]$	c_P $[kJ/°Ckg]$
1	0.01	25	100	61.59	63.41	300	500	3.0

Table 4.1: Steady-state data for heat-exchanger in Example 1. See also Figure 4.1

4.2 Introductory Example

Example 1. Heat-exchanger. Consider a heat-exchanger modelled using a single mixing tank on both the hot and cold side (see Figure 4.1). Neglecting variations in the liquid volumes yields a model with two states. The model is a reasonable approximation for heat-exchangers with large driving forces compared to temperature changes. Data for such a heat-exchanger are given in Table 4.1. In the following we only use the linearized version, $y(s) = G(s)u(s)$, of the model. The exact linear model is

$$G(s) = \frac{1}{(1+\tau_1 s)(1+\tau_2 s)} \begin{pmatrix} k_{11}(1+4.76s) & k_{12} \\ k_{21} & k_{22}(1+4.76s) \end{pmatrix} \tag{4.1}$$

$$\tau_1 = 100 \quad ; \tau_2 = 2.44 \quad ; k_{11} = -k_{22} = -1874 \quad ; k_{12} = -k_{21} = 1785$$

Here $y = [T_C \quad T_H]^T$ and $u = [q_C \quad q_H]^T$. Open-loop responses in the outlet temperatures to a 10% step change in hot inlet flow obtained from this model are shown by the solid lines in Figure 4.2. From the figure we observe that the responses in both outputs are close to first-order with a time-constant around 100 minutes. Indeed, as seen from the dashed lines in Figure 4.2, an excellent fit is obtained with the following model

$$G(s) = \frac{1}{1+\tau_1 s} \begin{pmatrix} k_{11} & k_{12} \\ k_{21} & k_{22} \end{pmatrix} \tag{4.2}$$

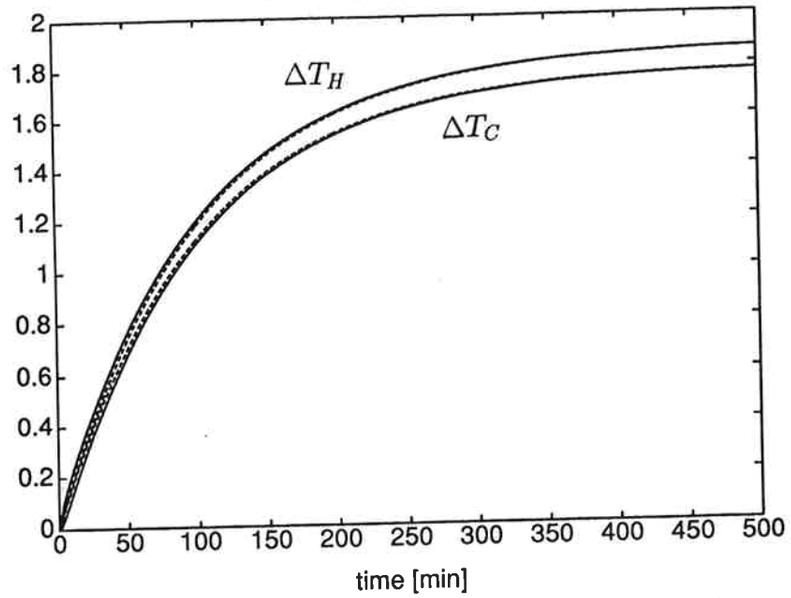

Figure 4.2: Open-loop dynamic response of heat-exchanger. Responses in outlet temperatures T_C and T_H to a 10 % step increase in hot inlet flow q_H. Solid line: Response of full model (4.1). Dashed line: Response of fitted model (4.2).

Although it may seem like this model only has a single time-constant of 100 minutes, the state-space realization contains two poles at $-1/\tau_1$.

We now want to study the behavior of the process under partial (one-point) feedback control, i.e., controlling one of the outlet temperatures. The cold outlet temperature T_C is controlled with the cold inlet flow q_C using a P-controller with gain $K = 0.015$ which yields a closed-loop time-constant for this loop of about 3.6 minutes. Figure 4.3 shows the responses to a 10% step change in hot inlet flow q_H with the loop closed. The solid lines are obtained with the "full" linear model (4.1), whereas the dashed lines are obtained with the fitted model (4.2). For the response in the uncontrolled output, T_H, there is a significant difference between the two models. The full model yields a "fast" response in T_H (similar to that of the controlled output T_C), whereas the fitted model yields a slow settling towards the new steady-state. The reason for the large difference in behavior is, as we shall see, the different number of slow poles in the two models.

4.3 Minimum Number of States in Multivariable Models.

Consider a linear system described by the model

$$\dot{x} = Ax + Bu \quad ; y = Cx + Du \tag{4.3}$$

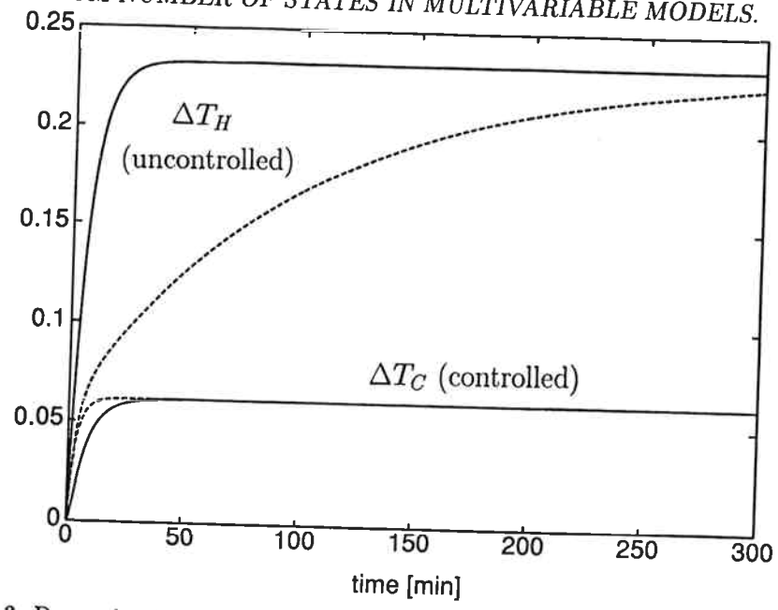

Figure 4.3: Dynamic response of heat-exchanger with one loop closed. Responses in outlet temperatures to a 10 % step increase in q_H. Cold outlet temperature T_C is controlled by q_C using a pure proportional controller with gain $K = 0.015$. Solid line: Response of full model (4.1). Dashed line: Response of fitted model (4.2).

Here x denotes states, u inputs, y outputs and $\dot{x}$ the time-derivative of x. Laplace transformation of (4.3) yields the transfer-matrix

$$G(s) = C(sI - A)^{-1}B + D \tag{4.4}$$

For a system with n states, m inputs and p outputs we have $dim(A) = nxn$, $dim(B) = nxm$, $dim(C) = pxn$ and $dim(D) = pxm$. The maximum rank of $G(s)$ is $r_{max} = min(p, m)$. Assume that $G(s)$ has rank $r > 1$ at some frequency, that is, the system is non-singular. With $D \neq 0$ we may define a model with a single state (time-constant) by making the dynamic part of the model , $C(sI - A)^{-1}B$, singular and let D account for the non-singularity at steady-state. However, such a model yields a very poor initial response for most processes and is therefore not considered. With $D = 0$, which is more reasonable from a physical point of view, it is easily seen from (4.4) that we need at least r states to describe the system.

In the heat-exchanger example we had a non-singular steady-state matrix $G(0)$ with rank $r = 2$, and consequently we need at least two states to describe the system using a state-space description. Thus, when attempting to describe the system using only one pole (state) we obtained the simplified model (4.2) with two poles at $-1/\tau_1$. Some readers might believe that also the full model has two poles at $-1/\tau_1$ since there are two mixing tanks which isolated would have a time-constant of $V/q = 100$ minutes each. However, an analysis of the full model reveals that it has only one pole at $-1/\tau_1$, shared by all transfer-function elements. This single time-constant is a result of the interactions between the

two sides of the heat-exchanger. In addition the full model has a significantly faster pole corresponding to a time-constant $\tau_2 = 2.44$ min. This is not obvious from open-loop simulations, but becomes clear when applying feedback control to the models. Applying one-point feedback control to the full model (4.1) causes the shared pole $-1/\tau_1$ to move, and also the uncontrolled response to become fast. However, this is not the case when the simplified model (4.2) is used, because here only one of the two poles at $-1/\tau_1$ is moved. This is shown in the next section.

4.4 Behavior of Low-Order Models with Excessive Slow Poles under Partial Feedback Control.

Consider applying the control law

$$du_1 = -K(dy_1 - dy_{1s}) \tag{4.5}$$

to the simplified model (4.2) (here subscript s denotes setpoint). The closed-loop transfer-matrix becomes

$$\begin{pmatrix} dy_1 \\ dy_2 \end{pmatrix} = \frac{1}{1+\tau_{CL}s} \begin{pmatrix} \frac{Kk_{11}}{(1+Kk_{11})} & \frac{\frac{k_{12}}{(1+Kk_{11})}}{k_{22}(1+\tau_{CL}s)-\frac{Kk_{12}k_{21}}{1+Kk_{11}}} \\ \frac{Kk_{21}}{(1+Kk_{11})} & \frac{}{(1+\tau_1 s)} \end{pmatrix} \begin{pmatrix} dy_{1s} \\ du_2 \end{pmatrix} \tag{4.6}$$

Thus three of the elements are first-order with the time-constant $\tau_{CL} = \tau_1/(1+Kk_{11})$. However, the transfer-function $g_{22}(s)$ from u_2 to the uncontrolled output y_2 is second order as it contains the open-loop dominant time-constant τ_1 in addition to the closed-loop time-constant. To see how these two poles contribute to the overall response write $g_{22}(s)$ on the form

$$g_{22}(s) = \frac{X_1}{1+\tau_1 s} + \frac{X_{CL}}{1+\tau_{CL}s} \tag{4.7}$$

The ratio between the gains X_1 and X_{CL} becomes

$$\frac{X_1}{X_{CL}} = (1+Kk_{11})\frac{1-Y}{Y} \quad ;Y = \frac{k_{12}k_{21}}{k_{11}k_{22}} \tag{4.8}$$

Y is the ratio between the off-diagonal and diagonal steady-state gains, and is a well known measure of interactions (e.g., Balchen, 1958, Rijnsdorp, 1965). It is also related to the $1,1-$element of the Relative Gain Array (Bristol, 1966) for 2×2 systems

$$RGA = \frac{1}{1-Y} \tag{4.9}$$

The RGA is again closely related to the minimized condition number (Skogestad and Morari, 1987a) and so Y is a measure of the ill-conditioning of the model.

Consider Y in the range 0 to 1. For cases with $Y = 1$ (RGA$= \infty$) we see from (4.8) that X_1 becomes zero, i.e., there is no gain related to τ_1, and only τ_{CL} remains in (4.6). This is as expected since $Y = 1$ implies that the system is singular at all frequencies and the minimal realization of (4.2) will only have one state. On the other hand, if $Y = 0$

(RGA=1) we see from (4.8) that the gain related to τ_{CL} will be zero and only τ_1 will be left in (4.6). This is also as expected since $Y = 0$ implies that the steady-state matrix is triangular or diagonal, in which case it is likely that the identified process actually contains two poles at $-1/\tau_1$ (see section 4.1). For values of Y between 0 and 1 (RGA$>$ 1), both poles will be present in (4.7).

From (4.8) we see that the ratio X_1/X_{CL} also depends on the gain K used in the controller. The higher gain that is used, the larger will the ratio X_1/X_{CL} be. This means that the faster the response in the controlled output is, the more marked is the large time-constant τ_1 in the uncontrolled output.

Example 1, continued. For the heat-exchanger example we have $Y = 0.907$ and $Kk_{11} = 28.1$ which yields $X_1/X_{CL} = 2.98$. That is, the major part of the response in the uncontrolled output is related to τ_1, which is confirmed by the simulations in Figure 4.3. In the "full" model of the heat-exchanger the single time-constant τ_1 is affected by the feedback control, and there will consequently be no slow settling corresponding to τ_1 in the uncontrolled output.

Example 2. PI-control of Wahl and Harriot column (1970).

High-purity distillation columns operating with reflux L and boilup V as independent variables are known to be strongly ill-conditioned. Furthermore, it is well known that the individual open-loop responses may be well approximated using only one dominating time-constant. This has been shown both from plant data (McNeill and Sachs, 1969) and in several theoretical papers (e.g., Davidson, 1956; Moczek et.al., 1965; Wahl and Harriot, 1970; Kim and Friedly, 1974; Skogestad and Morari, 1987b). Due to this, first order models are commonly used in the distillation control literature.

Wahl and Harriot (1970) used a simple low-order model to study the behavior of a high-purity column under one-point control. They controlled the composition on plate 4 below the top using reflux, and considered the response in top composition for a disturbance in feed-composition. All the data needed for the full model and the low-order model are given in their paper. The low-order model suggested by Wahl and Harriot was somewhat more complicated than pure first-order transfer-functions as given in (4.2), but the minimal realization of the model contains two time-constants equal to 365 min., while the full model only has one time-constant at 365 min.

The dashed lines in Figure 4.4 show the response of the Wahl and Harriot low-order model to a step change in feed composition with the composition on plate 4 under feedback control. The controller tuning (PI-controller) used here is somewhat different than the one used by Wahl and Harriot, but the responses resemble closely the ones shown in Wahl and Harriot (1970)[1], i.e., a fast response in the composition on plate 4 with a slow settling towards steady-state for the top composition. The slow settling was noticed by Wahl and Harriot, but they assumed it to be a property of the process. However, as shown above, the slow settling to steady-state is simply a result of a modelling error, that is, the model has an excessive slow pole. This is seen from the solid lines in Figure 4.4 which shows the responses obtained using the full linear model. The full model yields a fast response in both compositions.

[1] Actually Wahl and Harriot have the wrong sign on the change in top composition

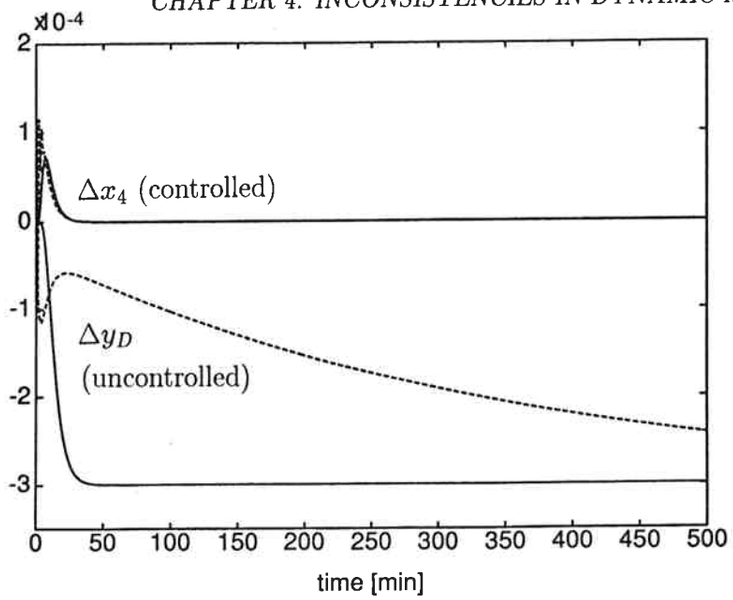

Figure 4.4: Wahl and Harriot column. Response in top-composition y_D and x_4 to a disturbance in feed composition with x_4 controlled by reflux. Dashed lines: Simulations with low-order model given by Wahl and Harriot (1970). Solid lines: Simulations with full linear model.

Also several other authors (e.g., Skogestad et.al., 1990; Sandelin et.al., 1991) have used inconsistent models for studies of partial feedback control in distillation. This may be seen from their figures by observing the slow settling in the uncontrolled output.

4.4.1 Relationship to ill-conditioned processes

We have seen that low-order models with excessive slow poles predict an erroneous slow response in the uncontrolled output to disturbances, and that the size of the gain related to the slow mode is largest for models with a small value of Y. From this it seems like the less interactive (ill-conditioned) the process is at steady-state (which is assumed to be well fitted by the simple model), the larger is the "error" in the response under one-point control for models with excessive slow poles.

However, this conclusion is misleading as it is for Y close to 1 we most likely will identify a model with too many slow poles. To see this consider a 2×2 model which is reduced to have two states. The two poles left should be the ones with the largest effect on the input-output behavior of the full model. Each of the two poles will have an input direction related to them, that is, a set of inputs that cancels the other pole. A similarity transformation of the state-space model, so that the A-matrix becomes diagonal, will reveal these directions in the rows of the transformed B-matrix. Changes in one input at the time, i.e., the input vectors $[1 \quad 0]^T$ and $[0 \quad 1]^T$, will span the input space. If one of the poles dominates the responses to both these input perturbations, it means that the gain related to the "hidden" pole must be small compared to the gain related to the

dominating pole. This implies that the system has two directions with widely differing gains, i.e., the system is ill-conditioned[2]. From this we conclude that it is only for ill-conditioned systems that the open-loop responses are likely to be well approximated using a single time-constant. A diagonal or triangular 2×2 process which has $Y = 0$ (RGA and minimized condition number γ^* unity) and is well described using only one time-constant τ_1 is thus likely to actually contain two poles at $-1/\tau_1$.

Example 1, continued. A similarity transformation of the state-space realization of the full heat-exchanger model (4.1) shows that the input direction cancelling τ_2 is $[1 \quad -1]^T$ and the input direction cancelling τ_1 is $[1 \quad 1]^T$. A singular value decomposition of the model gives a (minimized) condition number of 41 with the high-gain input direction being $[1 \quad -1]^T$ and the low-gain input direction being $[1 \quad 1]^T$. In this case we therefore have a perfect alignment of the singular input vectors and the pole-cancelling vectors, i.e the high-gain input direction has a pole $-1/\tau_1$ and the low-gain input direction a pole $-1/\tau_2$. The gain in the direction of the slow pole $-1/\tau_1$ is consequently 41 times the gain in the direction of the fast pole $-1/\tau_2$, and the fast pole is thus only weakly visible in open-loop simulations with perturbations in single inputs. This explains why a model using only one time-constant yields an excellent fit of the open-loop responses in Figure 4.2.

4.5 Behavior of Low-Order Models with Excessive Slow Poles with all Outputs under Feedback Control.

We have seen that models with excessive slow poles compared to the process yield a poor prediction of the behavior of the uncontrolled output under partial feedback control. One might expect that by closing the second loop we correct the slow behavior of the previously uncontrolled output and thereby obtain two closed-loop time-constants of similar magnitude. However, as we shall see, this is not the case.

We consider only decentralized (single-loop) controllers. In order to keep the expressions simple we limit ourselves to use pure proportional controllers. Similar results would be obtained when using single-loop PID- (see example below) or more complex decentralized controllers.

The state-space realization of (4.2) may be written

$$\dot{x} = -\frac{1}{\tau_1} I x + \frac{1}{\tau_1} G(0) u \quad ; y = Ix \tag{4.10}$$

We want to apply the control-law

$$du_1 = -\frac{K}{k_{11}}(dy_1 - dy_{1s}) \quad ; du_2 = -\frac{K}{k_{22}}(dy_2 - dy_{2s}) \tag{4.11}$$

[2]Note that some ill-conditioned systems may have the directions of the poles closely aligned with the input vectors of the perturbations. In this case both poles will show up in the simulations.

to (4.10). This yields the closed-loop time-constant $\tau_{CL} = \tau_1/(1+K)$ for both of the individual loops, but we shall see that the interactions may change the dynamics. The closed-loop model becomes

$$\dot{x} = -\frac{1}{\tau_1}\begin{pmatrix} 1+K & K\frac{k_{12}}{k_{22}} \\ K\frac{k_{21}}{k_{11}} & 1+K \end{pmatrix} x + \frac{K}{\tau_1}\begin{pmatrix} 1 & \frac{k_{12}}{k_{22}} \\ \frac{k_{21}}{k_{11}} & 1 \end{pmatrix} y_s \quad ; y = Ix \tag{4.12}$$

The eigenvalues of the closed-loop system are given by

$$\lambda_{1,2} = -\frac{1}{\tau_1}(1 + K(1 \pm \sqrt{Y})) \tag{4.13}$$

Thus if Y is zero, corresponding to a diagonal or triangular system, we have two equal closed-loop time-constants $\tau_{CL1} = \tau_{CL2} = \tau_1/(1+K)$ as found for the individual loops. However, as Y increases towards 1, τ_{CL1} and τ_{CL2} becomes more different and for $Y = 1$ we get $\tau_{CL1} = \tau_1/(1+2K)$ and $\tau_{CL2} = \tau_1$. Thus, the difference between the closed-loop time-constants is large for models of ill-conditioned plants when the feedback gain is large.

From (4.13) we see that for Y less than 1 instability is impossible with pure proportional controllers. For cases with Y greater than 1 we get closed-loop instability for $K > 1/(\sqrt{Y}-1)$.

Too see how the two closed-loop poles affect the input-output behavior, we determine the two vectors of setpoint changes that cancels each pole. This is done by multiplying the inverse of the closed-loop B-matrix (4.12) with the eigenvectors of the closed-loop A-matrix. This yields (after some simplification)

$$y_{s1} = \begin{pmatrix} \sqrt{\frac{k_{11}k_{12}}{k_{21}k_{22}}} \\ 1 \end{pmatrix} \tag{4.14}$$

$$y_{s2} = \begin{pmatrix} -\sqrt{\frac{k_{11}k_{12}}{k_{21}k_{22}}} \\ 1 \end{pmatrix} \tag{4.15}$$

Here y_{s1} and y_{s2} corresponds to vectors cancelling the slow and fast pole, respectively. Furthermore, these vectors corresponds to the easiest and most difficult setpoint directions, respectively. To see this we refer to Grosdidier et.al. (1985) who give the input and output scaling which yields the minimized condition number of a 2×2 matrix. Multiplying y_{s1} and y_{s2} with the output-scaling given in their paper yields the scaled version of $y_{s1} = [1 \quad 1]^T$ and $y_{s2} = [-1 \quad 1]^T$. From this we find that the two directions (4.14) and (4.15) correspond to disturbance condition numbers (see Skogestad and Morari, 1987c) $\gamma_d = 1$ and $\gamma_d = \gamma^*$, respectively. Here γ^* is the minimized condition number of the model. Thus for a setpoint change (4.14) corresponding to $\gamma_d = 1$ we will only observe the fast pole while we for a setpoint change (4.15) corresponding to $\gamma_d = \gamma^*$ only will observe the slow pole.

Example 3. High-purity distillation. Data for a column with relatively high product purities are given in Table 4.2. Open-loop simulations of step changes in reflux L using a full linear model with 82 states are shown in Figure 4.5. Note that liquid flow-dynamics

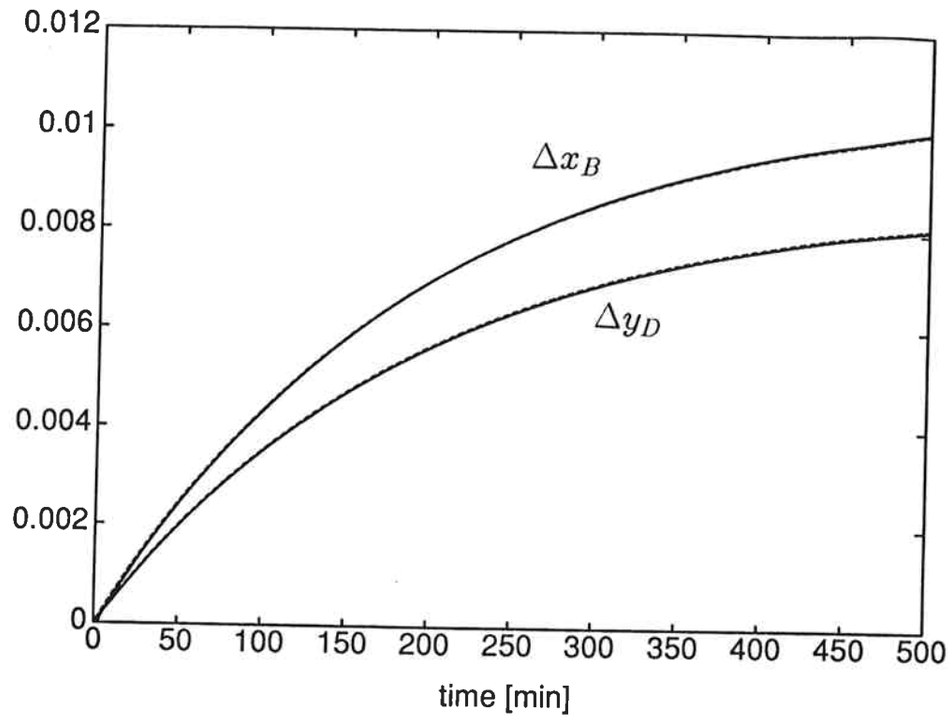

Figure 4.5: Open-loop responses of distillation column in Example 3 to 1 % step change in reflux L. Solid lines: responses of full linear model. Dashed lines: responses of fitted low-order model N1 (4.16).

z_F	α	N	N_F	$1-y_D$	x_B	D/F	L/F	V/F
0.5	1.5	40	21	0.01	0.01	0.500	2.706	3.206

- Feed is saturated liquid

Table 4.2: Steady-state data for distillation column in Example 3.

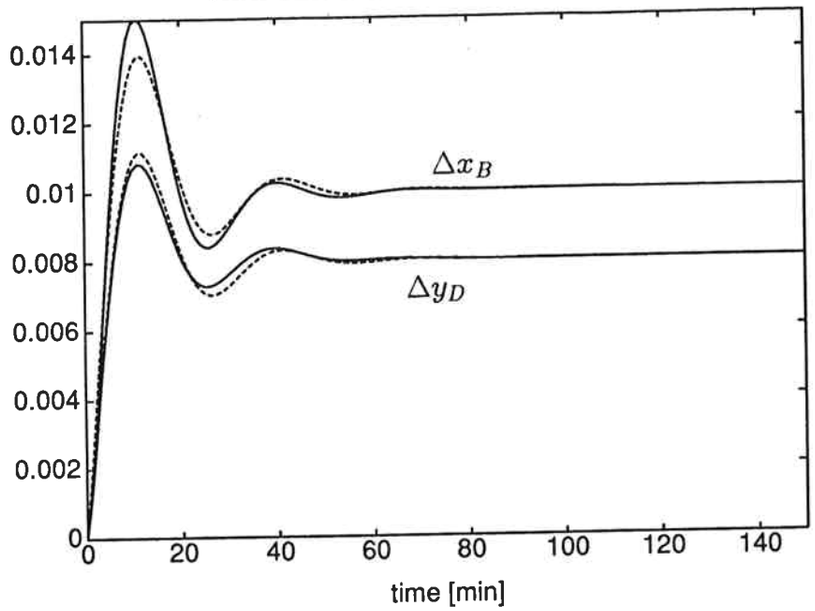

Figure 4.6: Closed-loop responses of distillation column in Example 3 to setpoint change corresponding to $\gamma_d = 1$. Solid lines: responses of full linear model. Dashed lines: responses of simplified model N1 (4.16).

are included in the model. The responses seem to be almost pure first-order with a time-constant approximately 194 min. Fitting each transfer-matrix element to a first-order response with time-constant $\tau_1 = 194$ minutes yields a model on the same form as (4.2)[3]

$$\begin{pmatrix} dy_D \\ dx_B \end{pmatrix} = \frac{1}{1+\tau_1 s} \begin{pmatrix} 0.878 & -0.864 \\ 1.082 & -1.096 \end{pmatrix} \begin{pmatrix} dL \\ dV \end{pmatrix} \tag{4.16}$$

This model is denoted N1. N means no flow dynamics and 1 indicates one time constant. This simple model gives an almost perfect fit of the overall open-loop responses of the full model with 82 states as seen from Figure 4.5; the differences between the responses are hardly visible.

We apply a two-point PI-controller with $K = 15$ and $\tau_{Iy} = \tau_{Ix} = 3$ min. to the first-order model (4.16). This controller tuning would yield a closed-loop time-constant of approximately 10 min. in the controlled outputs when used for one-point control. The dashed lines in Figure 4.6 shows the closed-loop response of the simplified model (4.16) to a setpoint change in the "easy direction" $y_{s1} = [0.80 \quad 1]^T$ as given by (4.14). We see that we get a reasonably fast response in both outputs. The response of the full linear model is shown with solid lines in Figure 4.6, and we see that the low-order model yields a good prediction of the behavior of the full model for this setpoint change.

Figure 4.7 shows the closed-loop response to a setpoint change in the "difficult direction" $y_{s2} = [-0.80 \quad 1]^T$, corresponding to a disturbance condition number $\gamma_d = \gamma^* =$

[3]Note that we could have fitted four slightly different time-constants instead. However, the results would have been similar.

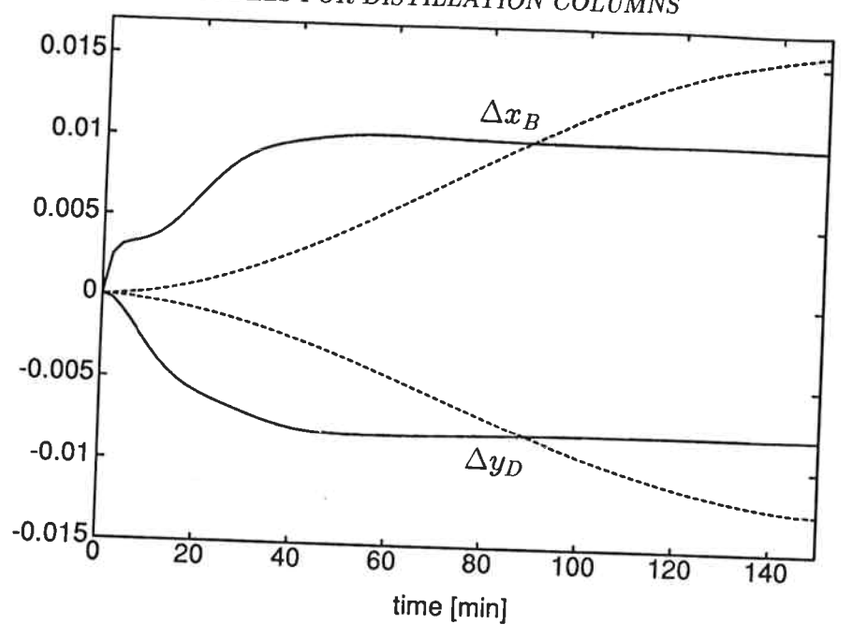

Figure 4.7: Closed-loop responses of distillation column in Example 3 to setpoint change corresponding to $\gamma_d = \gamma^* = 138.1$. Solid lines: responses of full linear model. Dashed lines: responses of simplified model N1 (4.16).

138.2. We see that for this setpoint change the simplified model (4.16) predicts a very slow response (the behavior is also oscillatory) which is as expected from the above analysis. The full model, on the other hand, predicts a reasonably fast response also for this setpoint change. Thus the low-order model (4.16) yields a poor prediction of the behavior of the full linear model, especially for "difficult" setpoint changes corresponding to high disturbance condition numbers.

4.6 Low-Order Models for Distillation Columns with Flow-Dynamics Included

In this section we discuss the problem of obtaining good simple low-order models for distillation columns. In the previous section we presented the simple model N1 (4.16) which gave an excellent fit to the open-loop responses of the column in Example 3. However, the model contained an excessive slow pole. In addition, the directions of the model are wrong at intermediate and high frequencies as seen from Figure 4.8. The simplified model (4.16) has an RGA=35 over all frequencies, that is, strong directional dependence at all frequencies. The full model, on the other hand, has a significantly lower RGA-value at intermediate and high frequencies than at steady-state as seen from Figure 4.8. The RGA of the full model breaks off at intermediate frequencies and becomes 1 at higher frequencies. The process is therefore only weakly directionally dependent at high frequencies.

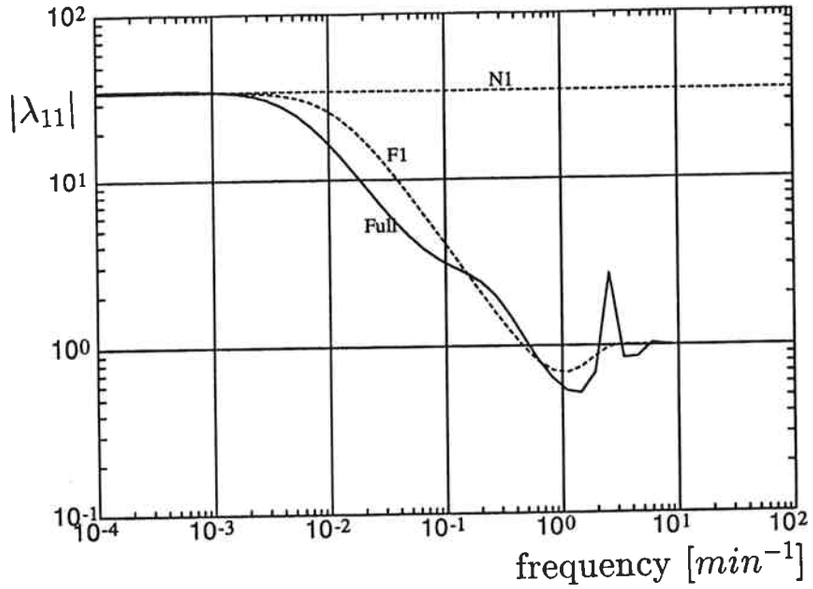

Figure 4.8: RGA as a function of frequency for distillation column in Example 3. N1: fitted low-order model without flow-dynamics (4.16). F1: fitted low-order model with flow-dynamics included (4.17). Full: full 82th order linear model.

This explains the similar responses of the full model to different setpoint changes in Figures 4.6 and 4.7. As shown by Skogestad et.al. (1990), the low RGA at intermediate and high frequencies is caused by the flow-dynamics, i.e., the lag in reflux from the top to the bottom of the column.

We now want to study how to develop a simple low-order model of a distillation column which 1) has correct directions at intermediate and high frequencies and 2) does not contain excessive slow poles. However, let us first consider the low-order models most commonly presented in the distillation literature.

Most low-order models of distillation columns presented in the literature are of the type first-order plus delay. With only measurement delays and/or input delays the sum of delays would be equal in the diagonal and off-diagonal elements. However, a study of models reported reveals that most of them have a larger sum of delays in the off-diagonal elements than in the diagonal elements (e.g., Wood and Berry, 1973, Waller et.al., 1988). This seems reasonable and is probably a result of the flow-dynamics. Note that most authors use pure dead-times in their models, while the flow-dynamics physically is a high-order lag.

Let us now try to improve the simplified model N1 (4.16) to get a reasonable low-order model. Because the flow-dynamics reduce the RGA at high frequencies, we will first try to add this to the model. We introduce a lag term of 2.5 minutes in the 2,1 element of model N1 (4.16), corresponding to the reflux lag of the full model, and obtain the model

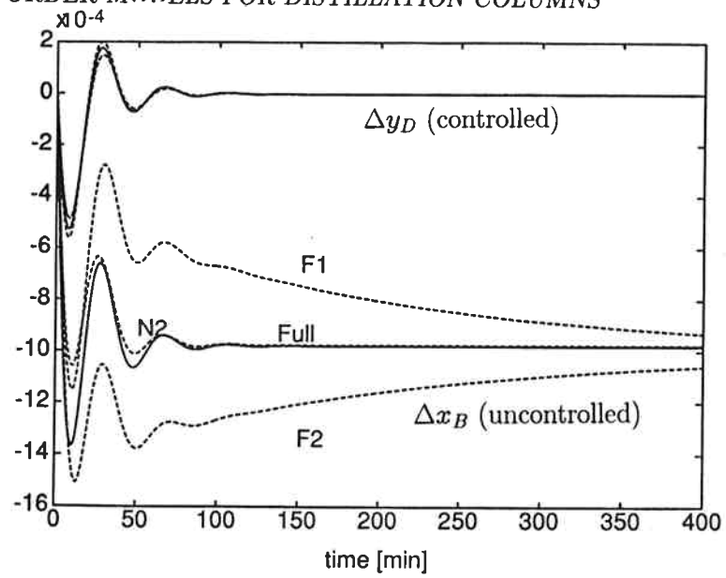

Figure 4.9: Dynamic response of distillation column in Example 3 with one loop closed. Response to a 1 % increase in boilup. Top composition y_D controlled by reflux L using a PI-controller. Full: full 82th order linear model. F1: fitted low-order model with flow-dynamics included (4.17). N2: two time-constant model (4.18) F2: two time-constant model (4.18) with flow-dynamics included.

F1 (F denotes flow dynamics)

$$\begin{pmatrix} dy_D \\ dx_B \end{pmatrix} = \frac{1}{1+\tau_1 s} \begin{pmatrix} 0.878 & -0.864 \\ 1.082/(1+0.5s)^5 & -1.096 \end{pmatrix} \begin{pmatrix} dL \\ dV \end{pmatrix} \tag{4.17}$$

(the full model actually has a 39th order lag, but a good approximation is obtained with a 5th order lag). We see from the RGA-plot in Figure 4.8 that we now obtain a much better fit of the directionality of the process. The model F1 has been studied by Skogestad et.al. (1990) and Jacobsen et.al. (1991), and they concluded that it was a reasonably good model for *two-point* control studies. However, we find that including the flow-dynamics does not correct the fundamental error of excessive slow poles, and the model will be poor for studies of partially controlled distillation columns. This is seen from Figure 4.9 which shows the response of the model under one-point control. As seen from curve F1, the model yields an incorrect slow settling towards steady-state for the uncontrolled output. As F1 represents the type of model most commonly presented in the literature, it is likely that most of the models presented contain excessive slow poles.

Skogestad and Morari (1988) suggested to use a two time-constant model with the dominant time-constant τ_1 for the high-gain direction ($dL = -dV$) and a smaller time-constant τ_2 for the low-gain direction ($dL = dV$) (model N2)

$$\begin{pmatrix} dy_D \\ dx_B \end{pmatrix} = \begin{pmatrix} \frac{k_{11}}{1+\tau_1 s} & \left(\frac{k_{11}+k_{12}}{1+\tau_2 s} - \frac{k_{11}}{1+\tau_1 s}\right) \\ \frac{k_{21}}{1+\tau_1 s} & \left(\frac{k_{21}+k_{22}}{1+\tau_2 s} - \frac{k_{21}}{1+\tau_1 s}\right) \end{pmatrix} \begin{pmatrix} dL \\ dV \end{pmatrix} \tag{4.18}$$

For the column in Example 3, $\tau_1 = 194$ min. and $\tau_2 = 15$ min. The minimal realization of this model contains two poles (not four as one might expect), one dominating at $-1/\tau_1$ and one fast at $-1/\tau_2$, and gives an excellent fit of a full 41th order model which results from neglecting flow dynamics. The N2 model also agrees well with the 82th order full model with flow dynamics for the case of one-point control. This is seen from curve N2 in Figure 4.9. However, model N2 (4.18) does not include flow-dynamics and may therefore be relatively poor for two-point control studies. To improve the model one may try to add flow-dynamics to (4.18). The resulting model F2 yields good results for two-point control studies as reported by Jacobsen et.al. (1991). However, adding a lag term to the 2,1 element of (4.18) will again result in a minimal realization with two slow poles at $-1/\tau_1$, and therefore a poor model for one-point control studies. This is seen from curve F2 in Figure 4.9 where we again get an incorrect slow settling towards the new steady-state for the uncontrolled output.

In fact, we have not been able to obtain a simple low-order model for high-purity columns which includes flow-dynamics and is consistent in terms of the number of slow poles. In particular, it seems difficult to include the effect of disturbances, i.e., inputs not used for control. On the other hand, by mathematical model reduction of the full linear model it is possible to obtain low-order models with only two states which are good representations for both one- and two-point control studies (Jacobsen et.al., 1991). For instance, applying the Optimal Hankel Approximation without balancing (Safonov et.al., 1987) to the full linear model of the column in Example 3 yields the model (Jacobsen et.al., 1991)

$$G(s) = \frac{1}{(1.61s+1)(194s+1)} \begin{pmatrix} 0.871(2.17s+1) & -0.861(0.721s+1) \\ 1.089(0.45s+1) & -1.101(3.48s+1) \end{pmatrix} \tag{4.19}$$

This model has a minimal realization with only one slow pole at $-1/\tau_1$ and is a good model for both one- and two-point control studies. However, the model structures resulting from mathematical model reduction are not parameterized in terms of a few physical parameters and therefore difficult to use for fitting experimental data. For instance, in model (4.19) the decoupling at high frequencies, physically caused by the flow dynamics, is described by letting the zeros in the off-diagonal elements be smaller than in the diagonal elements.

4.7 Disturbance Modelling.

We have so far in this paper only discussed low-order models for the effect of inputs. However, the main purpose of process control is to reject the effect of disturbances entering the process, and so a disturbance model is usually also required. The common approach is to identify an isolated model for the effect of disturbances (e.g., Shunta and Luyben, 1972, Waller et.al., 1988). In this case it is important that the model reflects whether the poles of the disturbance and input responses physically are shared in the process. For the processes studied in this paper the dominating pole seen in the individual open-loop responses to inputs will also dominate the open-loop responses to disturbances. If the fitted disturbance model is inconsistent with the input model, the poles of the two models will be affected differently by feedback control. For instance, using the low-order model

in example 3 with flow-dynamics included (4.17) together with a pure first-order model for a disturbance in feed flow-rate F would yield a poor prediction of the closed-loop disturbance response of the process with both composition loops closed. The responses to setpoint changes would be reasonably fast with a properly tuned controller. However, the responses to a disturbance in F would be slow due to erroneous slow poles left in the closed-loop disturbance model. Thus, care needs to be taken also when identifying the disturbance model of an ill-conditioned process.

4.8 Identification.

The processes studied in this paper contain only one slow pole, and since a rank 2 model requires two states, we need to identify at least one more time-constant. For the heat-exchanger example the correct model is given by (4.1) and the small time-constant τ_2 may be identified by doing a simultaneous step increase in hot and cold flow, i.e., applying the input vector $[1 \quad 1]^T$. However, this is impossible in practice, and with a small deviation the low-gain direction disappears. Due to this one should try to explicitly model the "weak" direction of the plant and be careful about only fitting open-loop data.

Although all the process studied in this paper contains only a single slow pole, there are of course many processes that contain several slow poles. When doing open-loop identification it is necessary to know in advance how many slow poles the process actually contains. In a well designed high-purity distillation column there will usually only be one slow pole, while an overdesigned high-purity column with a pinch in the composition profile usually will have two slow poles (one pole related to each of the two column sections). An open-loop black-box identification method will not be able to discriminate between the two cases, and some physical knowledge needs to be added. Using closed-loop identification on the other hand is likely to reveal the fact that it only is one dominating time-constant in the processes we have studied. Thus, for ill-conditioned processes where physical knowledge is lacking, one should apply some closed-loop identification method when obtaining low-order models.

4.9 Conclusions

- The open-loop responses of ill-conditioned processes will often take the form of almost pure first-order dynamics. The responses are dominated by a single slow pole resulting from interactions in the process. The open-loop dynamics of such processes are seamingly well approximated by a low-order model containing only the dominant time-constant. However, the model will contain an excessive number of slow poles and is therefore physically inconsistent.

- Inconsistent models containing excessive slow poles yield a poor prediction of the process behavior under partial feedback control. Erroneous slow dynamics will dominate the responses for uncontrolled outputs to disturbances.

- Inconsistent models containing excessive slow poles will also often yield a poor prediction of the process behavior with *all outputs* controlled. This may be explained

by the fact that the directionality at high frequencies often is poorly predicted by the simplified model.

Acknowledgements: Financial support from the Royal Norwegian Council for Scientific and Industrial Research (NTNF) is greatfully acknowledged.

NOMENCLATURE

A - heat transfer area (m^2)
c_P - heat capacity ($kJ/^oCkg$)
D - distillate flow (kmol/min)
F - feed flow (kmol/min)
$G(s)$ - process transfer-matrix
$g_{ij}(s)$ - transfer matrix element i,j
k_{ij} - steady state process gains
I - identity matrix
K - controller gain
L - reflux rate ($kmol/min$)
N - number of theoretical trays
N_F - feed tray
q_C - cold inlet flow (m^3/min)
q_H - hot inlet flow (m^3/min)
T_C - cold outlet temperature (^oC)
T_H - hot outlet temperature (^oC)
U - heat transfer coefficient ($kJ/m^2\ ^oCmin$)
u_i - process input i
V - boilup rate ($kmol/min$)
V_C - liquid volume cold side (m^3)
V_H - liquid volume hot side (m^3)
x_B - bottoms composition
$Y = \frac{k_{12}k_{21}}{k_{11}k_{22}}$ - interaction measure
y_D - distillate composition
y_i - process output i
z_F - feed composition

Greek symbols
α - relative volatility
γ - condition number
γ^* - minimized condition number
γ_d - disturbance condition number
λ - eigenvalue
λ_{11} - 1,1 element of RGA
τ_1 - dominant (largest) process time-constant (min.)
τ_2 - smaller process time-constant (min.)
τ_{CL} - closed-loop time-constant (min.)
τ_{Iy} - integral-time for distillate composition loop (min.)
τ_{Ix} - integral-time for bottoms composition loop (min.)

Subscripts
s - setpoint change

REFERENCES

Andersen, H.W., M. Kümmel, and S.B. Jørgensen, 1988, "Dynamics and identification of a binary distillation column", AIChE Annual Meeting, Washington DC, Nov. 1988.

Balchen, J.G., 1958, *Lecture Notes*, Norwegian Institute of Technology, Trondheim, Norway (In Norwegian).

Bristol, E. H., 1966, "On a New Measure of Interactions for Multivariable Process Control", *IEEE Trans. Automat. Contr.*, **AC-11**, 133-134.

Davidson, J.F., 1956, "The Transient Behavior of Plate Distillation Columns", *Trans.Inst.Chem.Er* **34**, 44-52.

Grosdidier, P., M. Morari and B.R. Holt, 1985, "Closed-Loop Properties from Steady-State Gain Information", *Ind. & Eng. Chem. Fundamen.*, **24**, 221-235.

Jacobsen, E.W., P. Lundström and S. Skogestad, 1991, "Modelling and Identification for Robust Control of Ill-Conditioned Plants - A Distillation Case Study", *Proceedings of 1991 American Control Conference*, Boston, MA.

Kim, C. and C. F. Friedly, 1974, "Dynamic Modeling of Large Staged Systems", *Ind.Eng.Chem. Process Des.Dev*, **13**, 13, 177-181.

McNeill, G.A. and J.D. Sachs, 1969, "High Performance Column Control", *Chem.Eng.Prog.*, **65**, 3, 33-39.

Moczek, J.S., R.E. Otto and T.J. Williams, 1965, "Approximation Models for the Dynamic Response of Large Distillation Columns", *Chem.Eng.Prog.Symp.Ser*, **61**, 55, 136-146.

Rijnsdorp, J.E., 1965, "Interaction in Two-Variable Control Systems for Distillation Columns - I", *Automatica*, **1**, 15-28.

Safonov, M.G., R.Y. Chiang and D.J. Limebeer, 1987, "Hankel Model Reduction without Balancing - A Descriptor Approach", *Proc. IEEE Conf. on Dec. and Contr.*

Sandelin, P.M., K.E. Häggblom and K.V. Waller, 1991, "Disturbance Rejection Properties of Control Structures at One-Point Control of a Two-Product Distillation Column", *Ind.Eng.Chem.Res.*, **30**, 6, 1187-1193.

Shunta, J.P. and W.L. Luyben, 1972, "Sampled-Data Noninteracting Control for Distillation Columns", *Chem.Eng.Sci*, **27**, 6, 1325-1335.

Skogestad, S. and M. Morari, 1987a, "Implications of Large RGA-Elements on Control Performance", *Ind.Eng.Chem.Res.*, **26**, 11, 2323-2330.

Skogestad, S. and M. Morari, 1987b, "The Dominant Time-Constant for Distillation Columns", *Comp.Chem.Eng.*, **11**, 6, 607-617.

Skogestad, S. and M. Morari, 1987c, "The Effect of Disturbance Directions on Closed-Loop Performance", *Ind.Eng.Chem.Res*, **26**, 10, 2029-2035.

Skogestad, S. and M. Morari, 1987d, "LV-Control of a High-Purity Distillation Column", *Chem.Eng.Sci.*, **43**, 1, 33-48.

Skogestad, S. and M. Morari, 1988, "Understanding the Dynamic Behavior of Distillation Columns", *Ind. & Eng. Chem. Res*, **27**, 10, 1848-1862.

Skogestad, S., M. Morari and J.C. Doyle, 1988, "Robust Control of Ill-conditioned Plants: High-Purity Distillation", *IEEE Trans. Autom. Control*, **33**, 12, 1092-1105.

Skogestad, S., E.W. Jacobsen and P. Lundström, 1990, "Modelling Requirements for Robust Control of Distillation Columns", *Preprints 11th IFAC Conference*, Tallinn, Estonia.

Wahl, E.F. and P. Harriot, 1970, "Understanding and Prediction of the Dynamic Behavior of Distillation Columns", *Ind.Eng.Chem. Process Des.Dev.*, **9**, 3 396-407.

Waller, K.V., K.E. Häggblom, P.M. Sandelin and D.H. Finnerman, 1988, "Disturbance Sensitivity of Distillation Control Structures", *AIChE J.*, **34**, 5, 853-858.

Wood, R.K. and M.W. Berry, 1973, "Terminal composition control of a binary distillation column", *Chem. Eng. Sci.*, **28**, 1707-1717.

Chapter 5

Modelling and Identification for Robust Control of Ill-Conditioned Plants - a Distillation Case Study

Elling W. Jacobsen, Petter Lundström and Sigurd Skogestad

Chemical Engineering
University of Trondheim - NTH
N-7034 Trondheim
Norway

Presented at 1991 American Control Conference, Proceedings p.242-248

Abstract

The problem of obtaining linear models for effective control is discussed. First a suitable model structure is identified by comparing different models. It is demonstrated that the high-frequency behavior (initial time response) of the model is much more important for controller design than the steady-state characteristics. Finally, having determined a good model structure, the problem of obtaining models from experiments is discussed. It is shown that by combining experimental open-loop step responses with theoretically established structural properties one may obtain reasonably good models for two-point control studies.

Please Note: *This article was finished before the results in Chapter 4 were found, and several of the models presented, specifically models* $N1, F1, F2, F1X, F1fit$ *and* $F2fit$*, are actually inconsistent according to Chapter 4. However, we discuss only two-point control here, and for this purpose several of the models are shown to be reasonably good. However, the models based on "physical insight" would be poor if used for studies of partial (one-point) control.*

5.1 Introduction

When obtaining dynamic models for process control one is usually interested in simple linear models. In this paper we discuss how such models may be obtained. We investigate which effects that should be included in a model to be used for design of feedback controllers, and subsequently discuss how the models may be obtained from experiments.

It is stressed that we are looking for a multivariable model. The main difference between single-input-single-output (SISO) models and multivariable models is the presence of "directions" or "interactions" in the latter case. It seems likely that our model should capture these multivariable effects in a reasonable way. From the Ziegler-Nichols tuning rules, which are widely used for SISO control, we know that the plant behavior at high frequencies (at "crossover" , i.e., where the plant has a phase lag of about 180°) is of primary importance for feedback control. This fact often seems to be forgotten when developing multivariable control models, and engineers often emphasize the steady-state behavior. There are probably two reasons for this: 1) Steady-state gain data are easily obtained, 2) Up to now most tools for analyzing directions and interactions, for example the Relative Gain Array (Bristol. 1966), have been used at steady state only. In this paper we want to demonstrate that also for multivariable plants it is the high-frequency behavior, and not the steady state, which is of primary importance for feedback control. However, we shall see that it is important that the sign of the plant (expressed by the sign of the determinant or sign of the RGA-elements) is correct at steady state.

Distillation control is used as a case study throughout the paper. Composition control of distillation columns (Figure 5.1) has proven difficult to implement in practice. One-point control (one composition under feedback control and the other uncontrolled) is fairly common, while two-point control (feedback control of both compositions) is rarely used. One reason for this is that on-line tuning of two composition loops on a strongly interacting distillation column is very difficult (e.g., Wood and Berry, 1973). It is therefore desirable to obtain controller tunings based on some model of the column.

The linear model of the plant is written

$$\begin{pmatrix} dy_D(s) \\ dx_B(s) \end{pmatrix} = G(s) \begin{pmatrix} dL(s) \\ dV(s) \end{pmatrix} \tag{5.1}$$

where $G(s)$ is a 2×2 transfer matrix expressing the effect of small changes in the independent flows on the compositions. Note that we have assumed that the product flows D and B are used for level control such that reflux L and boilup V are used for composition control. This corresponds to the LV-configuration. This may certainly not be the best configuration for two-point control, but it is the most commonly used configuration in industry; probably because it works well for one-point control (Skogestad et.al., 1990).

The traditional approach for distillation columns has been to obtain the four elements of $G(s)$ *independently*, for example, by fitting open loop responses of steps or pulses in reflux and boilup to simple transfer function models (Luyben, 1970, Toijala and Fagervik, 1972, Wood and Berry, 1973). This approach might work for columns that are simple to control. However, as pointed out by Skogestad and Morari (1988b), for columns with large interactions between top and bottom, this approach will most probably yield poor models. The main reason is that it is very difficult to obtain a good model based on open-loop experiments or simulations unless one explicitly takes into account the expected

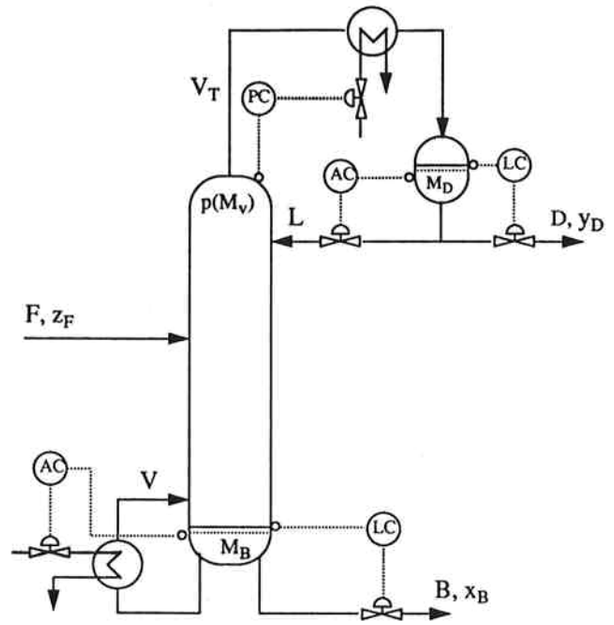

Figure 5.1: Two-product distillation column with LV-configuration.

couplings between the elements when formulating the model. In particular, one is not able to obtain a good model of the low-gain direction of the plant (Skogestad and Morari, 1988b, Andersen et.al., 1988). However, as we show in this paper, models obtained from fitting individual step responses may work if one: 1) uses a reasonable model structure, 2) fits only the initial part of the response and 3) corrects the obtained model according to theoretically established model properties.

We start the paper by evaluating what kind of modelling detail that is needed in a model used for controller design (part I). We then use the information gained here to fit models from experimental data (part II).

Part I: Modelling Requirements

5.2 Nonlinear Model

Data for the example column ("column A") are summarized in Table 5.1. The column has 40 theoretical trays (N-1 trays and a reboiler) plus a total condenser. The following modelling assumptions are used: binary separation, constant relative volatility, constant molar flows (neglected energy balance), negligible vapor holdup, and vapor-liquid equilibrium as well as perfect mixing on all stages. Neglecting the vapor holdup implies immediate vapor

z_F	α	N	N_F	$1-y_D$	x_B	D/F	L/F	V/F
0.5	1.5	40	21	0.01	0.01	0.500	2.706	3.206

- Feed is saturated liquid

Table 5.1: Steady-state data for distillation column example (column A).

flow responses throughout the column. Note that liquid flow-dynamics are not neglected; a simple linear relation is assumed between liquid holdup M_i and liquid flow L_i:

$$M_i = M_i^0 + \tau_{Li}(L_i - L_i^0) \tag{5.2}$$

where superscript 0 denotes nominal steady-state values given in Table 5.1. $M_i^0/F^0 = 0.5$ min. for all stages, including reboiler and condenser. The reboiler and condenser holdups are controlled by bottoms and distillate rate respectively. Note that the LV-configuration is insensitive to how tight these loops are tuned. The hydraulic time-constant τ_{Li}=0.063 min. for all stages, except for the reboiler and condenser. The variation in liquid holdup with liquid load yields an effective lag θ_L=2.46 min. in a change in liquid flow rate from the top to the bottom of the column. These modelling assumptions yield for each tray two nonlinear differential equations, one for composition and one for liquid holdup, resulting in a total of 82 states for the column studied. A linear model, denoted "full" linear model in the following, is obtained by linearizing the nonlinear model around the nominal steady-state.

5.3 Simple Linear Models

5.3.1 Reduced models from physical insight

It is well known that the composition dynamics in distillation columns may be well approximated by first order responses. Skogestad and Morari (1988b) found that there in general will be two time-constants; one for the strong direction of the plant (change in external flows) and one for the weak direction (change in internal flows). We will use this as a model basis in the following, but will in addition introduce the flow-dynamics (5.2):

$$G(s) = \begin{pmatrix} \frac{k_{11}}{1+\tau_1 s} & \left(\frac{k_{11}+k_{12}}{1+\tau_2 s} - \frac{k_{11}}{1+\tau_1 s}\right) \\ \frac{k_{21}}{1+\tau_1 s} g_L(s) & \left(\frac{k_{21}+k_{22}}{1+\tau_2 s} - \frac{k_{21}}{1+\tau_1 s}\right) \end{pmatrix} \tag{5.3}$$

$$g_L(s) = \frac{1}{(1+(\theta_L/n)s)^n} \tag{5.4}$$

The numerical values used are:

$$G(0) = K = \begin{pmatrix} k_{11} & k_{12} \\ k_{21} & k_{22} \end{pmatrix} = \begin{pmatrix} 0.878 & -0.864 \\ 1.082 & -1.096 \end{pmatrix} \tag{5.5}$$

$$\tau_1 = 194 \text{ min}; \quad \tau_2 = 15 \text{ min}; \quad \theta_L = 2.46 \text{ min}; \quad n = 5 \tag{5.6}$$

The flow-dynamics is described by (5.4) where n is the number of trays in the column. n should equal $N-1$, but is throughout this paper chosen to be 5 to avoid models of unnecessary high order. The steady-state gains k_{ij} and τ_1 were obtained from the full linear model. τ_2 is taken from Skogestad and Morari (1988b) and were obtained from fitting a model without flow-dynamics. When flow-dynamics are included in the model, the dynamics for changes in internal flows becomes somewhat more complicated, and there should be two poles in addition to a minimum phase zero close to the imaginary axis. This is caused by the fact that there will be a temporary change in the external flows when L and V are changes equally, and there will be a marked overshoot in the response of the bottom composition.

To study what level of modelling detail that is needed for a good model to be used for two-point control, we will study the following models:

N1: $\tau_2 = \tau_1$=194 min, $\theta_L = 0$. Simplest model with only the dominant time constant τ_1 and neglected flow-dynamics.

F1: $\tau_2 = \tau_1$=194 min. One time-constant model with flow dynamics.

F2: Two time-constant model (Eq.5.3) with τ_1, τ_2 and θ_L.

F1X: Same as F1, but with gains and time-constant reduced by a factor of 10.

Here "N" denotes no flow-dynamics, "F" denotes flow-dynamics, and "1" and "2" denotes one- and two-time-constant model, respectively. Note that all these models, except F1X, are identical to the full linear model at steady-state, but the high-frequency dynamics differ. Model $F1X$ will be identical to $F1$ at high frequencies, but the steady-state gains are incorrect. Also note that none of the models have multivariable zeros in the right half plane.

5.3.2 Mathematical model reduction

There exists many methods for reducing the order of a linear dynamic model. Most of the methods are based on computing the Hankel singular values[1], and then removing states corresponding to relatively small singular values. States with relatively small Hankel singular values corresponds to states having little effect on the input/output behavior of the system. In this work we applied 4 different methods to the full linear model of column A. All the methods are implemented in one of the MATLAB toolboxes:

B1: Balanced Truncation Approximation (Moore, 1981). (Robust Control Toolbox, Chiang and Safonov, 1988.

B2: Balanced Truncated Approximation without balanced minimal realization (Safonov and Chiang, 1988). (Robust Control Toolbox).

[1]The Hankel Singular Values are square roots of eigenvalues of PQ, where P and Q are the controllability and reachability grammians of the state-space system.

H1: Hankel Norm Approximation (Glover, 1988). (μ-Toolbox, Balas et.al., 1990).

H2: Optimal Hankel Approximation without balancing (Safonov et.al., 1987). (Robust Control Toolbox).

All methods possess the same infinity-norm error bound for a reduced model of order k. Method $H1$ allows for the D-matrix of the state-space description to be used, and guarantees in this case half the error compared to the other methods. However, this is not considered here. Methods $B1$ and $B2$ are quite similar, as are $H1$ and $H2$, but method $B1$ and $H1$ use a preliminary balanced realization of the original model while method $B2$ and $H2$ do not.

Due to their similarities in guaranteed maximum error one might expect that all methods yield similar reduced models. However, when reducing the model of column A from 82 to 2 states we found that the methods yielded very different models. Methods $B2$ and $H2$ gave significantly better models (though quite different) than methods $B1$ and $H1$. (see section 5.5 on controller design.)

The main reason why methods $B2$ and $H2$ yield the best results is probably that they do not use the numerically ill-conditioned minimal realization step (Safonov et.al., 1987) which is used by the two other methods. The results we find here may of course be case dependent, but at least they demonstrate that model reduction methods should be chosen with caution.

Reducing the full nonlinear model of column A from 82 to 2 states with the algorithm described in Safonov et.al. (1987) (method $H2$) yields the model $H2(s)$=

$$\frac{1}{(1.61s+1)(194s+1)}\begin{pmatrix}0.871(2.17s+1) & -0.861(0.721s+1)\\ 1.089(0.45s+1) & -1.101(3.48s+1)\end{pmatrix} \tag{5.7}$$

We see that the gains and the dominant time-constant are similar to the full linear model, but the model structure is quite different from those obtained from physical insight. The decoupling at high-frequencies due to the flow-dynamics is described by making the zeros in the off-diagonal elements smaller than in the diagonal elements.

5.4 Analysis of Models

In order to evaluate the quality of the above five reduced models (N1,F1,F1X,F2,H2) we will consider:

1. Open-loop simulations,
2. The Relative Gain Array, and
3. Robust Controller design.

In the two first cases we use the model as a plant and analyze the behavior of the model. In the last case we use the reduced models for controller design and analyze how the resulting controller works on the full-order model. Since the goal is to find a model that is good for controller design, case 3 is of primary importance.

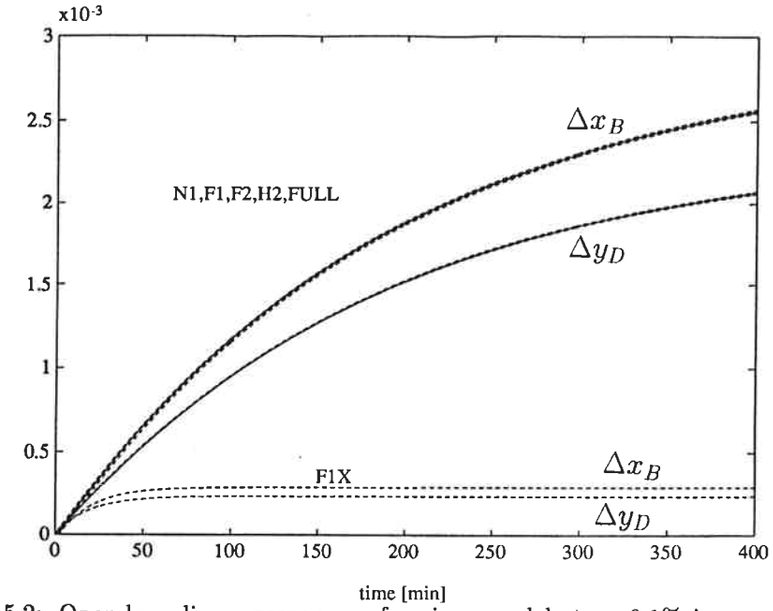

Figure 5.2: Open-loop linear responses of various models to a 0.1% increase in reflux, $\Delta L = 0.0027$.

5.4.1 Open-loop simulations

Small changes in external flows

Open-loop responses in y_D and x_B to a step change in L keeping V constant (change in external flows) using the five linear models are shown in Figure 5.2. We see that the models $N1$, $F1$, $F2$ and H2 are almost indistinguishable from the full linear model. The "wrong" model $F1X$ have a correct initial response, but the steady state gains are too low. The response for a step change in V is not shown, but would yield the same conclusion. The fact that the simple model $N1$ gives such a good fit implies that the responses are essentially 1.order with a time-constant of 194 min.

Most engineers would use these responses to compare the models, and would thus have concluded that only $F1X$ is a poor model.

Small changes in internal flows

Figure 5.3 shows responses in y_D and x_B to simultaneous and equal changes in L and V (change in internal flows). We note that there are significant differences between the models. Model $F2$ and H2 seems to be closest to the full model, especially for the initial response. Note that the steady-state gain for changes in internal flows is about one hundreth of that for external flows. This is the reason for the ill-conditioning (high interactions) of the plant. In a real plant operating open-loop, the effect of external flows will dominate and it will not be possible to observe effects of changes in internal flows alone. However, under feedback control the effect of internal flows may be observed also in practice. The reason is that the controller in order to keep the compositions constant

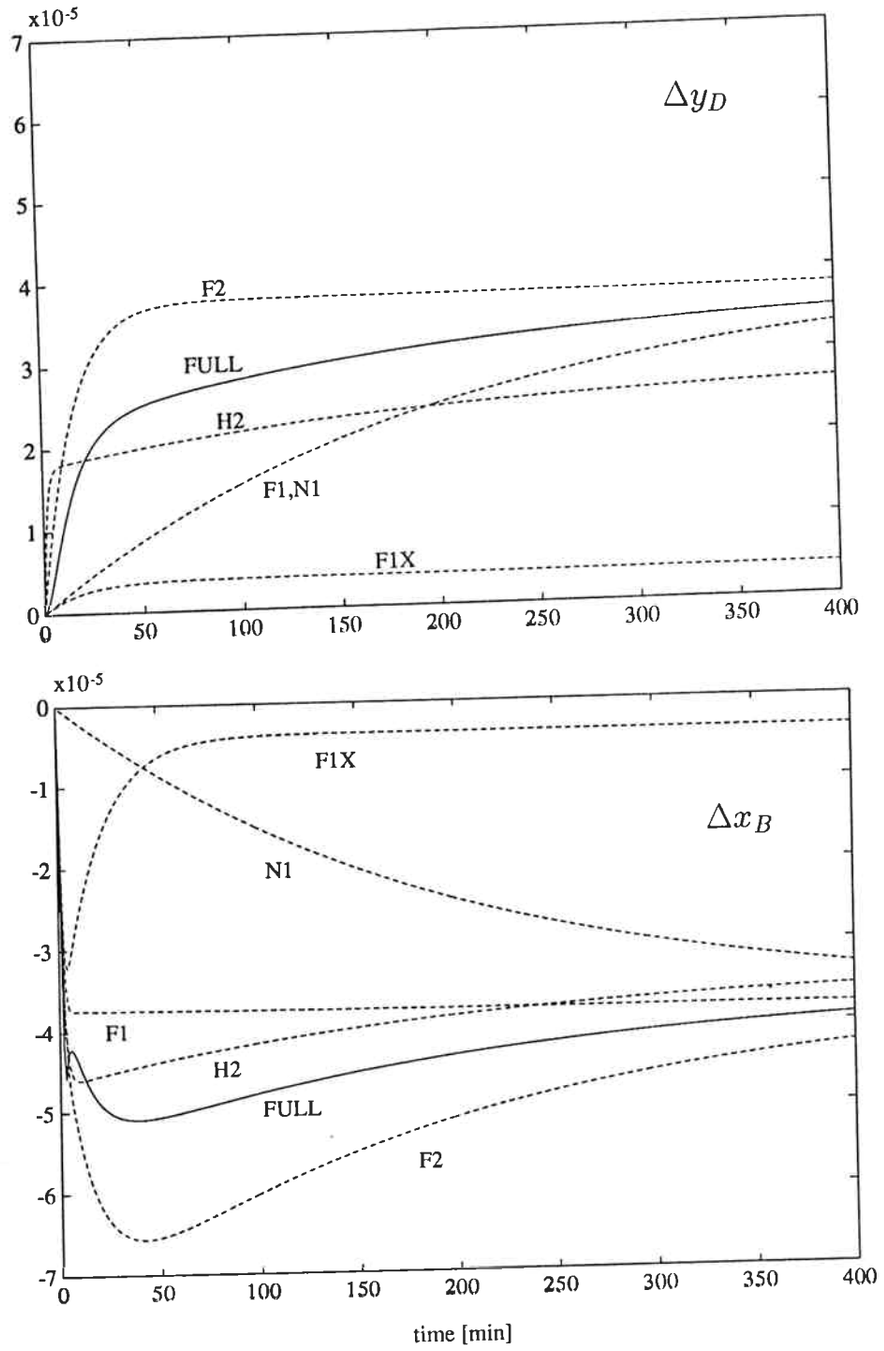

Figure 5.3: Open-loop linear responses of various models to a simultaneous increase in L and V. $\Delta L = \Delta V = 0.0027$.

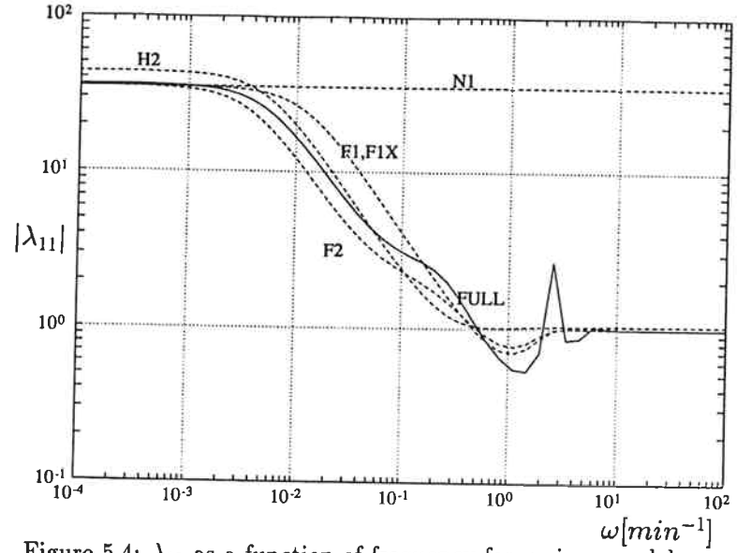

Figure 5.4: λ_{11} as a function of frequency for various models.

may have to make large changes in internal flows and thereby amplify the importance of the low-gain direction.

We rank the models from these simulations $F2, H2 > F1 > F1X > N1$.

5.4.2 Relative Gain Array

The 1,1 element of the RGA for 2×2 systems is given by

$$\lambda_{11}(j\omega) = \left(1 - \frac{g_{12}(j\omega)g_{21}(j\omega)}{g_{11}(j\omega)g_{22}(j\omega)}\right)^{-1} \tag{5.8}$$

The RGA has traditionally been evaluated at steady-state only (Bristol, 1966), but more recently the usefulness of the RGA plotted as a function of frequency has become clear. For example, Skogestad and Morari (1987b) argue that the value of the RGA at frequencies close to the expected closed-loop bandwidth is a good indicator of expected control performance and that large values indicate a plant that is fundamentally difficult to control. One important property of the RGA is that it is scaling independent. This means that that the RGA-elements are unchanged if actuator (valve) or measurement dynamics are included. For example, the RGA would be unchanged if we added the same time delay to each column or row of $G(s)$.

The magnitude of λ_{11} is shown as a function of frequency in Figure 5.4. At low frequencies the correct value is 35, and it falls down to 1 at high frequency where the responses becomes decoupled due to the flow-dynamics. Models $N1$, $F1$, $F1X$ and $F2$ yields a correct steady-state value, $\lambda_{11}(0) = 35$, while model H2 yields a steady-state value of 43. Model $N1$ has a constant value of 35 at all frequencies which clearly is incorrect. Model H2, while being incorrect at steady-state, yields a reasonably correct value of the RGA at high frequencies. Models $F1$, $F1X$ and $F2$ gives a reasonably correct value of

Model	μ_{RP}	k_y	k_x	τ_{Iy} [min]	τ_{Ix} [min]	τ_{Dy} [min]	τ_{Dx} [min]
N1	1.32	438	130	178.86	1.87	0.32	0.23
F1	0.91	85	38	7.77	3.61	0.81	1.11
F1X	1.12	96	93	2.48	2.23	0.68	1.10
F2	0.80	38	36	6.49	5.80	1.13	0.91
H1	0.95	2.2	10.8	0.73	0.92	1.20	4.98
B1	1.23	6.0	13.9	2.08	2.53	1.26	0.23
H2	0.78	32	34	4.39	4.14	1.03	0.41
B2	0.80	36	35	5.48	4.52	1.45	0.40
Full	0.86	22	32	3.51	4.71	1.22	0.61

- $C_{PID}(s) = k\frac{1+\tau_I s}{\tau_I s}\frac{1+\tau_D s}{1+0.1\tau_D s}$

Table 5.2: μ_{RP}-optimal PID-tunings for various column models.

the RGA at all frequencies. Note that $F1$ and $F1X$ yields identical RGA-values as they only differ by a scaling.

We rank the models based on the RGA-plot: $F2, H2 > F1, F1X >> N1$

5.5 Controller Design

Here we use the various models to design single-loop PID controllers, that is, top composition y_D is controlled by reflux L and bottom composition x_B is controlled by boilup V. Single loop controllers is a preferred choice in the industry, and seems to be a good one for the LV-configuration if properly tuned (Skogestad and Lundström, 1990).

To allow for differences also between the full linear model and the true plant we shall include model uncertainty in the controller design. The structured singular value, μ, is then a reasonable performance index. Robust performance (worst case response acceptable) is satisfied if μ_{RP} is less than 1, and designs with low μ_{RP}-values are preferable. Uncertainty and performance are defined as in Skogestad and Morari (1988a). The uncertainty corresponds to 1 minute deadtime and 20 % uncertainty in each input. The performance requirement corresponds to a maximum peak of 2 in the sensitivity function and a closed-loop time-constant of 20 min. Single-loop PID-controllers were tuned for the various models by minimizing μ_{RP}. The results are summarized in Table 5.2. Comparing the results for model $N1$, $F1$ and $F2$ we see that the optimal μ_{RP}-value becomes lower as flow-dynamics (θ_L) and internal flow-dynamics (τ_2) are included. This may be explained in terms of lower RGA-values at high frequency which makes control easier.

However, it is of course of no practical significance how well the *models* may be controlled; the interesting point is how well the controllers tuned based on the simplified models perform on the full-order model. This is summarized in Table 5.3. We see that

Controller (Table 5.2)	μ_{RP} Original	μ_{RP} Full model
N1	1.32	2.37
F1	0.91	1.16
F1X	1.12	1.44
F2	0.80	0.95
H1	0.95	1.24
B1	1.23	1.28
H2	0.78	0.94
B2	0.80	0.98
Full	0.86	0.86

Table 5.3: μ_{RP}-values for PID-controllers of Table 5.2 when applied to original simplified model and to full linear model.

the controllers based on the models $F1$, $F2$ and H2 perform well, with H2 and $F2$ giving the best design. Model $N1$ gives a poor controller for the full plant; it will in fact give an unstable system. We see that model $F1X$, which is close to the full model only the initial 10 minutes of the open-loop response, yields a far better controller than $N1$, which is correct at steady-state.

To compare the four different mathematical methods for model reduction discussed in section 5.3.2, we also designed controllers for models reduced from 82 to 2 states with each method. The results are given in Table 5.2 and 5.3. The results confirm that the methods *not* using the minimal balanced realization step (B2 and H2) yield controllers performing well on the full plant. The two other methods (B1 and H1) yield controllers that perform reasonably well on the full plant, but significantly poorer than B2 and H2. For the methods B1 and H1 one would have to include more states in the reduced models to get satisfactory results.

We rank the models based on the controller design: $H2, F2 > F1 > F1X >> N1$

5.6 Conclusions on Modelling Requirements

From the analysis presented above we conclude that models $F2$ and H2 seems to be the best models to be used for controller design. Most engineers would have considered mainly the open-loop responses for changes in external flows (see Figure 5.2), and would then conclude that $N1$ seems to be a reasonable model. However, as the RGA analysis demonstrated, model $N1$ is incorrect at high-frequencies and therefore useless for controller design. Model $F1X$ which is correct at high frequencies but incorrect at steady-state is in fact a much better model for controller design. These results simply support the well known fact that the high-frequency behavior is much more important than the steady-state properties for feedback control. An important conclusion is that the flow-dynamics should be included in a model to be used for controller design.

Part II: Model Identification From Experiments

In this section we discuss how low-order models may be obtained from open-loop experiments. From part I. we concluded that $F2$ and H2 were the best models. However, estimating τ_2 in model $F2$ will be difficult experimentally. Furthermore, the structure of model H2 is not physically motivated, and will be difficult to fit from experiments. However, model $F1$ seemed to be a reasonably good model structure, and should be well suited to fit from open-loop experiments. We will therefore use an $F1$-type model structure in the model identification.

All experiments are based on open-loop responses from the nonlinear model by doing step changes in one input at the time. This may seem a risky way to obtain a model as the plant is ill-conditioned and small errors in the gains may yield an erroneous model. On this background Andersen et.al. (1988) suggested using multivariable experiments. However, individual step responses are clearly the easiest way to obtain a model and, as we shall see, they may yield a good model if used together with theoretically established structural properties. The approach we suggest to use when obtaining the model is:

1. Fit only the initial part of the responses. This is motivated by the fact that we are mostly interested in capturing the high-frequency behavior correct. Furthermore, the initial part of the response is less affected by nonlinearities than the response towards steady-state (Skogestad and Morari, 1988b).

2. Make sure that the flow-dynamics are captured in the model. If there are several other deadtimes/lags in the process, one should make sure that the sum of lags in the off-diagonal elements are larger (actually θ_L larger) than the sum in the diagonal elements. The liquid lag θ_L may be obtained individually by measuring the time it takes for a change in liquid flow from the top to reach the bottom of the column.

3. Check the sign of the model at steady-state. It is important that the sign is correct also at steady-state. This may be checked by computing $\lambda_{11}(0)$ which should be greater than 1 for almost any column with the LV-configuration (see Appendix). Due to the ill-conditioning at steady-state, only small errors in the individual steady-state gains may yield an incorrect sign in the gain of the weak direction (corresponding to internal flows). If the steady-state sign of the model is incorrect, i.e., $\lambda_{11}(0) < 0$, change one of the individual steady-state gains so that the sign becomes correct. Correct also the corresponding time-constant so that the high-frequency dynamics are unchanged. Due to the flow-dynamics, the column will not be ill-conditioned at high frequencies, and it is therefore likely that the high-frequency directions are correctly captured.

We will demonstrate this approach by obtaining step responses from the nonlinear model of column A.

Experiment 1. In this experiment we use the LV-configuration and do step responses in reflux and boilup separately. We do a perturbation of 0.1 % in each input. This is of course an unrealistic small step change from a practical point of view, but as we shall see, even in this ideal case one may easily end up with an erroneous model. As we are mostly interested in the high-frequency behavior of the column we fit only the initial 60 minutes of the responses. The model thereby obtained is

$$\hat{G}(s) = \begin{pmatrix} \frac{0.728}{1+164s} & \frac{-0.903}{1+224s} \\ \frac{0.949}{1+154s} g_L(s) & \frac{-0.933}{1+144s} \end{pmatrix}, \theta_L = 2.5min. \tag{5.9}$$

Note that we have used four different time-constants. This was done to get the best fit of the responses.

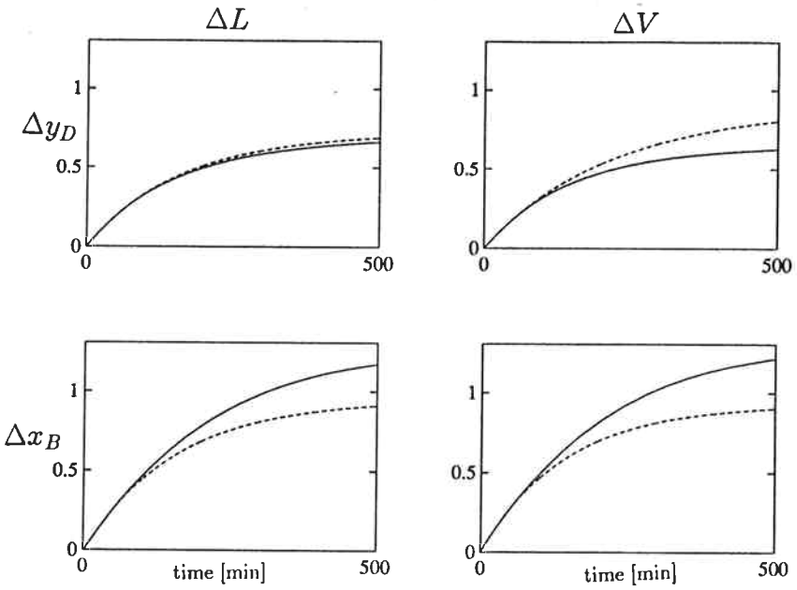

Figure 5.5: Open-loop responses for 0.1 % increase in reflux L and 0.1% decrease in boilup V. Responses are scaled so that it corresponds to $\Delta L = -\Delta V = 1$. Solid line: nonlinear response. Dashed line: fitted response.

Figure 5.5 shows the responses of the nonlinear model together with the responses of the fitted model. Note that the step changes where made so that the compositions increased in both experiments, i.e., we increased L and decreased V. From the figure we see that the initial 60 minutes are well fitted by the model, while there are quite large deviations at steady-state. The fitted model predicts a larger steady-state gain for top composition y_D than found for the nonlinear response. This is explained by the fact that the gain in the process decreases with increased purity, y_D (e.g., Skogestad and Morari, 1988b) , and this is reflected in the nonlinear response. The steady-state gain from L to y_D found in the nonlinear simulation is approximately 0.682, the fitted gain is 0.728 and the true linear gain is 0.87. For responses in bottom composition we see the same effect, but in this case the purity decreases (x_B increases) and the gain increases. This shows that even for these very small step changes, the responses becomes significantly affected by the nonlinearities. The change in gain due to change in purity is the main nonlinearity in distillation (Skogestad and Morari, 1988b).

From (5.9) we easily see that the sign of the gain for the weak direction of the plant is wrong. The steady-state gains tells us that an increase in internal flows ($dL = dV$)

will decrease purity in both ends, while we from theory know that this gain always will be positive in distillation, i.e., increased internal flows increase the separation. This is also seen when computing $\lambda_{11}(0)$ for (5.9), which yields a value of -3.8 which we from theory know is incorrect; $\lambda_{11}(0)$ should be larger than 1 (see Appendix). Computing the transmission zeros we also find that there is a multivariable right half plane zero at $0.0072min^{-1}$ which is closely linked to the negative $\lambda_{11}(0)$ (Hovd and Skogestad, 1990).

It is obvious that the fitted model, as is, is useless for designing controllers to be used on the plant. As we should always pair on positive RGA-elements, the model suggest the reverse pairing as compared to the correct model, i.e., L with x_B and V with y_D. Designing a controller with integral action for this pairing would yield an unstable system when applied to the true plan (Grosdidier et.al., 1985). If we paired the usual way, i.e., L with y_D and V with x_B, we would not obtain a stabilizing controller with the model. However, we have fitted only the initial part of the responses and know that these are less affected by nonlinearities than the steady-state responses. In addition the process is not ill-conditioned at high frequencies ($|\lambda_{11}(j\infty)| = 1$). We may therefore assume that the initial responses of the model are reasonably correct. Furthermore, we know that except for getting the correct sign of the plant at steady-state, the low-frequency behavior of the plant (and model) is of little importance for the control properties. We therefore propose to simply fix the sign of the model at low-frequency. This may be done by correcting one of the individual steady-state gains so that $\lambda_{11}(0)$ becomes greater than 1. To get a reasonably correct value of $\lambda_{11}(0)$ we use the simple expression (Skogestad and Morari, 1987a):

$$\lambda_{11}(0) = \frac{1}{Bx_B + D(1-y_D)} L \frac{2}{N} \frac{L+F}{F} \tag{5.10}$$

Inserting the nominal values in (5.10), we find $\lambda_{11}(0)$=50 (the correct value is 35). We choose to correct the off-diagonal element 2,1 to obtain $\lambda_{11}(0)$=50, and the new steady-state gain becomes k_{21}=0.737. Note that we scale the corresponding time constant accordingly so that the initial response is unchanged. This yields $g_{21}(s) = 0.737 g_L(s)/(1+120s)$. The corrected model has no RHP zeros. Figure 5.6 shows the RGA plotted as a function of frequency for the corrected model, denoted F1fit1. We see that we have a reasonably good fit of the RGA for the full linear model at high frequencies.

To check the quality of the obtained model, we use it for controller design as described in section 5.5, and apply the controller to the full plant. The results are given in Table 5.4. We see that the model yields a controller that performs reasonably well on the full plant. Comparing with the results in Table 5.3, we see that we obtain a controller with a performance similar to what was obtained with the "correct" $F1$-model. This is of course the best we could expect since we used a $F1$-type model structure.

Experiment 2. In experiment 1 we saw that even a 0.1 % perturbation in the inputs gave nonlinear effects in the responses. In practice one will of course have to make significantly larger changes in the inputs, and nonlinearities will affect the responses even more. One should be careful about trying to fit the nonlinearities into a linear model. To demonstrate this consider Figure 5.7 which shows the response in bottom composition x_B to a 1 % change in reflux L. The response now seems to be 2.order. However, as discussed above the gain will increase as x_B increases, and this explains the seemingly 2. order of the response. We know the linear responses in distillation columns should

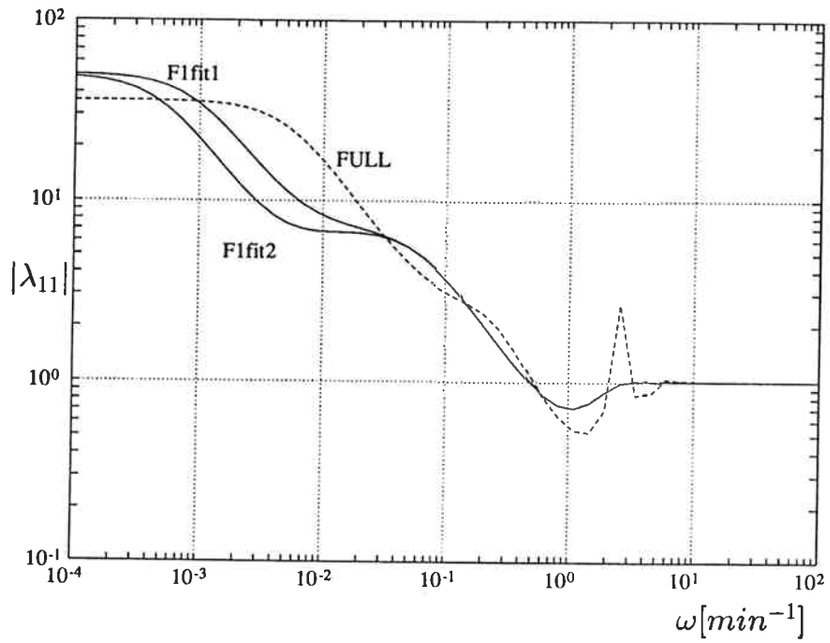

Figure 5.6: λ_{11} as a function of frequency for the fitted models F1fit1 and F1fit2.

Model	k_y	k_x	τ_{Iy}	τ_{Ix}	τ_{Dy}	τ_{Dx}	μ_{RP}-Original	$\mu_R P$-Full
F1fit1	37	44	3.53	4.00	1.54	0.94	0.87	1.05
F1fit2	53	41	4.00	3.11	1.31	0.89	0.91	1.11

Table 5.4: μ_{RP}-optimal PID-tunings for fitted models F1fit1 and F1fit2 and μ_{RP}-values when applied to fitted model and to full linear model.

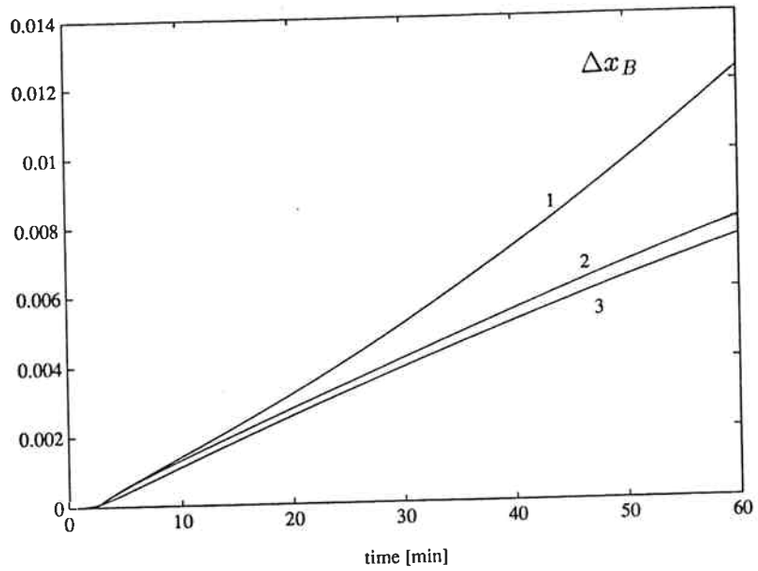

Figure 5.7: Open-loop response in x_B to a 1 % increase in reflux. 1) Nonlinear response. 2) Nonlinear logarithmic response ($\Delta log(x_B)/100$). 3) Linear response.

be almost pure 1.order. Trying to fit the response to a second order model would yield a poor model. However, as Skogestad and Morari (1988b) show, the nonlinearities may be partly counteracted by using the logarithm of the compositions as measurements, i.e. $log(1 - y_D)$ and $log(x_B)$. In particular the initial responses will be linearized by the logarithm. This is illustrated in Figure 5.7 which shows the nonlinear response in x_B with and without logarithmic measurements together with the linear response. The figure clearly demonstrates that the logarithm linearizes the initial response of the column.

In this case we therefore fit the logarithmic responses, and again we fit only the initial 60 minutes. This yields the model

$$\hat{G}(s) = \begin{pmatrix} \frac{0.456}{1+98s} & \frac{-0.423}{1+99s} \\ \frac{1.02}{1+168s} g_L(s) & \frac{-0.903}{1+141s} \end{pmatrix}, \theta_L = 2.5min. \tag{5.11}$$

For this model we find $\lambda_{11}(0) = -21$ which clearly is incorrect. Using the same procedure as above (change k_{21} to yield $\lambda_{11}(0)$=50) we find the new $g_{21} = 0.954 g_L(s)/(1 + 157s)$. The RGA of the corrected model, denoted F1fit2, is shown in Figure 5.6, and we see that we get a similar fit as obtained in Experiment 1.

The results obtained when using this model for controller design are given in Table 5.4. Again, we see that we get a model which yields a controller with a relatively good performance, and comparable to what was obtained with the $F1$-model.

5.7 Discussion

Other control configurations We have in this paper only discussed the LV-configuration,

i.e., using L and V as independent variables. However, other configurations are possible, and the model determined for one configuration may easily be transformed to another configuration by using simple algebraic relations (e.g., Skogestad et.al., 1990). For the DV-configuration the input D will correspond to external flows and input V to internal flows. One might think that it should be relatively easy to obtain the weak direction of the plant from a step change in V. This is, however, not necessarily true: because of the flow-dynamics there will be a temporary change in external flows when changing V. This results in a significant overshoot in bottom composition, and the transfer-function should contain a minimum phase zero close to the imaginary axis in addition to two poles. Furthermore, the DV-configuration depends on the tuning of the level controllers, and one will observe that this affects the responses. There will for instance be a small inverse response in y_D for a change in V because of nonperfect level control. Due to these complications we found it difficult to obtain a good model using the DV-configuration. Using the LV-configuration (which is independent of the level controllers) and correcting the model as discussed above yielded far better models.

Effect of deadtimes. We have assumed an input deadtime of 1 minute when designing controllers. This implies that we are able to have a relatively small closed loop time-constant (20 min.). However, if the deadtime in the system is significantly larger, the closed-loop constant will have to be reduced accordingly. In this case it will be necessary to have a good fit of the model also at lower frequencies, and the models we have obtained from open-loop experiments may not be sufficient. In cases with large deadtimes it will be difficult to obtain a good model from single step open-loop responses.

Measurement noise. We have not included any measurement noise in our simulations. However, when fitting the responses to 1.order transfer-functions with only two parameters, it is unlikely that randomly distributed noise will affect the results significantly.

Multivariable controllers. One might argue that when true multivariable controllers are to be applied to the plant one needs a better fit of the individual elements in the model. This may certainly be true. However, it is also clear that due to uncertainty in the inputs, a multivariable controller, which tends to decouple the process, will perform poorly on an ill-conditioned plant (Skogestad and Morari, 1987b).

5.8 Conclusions

1. The most important model characteristic for controller tuning is the high-frequency dynamics (initial response) corresponding to the time-constant of the closed-loop system.

2. Because of the importance of the high-frequency behavior, the flow-dynamics should be included in the model.

3. An accurate model of the steady-state behavior is not very important for controller design. However, it is important to know the sign of the plant, that is, one must know the sign of the steady-state RGA. For almost any column with the LV-configuration $\lambda_{11}(0)$ should be larger than 1.

4. Models obtained simply by fitting individual transfer-functions from open-loop experiments may prove entirely useless for controller design. However, if the obtained model is corrected according to established structural properties, the resulting model will most likely be good.

5. One may easily enter the nonlinear region when doing open-loop experiments. The nonlinearities may effectively be counteracted by using logarithmic measurements.

Acknowledgements: Financial support from the Royal Norwegian Council for Scientific and Industrial Research (NTNF) is greatfully acknowledged.

APPENDIX. $\lambda_{11}(0)$ for distillation columns with LV-configuration.
Consider a binary separation. Define the separation factor

$$S = \frac{y_D/(1-y_D)}{x_B/(1-x_B)} \tag{5.12}$$

and assume that the following component and overall material balance apply

$$Fz_F = Dy_D + Bx_B \tag{5.13}$$

$$F = D + B \tag{5.14}$$

F and z_F are assumed constant in the following (disturbances not considered). Differentiating these equations yields

$$Ddy_D + Bdx_B = -(y_D - x_B)dD \tag{5.15}$$

$$\frac{1}{y_D(1-y_D)}dy_D - \frac{1}{x_B(1-x_B)}dx_B = d\ln S \tag{5.16}$$

and the steady-state gains may be evaluated by eliminating dy_D or dx_B from these equations. The 1,1-element in the RGA is given by

$$\lambda_{11} = k_{11}k_{22}/\det K \tag{5.17}$$

where by definition for the LV-configuration

$$k_{11} = \left(\frac{\partial y_D}{\partial L}\right)_V; \quad k_{22} = \left(\frac{\partial x_B}{\partial V}\right)_L \tag{5.18}$$

and by manipulating (5.15)-(5.16) we derive for the LV-configuration

$$\det K = \frac{(y_D - x_B)}{\beta(\partial D/\partial L)_V}\left(\frac{\partial \ln S}{\partial L}\right)_D \tag{5.19}$$

where β is a positive constant defined as

$$\beta = \frac{D}{x_B(1-x_B)} + \frac{B}{y_D(1-y_D)} \tag{5.20}$$

Make the following physical assumptions

A1. $k_{11} > 0, k_{22} < 0$. This applies to any column with constant molar flows (Jacobsen and Skogestad, 1991).

A2. $\left(\frac{\partial \ln S}{\partial L}\right)_D > 0$. This is equivalent to requiring $\left(\frac{\partial y_D}{\partial L}\right)_D = -\frac{B}{D}\left(\frac{\partial x_B}{\partial L}\right)_D > 0$. This means that an increase in internal flows (D constant) should improve separation.

A3. $\left(\frac{\partial D}{\partial L}\right)_V < 0$. This must hold for any column with constant molar flows (Jacobsen and Skogestad, 1991) provided flooding does not occur as L is increased.

With these assumptions, which should apply to any column assuming constant molar flows and no flooding, we get for the LV-configuration $\det K < 0$ and $\lambda_{11} > 0$. If we in addition make the assumption

A4. $k_{21} = \left(\frac{\partial x_B}{\partial L}\right)_V > 0; \quad k_{12} = \left(\frac{\partial y_D}{\partial V}\right)_L < 0$

which is closely related to Assumption A1, then $\frac{k_{12}k_{21}}{k_{11}k_{22}}$ is positive and λ_{11} cannot be between 0 and 1 . We conclude that for columns where Equations (5.13) and (5.14) and Assumptions A1-A4 hold, the 1,1-element in the steady-state RGA of the LV-configuration is always larger than 1. The results may be extended to multicomponent mixtures if flows and compositions are evaluated on a pseudo-binary basis. It should also be noted that if both A1 and A4 hold, then A3 is not needed since it follows as a special case from (5.15).

NOMENCLATURE (see also Figure 5.1) .

B - bottoms flow (kmol/min)
D - distillate flow (kmol/min)
F - feed flow (kmol/min)
$G(s)$ - linear model of column
$\hat{G}(s)$ - experimentally fitted model
g_{ij} - elements of $G(s)$
$K = G(0)$ - steady-state gain matrix
k_{ij} - steady state gains for column
L - reflux (kmol/min)
M - liquid holdup (kmol)
N - number of theoretical trays

N_F - Feed tray
RGA - Relative Gain Array, elements are λ_{ij}
S - separation factor
V - boilup (kmol/min)
x_B - mole fraction of light component in bottoms product
y_D - mole fraction of light component in distillate (top product)
z_F - mole fraction of light component in feed

Greek symbols

$\alpha = \frac{y_i/x_i}{(1-y_i)/(1-x_i)}$ - relative volatility
$\lambda_{11}(j\omega) = (1 - \frac{g_{12}(j\omega)g_{21}(j\omega)}{g_{11}(j\omega)g_{22}(j\omega)})^{-1}$ - 1,1-element in RGA.
ω - frequency (min^{-1})
τ_1 - dominant time constant for external flows (min)
τ_2 - time constant for internal flows (min)
$\tau_L = (\partial M_i/\partial L)_V$ - hydraulic time constant (min)
$\theta_L = (N-1)\tau_L$ - overall lag for liquid response (min)

REFERENCES

Andersen, H.W., M. Kümmel, and S.B. Jørgensen, 1988, "Dynamics and identification of a binary distillation column", AIChE Annual Meeting, Washington DC, Nov. 1988.

Balas, G.J., J.C. Doyle, K. Glover, A.K. Packard and R. Smith, 1990, *μ-Analysis and Synthesis Toolbox, Beta Test Version*, MUSYN Inc.

Chiang, R.Y. and M.G. Safonov, 1988, *Robust Control Toolbox*, MathWorks Inc.

Bristol, E. H., 1966, "On a New Measure of Interactions for Multivariable Process Control", *IEEE Trans. Automat. Contr.*, **AC-11**, 133-134.

Glover, K., 1984, "All Optimal Hankel Norm Approximation of Linear Multivariable Systems, and Their L^∞-error bounds", *Int.J.Control*, **39**, 6, 1145-1193.

Grosdidier, P., M. Morari and B.R. Holt, 1985, "Closed-Loop Properties from Steady-State Gain Information", *Ind. & Eng. Chem. Fundamen.*, **24**, 221-235.

Hovd, M. and S. Skogestad, 1990, "Use of Frequency Dependent RGA for Control System Analysis, Structure Selections and Design", Accepted for publication in *Automatica.*

Jacobsen, E.W. and S. Skogestad, 1991, "Multiple Steady-States in Ideal Two-Product Distillation", *AIChE J.*, **37**, 4, 499-511.

Luyben, W.L., 1970, "Distillation decoupling", *AIChE J.*, **16**, 2, 198-203.

Moore, B.C., 1981, "Principal Component Analysis in Linear Systems: Controllability, Observability and Model Reduction", *IEEE Trans. on Automat. Contr.*, **AC-32**,115-122.

Safonov, M.G. and R.Y. Chiang, 1988, "Schur Balanced Model Reduction", *Proc. American Contr. Conf.*.

Safonov, M.G., R.Y. Chiang and D.J. Limebeer, 1987, "Hankel Model Reduction without Balancing - A Descriptor Approach", *Proc. IEEE Conf. on Dec. and Contr.*

Skogestad, S. and M. Morari, 1987a, "A systematic Approach to Distillation Column Control", *I.Chem.E.Symp.Series*,**No. 104**, A71-A76.

Skogestad, S. and M. Morari, 1987b, "Implication of Large RGA-Elements on Control Performance", *Ind. & Eng. Chem. Res.*, **26**, 11, 2121-2330.

Skogestad, S. and M. Morari ,1988a, "LV-control of a High-Purity Distillation Column", *Chem. Eng. Sci.*, **43**, 1, 33-48.

Skogestad, S. and M. Morari, 1988b, "Understanding the Dynamic Behavior of Distillation Columns", *Ind. & Eng. Chem. Res*, **27**, 10, 1848-1862.

Skogestad, S. and P. Lundström, 1990, "Mu-optimal LV-control of Distillation Columns", *Computers & Chem. Eng*, to appear.

Skogestad, S., P. Lundström and E.W. Jacobsen, 1990, "Selecting the Best Distillation Control Configuration", *AIChE J.*, **36**, 5, 753-764.

Toijala (Waller), K.V. and K. Fagervik, 1972, "A Digital Simulation Study of Two-Point Feedback Control of Distillation Columns", *Kemian Teollisuus*, **29**, 1, 1-12.

Wood, R.K. and M.W. Berry, 1973, "Terminal composition control of a binary distillation column", *Chem. Eng. Sci.*, **28**, 1707-1717.

Chapter 6

Design Modifications for Improved Controllability of Distillation Columns

Elling W. Jacobsen and Sigurd Skogestad

Chemical Engineering
University of Trondheim - NTH
N-7034 Trondheim
Norway

Submitted to *Computers Chem.Engng.*

Abstract

High-purity distillation columns have several characteristics that make them inherently difficult to control. One of the main control limitations is the strong interactions between the top and bottom of the column. In this paper we study some design modifications of the column which may improve the controllability. These modifications include introducing sidestreams, changing the number of trays and use of a feed preheater for feedback control. It is shown that some of the modifications may yield a significant reduction in the interactions as well as in disturbance sensitivity.

6.1 Introduction

High-purity distillation columns are known to be inherently difficult to control. The main reasons are strong interactions (ill-conditioning) and high disturbance sensitivity (e.g., Skogestad et.al., 1988). The problem of controlling the product compositions of such columns has been studied extensively in the literature over the last decades. However, most authors have considered columns that are close to optimally designed from a steady-state point of view. This reflects common practice in industry; a process unit is designed for steady-state optimality and the control engineer is left with the problem of designing controllers. However, in many cases the operational (dynamic) performance of the column will be poor, even with the "best" possible controller, due to inherent control limitations. That is, the "controllability" is poor. In this paper we discuss possible trade-offs between steady-state optimality and controllability. Relaxing the demands for steady-state optimality may be warranted in terms of improved dynamic performance. The issue of design modifications for improved control in distillation has so far gained little attention in the literature.

In this paper we consider 5 different design modifications: 1) Wachter and Andres (1989) suggested to introduce sidestreams with recycling to the feed to improve controllability of high-purity separations. In this paper we consider the effect of sidestreams with and without recycling to the feed. We find that a sidestream by itself has little effect on controllability, and if it is recycled to the feed as suggested by Wachter and Andres it has almost no effect. 2) Kropholler and Guesalaga (1990) suggested to use a bypass in reflux, i.e., to introduce parts of the reflux further down the column. However, this bypass has essentially no effect on interactions and disturbance sensitivity. Furthermore, when designing controllers for optimized robust performance we found that the optimal controller did not make any use of the bypass. We will therefore not pursue this idea any further. 3) Loe (1976) considered the use of a feed preheater for control. His idea was that manipulation of the feed preheater in a certain way would yield reduced interaction between the top and bottom of the column. In this paper we apply a slight modification of his idea and find that the improvement in controllability may be significant. 4) In addition to the above previously proposed modifications, we analyze the effect of "overdesign" by introducing extra trays in the column. Overdesign is fairly common in industry, mainly to allow for flexibility in the operation and in some cases to overfractionate the products. In this paper we find that overdesign may improve the controllability in some cases. 5) An important issue is the selection of which inputs to use for composition control. This is often specified as a part of the column design, but the decision made here is of vital importance for the remaining control problem. The selection of a proper configuration has been treated quite extensively in the literature during the last decade (e.g., Shinskey, 1984, Häggblom and Waller, 1990, Skogestad et.al, 1990) and is therefore not treated in detail here.

6.2 Example Columns

Data for the "base case" example columns we will use ("Column A and F") are given in Table 6.1. The columns have 40 and 10 theoretical stages, respectively, and both have high-purity products. Column F is somewhat unusual with its large relative volatility and corresponding low reflux. The controllability of both columns have been studied quite extensively in several papers by Skogestad and coworkers (e.g., Skogestad et.al., 1990).

The following modelling assumptions are used: binary separation, constant relative volatility, constant molar flows (neglected energy balance), negligible vapor holdup, and vapor-liquid equilibrium as well as perfect mixing on each stage. Neglecting the vapor holdup implies immediate vapor flow responses throughout the column. The liquid flow-dynamics are described by a linear relation between between liquid flow L_i and liquid holdup M_i;

$$L_i = L_i^0 + (M_i - M_i^0)/\tau_L \tag{6.1}$$

where superscript 0 denotes nominal steady-state values. The hydraulic time-constant τ_L is computed from a linearized Francis weir formula

$$\tau_L = \frac{2}{3}\frac{M_{oi}}{L_i} \tag{6.2}$$

where M_{oi} denotes liquid over weir. We use a liquid holdup on each tray equal to $M_i/F = 0.5$ min. and assume half the liquid over weir. This yields $\tau_L = 0.063$ min. for column A and $\tau_L = 0.733$ min. for column F. The total lag from a change in reflux to a change in the liquid flow to the reboiler becomes $\theta_L = N\tau_L = 2.46$ min. for column A and $\theta_L = N\tau_L = 6.60$ min. for column F.

The modelling assumptions yield a nonlinear dynamic model with two differential equations per tray; one for composition and one for liquid holdup. This results in a total of $2(N+1)$ states in the full model, with N denoting the number of theoretical trays. In the analysis we will use linear models which are obtained by linearizing the full nonlinear models around the nominal steady-state.

We will in the following mainly consider the LV-configuration, that is, with reflux L and boilup V used for composition control. This may not be the best choice of configuration with respect to control properties (e.g., Skogestad et.al, 1990), but it is the most widespread configuration in industry.

Column	z_F	α	N	N_F	$1-y_D$	x_B	D/F	L/F	V/F
A	0.5	1.5	40	21	0.01	0.01	0.500	2.706	3.206
F	0.5	15	10	5	0.0001	0.0001	0.500	0.227	0.727
•	Feed is saturated liquid								

Table 6.1: Steady-state data for distillation columns A and F.

When considering various design modifications we always adjust the steady-state values of L and V so that the product purities $1 - y_D$ and x_B remain at the values given in Table 6.1, that is, 0.01 for column A and 0.0001 for column F.

6.3 Analysis Tools

6.3.1 The Relative Gain Array

The Relative Gain Array (RGA) was originally proposed by Bristol (1966) as a steady-state interaction measure, and has found widespread applications for selecting single loop pairings in decentralized control. Furthermore, the RGA is closely related to the minimized condition number and so large RGA-values indicate that decouplers will perform poorly on the plant. One of the main advantages of the RGA is that it depends only on the plant model itself, and does therefore not require any preliminary controller design. This is due to an assumption of perfect control. Another advantage of the RGA is that it is scaling independent.

The RGA may easily be extended to a frequency dependent measure (e.g., Bristol, 1978), and will in this case contain more useful information with respect to feedback control. We are here primarily interested in the frequency region around the expected closed-loop bandwidth. The definition of the elements in the RGA is given by

$$\lambda_{ij} = \frac{(\partial y_i/\partial u_j)_{u_{l\neq j}}}{(\partial y_i/\partial u_j)_{y_{l\neq i}}} = g_{ij}(s)[G^{-1}(s)]_{ji} \tag{6.3}$$

As the elements in each row and column sums up to unity in the RGA, we only have to consider the 1,1 element for the 2×2 case.

Skogestad et.al. (1990) have successfully used the frequency dependent RGA for selecting control configurations for several distillation columns, and Hovd and Skogestad (1991) have proven its usefulness on a more general basis.

6.3.2 Closed Loop Disturbance Gain

The Relative Gain Array is independent of disturbances. However, the main reason for applying feedback control in distillation is rejection of disturbances that enters the process. In the literature it has been common to consider the open-loop disturbance gains at steady-state when evaluating sensitivity to disturbances. However, one should also for disturbances put emphasis on the dynamic behavior. In addition the direction of the disturbance effect should be considered in the multivariable case. Some disturbances may be easier to reject than others due to a good alignment with the strong input directions of the plant. Stanley et.al. (1985) introduced the Relative Disturbance Gain (RDG) which takes the directions into account. For a particular disturbance z_k the RDG, β_{ik}, is defined for each loop i as the ratio of the change in u_i needed for perfect disturbance rejection in all outputs to the change in u_i needed for perfect disturbance rejection in the corresponding output y_i when all other inputs are kept constant.

$$\beta_{ik} = \frac{(\partial u_i/\partial z_k)_{y_l}}{(\partial u_i/\partial z_k)_{y_i, u_{l\neq i}}} \tag{6.4}$$

Hovd and Skogestad (1991) suggested a measure, the Closed-Loop Disturbance Gain (CLDG), δ_{ik}, based on the RDG but which also takes the disturbance gain g_{dik} into account,

$$\delta_{ik} = \beta_{ik} g_{dik} \tag{6.5}$$

A matrix of CLDG's may be computed from

$$\Delta = \{\delta_{ik}\} = G_{diag} G^{-1} G_d \tag{6.6}$$

where G_{diag} are the diagonal elements of G. Hovd and Skogestad (1991) found that this measure enters nicely into the relation between control off-set e_i and disturbances z_k while the RGA enters in a similar way into the relation between off-set and setpoint changes r_j. We have for the case of decentralized control

$$e_i \approx -\lambda_{ji}\frac{1}{g_{ji}c_i} r_j + \delta_{ik}\frac{1}{g_{ii}c_i} z_k; \quad \omega < \omega_B \tag{6.7}$$

Assume the model is scaled such that the allowed control error, $e_i = y_i - r_i$, is of magnitude 1, and the disturbance model is scaled such that the expected disturbances, z_k, are of magnitude 1. Then (6.7) implies that $|\delta_{ik}(j\omega)|$ is approximately equal to the minimum loop gain, $|g_{ii}c_i(j\omega)|$, needed to reject disturbance z_k. Due to bandwidth limitations the required gain should not be too high. That is, small values of $|\delta_{ik}|$ are preferred. Similar reasoning applies to the RGA for setpoint changes.

In this paper we scale the outputs such that setpoint changes of 0.01 mole-fraction units for column A and 0.0001 mole-fraction units for column F corresponds to magnitude 1 setpoint changes. We consider disturbances in feed flow F and feed composition z_F. For both columns the disturbances are scaled so that a 30 % change in F and a 20 % change in z_F corresponds to magnitude 1 disturbances.

6.4 RGA and CLDG for Example Columns.

The RGA for column A is shown as a function of frequency as the solid line in Figure 6.1a. The RGA starts out at a value of 35 at steady-state but breaks off at intermediate frequencies and reaches a value of 1 at high frequencies. The RGA value of 1 at high frequencies is due to the liquid lag which introduces a one-way decoupling at high frequencies. The frequency where the RGA-value becomes unity is given by $\omega_1 \approx 1/\theta_L$ (Skogestad et.al., 1990), where θ_L is the total liquid lag for the flow-dynamics as defined in Section 2.

The RGA for column F is shown in Figure 6.2a. The RGA starts out at a value of 499 at steady-state, but as for column A it breaks off at intermediate frequencies and reaches a value of 1 at higher frequencies due to the flow-dynamics.

The large RGA-values for the two columns imply that decouplers can not be used as a part of the controller design (Skogestad and Morari, 1987).

The interactions in distillation columns operated with the LV-configuration may be understood as follows: The initial composition responses are dominated by intermixing between adjacent stages as a result of the change in flows L and V. Due to the lag

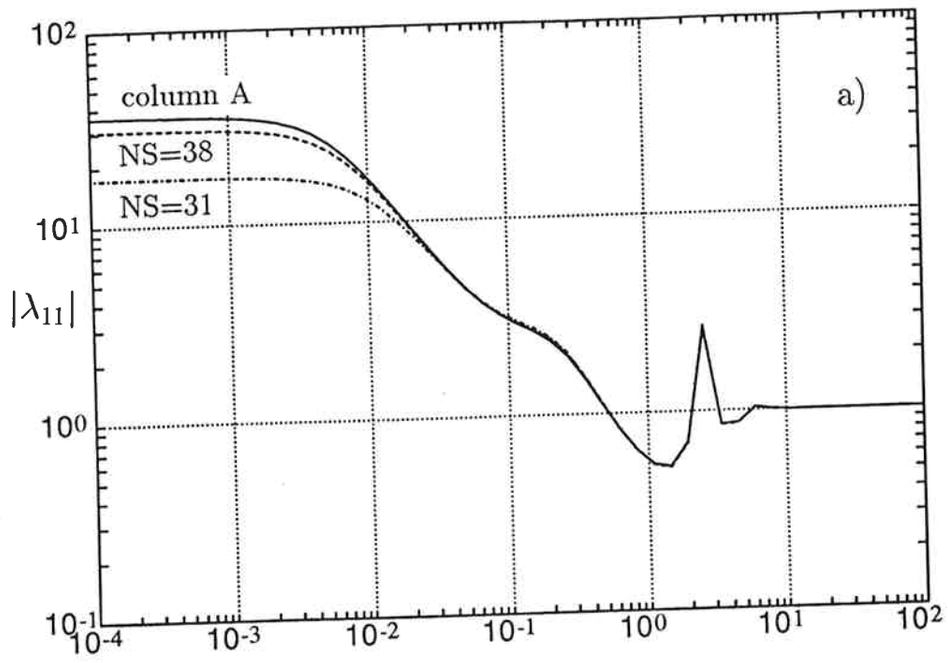

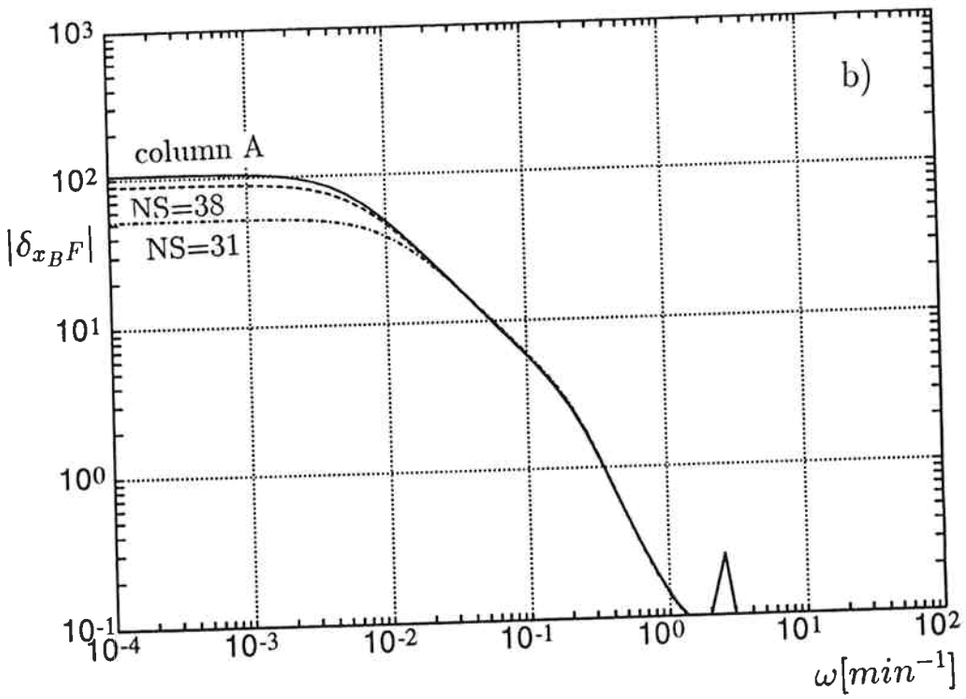

Figure 6.1: (a) RGA and (b) CLDG (effect of F on x_B) as functions of frequency for column A with and without sidestream. Sidestreams $S = 0.1F$ from trays 31 and 38 respectively.

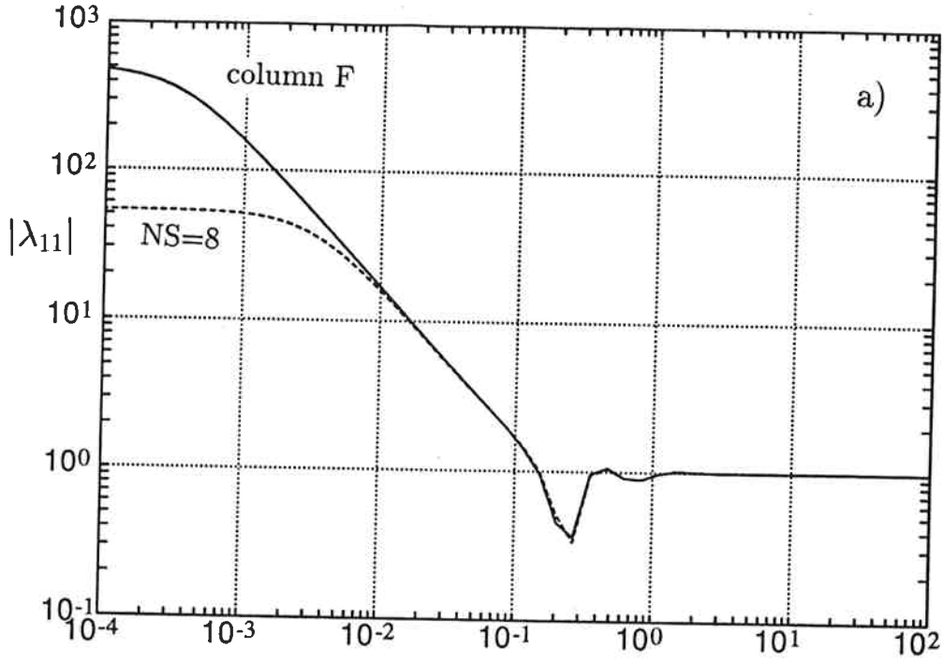

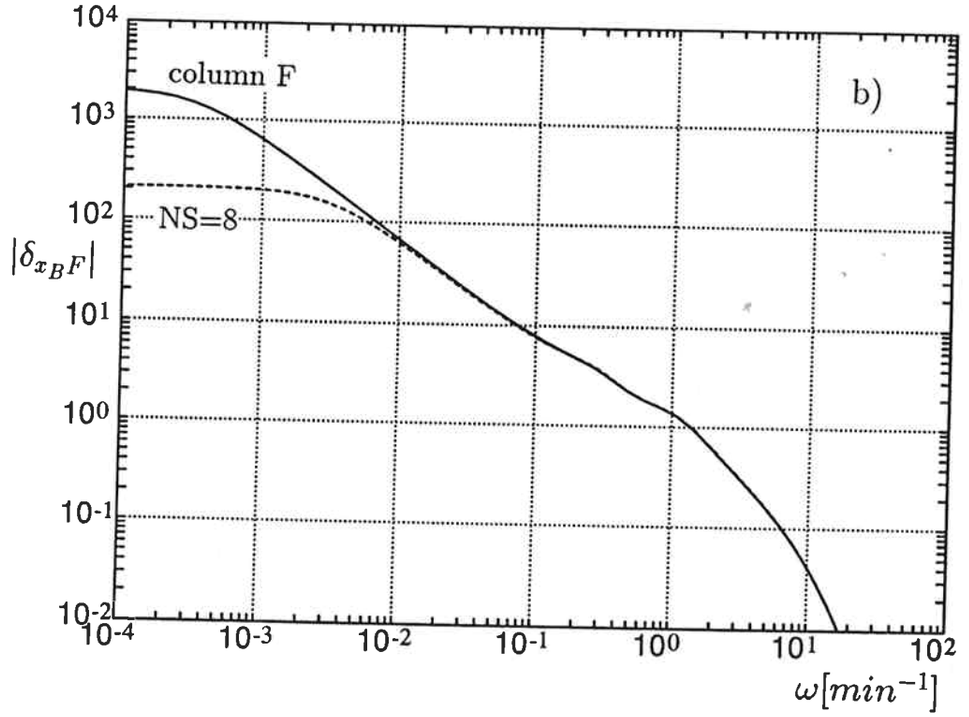

Figure 6.2: (a) RGA and (b) CLDG (effect of F on x_B) as functions of frequency for column F with and without sidestream. Sidestream $S = 0.02F$ from tray 8.

for changes in reflux flow L, the interactions are small initially. The slower part of the responses are dominated by interactions between the compositions on *all* stages (eg, Rademaker et.al, 1975). In a well designed column without any pinch in the composition profile this results in strong interactions between the top and bottom of the column.

Figure 6.1b shows the CLDG as a function of frequency for the effect of a disturbance in feed flow F on bottom composition x_B (worst case disturbance) for column A. We see that the CLDG has its maximum at steady-state and breaks off at the same frequency as the RGA. The CLDG for a disturbance in F on x_B (worst case disturbance) for column F is shown in Figure 6.2b. As for column A the CLDG has its maximum at steady-state and then breaks off at the same frequency where the RGA breaks off.

When analyzing systems for feedback control properties one should emphasize the frequency region around the expected closed-loop bandwidth. The expected bandwidth of most columns will be in the frequency range 0.01 - 0.1 rad/min, depending mainly on the size of measurement delays. We see from Figure 6.1 and Figure 6.2 that the interactions and disturbance sensitivity are worse when the bandwidth is low.

6.5 Effect of Introducing Sidestreams

The high interactions in high-purity distillation (using LV-configuration) is closely related to the fact that the steady-state gains for "changes in internal flows" (change L and V with D and B constant) are significantly smaller than the gains for "changes in external flows" (change in D and B) (e.g., Skogestad et.al., 1988). The reason for the high gains for changes in external flows is easily seen from the overall material balance (e.g, Shinskey, 1984)

$$Dy_D + Bx_B = Fz_F \tag{6.8}$$

For high-purity columns we have $y_D \approx 1$ and $x_B \approx 0$ and thus $D \approx Fz_F$. Any change in D from this value will necessarily lead to an imbalance in (6.8) which will strongly influence the product compositions. One possible way to reduce the effect of external flows on product compositions is to withdraw a small sidestream from a plate inside the column (Wachter and Andres, 1989). The total material balance then becomes

$$Dy_D + Bx_B + Sx_S = Fz_F \tag{6.9}$$

Here S denotes the size of the sidestream and x_S its composition. The compositions inside the column will vary relatively much compared to the product compositions, and one might conjecture that a sidestream will absorb a large part of the imbalance for changes in D and B. Since a sidestream only will have a small effect on the gains for internal flows, we expect the RGA and CLDG to decrease with the introduction of a sidestream, at least at low frequencies. Note that we here use steady-state arguments.

The two dotted lines in Figure 6.1a shows the RGA for column A with a sidestream $S = 0.1F$ on tray 31 and tray 38, respectively. We see that the sidestream reduces the RGA at low frequencies from 35 to 17 and 31, respectively, but has no effect on the RGA at higher frequencies. The reduction in the RGA at low frequencies is expected from the above discussion. The RGA is unchanged at higher frequencies because the initial responses are dominated by the intermixing between adjacent stages due to the change in

flows, and as the composition profile is almost unchanged by the sidestream, the initial responses are unaffected. Figure 6.1a shows, as expected, that the effect of a sidestream on tray 31 is significantly larger than for a sidestream on tray 38, which is located only two trays below the top.

A sidestream has a similar effect on disturbance sensitivity as on the RGA. This is illustrated in Figure 6.1b which shows the CLDG for a disturbance in F on x_B for column A with and without sidestreams. We see that the disturbance sensitivity is reduced at low frequencies but is unchanged at higher frequencies. The effect on the other elements of the CLDG-matrix is similar.

Figure 6.2 shows the effect on the RGA and CLDG of introducing a sidestream $S = 0.02F$ in column F. The sidestream is withdrawn from tray 8, which is close to the top. The RGA is reduced from 499 to 53 at low frequency, but as for column A, there is no improvement in the frequency region most important for feedback control. The CLDG is similarly to the RGA significantly reduced at low frequencies but unchanged at higher frequencies.

We conclude from the analysis above that although the RGA and CLDG are reduced at low frequencies by introducing a sidestream, the controllability is almost unaffected as the high-frequency behavior is unchanged. The bandwidth will usually be in the frequency range 0.01 - 0.1 rad/min, and in this region there is no improvement in the RGA and CLDG. For manual operation, where "control" will be slow, a sidestream may ease the operation, especially in columns with high purities like column F. For column A, a relatively large sidestream is needed to yield a significant improvement in the low-frequency RGA, and this will be costly as the sidestream will have to be recycled somewhere in the process.

Wachter and Andres (1989) propose to introduce a sidestream and recycle it to the feed. However, then there is no effect on the overall material balance (6.8), and their solution does not yield any noticeable change in the RGA or CLDG.

6.6 Effect of Adding Trays

Industrial columns are often overdesigned in terms of number of trays to increase flexibility with respect to changing feed stocks, and sometimes also to overfractionate the products so that the product specifications are easier to keep when disturbances enter the column. Here we consider overdesigned columns with the product compositions kept at their specifications.

One of the characteristics of an overdesigned column is that is has a pinch in the composition profile. This is seen when plotting $log(x_L/x_H)$ against tray number, where x_L and x_H denotes fraction of light and heavy component respectively. Figure 6.3 shows a plot of $log(x_L/x_H)$ for column A with 40 trays and for column A60 with 60 trays (feed tray at 31). The product specifications are the same for both columns. We see that column A60 has a pinch in the profile around the feed, while column A has no pinch. As one of the main reasons for the interactions in distillation is the interaction between compositions on *all* trays, we expect the pinch zone in the overdesigned column to reduce the interaction between the sections above and below the pinch. Introducing extra trays will also reduce

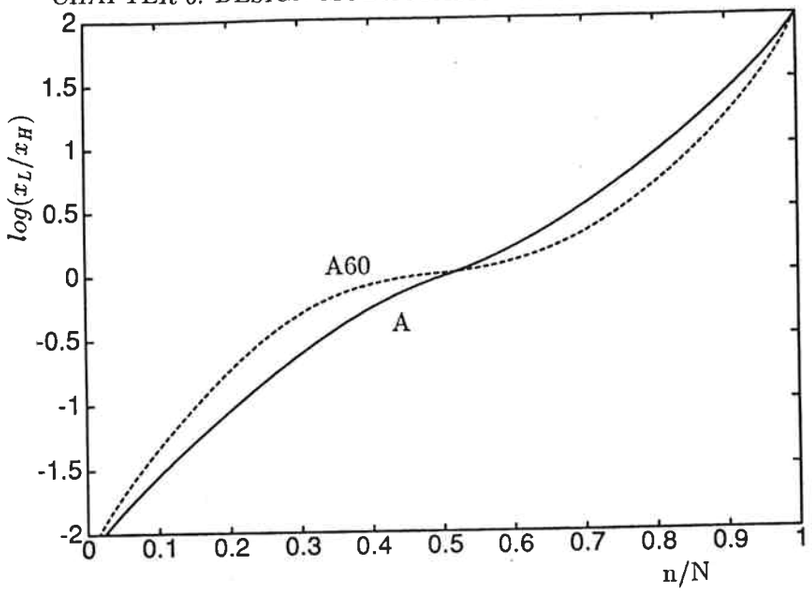

Figure 6.3: Composition profile [$log(x_L/x_H)$ against tray number n/N] for column A and column A60.

the internal flows and thus increase the effect of internal flows on compositions, while the effect of external flows will be almost unchanged.

Figure 6.4a shows the RGA as a function of frequency for column A and column A60. We see that the RGA is significantly reduced both at low and intermediate frequencies. The steady-state value is 35 for column A and 8 for column A60. The initial responses are, as for the case of sidestreams, almost unchanged. However, the lag in liquid flow (θ_L) is larger for column A60 as there are more trays and the liquid flows are smaller compared to the holdups (see (6.2)). This explains why the RGA for column A60 is lower also at high frequencies.

From Figure 6.4b we see that the overdesign also reduces the disturbance sensitivity from F to x_B (which is the largest element in the CLDG-matrix), but the reduction is significantly less than in the RGA for this example. As disturbance rejection usually is the most important in process control, overdesign will in this case not yield significant improvements in performance. However, we find that the improvement in other elements of the CLDG-matrix are significant (e.g., from F to y_D), and the conclusion with respect to overdesign may therefore be different for other columns with similar purities.

Note that we in column A60 introduced the feed at the optimal location $N_F = 31$, i.e. we added 10 trays to each section of column A. By adding the trays non-symmetrically we obtain somewhat different results. By adding 20 trays to the top section we find that y_D is the most sensitive output to disturbances, while adding 20 trays to the bottom section increases the sensitivity of output x_B to disturbances. However, these variations only appear at low frequencies. At intermediate and high frequencies there is almost no difference between the design alternatives; the effect of F on x_B represents the worst case CLDG with nearly the same magnitude for all design alternatives in the most important

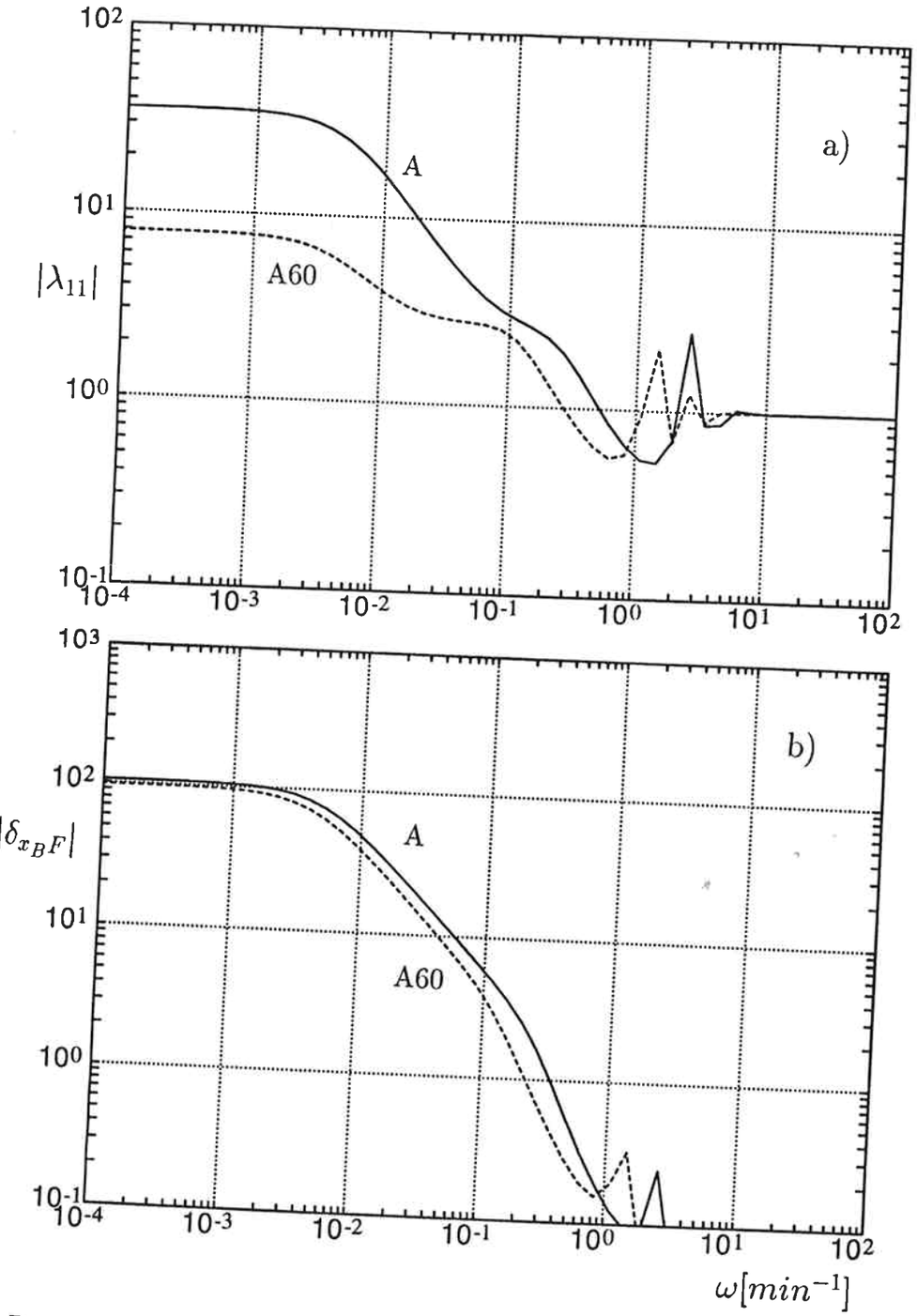

Figure 6.4: (a) RGA and (b) CLDG (effect of F on x_B) as functions of frequency for column A and column A60.

frequency region. Adding the trays symmetrically is the low cost solution in terms of utility consumption, and is therefore the best alternative for column A.

For column F we find that adding 5 extra symmetrically (optimal feed location) yields an improvement in the RGA, but yields a larger CLDG. However, for this column the best alternative seems to be to add the trays in the top section. The effect of this design modification, denoted F15, is shown in Figure 6.5. We see that the RGA is significantly reduced both at low and intermediate frequencies. Figure 6.5b shows the disturbance sensitivity (CLDG) of both y_D and x_B to disturbances in feed flow F. Note that the largest CLDG represents the control limitation at a given frequency. For column F, x_B is the most difficult output at all frequencies. For column F15, on the other hand, we see that y_D is the most sensitive at low frequencies (since we have introduced the extra trays in the top section), while x_B is the most sensitive at higher frequencies. Most important, however, is that the overall disturbance sensitivity is reduced both at low and intermediate frequencies by adding 5 trays to the top section.

The two columns studied here demonstrate that the effect of overdesign on controllability will depend both on the column studied as well as on where the extra trays are introduced. For column A none of the design alternatives considered yielded a significant improvement in controllability. For column F we got better controllability by introducing five extra trays in the top section, i.e., by using a non-optimal feed location. The effect of overdesign on controllability will thus depend on the column at hand, but should be considered for columns that prove hard to control.

With respect to the cost of overdesign, note that adding extra trays reduces the utility consumption needed for a given separation. For column F, the utility consumption in terms of $L+V$, is reduced by approximately 25 % by adding 50 % more trays. Thus, the surface around the steady-state optimal solution may be relatively flat, and the cost of overdesign may be relatively low.

6.7 Use of Feed Preheater for Control

Many columns have a feed preheater which heats the entering feed. Usually the amount of heat added is adjusted to keep the entering feed at a preset temperature, e.g., the bubble point temperature. However, in his thesis, Loe (1976) suggests that the feed preheater may be used more actively in controlling the column in order to reduce the interactions between the top and bottom composition control loops. More specifically, his idea is to counteract a change in boilup (V/F) by an equal change in the liquid fraction of the feed, q_F (such that $\Delta V_F = -\Delta V$ where $\Delta V_F = -F\Delta q_F$). In this way a change in the boilup will have a small effect on the flows in the top section, and one would obtain something close to a one-way decoupling of the column. This will, however, require that the available change in heat input to the feed preheater is almost as large as in the reboiler. Loe also discussed the possibility of using the feed preheater to control the feed-plate composition, but suggested to use a controller with integral action which obviously is not needed nor wanted since it would make the column profile very "stiff".

Here we will modify the idea of Loe somewhat and suggest to use a pure proportional controller between the feed-plate composition (or equivalently, for a binary mixture, the

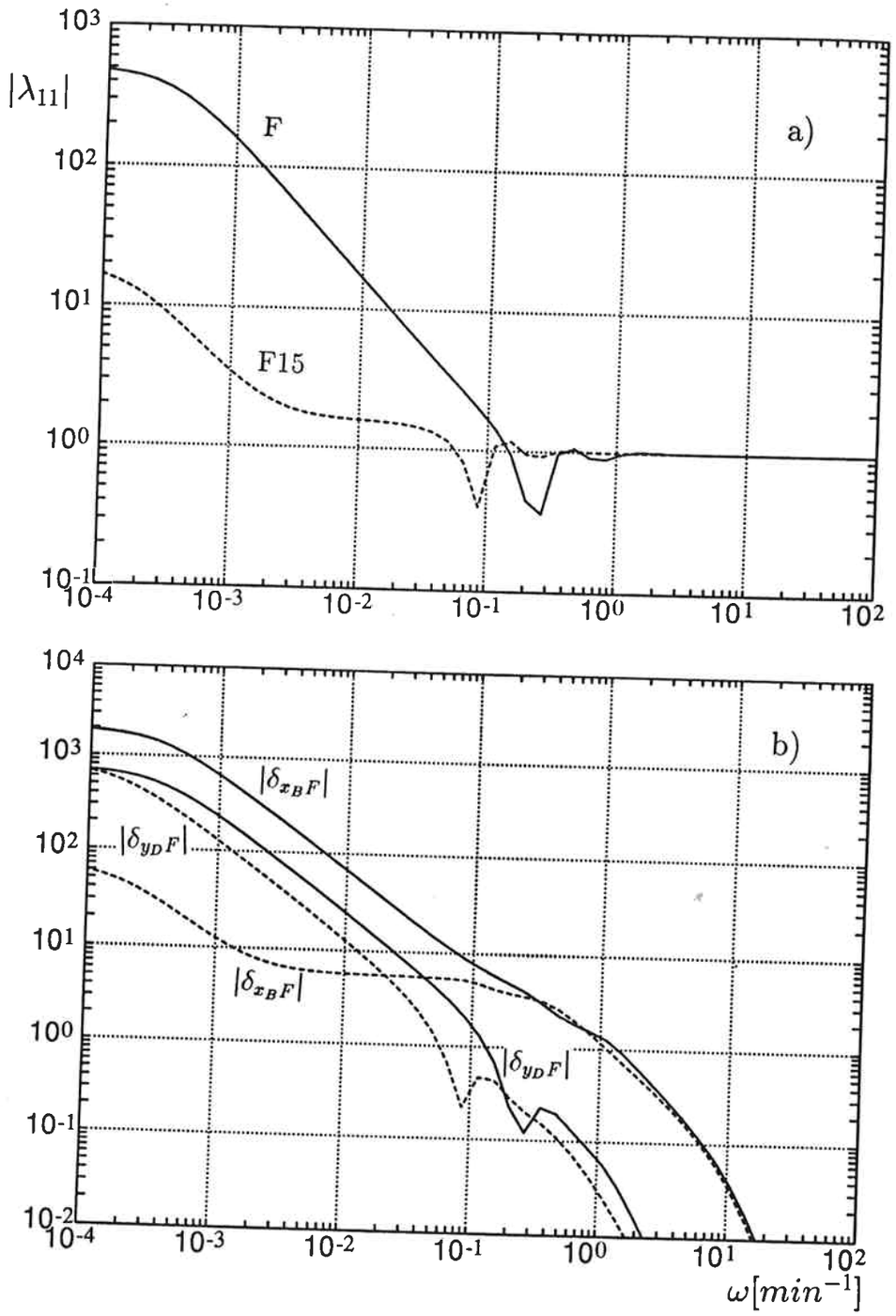

Figure 6.5: (a) RGA and (b) CLDG (effect of F on y_D and x_B) as functions of frequency for column F (solid line) and column F15 (dashed line).

temperature) and the feed preheater

$$dq_F = -k_{qF} dx_{NF} \tag{6.10}$$

By using a pure proportional controller one avoids making the column profile too stiff, and the controller gain may be adjusted so that the requirements for changes in the feed preheating does not exceed the available heating in the preheater. By using a feedback controller we also obtain a degree of two-way decoupling. An increase in reflux will be counteracted by a decrease in q_F and an increase in boilup will be counteracted by an increase in q_F.

Figure 6.6a shows the RGA as a function of frequency for column A using different gains k_{qF} for the feed preheater control. For our example, a gain k_{qF} of 1.0 implies that we for setpoint changes get approximately a 10 % change in Fq_F (feed preheater duty) compared to changes in V (reboiler duty). The largest change in q_F is found for changes in feed composition. A change in z_F from 0.50 to 0.60 yields a change in q_F from 1.0 to 0.91 (keeping y_D and x_B constant). From Figure 6.6a we see that the use of the preheater in control reduces the RGA for the remaining system significantly. The reduction increases with the controller gain used, and with a gain of 1.0 we get a reduction in the RGA at low frequencies from 35.0 to 4.0. The RGA is reduced at frequencies up to $0.1 min^{-1}$, but the reduction is largest at lower frequencies. This implies that we will gain most in terms of improved control performance when the bandwidth of the control system is small, e.g. due to large measurement delays.

The effect of the feed preheater control on disturbance sensitivity is illustrated in Figure 6.6b. We see that we obtain similar reductions in the CLDG as obtained in the RGA.

We do not show results for column F with feed preheater control here. However, similar results are obtained for this column as were obtained for column A, i.e., a significant reduction in both the RGA and CLDG.

Figure 6.7 shows nonlinear responses of column A to a 30 % step increase in feed rate F with and without feed preheater control ($k_{qF} = 2.0$). Single-loop PI-controllers are used for composition control. The controllers were designed for robust performance in both cases, i.e., taking uncertainties into account. A delay of 3 min. in the product composition measurements was included in the design and simulations. In the feed preheater loop a delay of 1 min. was included. The reason for using a smaller delay in this loop is simply that the composition measurement is not critical, and a fast temperature measurement will yield the desired effect. From Figure 6.7 we see that the control performance is improved by using the feed preheater for control. We get smaller overshoot as well as a faster settling to steady-state. This is as expect since the preheater reduces the interactions at low frequencies. Figure 6.7 also shows the response in the feed preheater. We see that the change in q_F only is temporarily, with a maximum change of about 3 %. The changes in reflux and boilup are 30 % with no overshoot for both cases.

We have here only considered using the feed-plate composition to manipulate the feed preheating. However, other strategies are of course possible. For example, one may use compositions at plates some distance away from the feed-plate. For column A, we for instance find that controlling the composition on plate 31, rather than 21, yields a similar

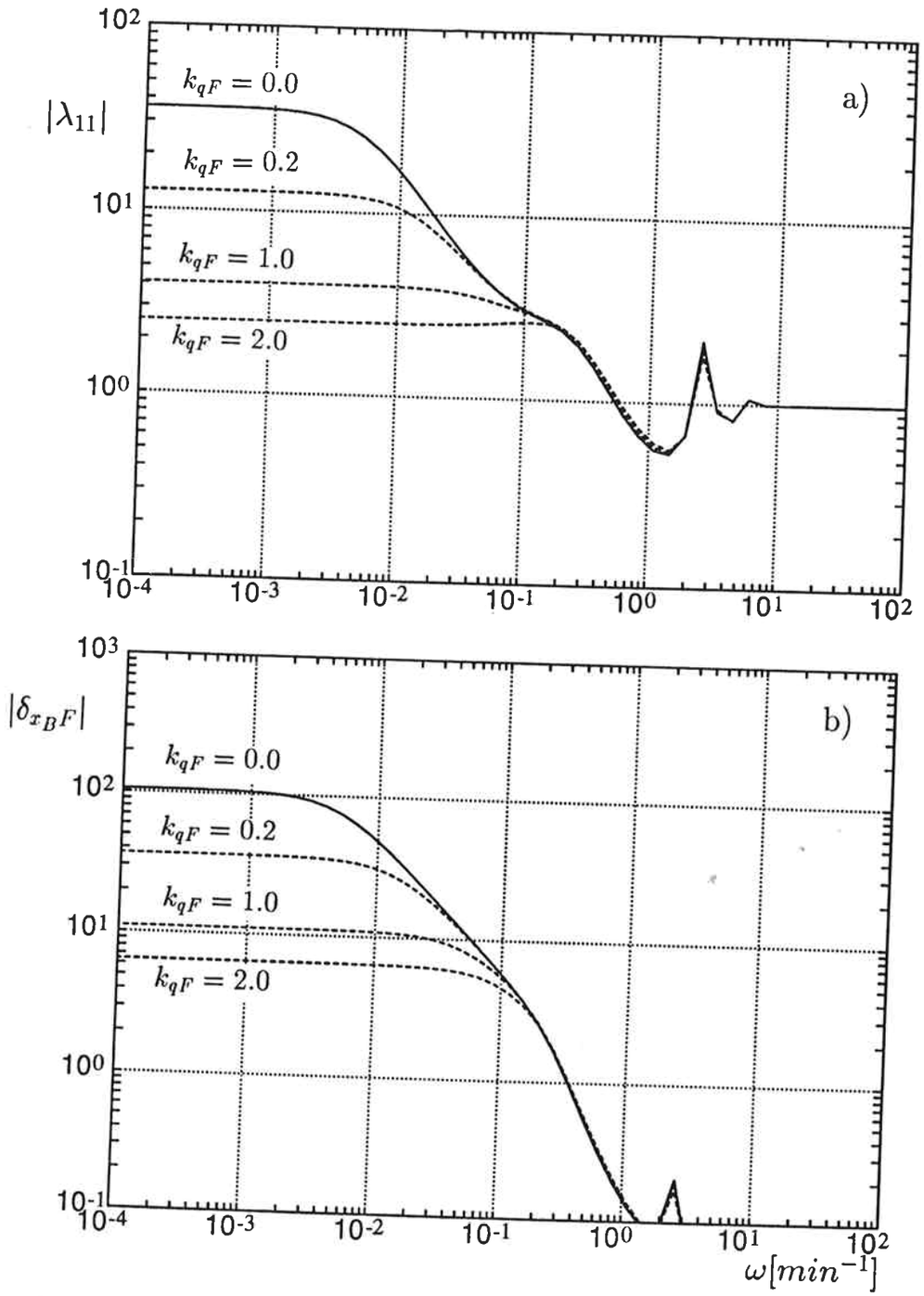

Figure 6.6: (a) RGA and (b) CLDG (effect of F on x_B) as functions of frequency for column A with control of feed preheater. k_{qF} denotes gain for feed preheater controller.

effect on the RGA and CLDG as in Figure 6.6, but with smaller requirements for changes in q_F.

One might believe that the utility consumption is increased significantly by using the feed preheater in control. However, the total change in heat input (i.e., $V - Fq_F$) is not increased significantly. The only exception is for large changes in feed composition. However, the heating of the feed will cost less than the heating used for boilup as we have more light component in the feed. In some cases the active use of a feed preheater in control may be optimal even from a steady-state point of view.

In summary, we have shown that there is a significant potential for improvements in control performance by using the feed preheater actively. In general, it is obvious that one may always improve the control performance by adding an additional manipulated input and/or measurement. For the feed preheater on may consider using other measurements or a multivariable controller. One may also consider adding other manipulated inputs, such as an intermediate reboiler or cooler, or in some cases even the feed rate and feed composition.

6.8 Control Configurations

We have in this paper only discussed the LV-configuration which is the most widespread configuration in industry. The selection of which inputs to use for composition control is made when configuring the level control system. This is often considered as a part of the column design. However, the choice made here is of vital importance for the remaining composition control problem. Different configurations will have different properties with respect to interactions and disturbance sensitivity (e.g., Shinskey, 1984, Häggblom and Waller, 1990, Skogestad et.al., 1990). Skogestad et.al. (1990) studied the control of a number of columns and found that the best choice for most columns were the ratio configuration $(L/D)(V/B)$. In many cases design modifications will not be neeeded if a proper control configuration is chosen. However, the modifications we have considered in this paper will have a similar effect on the $(L/D)(V/B)$-configuration as on the LV-configuration. For other configurations, e.g., the DV-configuration, the conclusions with respect to design modifications may be different.

6.9 Conclusions

We have in this paper considered several possible design modifications for improving the controllability of high-purity distillation columns. The most important conclusions are:

1. A sidestream will reduce interactions and disturbance sensitivity at low frequencies. However, the improvements will not affect the frequency region of the expected bandwidth of the control system. This implies that a sidestream will only be beneficial in high-purity columns which are operated in manual mode.

2. An overdesigned column with additional trays will have a pinch in the composition profile. The pinch zone will reduce the interactions (in terms of the RGA) in the

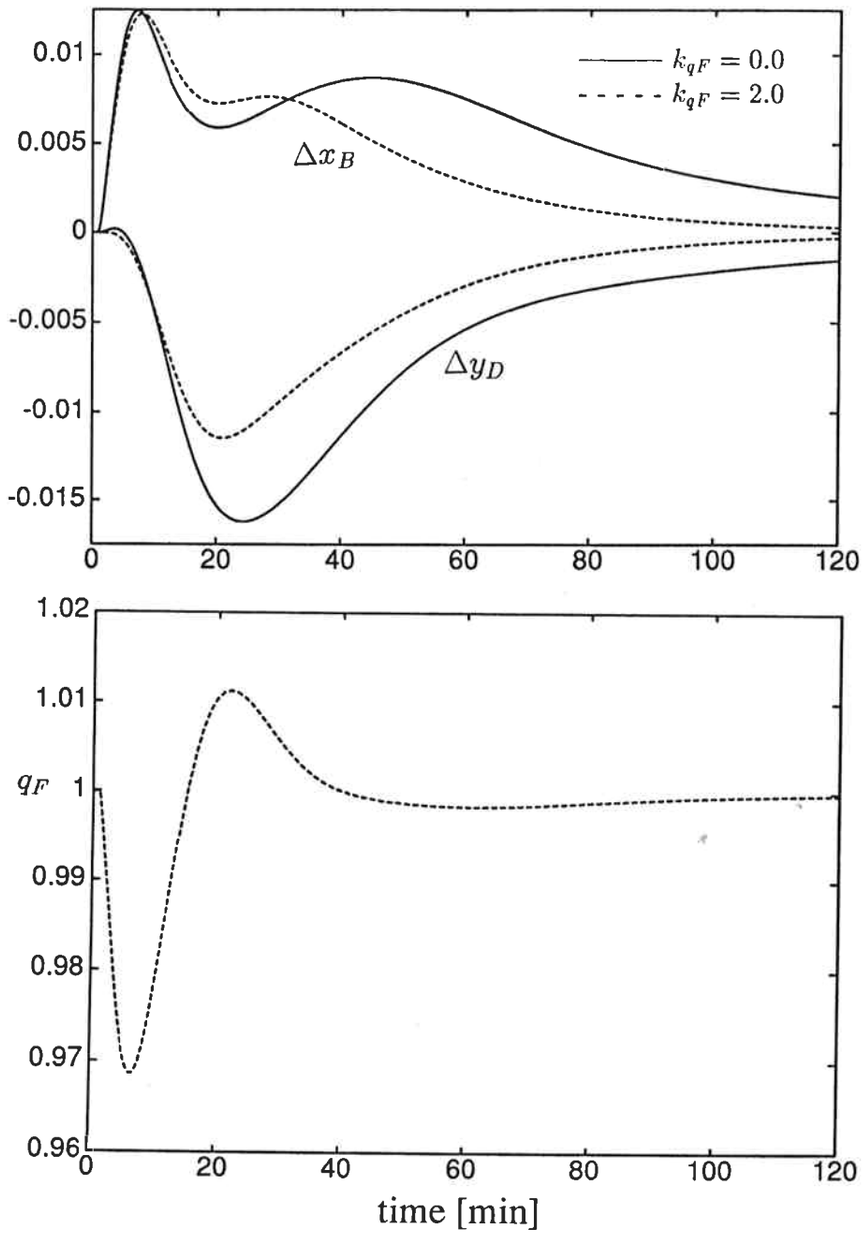

Figure 6.7: Nonlinear response of column A to a 30% increase in feed flow F with and without use of feed preheater for control. Product compositions controlled using single-loop PI-controllers. Lower plot shows response in q_F with feed preheater used for control.

frequency region important for feedback control. However, the reduction in disturbance sensitivity may be small in some cases, while it may be significant in other cases. Thus, the conclusion with respect to the effect of overdesign will depend on the column at hand.

3. Using the feed preheater to control a composition inside the column may yield significant improvements in both the RGA and CLDG, and should be considered as a design modification for columns which prove difficult to control.

We stress that we in this paper only have considered relatively few specific examples, and there is a definite need for additional studies.

Acknowledgements: Financial support from the Royal Norwegian Council for Scientific and Industrial Research (NTNF) is greatfully acknowledged.

NOMENCLATURE

B - bottoms product rate (kmol/min)
D - distillate product rate (kmol/min)
e_i - control off-set in output i
F - feed flow rate (kmol/min)
$G(s)$ - input transfer matrix
$G_d(s)$ - disturbance transfer matrix
$g_{ij}(s)$ -transfer matrix element
L - reflux rate (kmol/min)
M - liquid holdup (kmol)
N - number of theoretical trays
N_F - feed tray location
q_F - liquid fraction of feed
r_i - setpoint change in output i
S - sidestream rate (kmol/min)
u_i - input i
V - boilup rate (kmol/min)
x_B - bottoms composition
x_{NF} - feed plate composition
x_S - sidestream composition
y_D - distillate (top) composition
y_i - output i
z_F - feed composition
z_k - disturbance k

Greek symbols

α - relative volatility
β_{ij} - element i,j of RDG

Δ - CLDG matrix
δ_{ij} - element i,j of CLDG matrix
λ_{ij} - element i,j of RGA
ω - frequency (min^{-1})
τ_L - hydraulic time constant (min)
$\theta_L = (N-1)\tau_L$ - overall reflux lag (min)

REFERENCES

Bristol, E.H., 1966, "On a New Measure of Interactions for Multivariable Process Control", *IEEE Trans. Automat. Control*, **AC-11**, 133-134

Bristol, E.H., 1978, "Recent Results on Interactions in Multivariable Process Control", AIChE Meeting, Chicago.

Häggblom, K.E. and K.V. Waller, 1990, "Control Structures for Disturbance Rejection and Decoupling of Distillation", *AIChE J.*, **36**, 7, 1107-1113.

Hovd, M. and S. Skogestad, 1991, "Use of Frequency-Dependent RGA for Control System Analysis, Structure Selection and Design", *accepted for publication in Automatica*

Kropholler, H.W. and A.R. Guesalaga, 1990, "Dynamic Analysis of a Distillation Column with Bypass in Reflux", *Proc. IFAC World Congress '90*, Tallinn, Estonia.

Loe, I., *Dr.Ing. thesis*, University of Trondheim, NTH, 1976.

Rademaker, O., J.E. Rijnsdorp and A. Maarleveld, 1975, *Dynamics and Control of Continuous Distillation Units*, Elsevier, Amsterdam.

Shinskey, F.G., 1984, *Distillation Control*, 2nd Edition, McGraw-Hill, New York.

Skogestad, S. and M. Morari, 1987, "Implications of Large RGA elements on Control Performance", *Ind.Eng.Chem.Res*, **26**, 11, 2323-2330.

Skogestad, S., M. Morari and J.C. Doyle, 1988, "Robust Control of Ill-Conditioned Plants: High-Purity Distillation", *IEEE Trans. Autom. Control*, **33**,12, 1092

Skogestad, S., P. Lundström and E.W. Jacobsen, 1990, "Selecting the Best Distillation Control Configuration",*AIChE J.*, **36** (5), 753

Stanley, G., M. Marino-Galarraga and T.J. McAvoy, 1985, " Shortcut Operability Analysis. 1. The Relative Disturbance Gain.", *Ind.Eng.Chem.Process Des.Dev*, **24**, 4, 1181

Wachter, J.A. and R.P. Andres, 1989, "Control of Binary High-Purity Distillation Columns", *Proc. DYCORD '89*, Maastricht, Netherlands.

Chapter 7

Robust Control of Homogeneous Azeotropic Distillation Columns

Elling W. Jacobsen *

Lionel Laroche †
Manfred Morari ‡
Chemical Engineering 210-41
California Institute of Technology
Pasadena, California 91125

Sigurd Skogestad
Chemical Engineering
University of Trondheim, NTH
N-7034 Trondheim, Norway

Henrik W. Andersen
Chemical Engineering
Technical University of Denmark
DK-2800 Lyngby, Denmark

Accepted for publication in *AIChE Journal*

Abstract

The entrainer feed used in homogeneous azeotropic distillation provides an extra degree of freedom in the steady state design compared to simple distillation. In this paper we discuss the control of azeotropic distillation columns in the region close to minimum entrainer feed. Both industrial experience and previous research indicate that this is a difficult task. However, by considering the high frequency behavior (initial response) of the column, we show that tight and robust control can be obtained with simple single-loop PI-controllers. The results depend on the presence of high-frequency phenomena such as flow dynamics.

*Presently: Chemical Engineering, University of Trondheim, NTH, N-7034 Trondheim, Norway
†Presently: Procter & Gamble, Canada
‡To whom all correspondence should be addressed: phone (818)356-4186, fax (818)568-8743, e-mail mm@imc.caltech.edu

7.1 Introduction

Binary mixtures forming minimum boiling azeotropes are commonly encountered in the chemical industry. The separation of such mixtures into the pure components is not possible by simple distillation and must be accomplished by other means. In homogeneous azeotropic distillation the separation is made feasible by adding a third component, called the entrainer. The entrainer alters the thermodynamic properties of the mixture, thereby enabling separation of the binary azeotrope into the pure components. This type of distillation is widespread in the process industry and the economic potential of improved operation is usually high.

Distillation is the unit operation that has received most attention in the process control community. However, almost all the work so far has been concentrated on ideal binary distillation. The main reason for this is probably that even simple distillation columns are hard to understand and control. In homogeneous azeotropic distillation several complexities are added: non-ideal thermodynamics, multicomponent mixtures and multiple feeds. Most papers in this area have concentrated on modelling the thermodynamics, selection of entrainers (e.g., Doherty and Caldarola, 1985; Laroche and Morari, 1990), steady state design (e.g., Levy and Doherty, 1985a-b) and optimizing the separation (e.g., Knight and Doherty 1989). Only a few papers have been devoted to the control problem: Abu-Eishah and Luyben (1985), Andersen et al. (1989), Anderson (1989), Bozenhardt (1988) and Gilles et al. (1980). Most of these papers have studied specific cases and few general conclusions are drawn. Andersen et al. (1989) presented a more general analysis, but mainly based on steady state arguments. The most significant conclusion to draw from the papers is that homogeneous azeotropic distillation columns seem to be much more difficult to control than simple distillation columns. This seems to be supported also by industrial experience.

The entrainer used in homogeneous azeotropic distillation columns provides an extra degree of freedom compared to simple distillation. As several authors have shown (e.g., Andersen et al., 1989), this degree of freedom may be used to optimize the operation in terms of entrainer and utility (heating and cooling) consumption. However, steady state arguments indicate a much more difficult control problem at the steady state optimal operating point than at operating points with higher utility consumption (Andersen et al., 1989). This has led some authors to concentrate also on non-optimal operating points (e.g., Knapp and Doherty, 1990). Industrial experience also shows that it is common practice to operate far from the steady state economic optimum, and this may be due to a belief of easier operation with increased entrainer consumption. Knight and Doherty (1989) studied an industrial column and found that it used seven times more entrainer than what would be optimal.

In this paper we will concentrate on the high frequency (initial response) dynamics of the system. It is the initial response of the open-loop system which determines the feedback control properties. The frequency region around the expected closed-loop bandwidth (approx. 0.01 - 1 min^{-1}) is most important. In our analysis we will make use of the frequency dependent Relative Gain Array (RGA) (Bristol, 1966, 1978) and the Closed-Loop Disturbance Gain (Hovd and Skogestad, 1990). The frequency dependent Relative Gain Array has proven to be an efficient tool for evaluating controllability of simple distillation columns, and the Closed-Loop Disturbance Gain seems to have promising properties when evaluating the effect of disturbances under feedback control.

F	z_F	E	z_{E1}	z_{E2}	N	N_F	N_E	y_D	r_{12}
1.0	0.90	*)	1.e-7	1.e-4	33	6	27	0.998	0.005

- Reboiler is tray no.1.
- Feed and Entrainer are saturated liquids.
- Total condenser with saturated reflux.
- Liquid holdups are M_i/F= 0.5 min., including reboiler/ condenser.
- Constant molar flows.
- Equilibrium calculated by Van Laar activity coefficient model.

*) Operating point	II_B	II_A	V_{min}	I_A	I_B
E :	0.46	0.50	0.57	1.00	2.00

Table 7.1: Data for Acetone-Heptane-Toluene Column.

We start the paper by giving a short presentation of the separation sequence in homogeneous azeotropic distillation. Thereafter we present the model used in the analysis. This model includes important high-frequency characteristics usually excluded in control studies of distillation columns. An analysis of the model is presented next. In this analysis we study both different operating points as well as different control configurations. The selection of an appropriate control configuration has proven to be essential for the control of simple distillation columns. The ultimate test of controllability is obviously design of controllers with an optimized performance. In this paper we make use of the structured singular value (e.g., Morari and Zafiriou, 1989) as a criterion. In this manner we may study the effect of model uncertainty which is of outmost importance when designing controllers for ill-conditioned plants (Skogestad et al., 1988). At the end of the paper we discuss how optimal operation may be obtained in practice.

Throughout the paper we will make use of an example column which separates a mixture of Acetone, Heptane and Toluene (AHT). Acetone and Heptane forms a minimum boiling azeotrope and Toluene is used as entrainer. Toluene is the least volatile component in the mixture. Data for the column are given in Table 7.1. Control design results will also be presented for a column separating a system of Ethanol, Water and Ethylene glycol. Data for this column are given in Table 7.2.

7.2 The Separation Sequence

In homogeneous azeotropic distillation an entrainer is added to make the separation feasible. Therefore the system consists of three components, and two columns are needed to separate the mixture. The sequence in which this separation takes place will be determined by the type of entrainer that is used. The entrainer most commonly used in the industry is a heavy boiler, that is, the entrainer is the least volatile component of the mixture. We only consider this type of system here. In the case of a heavy entrainer

F	z_F	E	z_{E1}	z_{E2}	N	N_F	N_E	y_D	r_{12}
1.0	0.87	*)	1.e-7	1.e-4	50	17	48	0.998	0.0001

- Reboiler is tray no.1.
- Feed and Entrainer are saturated liquids.
- Total condenser with saturated reflux.
- Liquid holdups are M_i/F= 0.5 min., including reboiler/ condenser.
- Constant molar flows.
- Equilibrium calculated by Van Laar activity coefficient model.

		II_B	II_A	V_{min}	I_A
*)	Operating point E:	0.35	0.75	1.00	2.00

Table 7.2: Data for Ethanol-Water-Ethylene glycol Column.

we recover in the first column, called the extractive column, the lightest component at the top and a mixture of the intermediate and the heavy component at the bottom. The bottom product is fed to the second column, the entrainer recovery column, for separation of the binary mixture. The entrainer product from the recovery column is fed back to the extractive column. In the case of heavy entrainer the entrainer will be fed into to the upper part of the column. The separation sequence is illustrated in Figure 7.1.

Because of the two feeds to the extractive column we have three sections in the column compared to two in the ideal binary case (see Figure 7.1). The main purpose of the extractive section is to separate the components of the binary azeotrope. In the rectifying section the entrainer is removed from the top product while in the stripping section light component is removed from the bottom product. For a more detailed discussion on the significance of the different sections we refer to the work by Andersen et al. (1989).

As pointed out by Andersen et al. one must be careful when making specifications in the bottom product of the extractive column as this will determine the achieveable separation in the recovery column. More specifically, all the light component in the bottom product of the extractive column will enter the top product of the recovery column as impurity. In order to make sure that the fraction of impurity does not exceed a desired value we must limit the fraction of light to intermediate component in the bottom product of the first column. As specifications for the extractive column we will therefore use

y_D - fraction of light component in the distillate

r_{12} - ratio of light to intermediate component in the bottom product.

The specifications for the AHT-column are $y_D = 0.998$ and $r_{12} = 0.005$.

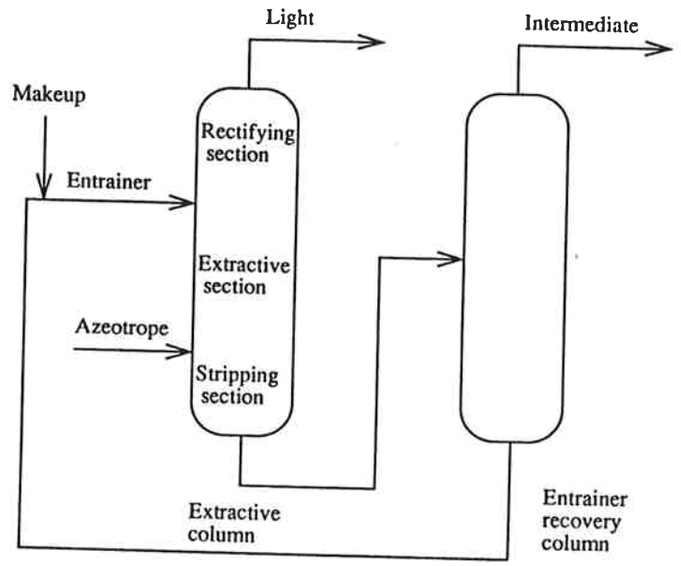

Figure 7.1: Separation sequence for the case of minimum boiling binary azeotrope and heavy entrainer.

7.2.1 Steady-state optimal operation

As stated above the entrainer feed may be used to optimize the column for a given separation. Andersen et al. (1989) showed that by varying the entrainer feed flow and adjusting the other flows accordingly for a given separation, one obtains a continuous set of possible operating points. They described the set in the form of an entrainer feed/boilup relation. For the AHT-column studied in this paper we obtain the set of operating points shown in Figure 7.2. The set of operating points may be divided into three distinct regions. In region I (see Figure 7.2) a decrease in entrainer feed leads to a decrease in boilup and thereby to a more optimal operation with decreased entrainer consumption. At a certain point the boilup reaches a minimum (V_{min}) and a further decrease in entrainer feed results in increased boilup (region II). This will continue until we reach the minimum entrainer needed for the separation (E_{min}). The optimal operating point will be between E_{min} and V_{min}, i.e. in region II. The exact location of the optimal operating point will depend on the cost of entrainer and heating/cooling. The third region (region III) is caused by an input multiplicity in the system and was discovered by Andersen et al. In this region an increased entrainer feed gives a sharp increase in boilup. Andersen et al. have discussed in detail the origin of the different regions.

The rest of the paper is devoted to analyzing the controllability in the different regions. The operating points we will consider are named I_A, I_B, V_{min}, II_A, II_B, III_A and III_B and are shown in Figure 7.2. We will assume operating point II_A to be optimal and will hence concentrate on this operating point. Operating point II_B is located almost at E_{min}.

We will not discuss the control of the recovery column as it basically may be considered as an ideal binary column. The coupling of the two columns is discussed briefly towards

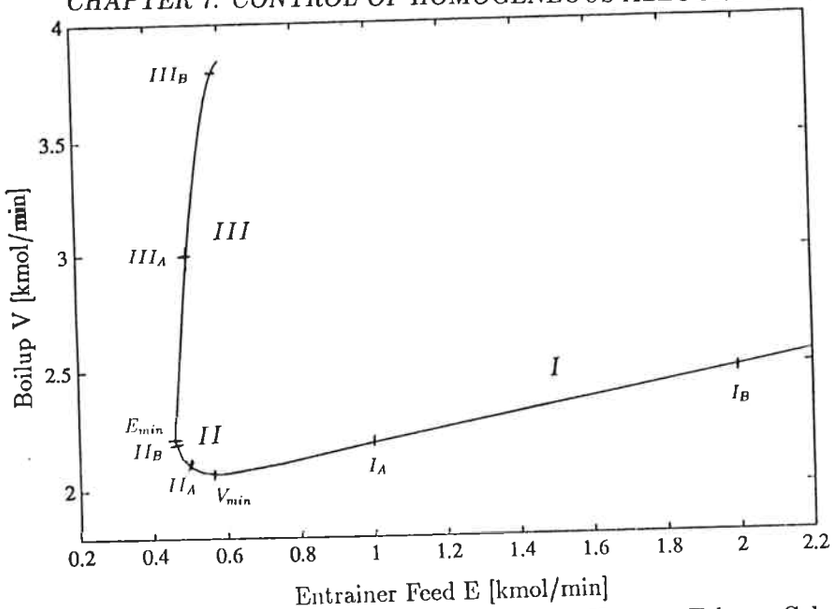

Figure 7.2: Set of operating points for the Acetone-Heptane-Toluene Column.

the end of the paper.

7.3 Modelling

The full non-linear dynamic model used in this paper has three states per tray. The states are expressed as fraction of two components plus liquid holdup on each tray. For the AHT- column this implies a total of 102 states. The flow-dynamics are described by a linear relation between liquid flow and liquid holdup:

$$L_i = L_i^0 + (M_i - M_i^0)/\tau_L \tag{7.1}$$

where superscript 0 denotes nominal steady state values. τ_L is computed from a linearized Francis weir formula

$$\tau_L = \frac{2}{3}\frac{M_{oi}}{L_i} \tag{7.2}$$

where M_{oi} denotes liquid over weir and L_i is the liquid flow. We use a holdup on each tray equal to $M_i/F = 0.5$ min and assume half of the liquid over the weir. The flow-dynamics are usually not included in models for control studies of distillation columns, but have an important high-frequency effect. As shown by Skogestad et al.(1990a) the flow dynamics introduce a lag in reflux from the top to the bottom of the column which leads to a decoupling at high frequencies.

The equilibrium is modelled by the Van Laar activity coefficient model. We assume constant molar flows, that is, we exclude the energy balance.

In the analysis and controller design we make use of linearized models. Due to the high order of the full models we use reduced models with 20 states. The models were reduced by means of a balanced minimal realization.

In simple distillation we have been successful using simplified models with only one or two time constants (e.g., Skogestad and Morari, 1988). We found it difficult to obtain good and general models in this way for the extractive column. Hence we will not use such models here.

Shinskey (1977) proposed using logarithmic composition measurements as a simple means of reducing the effect of nonlinearities. We will adopt this for the extractive column and will hence use the following measurements in the rest of the paper

$$log(1 - y_D) \tag{7.3}$$

$$log(r_{12}) \tag{7.4}$$

The logarithm does also give a good scaling of the outputs:

$$\Delta y_D^s = \frac{\Delta y_D}{1 - y_D} \tag{7.5}$$

$$\Delta r_{12}^s = \frac{\Delta r_{12}}{r_{12}} \tag{7.6}$$

where the superscript s denotes scaled variables.

7.4 Control Configurations

In control terms a distillation column may be viewed as a 5x5 system. That is, we have 5 manipulated variables (L, V, D, B, V_T) and 5 primary outputs (y_D, r_{12}, M_D, M_B, P). The feed streams are assumed to be given here (disturbances). One could design a full multivariable controller where all manipulated variables are coupled to all the measurements. This would of course be optimal from a theoretical point of view. However, for practical reasons it is common to design a decentralized controller with five single loops. Such a controller is easier to understand and to retune and will also be more failure tolerant. We will assume such a decentralized control structure in this work.

When using a decentralized control structure the first decision usually made is selection of level loops. The selection of which inputs to be used for level control is often considered part of the column design. However, the decision made here is of vital importance for the remaining control problem. Different control configurations will have different dynamic characteristics. This has been pointed out by several authors for the case of simple distillation (e.g., Shinskey, 1984; Skogestad et al., 1990a). In this paper we will consider four different configurations; the LV-, DV-, DB- and (L/D)(V/B)-configuration. The names indicate which inputs are left for composition control, e.g., the LV-configuration refers to using reflux L and boilup V to control compositions. The DB-configuration would be rejected from steady state arguments (D+B=F), but as shown by Skogestad et al. (1990b) it may be a good choice for simple distillation columns due to its high-frequency characteristics. It also shows how misleading steady state arguments can be when evaluating processes for controllability. Skogestad et al. (1990a) found the (L/D)(V/B)-configuration to be the overall best selection for a series of simple distillation column they studied.

7.5 Open-Loop Dynamics

Region III. Andersen et al. (1989) found that the operating points in the undesirable region III had severe right half plane zeros. They found that these right half plane zeros were due to a negative effect of internal flows ($dL = dV$) on separation in this region. The rhp-zeros are related to the input multiplicity found in the set of operating points (see Figure 7.2). For the AHT-column we find the worst rhp-zero at 0.234 at operating point III_A and at 0.128 at operating point III_B. Because these rhp-zeros impose serious bandwidth limitations and because the operating points in region III are clearly non-optimal it is unlikely that the column would be operated in this region. We will therefore exclude these operating points from any further analysis.

Region I and II. In order to get an idea of how the dynamics of the extractive column vary with operating conditions we will consider the open-loop gains of the LV-configuration at the different operating points. That is, we consider the gains in the transfer-matrix

$$\begin{bmatrix} dlog(1-y_D) \\ dlog(r_{12}) \end{bmatrix} = G^{LV} \begin{bmatrix} dL \\ dV \end{bmatrix} \tag{7.7}$$

Figure 7.3 shows the open-loop gains as a function of frequency for the LV-configuration at the different operating points. Note that the outputs are scaled according to (7.5) and (7.6).

For responses of the bottom composition we see that there are only small differences between the different operating points. The responses are essentially first order, as in most simple distillation columns, with a dominant time-constant around 500 min. From the figure we also see that the response from reflux to bottom composition breaks off at higher frequencies. This is caused by the lag introduced by the flow-dynamics.

For responses in the top composition we see that there are significant differences between the different operating points. Furthermore, the responses are dominated by higher order dynamics than those in the bottom. There is an initial effect with a time-constant around 4 min and a slower effect with a time-constant similar to what is observed for responses in the bottom composition. The two poles are separated by a zero, and the system is minimum phase.

In general there are two separate effects in distillation 1) the initial effect due to changes in flows (not to be confused with flow-dynamics) and 2) a slow effect due to interaction between adjacent tray compositions (e.g., Rademaker et al., 1975). Skogestad and Morari (1988) showed that for most simple distillation columns the slope of the initial response will usually be prolonged by the slow secondary response, thereby resulting in an overall first order response. This is mainly a result of the interaction between all the compositions in the column and will not be true for all columns.

In columns with pinches in the composition profiles (almost no difference in composition between two trays) the interaction between the top and bottom of the column will vanish, and we may get higher order responses. Extractive columns will usually have pinches for one or several components, and we may therefore experience higher order dynamics. In the AHT-column for instance, we have a pinch for acetone in the top of the extractive section.

Weigand et al. (1972) have also shown that in many cases the responses in the top and bottom of simple distillation columns may differ significantly. They found that the largest

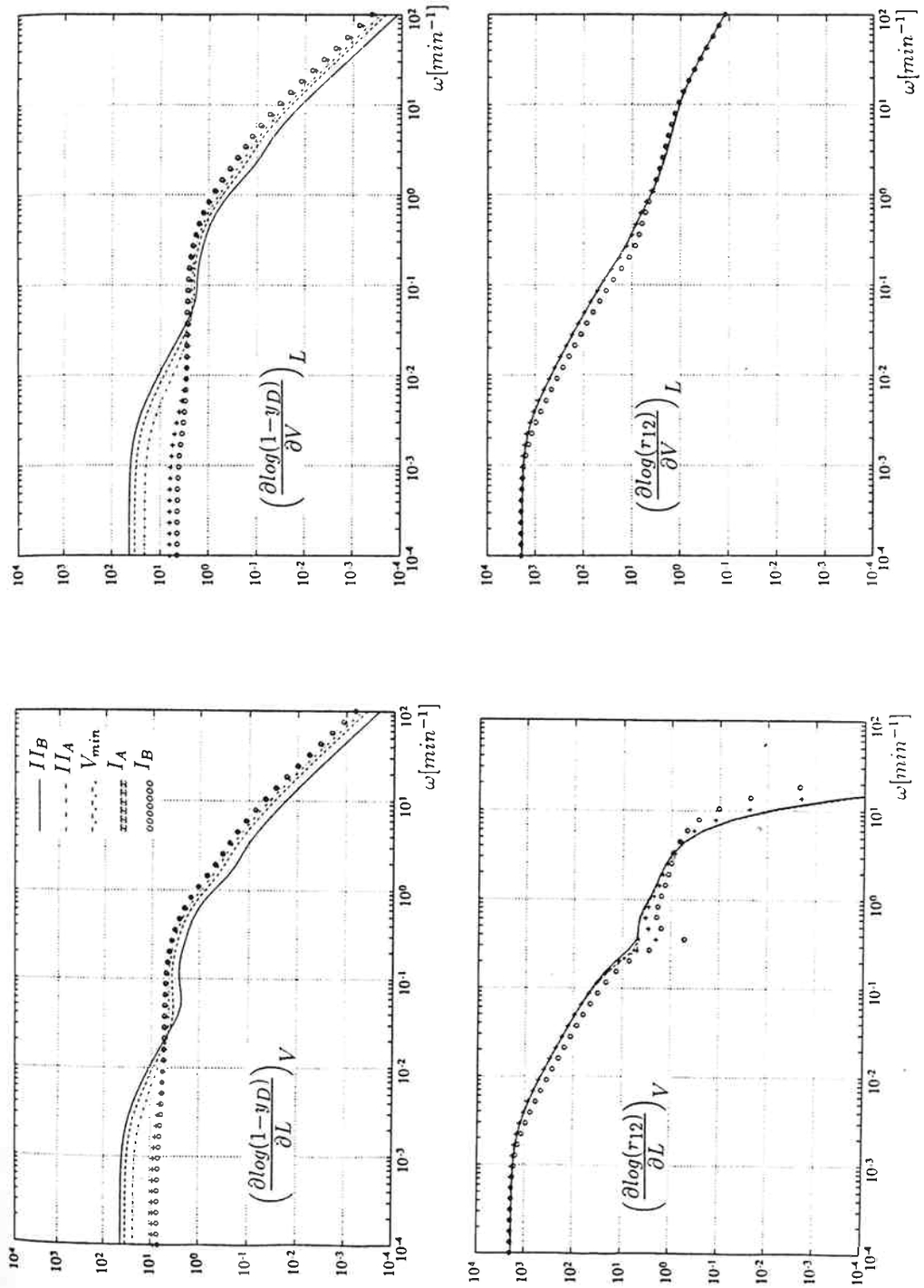

Figure 7.3: Open-loop gains for the LV-configuration at different operating points.

time-constant in general will apply only to the end with the largest absolute change in composition. This corresponds well to what we find here where the absolute change is largest in the bottom.

Comparing the different operating points we see that the main differences in the top composition responses are at low frequencies, while the high-frequency dynamics (initial responses) are similar at all operating points. The large difference in steady state gains between different operating points may be explained by the fact that different sections of the column will dominate at different operating points (Andersen et al., 1989). Skogestad and Morari (1988) found also for simple distillation that the initial responses are less dependent on the operating conditions than the low-frequency responses.

We conclude that while the low-frequency dynamics may differ widely between operating points, there are only small differences at high-frequencies for responses both in the top and bottom compositions. For control purposes the high-frequency dynamics are most important, and from the open-loop dynamics we would therefore not expect big differences between the control properties observed at the different operating points.

For the other configurations we find similar results, that is small differences between the high-frequency dynamics at the different operating points. The only exception is the (L/D) (V/B) -configuration. The gains for this configuration in terms of single flow gains may be expressed in the form

$$d(L/D) = \left(\frac{1}{D}\right) dL - \left(\frac{L}{D^2}\right) dD \tag{7.8}$$

and

$$d(V/B) = \left(\frac{1}{B}\right) dV - \left(\frac{V}{B^2}\right) dB \tag{7.9}$$

Between the different operating points we have only small variations in distillate D ($D \approx Fz_F$), while the bottoms product B will vary significantly since almost all the entrainer leaves in this product. Reflux L and boilup V will also vary somewhat (see Figure 7.2). The variations in flows imply that while the gains for the single flows vary only slightly, the gains for the ratios will vary significantly with the operating point. This may however be compensated for by measuring the flows, which is necessary anyway with this configuration.

7.6 The Relative Gain Array

The Relative Gain Array (RGA) was originally proposed by Bristol (1966) as a steady state interaction measure, and has found widespread application for selecting single loop pairings in decentralized control. One of the main advantages of the RGA is that it depends only on the model itself, and therefore does not require any preliminary controller design. This is due to the assumption of "perfect control". Another advantage of the RGA is that it is scaling independent.

The RGA may easily be extended to a frequency dependent measure (e.g., Witcher and McAvoy, 1977, Bristol, 1978), and will in this case contain more useful information with respect to feedback control. We are primarily interested in the frequency region

around the expected closed-loop bandwidth. The definition of the elements in the RGA is given by

$$\lambda_{ij} = \frac{(\partial y_i/\partial u_j)_{u_{l\neq j}}}{(\partial y_i/\partial u_j)_{y_{l\neq i}}} = g_{ij}(s)[G^{-1}(s)]_{ji} \tag{7.10}$$

As the elements in each row and column sum up to unity in the RGA (Bristol, 1966), we only have to consider the 1,1 element for the 2×2 case. The 1,1 element for the 2×2 case is given by

$$\lambda_{11} = \frac{1}{1 - \frac{g_{12}(s)g_{21}(s)}{g_{11}(s)g_{22}(s)}} \tag{7.11}$$

where g_{ij} denotes the (i,j) element of the transfer matrix G.

Skogestad et al. (1990a) successfully used the frequency dependent RGA for selecting control configurations in simple distillation, and Hovd and Skogestad (1990) have proven its usefulness on a more general basis. Besides giving information on interaction among single loops the RGA also contains useful information on sensitivity to input uncertainty. Another measure that is frequently used to assess controllability is the condition number, γ. However, the condition number is scaling dependent and the minimized condition number, γ^*, is used instead. Skogestad and Morari (1987a) give the following relationship between the RGA and the minimized condition number for 2×2 plants

$$\|\Lambda\|_1 - \frac{1}{\gamma^*} \leq \gamma^* \leq \|\Lambda\|_1 \tag{7.12}$$

where $\|\Lambda\|_1$ denotes the 1-norm of the RGA. Thus the difference between $\|\Lambda\|_1$ and γ^* is at most equal to $1/\gamma^*$. Since $\|\Lambda\|_1$ is much easier to compute it is the preferred quantity to use.

Figure 7.4 shows the RGA as a function of frequency for the four configurations at the different operating points. From the figure we see that for all configurations the RGA differs widely between the operating points at steady state. For the LV-configuration we have for instance a steady state value of 70 at operating point II_B and a steady state value of less than 3 in I_B. From the low-frequency RGA one would therefore have concluded that the control problem is much more difficult in the optimal region II than in the non-optimal region I. The same conclusion would be reached for the (L/D)(V/B)-configuration, while interesting enough one would reach the opposite conclusion for the DV- and DB-configuration. However, we stress that steady state arguments may be misleading in analysis for control. It is more important that the RGAs at higher frequencies are similar at all operating points. This is not surprising because we have seen that the high frequency dynamics are similar in the different operating points. At high frequencies all RGA-values reach a value of one due to the decoupling introduced by the flow dynamics.

The steady state RGA-values for the DV-configuration are less than 0.5 at all operating points, which would suggest to pair the distillate D with the bottom composition r_{12} and the boilup V with the top composition y_D. This is counter intuitive on physical grounds. We also note that this suggestion is only valid for low frequencies. At higher frequencies the RGA is above 0.5 and therefore the usual pairing is suggested, e.g., pairing D with y_D and V with r_{12}. Similar RGA-plots are also obtained for simple distillation columns with higher purity in the top than in the bottom (Skogestad et al., 1990).

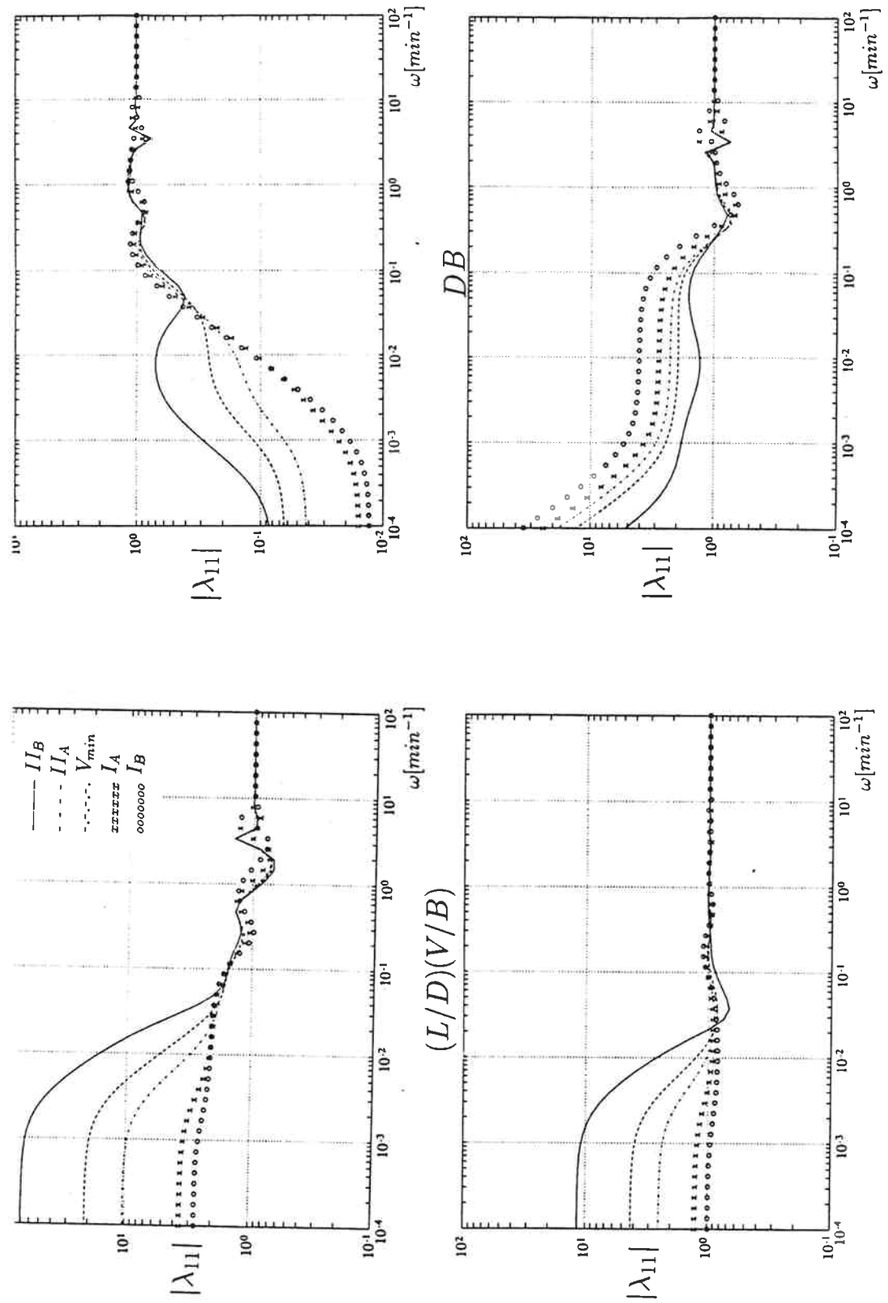

Figure 7.4: RGA as a function of frequency for the configurations LV, DV, DB and (L/D)(V/B) in different operating points.

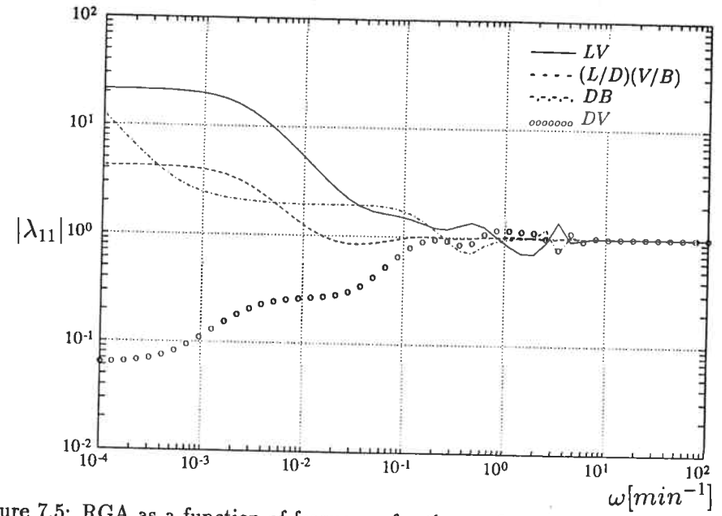

Figure 7.5: RGA as a function of frequency for the configurations LV, DV, (L/D)(V/B) in operating point II_A.

To compare the configurations we have plotted the RGA-values of the four configurations at the optimal operating point II_A in Figure 7.5. The plot shows that the (L/D)(V/B) has a RGA-value equal to one from a frequency of approximately 0.01 min^{-1} and upwards, and seems to be a favorable configuration. The RGA-plot also indicates that the control problem at operating point II_A is relatively simple when we use the (L/D)(V/B)-configuration.

We conclude from the RGA-analysis that with a properly tuned controller (reasonably high bandwidth) and a 'good' configuration we would not expect any worse control problems in the optimal region II than in region I. The RGA-values are also comparable to what has been found in simple distillation, and do therefore not indicate a more difficult control problem for the extractive column than for simple distillation columns with high-purity products.

7.7 Disturbance Sensitivity

The Relative Gain Array is independent of disturbances. However, an important issue when analyzing processes for feedback control properties is sensitivity to disturbances. The main reason for applying feedback control in distillation is rejection of disturbances that enter the process. In the literature it has been customary to consider the open-loop disturbance gains at steady state when evaluating sensitivity to disturbances. However, for disturbances one should also put emphasis on the high-frequency behavior. In addition the "direction" of the disturbance effect should be considered in the multivariable case. Some disturbances may be easier to reject than others due to a good alignment with the strong

input directions of the plant. Stanley et.al. (1985) introduced the Relative Disturbance Gain (RDG) which takes the directions into account. For a particular disturbance z_k the RDG, β_{ik}, is defined for each loop i as the ratio of the change in u_i needed for perfect disturbance rejection in all outputs to the change in u_i needed for perfect disturbance rejection in the corresponding output y_i when all other inputs are kept constant.

$$\beta_{ik} = \frac{(\partial u_i/\partial z_k)_{y_l}}{(\partial u_i/\partial z_k)_{y_i, u_{l\neq i}}} \tag{7.13}$$

Hovd and Skogestad (1990) suggested a measure, the Closed-Loop Disturbance Gain (CLDG), δ_{ik}, based on the RDG but which also takes the disturbance gain g_{dik} into account,

$$\delta_{ik} = \beta_{ik} g_{dik} \tag{7.14}$$

A matrix of CLDGs may be computed from

$$\Delta = \{\delta_{ik}\} = G_{diag} G^{-1} G_d \tag{7.15}$$

where G_{diag} are the diagonal elements of G. Hovd and Skogestad (1990) found that this measure enters nicely into the relation between control off-set and disturbances while the RGA enters in a similar way into the relation between off-set and setpoint changes.

$$e_i \approx -\frac{g_{ii}}{g_{ji}} \lambda_{ji} \frac{1}{g_{ii} c_i} r_j + \delta_{ik} \frac{1}{g_{ii} c_i} z_k; \quad \omega < \omega_B \tag{7.16}$$

This equation provides a good approximation within the bandwidth of the closed-loop system when all variables are scaled to be of magnitude one.

In this work we will use the closed-loop disturbance gain as a function of frequency to measure sensitivity to disturbances for the different configurations and operating points. We consider disturbances in the feed rate F, its composition z_F, the entrainer feed rate E, and its composition z_{E1} and z_{E2}. All disturbances are scaled with respect to the maximum expected disturbance size. We expect up to 30 % change in the feed rate F and entrainer feed rate E, up to 10 mole % in the azeotropic feed composition z_F, and up to 0.10 mol % in the entrainer impurities z_{E1} and z_{E2}.

We find that for the AHT-column we study in this paper the worst-case disturbances are disturbances in the feeds F and E. Due to limited space we will only present results for these disturbances here. We do however find similar results for all the disturbances encountered. All disturbances are taken into account in the controller design that follows later.

Figure 7.6 shows the Closed-Loop Disturbance Gains for disturbances in F and E as a function of frequency for the LV-configuration. Figure 7.7 shows the same measures for the (L/D)(V/B)-configuration. As for the RGA we see that there is a significant difference between the different operating points at low frequencies, while the responses are more similar at higher frequencies. There is however still a difference, although small, in the interesting frequency region (approx. 0.01 to 1 min^{-1}). The bottom composition r_{12} is most sensitive both to disturbances in E and F. The operating point V_{min} seems to be the best operating point with regards to disturbance sensitivity both at low and high frequencies.

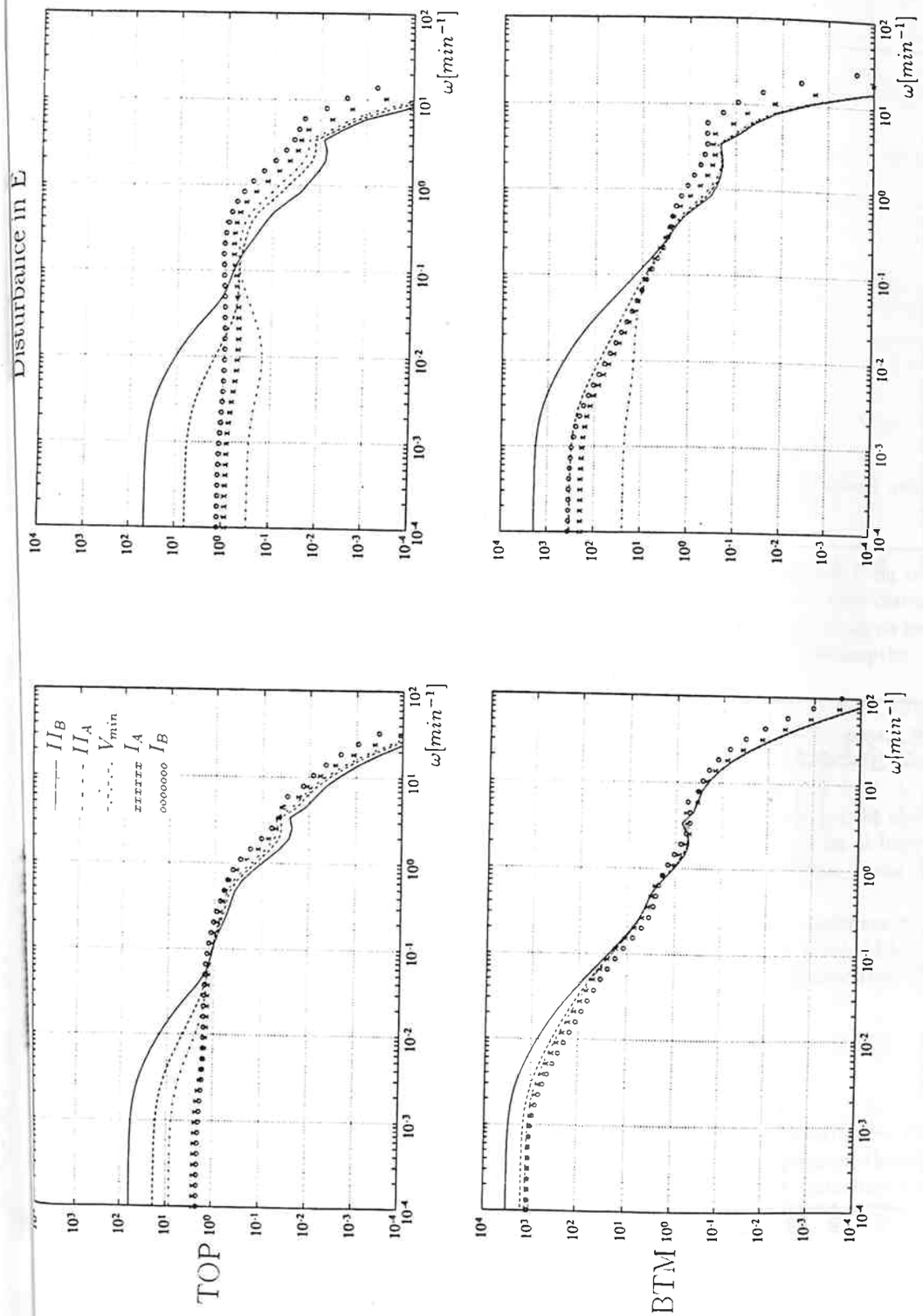

Figure 7.6: Closed-Loop Disturbance Gains for disturbances in F and E using configuration LV in different operating points.

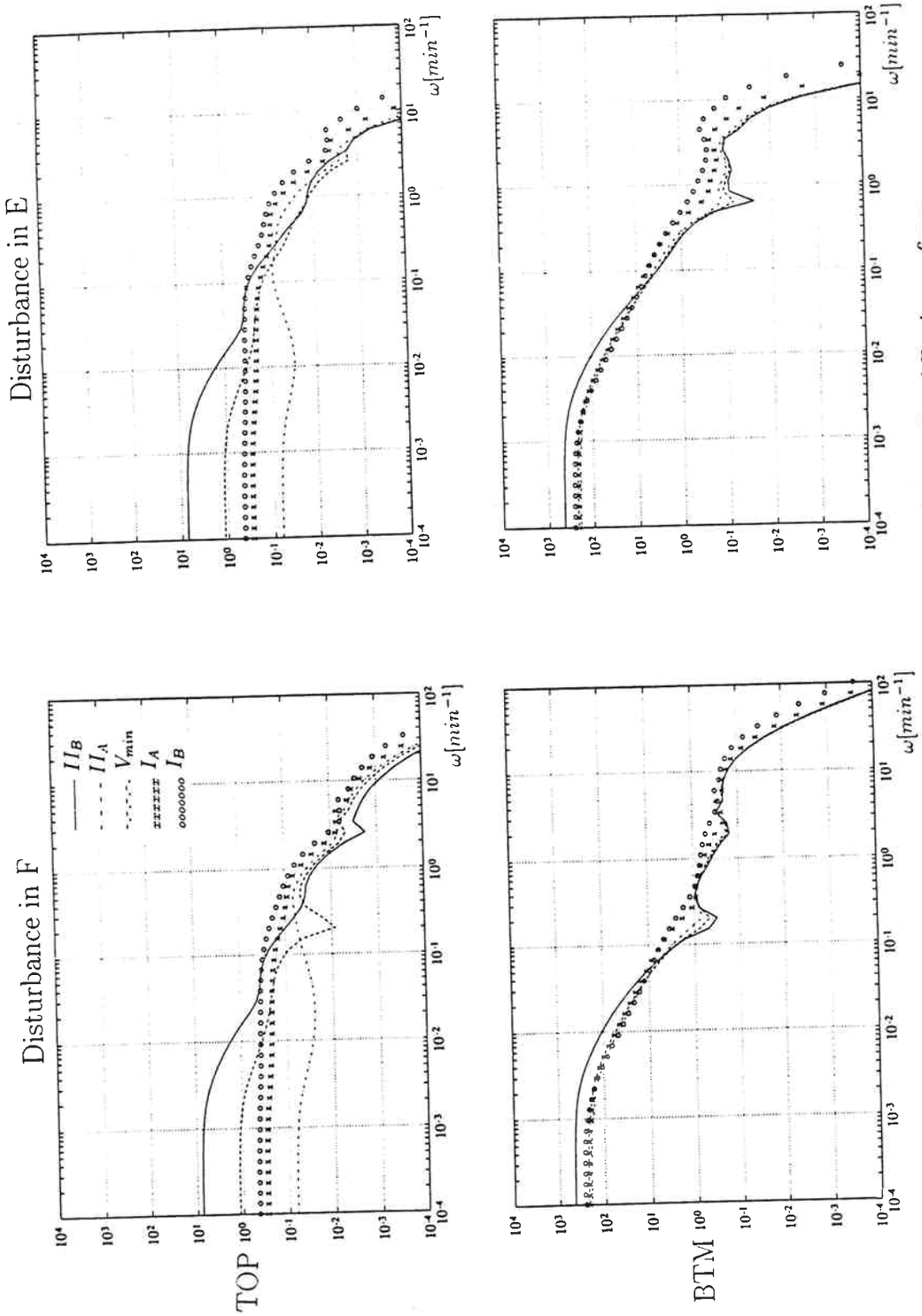

Figure 7.7: Closed-Loop Disturbance Gains for disturbances in F and E using configuration (L/D)(V/B) in different operating points.

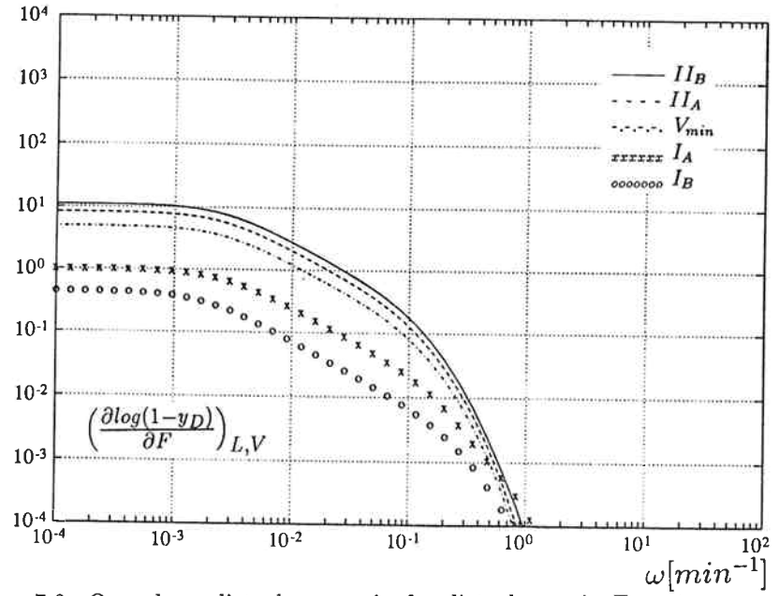

Figure 7.8: Open-loop disturbance gain for disturbance in F on top composition using the LV-configuration in different operating points.

For comparison consider the open-loop disturbance gain between feed flow F on top composition y_D for the LV-configuration in Figure 7.8. We see that the open-loop disturbance sensitivity gets worse as we get close to region II. From an open-loop analysis one would therefore incorrectly conclude that it easier to operate as entrainer consumption is increased.

In order to compare the configurations consider Figure 7.9 which shows the CLDG for disturbances in F and E in operating point II_A using the four configurations. We observe a significant difference between the configurations, and the (L/D)(V/B)- and DV-configuration seem to have the best disturbance rejection properties.

We conclude from the CLDG analysis that there is some difference between the operating points with regards to disturbance sensitivity, but the difference is smaller at higher frequencies than at steady state. The operating point V_{min} (between region I and II) seems to be the best with respect to disturbance rejection.

From the disturbance gains we see that overloading the column with entrainer does not make the control problem easier. This will be true regardless of what bandwidth the controller has; overall the operating point V_{min} will have the best disturbance rejection properties at all frequencies.

7.8 Controller Design

The analysis presented above gives an idea of what kind of control performance we may expect at the different operating points using different configurations. However, the ultimate test of achieveable performance is, of course, the design of optimal controllers for a

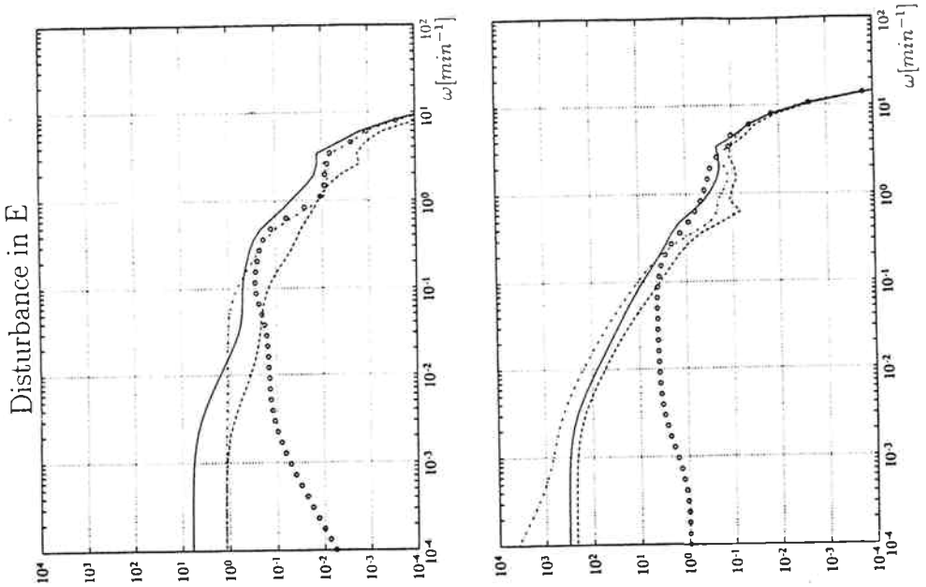

Figure 7.9: Closed-Loop Disturbance Gains for disturbances in F and E using configurations LV, DV, DB and (L/D)(V/B) in operating point II_A.

	I_B	I_A	V_{min}	II_A	II_B
LV	1.25	1.20	1.16	1.19	1.47
DV	1.35	1.49	1.53	1.67	1.63
$(L/D)(V/B)$	1.01	1.03	0.98	0.97	1.12
DB	1.48	1.43	1.35	1.33	1.28

Table 7.3: Optimal μ-values obtained at each operating point for Acetone-Heptane-Toluene Column.

chosen objective. In this work we use the structured singular value, μ, (see e.g., Morari and Zafiriou, 1989) as a design objective. That is, we design for robust performance. The controllers are optimized for setpoint changes as well as disturbances. We limit the structure of the controller to be two single-loop PI-controllers. This is done to simplify the computations and also because it is the preferred configuration in industry. Single loop PI-controllers have been designed successfully for simple distillation columns (Skogestad et al., 1990a) and seem to be close to optimal (Skogestad and Lundström, 1990).

The uncertainty weight we use on each input in this work is given by

$$w_I(s) = 0.2\frac{5s+1}{0.5s+1} \tag{7.17}$$

This includes one minute deadtime and 20 % uncertainty in each input and is the same uncertainty description as used by Skogestad et al. (1990a) for simple distillation columns.

The performance weight was adjusted to give robust performance for at least one operating point:

$$w_P(s) = 0.45\frac{15s+1}{15s} \tag{7.18}$$

This corresponds to a maximum closed-loop time constant of about 30 min for setpoint changes and a maximum amplification of 2.2 of high-frequency disturbances. This performance weight corresponds to somewhat less tight control than what Skogestad et al. (1990a) obtained for simple distillation columns (closed-loop time constant 20 min). They did however only optimize with respect to set point changes.

The disturbances were scaled as in the analysis. The outputs are naturally scaled by the logarithm, i.e. a magnitude of 1 corresponds to a change in y_D of 0.002 and a change in r_{12} of 0.005.

The results of the optimization in terms of μ-values for robust performance are given in Table 7.3. A μ-value less than one implies that the performance criteria is fulfilled for any model within the uncertainty-weight that was used. The results show that we can only guarantee robust performance (for the weights used) with the (L/D)(V/B)- configuration at the operating points V_{min} and II_A. This may be explained by the good disturbance rejection capabilities and low RGA-values observed close to the closed-loop bandwidth for this configuration at the two operating points. The (L/D)(V/B)-configuration does however get close to a μ-value of one at the operating points I_A and I_B as well, while II_B seems to be the worst operating point for this configuration. The LV-configuration

k_y	k_{r12}	τ_{Iy} [min]	τ_{Ir12} [min]
0.152	1.243	4.101	10.273

- $C(s) = k\frac{1+\tau_{Is}}{\tau_{Is}}$
- Parameters are for scaled compositions (Eq. 7.5 and 7.6)

Table 7.4: PI-settings for AHT-column with (L/D)(V/B)-configuration at operating point II_A.

also seems to work best at II_A and V_{min}, but the lowest μ-value is at 1.16. For the DV-configuration there is a clear trend that the control gets worse as we use less entrainer. It seems to be opposite for the DB-configuration, that is, control gets easier as we approach region II. These results demonstrate once again how important it is to choose a 'good' control configuration. Different configurations will give different conclusions with respect to operability at the different operating points.

In Figure 7.10 we have plotted the nominal closed-loop gains $|g_{ii}c_i|$ in both loops together with the RGA and all closed-loop disturbance gains for the (L/D)(V/B)-configuration at operating point II_A. The controller is μ-optimal and was designed above with the control parameters given in Table 7.4. From the figure we see that in both loops the closed-loop gain stays above both the RGA and the CLDG's up to the bandwidth. This is necessary to achieve the performance specification (see Eq.16). From Figure 7.10 we note that control of the bottom composition is most difficult. This is expected from the Closed-Loop Disturbance Gain analysis which showed that the bottom composition was most sensitive to disturbances. The bandwidth in this loop is much higher than for the top composition loop which is far less sensitive to disturbances. The difference in bandwidth between the two loops is also advantageous from an interaction point of view. (Because each loop has its main effect in a different frequency region, we avoid possible interaction problems because of non-perfect control (Balchen, 1988)) The distance between the closed-loop gain and the RGA and CLDGs give the offset e_i according to (16).

For comparison we optimized controllers also for the Ethanol-Water-Ethylene glycol (EWE) column. Data for the column are given in Table 7.2. We used the same uncertainty weight as for the AHT-column, but the performance requirements were somewhat looser

$$w_P(s) = 0.40\frac{20s+1}{20s} \tag{7.19}$$

Results of the optimization for the EWE-column are given in Table 7.5. The results are very similar to those for the AHT-column, and robust performance can only be guaranteed at operating points V_{min}, II_A and II_B with the (L/D)(V/B)-configuration.

7.9 Use of Entrainer Feed for Control

So far we have not considered the entrainer as a third degree of freedom in control. The main reason for this is that we did not want to complicate matters too much compared

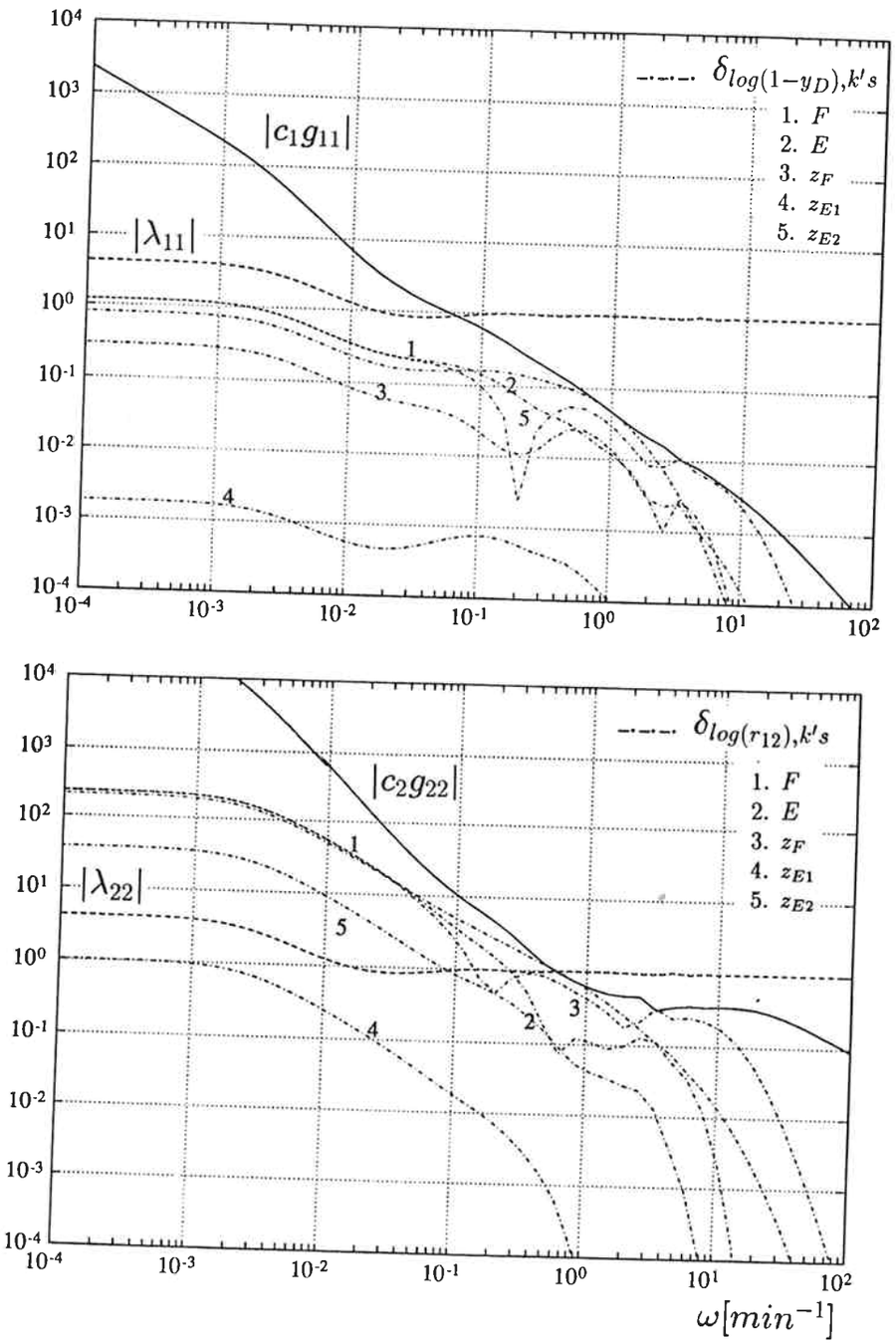

Figure 7.10: Closed-loop gains, RGA and CLDG's for all disturbances in the two single loops using the (L/D)(V/B)-configuration in operating point II_A. Controller parameters are given in Table 7.4.

	I_A	V_{min}	II_A	II_B
LV	1.18	1.13	1.14	1.50
DV	1.38	1.40	1.52	1.69
$(L/D)(V/B)$	1.11	0.99	0.99	0.99
DB	1.52	1.42	1.37	1.14

Table 7.5: Optimal μ-values obtained at each operating point for Ethanol-Water-Ethylene glycol Column.

to simple distillation. We did not seem to need this extra degree of freedom. However, there are two reasons why one may want to use the entrainer actively for control. First of all, it may be needed to ensure optimal operation under varying operating conditions. Second, we must avoid that the entrainer feed goes below the minimum needed for the desired separation. The entrainer may be used in a feedback or feedforward manner to accomplish this.

In order to get an idea when we need to change the entrainer feed in order to stay at the optimal operating point we need to know how different disturbances affect the optimality curve in Figure 7.2. It is obvious that the entrainer rate should simply be scaled by a factor $(E/F)^*$, where * denotes the nominal value, for disturbances in F. This may be done in a feedforward manner. As the dynamics for changes in E and F are very similar, dynamic compensation should not be necessary in the feedforward loop.

It is however not clear what happens to the trade-off curve for disturbances in feed and entrainer composition. As the separation in the recovery column is easy we do not expect large disturbances in the entrainer composition and therefore not in the trade-off. Figure 7.11 shows the trade-off curve for different azeotropic feed compositions. We see that the curve moves mostly in a vertical direction, that is the value of E_{min} is almost constant while V_{min} varies. We may therefore conclude that in order to stay close to the optimum, and thereby also avoid E_{min} under changing operating conditions, we only have to change the entrainer feed rate for disturbances in the azeotropic feedrate.

We suggest that this may be implemented in a feedforward loop. We do however realize that it is impossible to avoid "drift" with feedforward control, and that one therefore should consider using the entrainer feed in a feedback manner. It is not obvious how this should be done without limiting the flexibility of the column.

7.10 Nonlinear Simulations

Figure 7.12 shows the response to a setpoint change in y_D from 0.998 to 0.9964 ($\Delta y_D^s = -0.8$) in operating point II_A using the (L/D)(V/B)-configuration. The controller tunings are the ones obtained from the robust controller design and are given in Table 7.4. The simulations include one minute deadtime and 20 % uncertainty in the inputs. Figure 7.13 shows the response to a setpoint change in the bottom composition r_{12} from 0.005 to 0.001 ($\Delta r_{12}^s = -0.8$) in operating point II_A with the same controller. We see that the bandwidth for the bottom loop is significantly higher than for the top loop. The

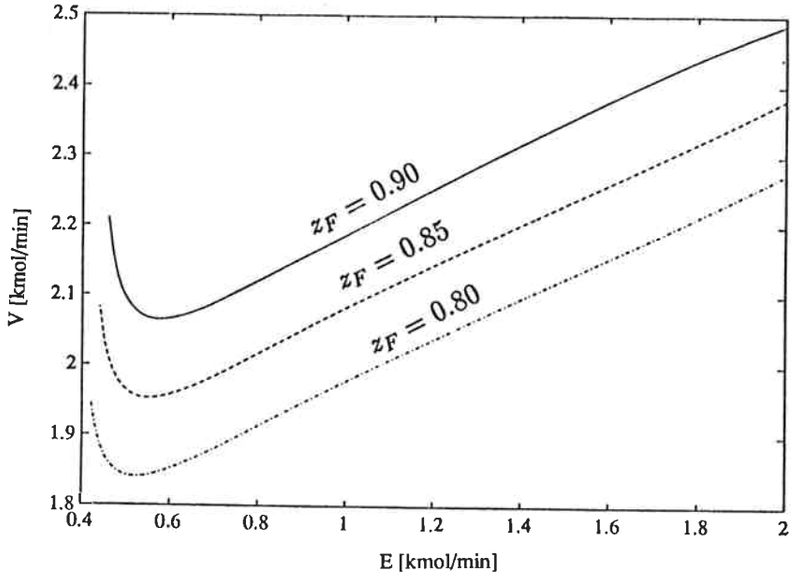

Figure 7.11: Set of solutions for the AHT-column for different azeotropic feed-compositions. Region III is not shown.

simulations demonstrate that setpoint changes are easily handled by the control system, and that the interaction between the control loops is small. Figure 7.14 shows the response to a 30 % increase in azeotropic feed rate F with feedforward action in entrainer feed rate. The same uncertainty was included in the controller as above, and we also assumed one minute deadtime and 20 % uncertainty in the entrainer feed rate change, i.e., we increased the entrainer feed rate by 24 % after one minute. Without the feedforward action, E would fall below E_{min} and the closed-loop system would become unstable. The simulations demonstrate that it is the bottom composition which is most difficult to control. We do however get an acceptable response also for this composition.

7.11 On-line Location of Optimal Operating Point

We discuss here briefly how the optimal operating point may be located on a column that is under operation. We assume that the starting point is in region I, i.e. in the non-optimal region. We know that as we decrease the entrainer feed rate in region I we will simultaneously decrease the boilup until we reach minimum boilup V_{min}, provided both compositions are kept constant (see Figure 7.2). By decreasing in E in a ramp-wise fashion with both compositions under feedback control we will therefore observe a decrease in boilup until we pass V_{min}. The ramp change should not be done too fast so that the composition controllers can follow. If the ramp change is done too fast we may go far beyond V_{min} before we actually observe an increase in boilup V. For a sufficiently slow ramp change we may continue the ramp until we observe an increase in boilup. This will provide a fairly accurate location of V_{min}. From this point on one can do small step

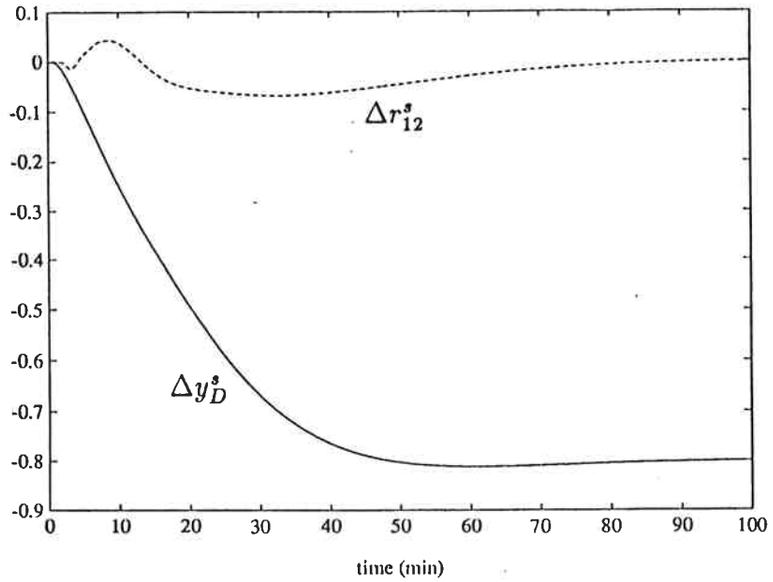

Figure 7.12: Nonlinear simulation of a set point change in top composition y_D in operating point II_A using the (L/D)(V/B)- configuration. Controller tunings from Table 7.4. The simulation includes input uncertainties as given in Eq.7.17.

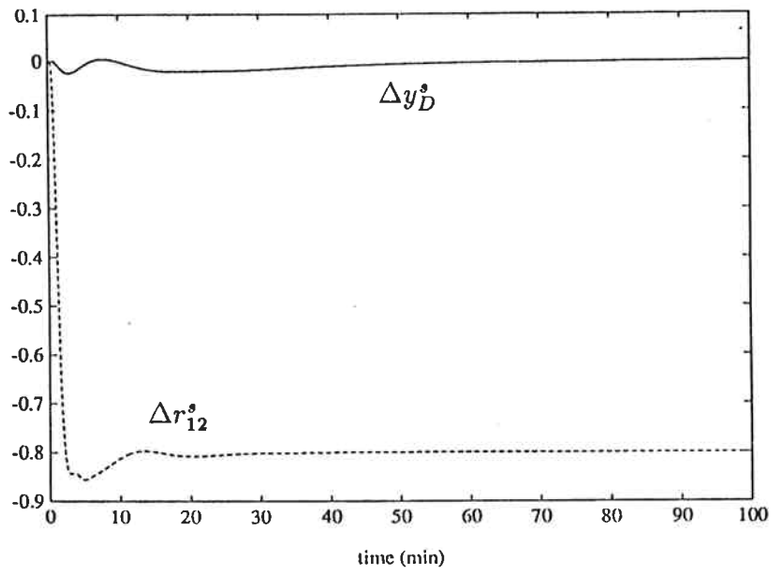

Figure 7.13: Nonlinear simulation of a set point change in bottom composition r_{12} in operating point II_A using the (L/D)(V/B)- configuration. Controller tunings from Table 7.4. The simulation includes input uncertainties as given in Eq.7.17.

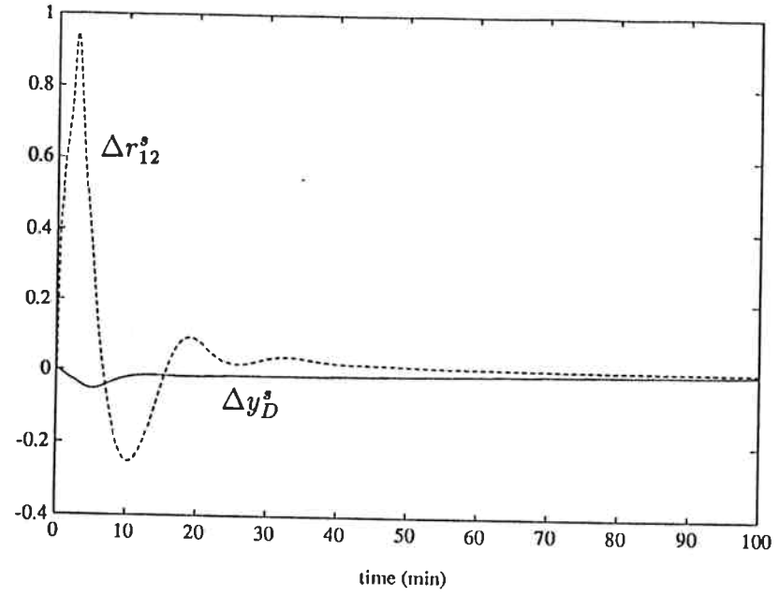

Figure 7.14: Nonlinear simulation of a 30 % increase in azeotropic feed flow rate F in operating point II_A using the (L/D)(V/B)- configuration. Controller tunings from Table 7.4. Feedforward action for entrainer feed is implemented by keeping (E/F) constant. The simulation includes input uncertainties as given in Eq.7.17.

changes in E until one reaches the desired trade-off between entrainer consumption and boilup.

Figure 7.15 shows non-linear simulation results for a ramp decrease in E from operating point I_B using the (L/D)(V/B)-configuration. The entrainer feed was decreased at a rate of 0.001 kmol/min. The controller given in Table 7.4. was used to control compositions. We see that the boilup starts to increase at a value of E around 0.56. The steady state minimum boilup is at E equal to 0.57. Thus we are able to determine the point of minimum boilup quite accurately by the proposed method. The simulation also demonstrates that the same controller may be used over a wide range of operation. This is explained by the similar initial responses in different operating points when logarithmic measurements are used.

7.12 Discussion

In this paper we have only studied two columns, both with heavy boiling entrainers, and one should therefore be careful about making general conclusions. However, the main results are explained by the fact that the initial responses of the columns are similar at all operating points and also to what is observed in simple distillation. The effects of the non-ideal thermodynamics are slow and do therefore not have a strong effect on the high-frequency dynamics which are most important for control. We expect this to be true also for other columns of the same class.

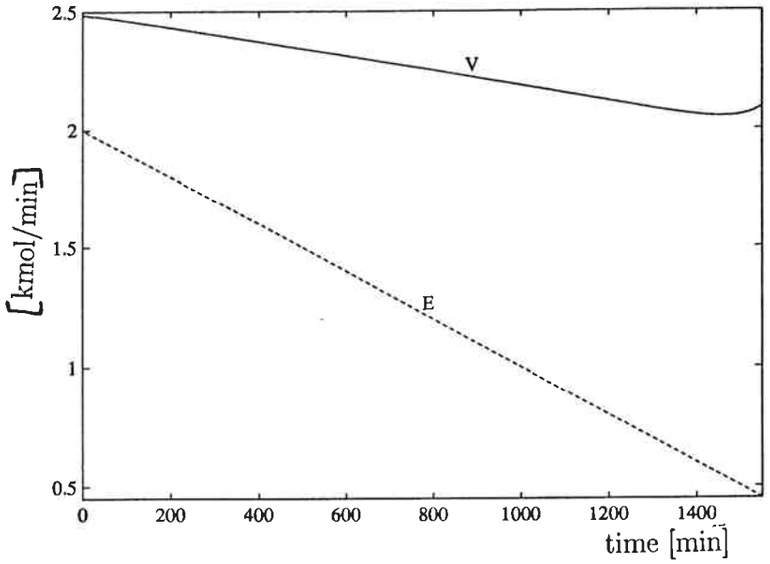

Figure 7.15: Response in boilup to a ramp decrease in entrainer feed from operating point I_B. Both compositions under feedback control with the (L/D)(V/B)-configuration. Controller tunings from Table 7.4. The simulation includes uncertainties as given in Eq.7.17.

It is clear for the columns studied that it is the bottom product composition that is most sensitive to disturbances and is limiting control performance. However, the ratio r_{12} is also sensitive to the inputs (e.g., L and V), which implies that it may be kept above specification at a small expense in terms of boilup and reflux. For instance one could decrease the ratio r_{12} from 0.005 to 0.001 at operating point II_A of the AHT-column by only increasing the boilup by 2.5 %. This is not a result of column overdesign as one might expect, as a decrease in number of trays would be expensive in terms of increased boilup. If crucial, we would recommend that the specification for the bottom product is set low enough to never complicate the separation in the recovery column. Another solution may be to add some trays in the stripping section, as this would reduce the high-frequency disturbance sensitivity of the bottom product.

All presented results indicate that the control problem in the optimal region II is not more difficult than in region I. These results are however based on reasonably tight control. Tight control depends on the choice of a 'good' configuration and on obtaining measurements without long delays. The results in this paper indicate that the ratio configuration (L/D)(V/B) is the best choice. This is similar to what is found in simple distillation (Skogestad et al., 1990a). The measurement problem has not been treated in this paper and may be a more difficult problem in azeotropic distillation than in simple distillation. This has been pointed out by several authors (e.g. Gilles et al., 1980), and is due to the more difficult temperature profile encountered in these columns. The measurement problem will be studied in a future paper.

The existence of a minimum necessary entrainer feed for a given separation may cause problems during the operation. If the azeotropic feed rate is increased by more than 10 % at operating point II_A of the AHT-column without adjusting the entrainer feed, the column will go closed-loop unstable as the specified separation is infeasible. In this paper we propose using a feedforward loop from azeotropic to entrainer feed to avoid E_{min}. However, this solution is sensitive to uncertainties in flow measurements. A better solution may be to use the entrainer in a feedback scheme in addition to feedforward action. The problem will be to select a measurement that will not limit the flexibility of the column. The control problem will also become more complicated because we get a 3×3 control system.

The problem associated with minimum entrainer feed may also be reduced by selecting a suboptimal operating point. For the AHT-column the operating point V_{min} is not far from the economic optimum but may tolerate significantly larger disturbances in F without the entrainer dropping below E_{min}. This operating point does also have good control properties as seen from the analysis and control design.

Another potential problem which we have not discussed in the paper is region III where we have severe right half plane zeros. If this region is entered dynamically during operation one can experience stability problems. The probability of entering this region is hard to predict analytically because it is a high order non-linear dynamic problem. One would have to use some kind of Lyapunov function in order to determine the regions of attraction. Because of the high order and complexity this is too difficult a problem to be handled in this paper. However, in all our simulations we have not been able to perturb the column into a region where we encountered problems resulting from changes in the sign of the gains. Thus, our experience indicates that region III should not pose any problems to practical operation in region II.

The paper has not discussed the control of the entrainer recovery column and the coupling between the two columns. However, the separation in the recovery column will usually be similar to simple distillation. The coupling between the two columns should not be a difficult problem either. A tank for the entrainer feed will be necessary due to variations in the entrainer feed rate, and this will dampen the effect of changes in entrainer flow and composition from the recovery column.

The use of a heavy entrainer which we have studied in this paper is most widespread in industry today. However, it is clear that other entrainers may be more favorable both from a steady state point of view (Laroche and Morari, 1990) and also from a control point of view. One kind of entrainer that may be advantageous is an entrainer which is an intermediate boiler. In this case we have two possible sequences of separation: 1) Light component and entrainer in the top of the extractive column 2) Heavy component and entrainer in the bottom of the extractive column. In both these cases the impurities from the extractive column will enter the entrainer product in the recovery column. This entrainer product will be fed back to the bottom of the extractive column in case 1 and to the top in case 2. This implies that the impurities in both cases are fed back to a section where they are easy to separate. Therefore the entrainer impurities should be easy to handle in the extractive column, and relatively high impurities may be optimal. By the same argument disturbances in the entrainer impurities should be easy to reject with feedback control, and the performance specification on the ratio (e.g., r_{12}) may be

loosened, thereby making control easier.

7.13 Conclusions

In this paper we have studied the control properties both at the optimal operating point (low entrainer feed) and at suboptimal operating points for two extractive columns with heavy entrainer. The analysis of the dynamic model does not indicate a more difficult control problem at the optimal operating point than at other operating points. The robust controller design supports the results of the preliminary analysis. In the optimal region of operation we obtain controller performance which is comparable to what is achieved for simple distillation columns. The results depend strongly on the choice of a "good" control configuration, and for the columns studied we find the ratio configuration (L/D)(V/B) to be the best choice. The results does also depend on relatively tight control as the low-frequency characteristics indicate a more difficult control problem if the bandwidth is significantly lower than what is used in this work. The results are explained by the fact that the initial response in an extractive distillation column is similar to what is found in simple distillation. The effect of non-ideal thermodynamics is slow. Therefore we expect the results obtained to be valid for most extractive columns of the type studied in this work.

The existence of a minimum entrainer feed rate for a desired separation may pose problems in the operation of extractive columns. In this work we have proposed a feed-forward scheme to avoid E_{min}. This may however not be satisfactory, and one should therefore consider using the entrainer in a feedback scheme.

NOMENCLATURE

B - Bottom flow [kmol/min].
c_i - controller transfer function, loop i.
G - process transfer matrix.
g_{ii} - i,i-element of G.
G_d - disturbance gain matrix.
g_{dik} - disturbance gain from disturbance k to output i.
D - Distillate flow [kmol/min].
E - Entrainer feed flow [kmol/min].
e_i - control off-set in loop i.
F - Azeotropic feed flow [kmol/min].
L - Reflux flow [kmol/min]
M_i - Liquid holdup on tray i.
N - Number of theoretical trays
NF - Feed tray location for azeotropic feed.

NE - Feed tray location for entrainer feed.
P - Pressure
r_{12} - ratio of light to intermediate component in bottom product.
r_j - set point change in output j.
V - boilup [kmol/min]
V_T - condensation rate [kmol/min]
w_P - Performance weight.
w_I - Uncertainty weight.
z_k - Disturbance k.
y_D - fraction of light component in distillate.
z_F - Fraction of light component in azeotropic feed.
z_{E1} - Fraction of light component in entrainer feed.
z_{E2} - Fraction of intermediate component in entrainer feed.

Greek symbols

β_{ik} - Relative Disturbance Gain form disturbance k to output i.
δ_{ik} - Closed Loop Disturbance Gain from disturbance k to output i.
γ^* - Minimized condition number.
λ_{ij} - ij'th element of the Relative Gain Array.
μ (mu) - structured singular value
τ_L - Hydraulic time constant for each tray [min].
ω_B - Closed-loop bandwidth [min^{-1}].

REFERENCES

Abu-Eishah, S.I. and W.L. Luyben, 1985, "Design and Control of a Two-Column Azeotropic Distillation System", *Ind.Eng.Chem.Res.Dev.*, **24**, 132-140.

Andersen, H.W., L. Laroche and M. Morari, 1989, "Effect of Design on the Control of Homogeneous Azeotropic Distillation Columns", AIChE Meeting, San Francisco (Nov., 1989).

Andersen, H.W., L. Laroche and M. Morari, 1991, "Dynamics of Homogeneous Azeotropic Distillation Columns", *Ind.Eng.Chem.Res.*, **30**, 1846-1855.

Anderson, J.E., 1986, "Multivariable Control of an Azeotropic Distillation Column", *Adv.Instrum.*, **42** (2), 469-476.

Balchen, J.G., 1988, *Process Control. Structures and Applications*, Van Nostrand Reinhold, New York.

Bozenhardt, H.F., 1988, "Modern Control Tricks to Solve an Old Problem: Azeotropic Distillation", *Hydrocarbon Process*, **67** (6), 47-50.

Bristol, E.H., 1966, "On a New Measure of Interactions for Multivariable Process Control", *IEEE Trans. Automat. Control*, **AC-11**, 133-134

Bristol, E.H., 1978, "Recent Results on Interactions in Multivariable Process Control", AIChE Meeting, Chicago.

Doherty, M.F. and G.A. Calderola, 1985, "Design and Synthesis of Homogeneous Azeotropic Distillation. 3. The Sequencing of Columns for Azeotropic and Extractive Distillation", *Ind.Eng.Chem.Fund.*, **24**, 474

Doyle, J.C., 1985, "Structured Uncertainty in Control System Design", *Proc. IEEE Conf. on Decision and Control*, Ft. Lauderdale.

Gilles, E.D., B. Retzbach and F. Silverberg, 1980, "Modelling, Simulation and Control of an Extractive Distillation Column", *ACS Symposium Series # 124*, American Chemical Society.

Hovd, M. and S. Skogestad, 1990, "Use of Frequency-Dependent RGA for Control System Analysis, Structure Selection and Design", *accepted for publication in Automatica*

Knapp, J.P. and M.F. Doherty, 1990, "Thermal Integration of Homogeneous Azeotropic Distillation Sequences", *AIChE J.*, **36**, 7, 969

Knight, J.R. and M.F. Doherty, 1989, "Optimal Design and Synthesis of Homogeneous Azeotropic Distillation Sequences", *Ind.Eng.Chem.Res*, **28**, 564-572.

Laroche, L. and M. Morari, 1990, "Entrainer Selection for Homogeneous Azeotropic Distillation", *AIChE J.*, In press.

Levy, S.G. and M.F. Doherty, 1985a, "Design and Synthesis of Homogeneous Azeotropic Distillation. 4. Minimum Reflux Calculations for Multiple Feed Columns.", *Ind.Eng.Chem.Fund.*, **25**, 269

Levy, S.G. and M.F. Doherty, 1985b, "Design and Synthesis of Homogeneous Azeotropic Distillation. 5. Columns with nonnegligible Heat Effects", *Ind.Eng.Chem.Fund.*, **25**, 279

Morari, M. and E. Zafiriou, 1989, *Robust Process Control*, Prentice-Hall, New Jersey.

Rademaker, O., J.E. Rijnsdorp and A. Maarleveld, 1975, *Dynamics and Control of Continuous Distillation Units*, Elsevier, Amsterdam.

Shinskey, F.G., 1977, 1984, *Distillation Control*, 1st & 2nd Edition, McGraw-Hill, New York.

Skogestad, S. and M. Morari, 1987a, "Implication of Large RGA-elements on Control Performance", *Ind.Eng.Chem.Res.*, **26**, 11, 2323

Skogestad, S. and M. Morari, 1987b, "The Effect of Disturbance Directions on Closed-Loop Performance", *Ind.Eng.Chem.Res.*, **26**, 10, 2029

Skogestad, S., M. Morari and J.C. Doyle, 1988, "Robust Control of Ill-Conditioned Plants: High-Purity Distillation", *IEEE Trans. Autom. Control*, **33**,12, 1092

Skogestad, S. and M. Morari, 1988, "Understanding the Dynamic Behavior of Distillation Columns", *Ind.Eng.Chem.Res.*, **27**, 10, 1848

Skogestad, S., P. Lundström and E.W. Jacobsen, 1990a, "Selecting the Best Distillation Control Configuration",*AIChE J.*, **36** (5), 753

Skogestad, S., E.W. Jacobsen and M. Morari, 1990b, "DB-Control of Distillation Columns: Inadequacy of Steady-State Analysis for Feedback Control", *Accepted for publication in Ind.Eng.Chem.Res.*

Skogestad, S. and P. Lundström, 1990, "Mu-optimal LV-Control of Distillation Columns", *Comp. and Chem. Eng.*, **14**, 4/5, 401

Stanley, G., M. Marino-Galarraga and T.J. McAvoy, 1985, " Shortcut Operability Analysis. 1. The Relative Disturbance Gain.", *Ind.Eng.Chem.Process Des.Dev*, **24**, 4, 1181

Witcher, M. and T.J. McAvoy, 1977, "Interacting Control Systems: Steady State and Dynamic Measurement of Interaction", *ISA Trans.*, **16**, 35.

Weigand, W.A., A.K. Jhawar and T.J. Williams, 1972, "Calculation Methods for the Response Time to Step Inputs for Approximate Dynamic Models of Distillation Columns", *AIChE J.*, **18**, 6, 1243.

Chapter 8

Conclusions

The thesis addresses different aspects of distillation dynamics and control. The research has been motivated by the need to better understand the behavior of distillation columns, which subsequently may lead to improved composition control. The main contributions of the thesis are summarized below:

I. Multiple steady-states and instability in homogeneous distillation

It is established that homogeneous distillation columns may have multiple steady-state solutions and that some of the solutions represent unstable operating points. The results apply even to the distillation of ideal binary mixtures. Two different sources for the multiplicity are presented. The first source is found for inputs on a mass or volume basis. It is shown that the transformation from the actual input units to molar units may become singular. As it is the size of the molar flows that determine the separation in distillation, the singularity results in output multiplicity, i.e., several possible solutions in terms of outputs (compositions) for a given set of inputs (flows). This type of multiplicity is found even for the case of constant molar flows, that is, with neglected energy balance. The second source of multiplicity depends on the presence of an energy balance. The interactions between compositions and flows through the material and energy balance may in some cases result in a singularity. Also in this case the singularity results in output multiplicity. For both cases it is shown that increased internal flows will increase the probability of instability.

It is demonstrated that an open-loop unstable operating point may be stabilized by the use of feedback control of a column composition or temperature. The column may go into a stable limit-cycle if the control is not sufficiently tight. Finally, it is shown that the instability will worsen the performance of composition controllers, in particular in columns with large measurement delays.

II. Low-order dynamic models for distillation columns

Most studies on distillation control employ low-order dynamic models. It is shown that such models often are physically inconsistent in that they contain an excessive number of slow poles compared to the process. The reason is that the open-loop responses of ill-conditioned processes, like high-purity distillation columns, usually are dominated by a single pole. It is consequently difficult to identify the other poles of the process. Attempting to define a model using only the dominating time-constant (pole) of the process corresponds to assuming singular dynamics. Because the steady-state part of the model is non-singular, the realization of the model will contain several poles equal to the dominating pole of the process. It is shown that such a model, although a reasonable approximation for open-loop dynamics, yields a poor prediction of the closed-loop behavior of the process. Partial feedback control as well as the case with both compositions under feedback control are discussed. An important conclusion for distillation is that it seems difficult to define a low-order model, based on physical insight, which includes flow dynamics and is consistent in terms of the number of slow poles.

The second chapter of part II compares different low-order dynamic models for distillation columns. Models obtained from physical insight as well as mathematically reduced models are considered. The main conclusion of the model comparison is that it is the initial responses of the models that are most important for feedback control, and consequently the flow dynamics should be included in the model. An accurate model of the steady-state behavior is not very important for feedback control. However, it is important to know the sign of the plant, that is, one must know the sign of the steady-state determinant. The problem of obtaining low-order models from experimental data is also addressed. It is shown that by combining experimental open-loop step responses with theoretically established structural properties one may obtain reasonably good models for two-point (dual composition) control. It should be noted that this study was finished before the results on inconsistencies in low-order models were found, and that several of the models considered actually are inconsistent in terms of the number of slow poles. However, it is shown that several of the models considered are reasonable for cases with both compositions under feedback control. All the models obtained from "physical insight" and experiments would, however, be poor for studies of partially controlled distillation columns.

III. Trade-offs between design and control of distillation columns

Most studies on distillation control aim at improving the control performance through improved control algorithms. However, high-purity distillation columns are known to have inherent control limitations which limits the achieveable performance even with the

"best" possible controller. In this thesis it is considered whether modifying the column design itself may reduce the control limitations, thereby improving the achieveable control performance. Modifications considered include: 1) Introducing sidestreams. It is shown that this modification reduces the interactions and disturbance sensitivity at low frequencies, but has little effect in the frequency region most important for feedback control. 2) Overdesigning the column in terms of the number of trays. This design modification may improve the controllability for some columns, but the conclusion will depend on the column studied. 3) Use of a feed preheater in feedback control. This modification may yield significant improvements in the interactions as well as the disturbance sensitivity of the column. It is stressed that the results are limited to a few case studies, and that further research is needed.

In homogeneous azeotropic distillation an entrainer is added to make the separation feasible. The entrainer flow represents an extra degree of freedom which may be used to optimize the column in terms of utility consumption. However, it has previously been believed that for these columns there is a strong trade-off between steady-state optimality and controllability. Many industrial columns are operating far from the steady state optimum, partly due to a belief of improved controllability. This thesis consider the high-frequency dynamics of such columns and compare different operating points with respect to controllability. It is concluded that, with a proper control configuration and reasonably fast composition measurements, the control problem in the optimal region of operation is similar to the control problem in the less optimal region. Furthermore, the achieveable control performance is found to be similar to what is found for ideal binary distillation columns with high purity products.

8.1 Suggestions for Future Research

Distillation modelling

There are still many aspects of the dynamic behavior of distillation columns which are poorly understood. This concerns for instance the effect of the energy balance and pressure variations. Furthermore, there is a need for further research on low-order dynamic models and experimental model identification in high-purity distillation.

1) Although most current simulation models probably include the energy balance, few analytical studies have included the effect of variations in flows due to the energy balance. As seen in this thesis, the energy balance may lead to multiplicity and instability even in the simplest cases. In addition, the author have indications of more complex types of bifurcations that may occur when the energy balance is included. For a binary system

with certain thermodynamic properties we have found that input multiplicity and period 2 limit cycles may occur (see Appendix). However, the results are based on artificial thermodynamic data which do not satisfy the Gibbs Duhem equation. Whether similar behavior may be found for real systems is therefore still an open question.

The influence of the energy balance on feedback control properties is also poorly understood. It is therefore a definite need for further studies on the effect of the energy balance on the behavior of distillation columns. These studies should consider binary as well as multicomponent mixtures.

2) The effect of pressure variations has also received little attention in the literature on distillation dynamics. The effect of pressure variations on the overall dynamic behavior as well as on the initial dynamic responses important for feedback control needs a closer investigation.

3) In studies of distillation control, low-order dynamic models are needed. However, as seen in this thesis, such models are difficult to formulate based on physical insight or experimental data. The problem of obtaining low-order models which are consistent and proper for feedback control studies needs to be studied closer. This concerns both the model for the effect of inputs as well as the disturbance model.

4) The more general problem of identifying dynamic models from experiments in ill-conditioned plants is also a subject that needs further investigation. Such studies should concentrate on the properties important for feedback control, and in particular emphasize the robustness properties. If the identification method is able to reveal something quantitative about the model uncertainty, the controller design may be made less conservative, resulting in tighter control of the plant.

Finally, although experiments on operating columns often yield case-specific results, it is important to confirm results found from mathematical models by performing experiments on a real column. The results on multiplicity presented in this thesis need to be confirmed by experiments. In addition, through experiments one may in some cases discover new and interesting effects which may have been left out of a model.

Distillation control

This thesis have discussed a few possibilities of design modifications for improving the controllability of distillation columns. The results are based on a case study of two example columns. There is obviously a need for more general research in this area. Improved control algorithms are only able to improve the control performance as far as the inherent control limitations of the process allows. Therefore, further improvements will require process design modifications. In a wider definition this includes modifying the steady-state design as well as selecting inputs and outputs for control. One of the

long term goals of this research should be to develop tools for evaluating controllability which relatively easily may be incorporated in a process design environment.

One important prerequisite for tight control of distillation columns is fast and reliable measurements. For ideal columns this has partly been solved by the use of composition estimators based on temperature measurements. However, it is unclear whether the same methods is applicable to more complex separations like homogeneous azeotropic distillation. This needs to be investigated as the conclusions in this thesis regarding control of such columns depend on the availability of relatively fast measurements which usually are not obtained with conventional composition analyzers.

APPENDIX. Input multiplicity in binary distillation.

This appendix presents some preliminary results on the existence of input multiplicity in binary distillation. The system studied has constructed thermodynamic properties which are unlikely to be found in any real homogeneous system. However, the results are presented here as they may yield some insight which may be used as a starting point for similar studies on real systems.

The system we study is a binary distillation column with N=40 trays, feed tray N_F=21, feed F=1.0 kmol/min, feed composition z_F=0.5 and constant relative volatility α=1.5. The heat of vaporization for the system, i.e., the difference between saturated vapor and liquid enthalpy, is shown as a function of composition in Figure 8.1. We see that the heat of vaporization is the same for the pure components while it has an extremum for a composition x=0.5. This enthalpy behavior may be explained by non-ideal mixing in the liquid phase, which yields an increase in the liquid enthalpy with mixing. The vapor phase may be assumed to be close to ideal.

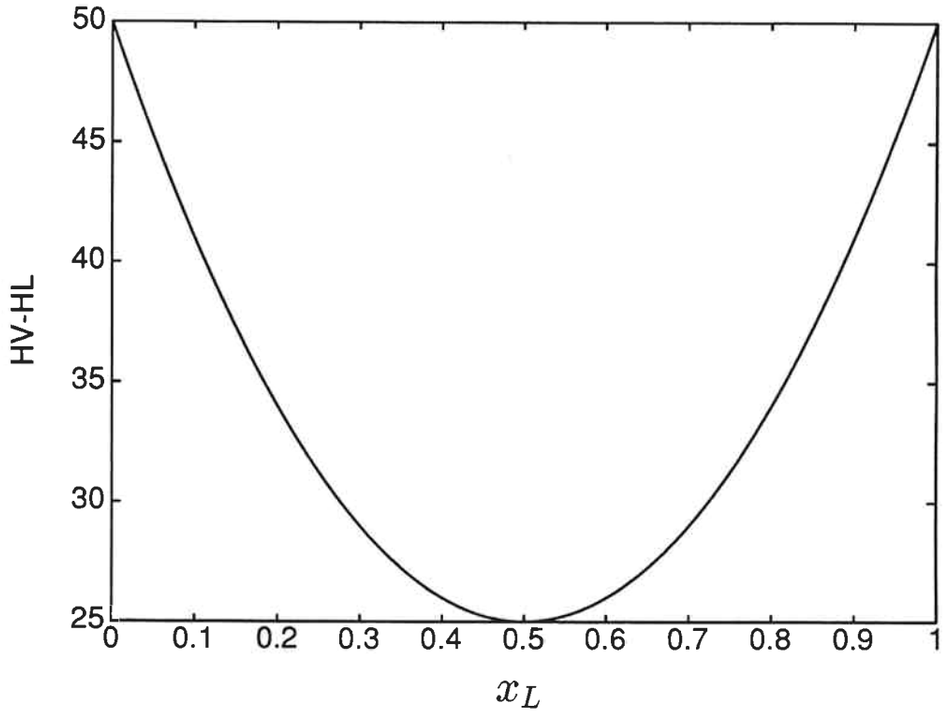

Figure 8.1: Saturated heat of vaporization as function of composition for system studied.

The system studied may have input multiplicity when distillate flow and boilup are used as independent variables. This is illustrated in Figure 8.2, which shows top composition y_D as a function of distillate flow D with boilup V fixed at 2.14 kmol/min. The figure

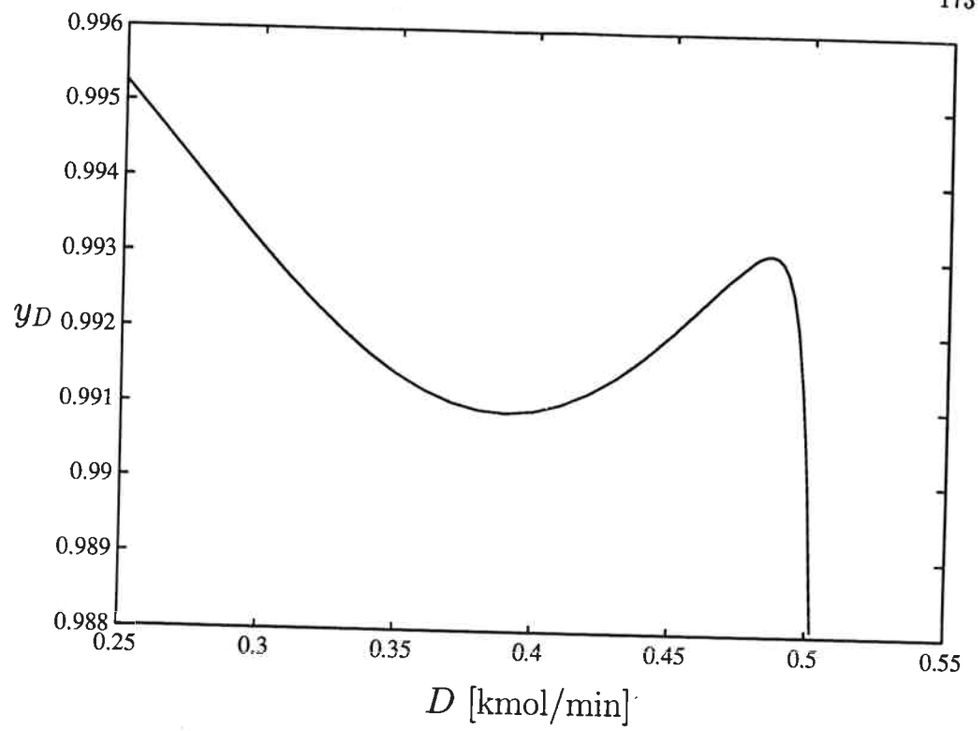

Figure 8.2: Top composition y_D as a function of distillate flow D for system studied. Boilup V=2.14 kmol/min.

shows that, with boilup V fixed, there exist several input solutions in terms of distillate flow D for a given output in terms of product composition y_D. Note that this is different from the results presented in Chapter 2 of this thesis, where we had output multiplicity, i.e., for a given input L_w there existed several solutions in terms of output y_D, and a pole crossed the imaginary axis resulting in instability for some of the solutions. The existence of input multiplicity is linked to a zero crossing the imaginary axis, i.e., a change in the sign of the steady-state gain.

The system studied may also undergo a Hopf bifurcation when the condenser level control is not sufficiently tight, as discussed in Chapter 3 of this thesis. However, in this case with do not only get period 1 limit cycles. The bottoms flow B will for instance have a period 2 limit cycle as seen from Figure 8.3a. A probable explanation for the period 2 solution for the bottoms flow is that a zero is crossing the imaginary axis, corresponding to a change in sign of gain. The compositions will on the other hand have a period 1 limit cycle, and the difference in periods for flows and compositions results in the somewhat exotic phase plot in Figure 8.3b.

At the moment we have no explanation of the input multiplicity for the system studied. However, it is likely that it is the special enthalpy properties of the mixture that causes the multiplicity. It is important to note that a system with this strong change in liquid enthalpy with mixing is likely to separate into two liquid phases, i.e., heterogeneous

mixture. Thus, the system studied does not represent any real homogeneous mixture. However, it is the belief of the author that similar results to the ones presented here may be found in real homogeneous systems with an extremum in the heat of vaporization. This needs to be studied closer in a future research project.

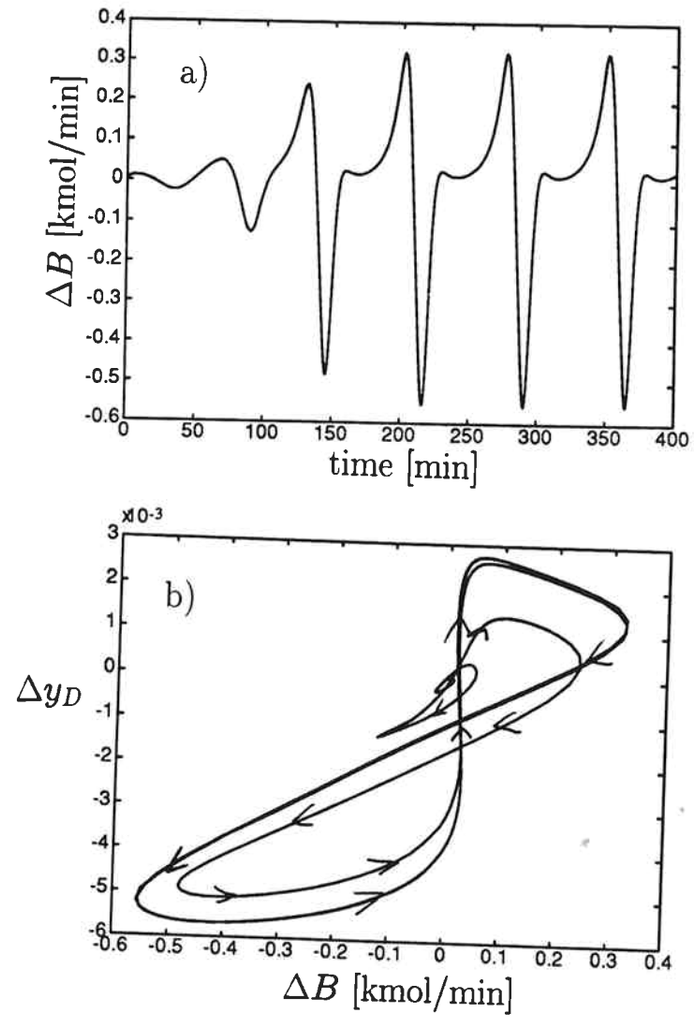

Figure 8.3: Limit cycle for system studied. Response to a small increase in distillate flow D keeping boilup V fixed at 2.14 kmol/min. a) Bottoms flow B against time. b) Top composition y_D against bottoms flow B.